DETERMINATION OF HEAVY METAL COMPOSITION OF PARTICULATE MATTER IN A TYPICAL CHROME AND PLATINUM MINE AREA IN THE LIMPOPO PROVINCE, SOUTH AFRICA

by

Cheledi Evans Tshehla

Submitted in fulfilment of the requirements for the degree
PhD in Air Quality Management

in the

Department of Geography Geoinformatics and Meteorology
Faculty of Natural and Agricultural Sciences

UNIVERSITY OF PRETORIA

8 February 2020

ABSTRACT

The Greater Tubatse Municipality (GTM) is found in the northern part of the Sekhukhune District Municipality in the Limpopo Province of South Africa. It is an area plagued by poor air quality resulting from the activities of chrome and platinum mining, ferrochrome smelters, agricultural and forestry activities, domestic and waste burning practices, as well as vehicular traffic and road dust. This study aimed to contribute to current knowledge on the characteristics and sources of ambient particulate matter (PM) in the area. It also sought to identify the relevant sources, the chemical composition of the pollution stemming from these sources, the amount that each source contributes to PM and the influence of meteorological processes on the spatial distribution of PM in the GTM.

PM, PM_{10} and $PM_{2.5}$ were measured using inexpensive University of North Carolina gravimetric passive samplers. Computer Controlled Scanning Electron Microscopy was used to characterise the mass concentrations of the PM. The mean annual concentration values for PM_{10} for the various measurement sites in the area were: Site 1 (32.02 $\mu g.cm^{-3}$), Site 2 (31.28 $\mu g.cm^{-3}$), Site 3 (38.11 $\mu g.cm^{-3}$), Site 4 (24.1 $\mu g.cm^{-3}$), Site 5(24.65 $\mu g.cm^{-3}$), and Site 5 (20.98 $\mu g.cm^{-3}$). These values were below the South African annual NAAQS of 40 $\mu g.cm^{-3}$. The $PM_{2.5}$ mean annual concentrations were as follows: Site 1 (11.8 $\mu g.cm^{-3}$), Site 2 (4.7 $\mu g.cm^{-3}$), Site 3 (4.8 $\mu g.cm^{-3}$), Site 4 (3.0 $\mu g.cm^{-3}$), Site 5(3.2 $\mu g.cm^{-3}$), and Site 5 (2.5 $\mu g.cm^{-3}$). The annual $PM_{2.5}$ concentration was below the South African annual NAAQS of 20 $\mu g.cm^{-3}$.

The spatial interpolation of PM chemical components showed that metal concentrations were highest closer to the industrial facilities with annual chromium concentrations exceeding the New Zealand annual limits for both Cr(III) (0.11 $\mu g.cm^{-3}$) and Cr(IV) (0.0011 $\mu g.cm^{-3}$) in the study area which is dominated by chromium mining and ferrochrome smelters. The HYSPLIT model was run to determine the regional and trans-boundary air transport to the receptor locations. The HYSPLIT cluster transport pathways indicated both regional and trans-boundary transport of air masses from the North-West Province in South Africa, Zambia (passing over the Limpopo Province in South Africa), Zimbabwe (passing over Limpopo Province), Mozambique and the Indian Ocean (passing over Northern KwaZulu-Natal Province and Swaziland).

The TAPM model and GIS software were used to determine the distribution of PM_{10} from industrial point sources and to consider their possible impacts on human health using modelled hourly data. Meteorological parameters such as Monin-Obukhov length, mixing height, ventilation coefficient and air pollution potential calculated using the TAPM model output data were unable to accurately predict the spatial variability of PM and its chemical components in a complex terrain.

Source contributions were analysed using the positive matrix factorization (PMF) model. The average source contribution in the study area were vehicle (15.1%), chrome smelter (17.3%), industrial coal combustion (19.7%), wood combustion (24.5%) and crustal material (23.6%). The PM_{10} spatial distribution from industrial sources showed the highest concentration of 27.3 µg.cm^{-3}. The seasonal distribution indicated that PM_{10} was high during winter (27.3 µg.cm^{-3}) and low in autumn (15.2 µg.cm^{-3}). The overall PM_{10} distribution was to the west and south-west of the industrial point sources.

The findings from this study on chemical composition, source profiling and source apportionment, and the analysis of the possible impacts from industrial point sources described here can inform the development and implementation of cost-effective strategies to mitigate the scourge of air pollution encountered in South Africa and many other low- and middle-income countries.

RESEARCH OUPUTS

Journal articles

1. Tshehla C. E, and Wright C.Y. 2019. Spatial variability of PM_{10}, $PM_{2.5}$ and PM chemical components in an industrialized rural area within a mountainous terrain. *S Afr J Sci* 115(9/10): 1-10. Doi: https://doi.org/10.17159/sajs.2019/6174
2. Tshehla C.E and Djolov G. 2018. Source profiling, source apportionment and cluster transport analysis to identify the sources of PM and the origin of air masses to an industrialized rural area in Limpopo. *Clean Air Journal*. 28(2): 54-66. Doi: http://dx.doi.org/10.17159/2410-972X/2018/v28n2a18
3. Tshehla C. E., and Wright C.Y. 2019. Spatial and temporal variation of PM_{10} from industrial point sources in a rural area in Limpopo, South Africa. *Int J Env Res Pub Health* 16: 1-14. Doi: https://doi.org/10.3390/ijerph16183455
4. Tshehla C. E. and Wright C.Y. 2019. 15 Years after the National Environmental Management Air Quality Act: Is legislation failing to reduce air pollution in South Africa. *S Afr J Sci* 115(9/10): 1-4. Doi: https://doi.org/10.17159/sajs.2019/6100

Conference presentations

1. Tshehla CE. Characterization of particulate matter, its chemical composition and source identification from the mining area in Limpopo, South Africa. NACA Conference 2016: Air Quality Week 2016, 5 – 7 October, Mbombela.
2. Tshehla CE. Source profiling and source apportionment of PM using PMF in an industrialised rural area in Limpopo, South Africa. 27th International Conference on Modelling, Monitoring and Management of Air Pollution, Air Pollution 2019, 26 – 28 June 2019, Portugal.

LIST OF ABBREVIATIONS

Ag	Silver
Al	Aluminium
APP	Air Pollution Potential
AQA	Air Quality Act
As	Arsenic
As_2S_3	Orpiment
As_4S_4	Pararealgar
Au	Gold
BC	Black Carbon
Fe	Iron
C	Carbon
Ca	Calcium
$CaCO_3$	Calcium Carbonate
$CaMg(CO_3)2$	Dolomite
CCN	Cloud Condensation Nuclei
CCSEM	Computer Controlled Scanning Electron Microscopy
Cd	Cadmium
Co	Cobalt
Co3As2	Linnaeite
CoAs2	Smaltide
CoAsS	Cobaltide
COD	Coefficient of Divergence
CSIRO	Commonwealth Scientific and Industrial Research Organisation
Cr	Chromium
Cu	Copper
DEA	Department of Environmental Affairs
DEFF	Department of Environment, Forestry and Fisheries
EDS	Energy Dispersive Spectrometry
EPA	Environmental Protection Agency
ARL	Air Resource Laboratory
Fe	Iron
FeAsS	Arsenopyride
$FeCr_2O_4$	Chromite

GIS	Geographic Information System
GTM	Greater Tubatse Municipality
HM	Heavy Metal
H_2O	Water
HSO_3	Hydrogen Sulphite
H_2SO_4	Sulphuric Acid
HYSPLIT	Hybrid Single Particle Lagrangian Integrated Trajectory
Ir	Iridium
K	Potassium
km	Kilometres
kV	kilovolt
m^{-3}	cubic meters
Mg	Magnesium
MH	Mixing Height
Mn	Manganese
MO	Monin-Obukhov
Na	Sodium
NACA	National Association of Clean Air
NAAQS	National Ambient Air Quality Standards
NAEIS	National Emissions Inventory System
NCAR	National Centre for Atmospheric Research
NCEP	National Centre for Environmental Prediction
NEMAQA	National Environmental Management Air Quality Act
Ni	Nickel
NOAA	National Oceanic and Atmospheric Administration
O_2	Oxygen
O_3	Ozone
Os	Osmium
OH	Hydroxyl Oxide
P	Phosphorus
PAH	Polyaromatic Hydrocarbons
Pb	Lead
PGE	Platinum Group Element
PM	Particulate Matter
PMF	Positive Matrix Factorization

Pt	Platinum
r	Pearson Correlation Coefficient
Rh	Rhenium
Ru	Ruthenium
RuS2	Ruthenium Sulphide
S	Sulphur
SEM	Scanning Electron Microscopy
Si	Silicon
SiO_2	Silicon Dioxide
SO_2	Sulphur Dioxide
SO	Sulphur Trioxide
TAPM	The Air Pollution Model
Ti	Titanium
TOMAS	Two-Moment Aerosol Section
TSV	Total Spatial Variance
UNC	University of North Carolina
US	United States
µg	micrograms
VC	Ventilation Coefficient
V	Deposition Velocity
VOC	Volatile Organic Compound
WHO	World Health Organization
Zn	Zinc

DECLARATION

I declare that the thesis, which I hereby submit for the degree PhD Air Quality Management at the University of Pretoria, is my own work and has not previously been submitted by me for a degree at this or any other tertiary institution.

ETHICS STATEMENT

The author, whose name appears on the title page of this thesis, has obtained, for the research described in this work, the applicable research ethics approval. The Ethics number is 180000149.

The author declares that he has observed the ethical standards required in terms of the University of Pretoria's Code of Ethics for Researchers and the Policy Guidelines for Responsible Research.

Signature:

Cheledi Evans Tshehla
8 February 2020

ACKNOWLEDGEMENTS

This project could not have been completed without the assistance of Ms Lydia Laka during the sampling period. I would also like to take this opportunity to thank the people who have contributed to this thesis and to the research documented herein. Thank you to Professor Phillip Hopke for assistance with information on the PMF model and staff at RJ Lee for assistance with the CCSEM chemical analysis of the PM samples. For the colleagues at the South African Weather Service who assisted with the logistics for sampling and courier of the samples to RJ Lee. I would like to thank Anzel Swart and the late Professor George Djolov for assistance with the TAPM model. Furthermore, I would like to thank my supervisors, the late Prof George Djolov for his advice and encouragement during the initial phase of this study and Dr Caradee Wright for her support and encouragement. Her confidence in my research inspired me, and her advice helped to shape my ideas. Her careful editing contributed enormously to the production of this thesis.

I thank my friends and family particularly Karabo, Mamohlomi and Thato for their understanding during my long abnormal working hours.

This project was supported by a bursary from the South African Weather Service.

TABLE OF CONTENTS

LIST OF TABLES

LIST OF FIGURES

CHAPTER 1
GENERAL INTRODUCTION

1.1 Introduction

Air pollution is formed by a mixture of gases and particles emitted into the atmosphere by natural and anthropogenic activities, and it can vary spatially and temporally (IHME, 2018). Pollutants in the atmosphere can be classified as either primary or secondary pollutants, with primary air pollutants being emitted directly into the atmosphere from sources, and they can have effects both directly and as precursors of secondary air pollutants (Lo *et al.*, 2006). Secondary air pollutants are those pollutants that are formed as a result of chemical reactions in the atmosphere. Secondary aerosols are formed either as a result of gas-phase reactions followed by condensation of the products, or by reactions taking place in the existing aerosol phase (Harrison and Perry, 1986). Airborne particulate matter (PM) may have a variety of sources that emit them directly into the atmosphere (Ediagbonya *et al*., 2013).

PM is defined by Khlystov (2001) as a complex mixture of particles varying in size range, morphology and composition such as sulphates, nitrates, ammonium, hydrogen ions, trace elements, organic material, black carbon, and crustal material. Particulates in the atmosphere come from a variety of natural and anthropogenic sources, with the latter being more predominant in urban and industrial areas (Borbély-Kiss *et al*., 1999). Anthropogenic activities such as metallurgical industries, metalliferous mining and smelting, use of fertilizers and soil amendments in high-production agriculture, and land disposal techniques for municipal / solid wastes are the major sources for metal contamination (Alloway, 1995; Adriano, 2001). These activities also contribute to the airborne particulates in the atmosphere (Harrison *et al*., 1997; Hien *et al*., 2001; Arditsoglou and Samara, 2005; Valavanidis *et al*., 2006).

Dust can be defined as particles less than 1000 µm that can either be suspended in the air or deposited on surfaces (Moja and Mnisi, 2013). Depending on the wind strength, dust can be suspended or transported from sources locally or across regions and continents and may contain both elemental and organic particles such heavy metals and polycyclic aromatic compounds (Adriaenssens, 2007).

Numerous epidemiological studies have associated ambient concentrations of inhalable (PM_{10}) and respirable ($PM_{2.5}$) particles with increased mortality, morbidity and decreased lung function (Costa and Dreher, 1997; Saskia *et al*., 1998; Martuzzi *et al*., 2002). However, while there are epidemiological correlations between particle concentrations and health effects, it must be kept in mind that particles contain a complex and variable mixture of chemical compounds that are emitted by different sources (Harrison and Yin, 2000; Nabi Bidhendi *et al*., 2007).

Heavy Metals (HMs) are some of the constituents of PM and those that are found in contaminated soil are listed as lead (Pb), chromium (Cr), arsenic (As), zinc (Zn), cadmium (Cd), copper (Cu), mercury (Hg), and nickel (Ni) (GWRTAC, 1997). These metal particles are stable and persistent environmental contaminants since they cannot be degraded or destroyed (Sevgí *et al*., 2010). HMs have a negative impact on human health and other living beings in terrestrial and aquatic environments and they also affect the food chain (Das *et al*., 2013).

In Limpopo province of South Africa, the Greater Tubatse Municipality (GTM) is home to three chromium smelters, a number of chrome and platinum mines and agricultural farms. Industrialization of the rural GTM has led to the increase in population size of the area, which in turn has led to an increase in the number of vehicles, wood burning activities for both space heating and cooking and domestic waste burning. These activities impact negatively on the environment due to an increase in the levels of PM from these anthropogenic activities. The GTM has no operational ambient air quality monitoring network that can be used to determine the status of air quality in the region. The area has a complex terrain that affects the wind circulation pattern and therefore affects the dispersion of pollutants. There have been no studies in the area to identify the major sources of metal pollutants. The meteorological impacts on the distribution of pollutants in a complex terrain (such as the one in the GTM) have not been considered.

2.2 Rationale

South Africa is one of the developing countries in the world, and as such, the country has considered economic growth, social and educational development and industrialization as key

development priorities. In the GTM, mining is viewed as one of the important economic activities which has the potential of contributing to the development of the area's economy (SANRAL, 2007). Though the contributions of mining activities to economic development of the GTM are well acknowledged, this might be achieved at significant environmental, health and social costs to the region due to urbanization, high traffic volumes and higher domestic waste production.

Environmental pollution due to heavy metals from mining activities, vehicular emissions, agricultural and biomass burning is a major concern in many parts of the world (UNEP, 2006). Extensive mining of chromite and platinum, and subsequent smelting of chromium in the GTM mining belt has the potential to pose a serious threat to the environment (Gericke, 1995; Beaver *et al*., 2009). Mining of these ores may release toxic metals such as hexavalent chromium and platinum group metals which are carcinogenic and mutagenic to human health (Zayed and Terry, 2003; Ravindra *et al*., 2004).

In South Africa, the National Environmental Management: Air Quality Act (DEA, 2004) was promulgated to manage air quality in the country. The Act requires national, provincial and local authorities to identify substances or mixtures of substances in ambient air which may reasonably be anticipated to endanger public health and welfare and whose presence in the ambient air results from numerous or diverse mobile or stationary sources, and to establish air quality standards to monitor noncompliance. However, to date, there are no local standards for metals in PM to define the level of air quality that is necessary to protect public health and wellbeing from any known or anticipated adverse effects of these pollutants. There is also little information from PM source apportionment studies to assist in developing effective policies to mitigate the impacts of PM on human health and the environment. The implications are that the control measures put in place to mitigate the impacts of pollution on the environment are based on scientific findings from other countries and as such may fail to effectively address the problem at hand given the complexity of the terrain in GTM and the non-existence of ambient monitoring data in such an industrialized area.

Source profiling and source apportionment is meant to provide information about pollution sources and how much each source contributes to the ambient air pollution levels. Developing an effective Air Quality Management System (AQMS) is a process that requires continuous

improvement, and the implementation of source apportionment techniques can contribute in a cost-effective manner to improve the existing systems or as an initial step to develop an AQMS. This information is crucial for air quality policy development and effective policy implementation. However, in South Africa there are no long-term speciated PM datasets, or studies on characterization of source profiles and source identification. This lack of information makes it nearly impossible to develop effective strategies to manage air quality. Priority needs (which are partly addressed in this study) that if applied may help to build effective AQMS in South Africa include: 1) Co-ordination of source characterization research strategies to inform air quality policy development in South Africa, and 2) Development of long-term PM chemical speciation datasets and source fingerprints for South Africa. For South Africa, source apportionment will offer policymakers and scientists the practical tools for identifying and quantifying the different sources of air pollution, and thereby increase the ability to put in place effective policy measures to reduce air pollution to acceptable levels.

2.3 Aim and objectives

The aim of this study was to contribute to current knowledge on the characteristics and sources of ambient PM in the GTM, South Africa. It also seeks to resolve the relevant sources, their chemical composition, the amount that each source contributes to PM and the influence of meteorological processes on the spatial distribution of PM in the GTM. This will improve understanding of the sources that should be included in air quality control strategies to improve the management of air quality in South Africa.

The objectives of this study were:

1. To collect particulate matter samples using University of North Carolina (UNC) gravimetric passive samplers in the GTM.
2. To characterize the mass concentrations of $PM_{2.5}$, PM_{10} and PM chemical components using Computer Controlled Scanning Electron Microscopy (CCSEM).
3. To characterize the spatial distribution of $PM_{2.5}$, PM_{10} and PM chemical components in the GTM.

4. To determine the relationship between calculated mixing height, Monin-Obukhov length, ventilation coefficient, and air pollution potential with PM_{10} concentration.
5. To determine source profiles of PM, the number of sources, and the contribution of identified sources in the GTM.
6. To determine the regional and trans-boundary air transport to the receptors' locations using the HYSPLIT model.
7. To determine the distribution of PM_{10} from industrial point sources and describe their possible impacts on human health using modelled hourly data from the TAPM model and GIS software.
8. To reflect on the findings of objectives (1) – (6) and consider gaps in the current implementation of the air quality management in South Africa.

2.4 Structure of this thesis

This thesis comprises Introductory and Literature Review Chapters followed by a set of published research manuscripts that describe the methods and results for each of the objectives provided in section 2.3 above. Chapter 2 gives a detailed description of aerosols, as well as a description of the Geographic Information Systems (GIS) and modelling applications. Chapter 3 gives results of the spatiotemporal variation of PM_{10}, $PM_{2.5}$ and PM chemical components and the impacts of meteorological parameters on the spatiotemporal variations. Results on source profiling and source apportionment of PM are given in Chapter 4 which also discusses the transport pathways of air masses prior to arrival at the receptor sites. Chapter 5 evaluates the spatial distribution of PM_{10} from industrial point sources using the TAPM model and GIS spatial analysis tool. Chapter 6 provides a reflection, having completed all of the tasks in objectives 1 to 7, on the implementation of the National Environmental Management Act, Air Quality Act No 39 of 2004 and air quality management in South Africa.

The contribution of the Candidate to each research output is outlined in the Introduction section of the Chapter preceding each paper. The Candidate was the lead author for each paper and drafted all versions of the manuscripts. The Candidate was responsible for circulating the manuscripts to the co-authors, reviewing co-authors' comments and suggestions before

integrating them into the manuscript as appropriate. All co-authors critically reviewed and approved the submitted manuscripts prior to submission.

1.5 References

Adriano, D.C., 2001: Trace elements in the terrestrial environment: Biogeochemistry, Bioavailability and Risks of Metals, 2nd Edition, Springer, New York.

Adriaenssens E., 2007. Analysis of heavy metals in ambient air. Spectroscopy Focus. *International Lab. mate*. 15:1.

Alloway, B.J., 1995: (Ed.). Heavy metals in soils, 2nd Edition, Blackie Academic & Professional, Glasgow, UK. pg. 368.

Arditsoglou, A. and Samara C., 2005: Levels of total suspended particulate matter and major trace elements in Kosovo: A source identification and apportionment study. Chemosphere 59: 669-678.

Beaver, L.M., Stemmy, E.J., Constant, S.L., Schwartz, A., Little, L.G., Gigley, J.P., Chun, G., Sugden, K.D., Ceryak, S.M. and Patierno, S.R., 2009: Lung injury, inflammation and Akt signalling following inhalation of particulate hexavalent chromium. *Toxicol. Appl. Pharm*. 235, 47-56. doi: 10.1016/j.taap.2008.11.018.

Borbély-Kiss, I., Koltay, E., Szabó, G.Y., Bozó, L., and Tar, K., 1999: Composition and sources of urban and rural atmospheric aerosol in Eastern Hungary. *J Aerosol Sci*. 30: 369-391. British Geological Survey, 2009. Platinum. Natural Environmental Research Council.

South African National Roads Agency (SANRAL), 2007: Community Empowerment Impact Assessment Report, Special Development Project: Tubatse - R37. c2007 [cited 2017 August04]. Available from: https://www.nra.co.za/content/Tubatse1.pdf.

Costa, D.L. and Dreher, K. L., 1997: Bioavailable transition metals in particulate matter mediate cardiopulmonary injury in healthy and compromised animal models. *Environ. Health Perspect.* 105(suppl. 5):1053–1060.

Das, J., Das, S., Bakar, M., Biswas, A. and Uddin, M., 2013: Evaluation of essential and toxic metals in bakery foods consumed in Chittagong (Bangladesh). Analytical Chemistry. *Indian Journ*. 13(3): 188-125.

South African Department of Environmental Affairs (DEA). National ambient air quality standards [document on the Internet]. c2012 [cited 2018 June29]. Available from: https://www.environment.gov.za/content/national-environmental-management-air-quality-act-2004-act-no-39-2004-national-ambient-air-q.

Ediagboya, T.F., Ukpebor, E.E. and Okiemen, F.E., 2013: Heavy metal in inhalable and respirable particles in urban atmosphere. *Environ. Skeptics and Critics*. 2(3): 108-117.

Gericke, W.A., 1995: Environmental aspects of ferrochrome production. https://www.pyro.co.za/InfaconVII/131-Gericke.pdf

GWRTAC, 1997: Remediation of metals-contaminated soils and groundwater. *Tech. Rep.* TE-97-01, GWRTAC, Pittsburgh, PA.

Harrison, R.M. and Perry, R.A., 1986: Handbook of Air Pollution Analysis. Springer, 2nd Edition, pg 343.

Harrison, R.M., Deacon, A.R., Jones, M.R. and Appleby, R.S., 1997: Sources and processes affecting concentrations of PM10 and PM2.5 particulate matter in Birmingham. *Atmos. Environ.* 31: 4103–4117.

Harrison, R.M. and Yin, J., 2000: Particulate matter in the atmosphere: which particle properties are important for its effect on health? *Sci. Total Environ*. **249:** 85-101.

Hien, P.D., Binh, N.T., Truong, Y., Ngo, N.T. and Sieu, L.N., 2001: Comparative receptor modelling study of TSP, PM2.5 and PM10 in Ho Chi Minh City. *Atmos. Environ*. 35: 2669-2678.

Institute of Health Metrics and Evaluation (IHME), 2018: State of global air: A special report on global exposure to air pollution and its disease burden.

Khlystov, A., 2001: Quality Assurance Project Plan for Pittsburgh Air Quality Study (PAQS), Department of Chemical Engineering. Carnegie Mellon University.

Lo, J.C.F., Lau, A.K.H., Yuan, Z.B., Fung, J.C.H. and Chen, F., 2006: A physical modelling approach for identification of source regions of primary and secondary air pollutants. *Atmos. Chem. Phys. Discuss*. 6: 6467-6496.

Martuzzi, M., Krzyzanowski, M. and Bertollini, R., 2003: Health impact assessment of air pollution: providing further evidence for public health action. *Eur. Respir. J.* **21:** 86-91.

Moja, S.J. and Mnisi, J.S., 2013: Seasonal variation in airborne heavy metals in Vanderbijlpark. *S. A. Journ. Environ. Chem. and Toxicol.* 5(9): 227-233.

Nabi Bidhendi, G.R., Karbassi, A.R., Nasrabadi, T. and Hoveidi, H., 2007: Influence of copper mine on surface water quality. *Int. J. Environ. Sci. Tech.* 4 (1): 85-91.

Ravindra, K., Bencs, L. and Van Grieken, R., 2004: Platinum group elements in the environment and their health risk. *The Science of the Total Environment*, 318: 1-43.

Saskia, C., Van Der Zee, S.C., Hoek, G., Harrssema, H. and Brunekreef, B., 1998: Characterization of particulate air pollution in urban and non-urban areas in the Netherlands. *Atmos. Environ.* 32: 3717–3729.

Sevgí, E., Coral, G., Gìzìr, A.M. and SanGün, M.K., 2010: Investigation of heavy metal resistance in some bacterial strains isolated from industrial soils. *Turk. J. Biol*. 34: 423-43.

United Nation Environment Programme (UNEP), 2006: Ground Contamination Assessment Report – Military Waste Storage Site, Astana, Afghanistan. Accessed February 5, 2018.

Valavanidis, A., Fiotakis, K., Vlahogianni, T., Bakeas, E.B., Triantafillaki, S., Paraskevopoulou, V. and Dassenakis, M., 2006: Characterization of atmospheric particulates, particle bound transition metals and polycyclic aromatic hydrocarbons of urban air in the centre of Athens (Greece). *Chemosphere*, 65: 760-768.

Zayed, A.M. and Terry M., 2003: Chromium in the environment: factors affecting biological remediation. *Plant and Soil*, 249: 139–156.

CHAPTER 2

Literature Review: Aerosols, Geographic Information Systems and Modelling Applications

Understanding and characterising aerosol formation is important because aerosols can modify cloud formation process (de Leeuw *et al*., 2011) and affect the amount of rainfall, which in turn will affect the level of pollution in the atmosphere (through wet deposition processes, for instance). Elucidating how aerosol formation occurs is critical to understand aerosol contribution to the Earth's radiation budget, given that atmospheric aerosols have a profound effect on scattering or absorption of radiation even at low concentrations (Mahlman, 1997). This chapter focuses on the formation of aerosols in the atmosphere and the methods used in measuring atmospheric aerosols in ambient air. It also looks at the influence of complex terrain on the meteorology of a region and how it may impact on the dispersion of pollutants.

2.1 Aerosols

An aerosol is a general term used to define suspended liquid or solid particles in a gaseous medium such as air, with particle diameters in the range of 10^{-9} -10^{-4} m. Aerosols are present in the atmosphere in the form of clouds, dust, smog, mist, fog, haze, and smoke (Seinfeld and Pandis, 1998; Hind, 1999). Naturally-occurring aerosols in the atmosphere are called “atmospheric aerosols”, those that are produced in the laboratory or field space by man-made chemical, thermal, or mechanical means are called “artificial aerosols” and those generated as by-products of human activity, such as burning of fossil fuels are often referred to as “anthropogenic aerosols” (Seinfeld and Pandis, 1998).

Atmospheric aerosols may be formed as the result of wind motion at the Earth’s surface (land or ocean) or formed in-situ by condensation from the gaseous phase. Gaseous precursors may be formed by chemical reactions of naturally- or anthropogenically-produced gases in the presence of sunlight. Aerosols are subject to changes in size and composition by processes of condensation, evaporation, and coagulation. Aerosols found in the troposphere are often mixtures of different chemical components. One such mixture occurs when a solid aerosol

passes through an industrial plume and the individual particle acquires a layer of sulphates or nitrates. Atmospheric aerosols are also involved in the cloud formation process in which they act as condensation nuclei around which cloud droplets are formed, and they can later be removed from the atmosphere through wet deposition in the form of rain or snow. The concentrations and composition of aerosols depend on location relative to source regions, production and removal rates, transport, and altitude. Aerosols can be characterized according to their sources and the most significant sources for atmospheric aerosols lie within the planetary boundary layer where concentrations are found in large numbers. Aerosol sources are not only localised but may also vary in time. These variations depend on meteorological conditions which change seasonally (Finlayson-Pitts and Pitts, 1999; Seinfeld and Pandis, 1998) such as in the formation of dust plumes by surface wind erosion or biomass burning and smoke often observed during the winter season in southern Africa.

Aerosols impact on the Earth's climate, biosphere and other atmospheric phenomena. Depending on the size of aerosols, solid and liquid particles will influence the radiation and energy budget of the Earth, the hydrological cycle, atmospheric circulation and the abundance of trace gases differently. Aerosols' concentration, size distribution, structure and chemical composition are temporally and spatially highly variable (Lagzi *et al*, 2013).

2.1.1 Aerosol formation process

The atmospheric sources of aerosols can either be of natural or anthropogenic origin. Human activities in recent years have resulted in the emission of liquids or solid aerosols from sources such as incomplete combustion of fossil fuel, biomass burning, industrial processes, fugitive sources (wind-blown dust from unpaved roads, crop land), traffic and mineral dust. Aerosol size measurements are characterized by their cross-sectional diameter and particle, surface area, volume and mass distribution (Finlayson-Pitts and Pitts, 1999). Atmospheric aerosols vary in shapes and size and this in turn determines their optical properties and their removal mechanism from the atmosphere (Finlayson-Pitts and Pitts, 1999; Seinfeld and Pandis, 1998). Primary aerosols are formed by dispersal of material at the Earth's surface and include material such as volcanic dust, organic materials from biomass burning, soot from combustion and mineral dust from wind-blown processes (Seinfeld and Pandis, 1998). Significant natural surface sources of primary aerosol particles include the emission of sea spray, release of soil

and rock debris (mineral dust) and biogenic aerosols, emission of biomass burning smoke, and injection of volcanic debris at tropospheric altitudes by violent eruptions. A negligible contribution to the overall atmospheric aerosol loading is also given by space, in the form of cosmic aerosols (Tomasi and Lupi, 2017).

Secondary aerosols are formed by reaction of gases in the atmosphere and include sulphates from the oxidation of sulphur-containing gases during the burning of fossil fuels, nitrates from gaseous nitrogen species, and products from the oxidation of volatile organic compounds (Seinfeld and Pandis, 1998). A combination of physical, chemical processes and sometimes biological processes occur to form new particles either by: (1) nucleation (i.e., gas molecules coming together to form a new particle), (2) condensation of gases onto existing particles, and (3) by reaction in the liquid phase. Homogeneous nucleation (Figure 2.1) involves the spontaneous formation of liquid droplets directly from the gas phase, while heterogeneous nucleation is the result of the interaction of aerosols with large surface area (Seinfeld and Pandis, 1998).

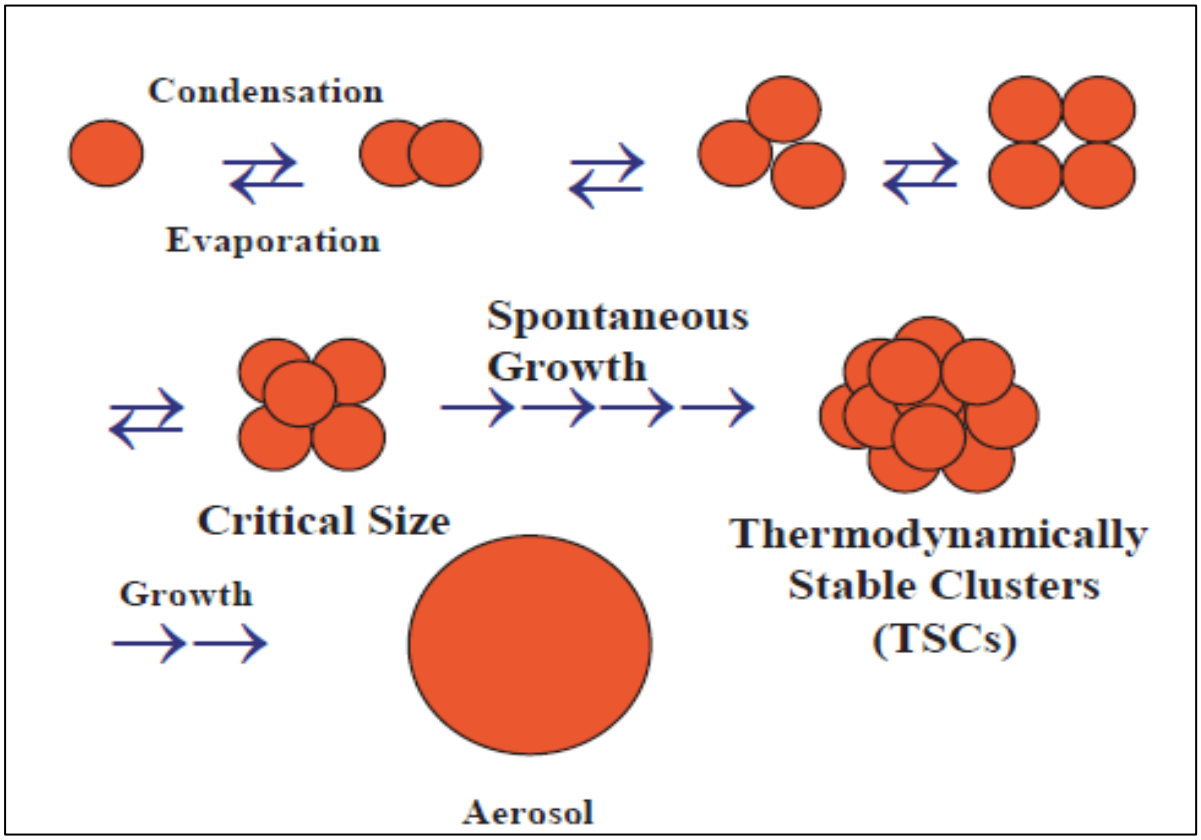

Figure 2.1: Gas phase homogeneous nucleation (Seinfeld and Pandis, 1998).

Nucleation involves the following reaction steps (Seinfeld and Pandis, 1998):

$SO_2 + OH \rightarrow HSO_3$ (Rate limiting step) 2.1,

$HSO_3 + O_2 \rightarrow HO_2 + SO_3$ 2.2,

$SO_3 + H_2O \rightarrow H_2SO_4$ 2.3,

SO_2 is emitted by combustion of fossil fuels or formed through the oxidation of organic sulphur compounds emitted by biogenic material. The OH formation result from photolysis of ozone molecules:

$h\gamma$

$O_3 \rightarrow O(1D) + O_2$ 2.4,

$O(1D) + H_2O \rightarrow 2OH$ 2.5,

Once formed, H_2SO_4 immediately becomes hydrated. The hydrated H_2SO_4 molecules act as nuclei, and the H_2SO_4 molecules collide. The collision of H_2SO_4 monomers forms H_2SO_4 dimers, and the H_2SO_4 dimers forms trimers, and so on.

$H_2SO_4 + H_2SO_4 \rightarrow 2\ H_2SO_4$ 2.6,

$2\ H_2SO_4 + H_2SO_4 \rightarrow 3\ H_2SO_4$ 2.7,

$3\ H_2SO_4 + H_2SO_4 \rightarrow 4\ H_2SO_4$ 2.8,

Adams and Seinfeld (2002) described the condensation of gas-phase species to existing aerosol particles as an important source of aerosol mass and a means by which small particles grow to Cloud Condensation Nuclei (CCN) sizes. Gaydos *et al*., (2005), used the Two-Moment Aerosol Sectional (TOMAS) algorithm to simulate the condensation/evaporation of sulphuric acid, ammonia, and organic vapours, using particle diameters. The driving force for condensation of a vapour to an aerosol particle is the difference between its ambient vapour partial pressure and the equilibrium vapour pressure over the particles, or

$$\Delta p_i = pi - p_i^* x_i(D_p) \exp\left(\frac{4\sigma Mi}{RT\rho Dp}\right) \quad 2.9,$$

where Δp_i is the condensational driving force of the organic vapour i (the difference between the partial pressure of condensing vapour and its equilibrium vapour pressure), p_i is the ambient partial pressure, x_i is the mole fraction of i, p_i^* is the effective saturation pressure over a flat surface, σ is the surface tension, M_i is the molecular weight of i, R is the ideal gas constant, T is the temperature, ρ is the liquid-phase density, and D_p is the diameter of the particle. The exponential term is known as the Kelvin effect due to the curvature of the particles. The exponential term is large for small particles to prevent the condensation of organic vapours on these. As a result, the Kelvin effect is important for the growth of newly formed particles. Two-Moment Aerosol Section (TOMAS) is used with an adaptive time step to efficiently solve the equations for condensation. The time step is chosen so that individual particles in any size bin do not grow by more than 10 %, the partial pressure of the organic vapour does not fall below 25% of its original value, and the time step is never longer than 15 min. The TOMAS could be a useful tool to predict the concentration of $PM_{2.5}$ in remote areas of South Africa where there is no continuous monitoring. This is because passive sampling tends to lose some of the $PM_{2.5}$ particles due to evaporation of sulphates and nitrates when deployed for a long period.

2.1.2 Aerosol size distribution

Aerosols are characterized by their physical and chemical properties, such as size, shape, and material composition. The atmosphere contains up to 108 cm^3 concentrations of aerosols with a diameter ranging from 0.002 to 100 µm. Size distribution of aerosols is crucial to understanding the chemistry and physics of atmospheric particles and their effects as well (Finlayson-Pitts and Pitts, 1999). Particles generated by combustion such as those from power generation, vehicles and wood and coal burning can range from a few nanometres to 1 µm. Atmospheric particles smaller than 1 µm are generally produced by photochemical processes, and those larger than 1 µm are generated by windblown dust, pollens, plant fragments and sea salt (Seinfeld and Pandis, 1998). The difference in size of these particles influences their lifetime in the atmosphere and their physical and chemical properties. The distinction between various modes of particles is fundamental for distinguishing the differences in physical, chemical, measurement and health effects of aerosols (Seinfeld and Pandis, 1998).

2.1.3 The number distribution

The atmospheric aerosol distribution is characterized by several modes (Figure 2.2).

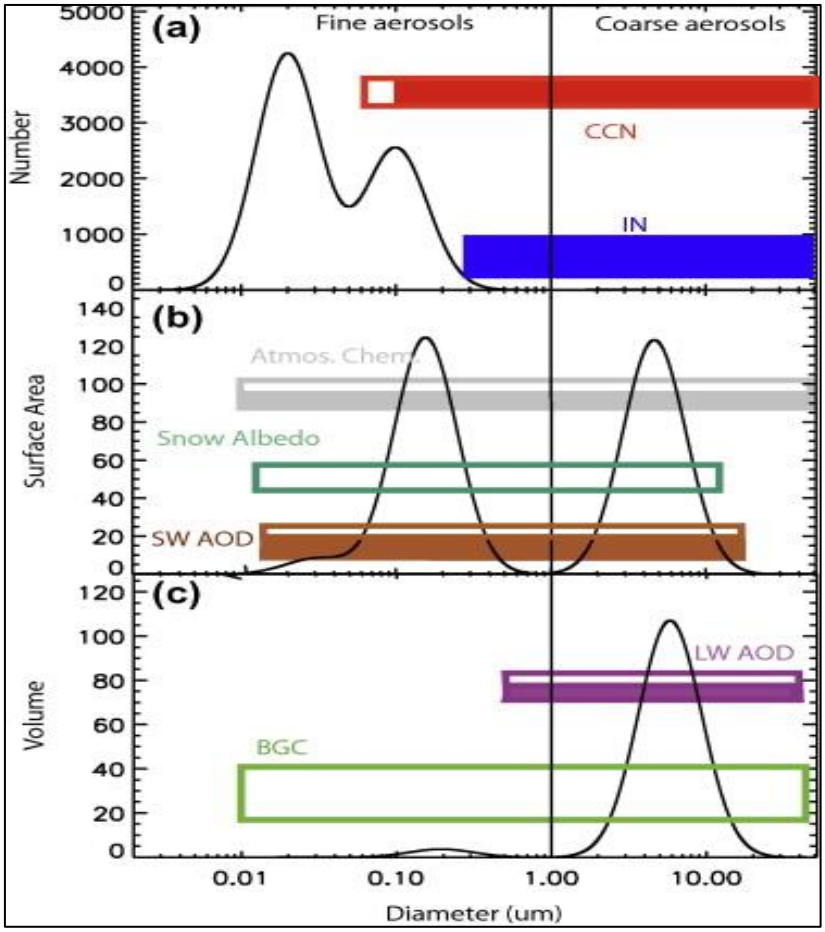

Figure 2.2: (a) Aerosol number, (b) surface area, and (c) volume for a typical trimodal aerosol distribution (Mahowald *et al*., 2011).

Particles with a diameter in the range of 10^{-3} µm to 10^{-2} µm are referred to as nucleation mode, particles with 10^{-2} µm to 0.1 µm diameter are Aitken mode, 0.1 µm to 1 µm diameter are accumulation mode and particle with a diameter greater than 1 µm are coarse mode. Fine particles with a diameter less than 0.1 µm are larger in numbers compared to those with a diameter greater than 0.1 µm which constitute all the aerosol mass size. Aerosol distribution values for a number of diameters can be reported using a table. However, for many applications including hundreds or thousands of aerosol distribution values will be impossible. Therefore, mathematical functions such as equation 2.10 to 2.11 are convenient for use because they match

observed shapes of ambient distributions (Aitchison and Brown, 1957). Atmospheric aerosols can be described as the sum of n lognormal distributions:

$$n°_N(logD_p) = \sum_{i=1}^{n} \frac{N_i}{(2\pi)^{1/2}\log\sigma_i} \exp\left(\frac{(\log D_p - log\bar{D}_{pi})^2}{2log^2\sigma_i}\right) \quad 2.10,$$

Where $n°_N(\log D_p)$ is the number of particles with diameter D_p, N_i is the number concentrations, $\bar{D}_{pi}$ is the median diameter, and σ_i is the standard deviation of the i^{th} lognormal mode (Seinfeld and Pandis, 1998).

2.1.4 The surface area, volume, and mass distribution

Aerosols size cannot only be presented in terms of number distribution. Surface area of aerosols is suitable for describing their chemical interaction, while the volume distribution is more suitable for describing their mass loading and conservation (Finlayson-Pitts and Pitts, 1999). Figure 2.3 shows the number, surface and volume distribution of aerosols for a typical urban aerosol distribution (Whitby, 1978). The three modes of aerosol distribution structure are summarized in Figure 2.4 which depicts the sources of each mode and the removal process (Finlayson-Pitts and Pitts, 1999). Analogous to the number size distribution, the volume size distribution is given as follows:

$$n_v(D_p) = \frac{4\pi}{3}\left(\frac{Dp}{2}\right) 3\, nN = \sum_{i=1}^{n} \frac{\frac{\pi}{6} N i D_p^3}{\sqrt{2\pi}\, Dp ln\sigma i} \exp\left(\frac{-(lnDp - ln\bar{D}pi)2}{2ln^2\sigma g}\right) \quad 2.11,$$

which represents the contribution of all particles in a size d$\log D$ around the diameter D to the total volume of all aerosol particles in one cm^{-3}. If the geometric mean diameter $\bar{D}_p$ and the geometric standard deviation σ_g are known, the geometric mean volume diameter $\bar{D}_{pv}$ given as follows (Seinfeld and Pandis, 1998):

$$\ln \bar{D}pv = \ln \overline{Dp} + 3 \ln 2\sigma_g \quad 2.12,$$

The geometric mean volume diameter D_{pv} is the aerosol diameter that divides the volume distribution in half.

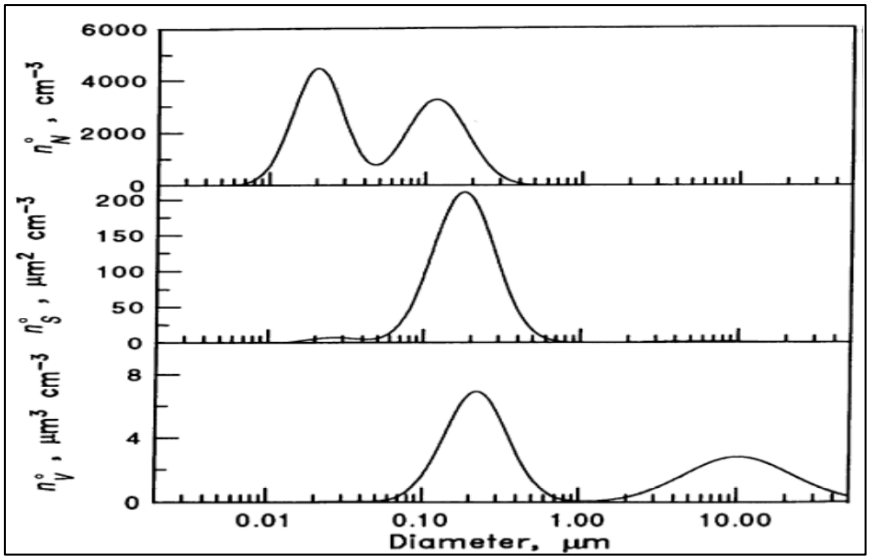

Figure 2.3: Illustration of number, surface, and volume distributions for a typical urban model aerosol (Whitby and Sverdrup, 1980).

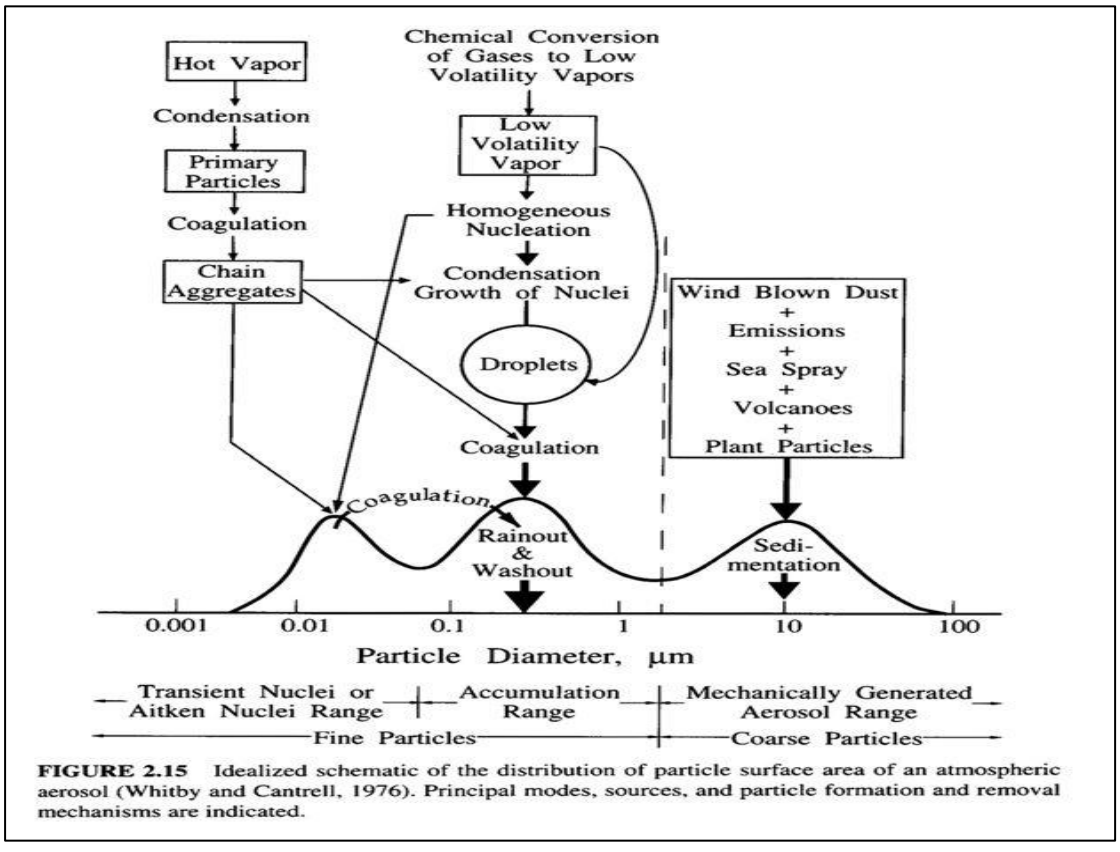

FIGURE 2.15 Idealized schematic of the distribution of particle surface area of an atmospheric aerosol (Whitby and Cantrell, 1976). Principal modes, sources, and particle formation and removal mechanisms are indicated.

Figure 2.4: Aerosol size distribution showing sources of the three modes (Whitby and Sverdrup, 1980).

2.1.5 Aerosol vertical distribution

An atmospheric layer known as the free troposphere is found above the surface boundary layer (Kumar *et al*, 2013). This is the region where aerosols movement is decoupled from surface friction, though they are influenced by the underlying surface characteristics. Aerosol concentrations in free troposphere are lower and have a longer lifetime than those in the boundary layer, and hence the free tropospheric aerosols can be transported across neighbouring countries. The vertical distribution of aerosol mass concentration (Figure 2.5) illustrates that they decrease exponentially with altitude to height (H_p) and become constant with height above level Hp. The aerosol mass concentration is described by:

$$p = p_o\{\exp\left(\frac{-z}{|Hp|}\right) + \left(\frac{Pb}{Po}\right)^{v}\}^{v} \qquad 2.13,$$

$$n = n_o\{\exp\left(\frac{-z}{|Hn|}\right) + \left(\frac{ns}{no}\right)^{v}\}^{v} : H_n \neq 0;\ v = Hn/(|Hn|)\ ,\ \text{Hp} \neq 0 \text{ and } \text{v} = Hp/(|Hp\ |) \qquad 2.14,$$

where p is either mass or number concentration at altitude z, p_o is the value of p at the Earth's surface, p_b is the corresponding background value, and H_p is the scale-height of the aerosol (Finlayson-Pitts and Pitts, 1999).

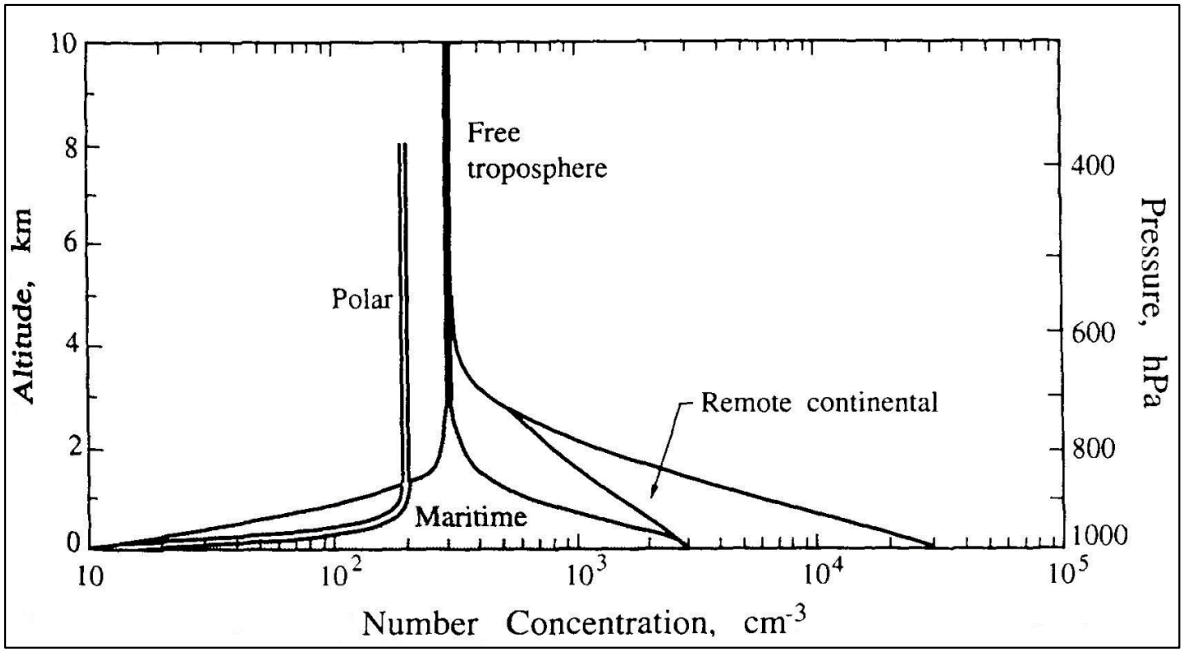

Figure 2.5: Vertical distribution of aerosol mass concentration (Jaenicke, 1993).

2.2 Aerosol emissions

Aerosols are emitted into the atmosphere by natural or anthropogenic activities. The natural sources of aerosols include soil dust and sea salt as a result of wind action on the Earth's and Oceans' surfaces. Biomass burning is also one of the natural emitters of black carbon, polycyclic aromatic hydrocarbons (PAHs) and unburnt carbon from incomplete biomass combustion, and mineral matter and heavy metals from complete combustion. Another important source of natural aerosols is the nucleation and condensation of naturally produced precursor gases to form aerosols containing sulphate and nitrates, as well as organic materials. Anthropogenic aerosols are generated by activities such as domestic / industrial fuel combustion, industrial processes, fugitive sources, and transport fleets. Globally, the natural aerosols are larger in magnitude compared to the anthropogenic aerosols, however, the ratio can be greatly influenced by human activities in industrialised regions (Gray *et al*., 1986; Mazurek *et al*., 1989; Hildemann *et al*., 1994). Table 2.1 summarises emissions from both natural and anthropogenic sources.

Table 2.1: Particle emission estimates (1 Tg/yr = 10^6 Ton/yr) (Tomasi and Lupi, 2017).

Particles	**Emissions (Tg/yr)**	**Source**
Sea salt (total, sizes <16 μm)	3 344	IPCC, 2001
Sea salt (sizes <1 μm)	54	IPCC, 2001
Sea salt (1–16 μm size range)	3 290	IPCC, 2001
Sea salt (overall)	10 100 3 300 7 804 3 000-20 000	Gong *et al*., 2002 Jaenicke, 2005 Tsigaridis *et al*., 2006 Andreae and Rosenfeld, 2008
Mineral (soil) dust (total, sizes <20 μm)	2 150	IPCC, 2001
Mineral (soil) dust (sizes <1 μm)	110	IPCC, 2001
Mineral (soil) dust total (1–2 μm size range)	290	IPCC, 2001
Mineral (soil) dust total (2–20 μm size range)	1 750	IPCC, 2001

Mineral dust (0.1–10 μm size)	1 000-2 150	Zender *et al*., 2003
Mineral dust (overall)	2 000 1 704 1 000-2 150	Jaenicke, 2005 Tsigaridis *et al*., 2006 Andreae and Rosenfeld, 2008
Volcanic dust (coarse particles)	30	Seinfeld and Pandis, 1998
Sulphates from volcanic SO2	10	Hobbs, 2000
Volcanic sulphates (as NH4HSO4)	21	IPCC, 2001
Volcanic SO2	9.2	Tsigaridis *et al*., 2006
Cosmic dust in the upper mesosphere	$3x10^{-2}$ – $1.1x10^{-1}$	Plane, 2012
Cosmic dust in the middle atmosphere	$2x10^{-3}$ – $2x10^{-2}$ $1.5x10^{-4}$ – $4x10^{-2}$	Plane, 2012 Gardner *et al*., 2014
Biogenic aerosol	1 000	Jaenicke, 2005
Biogenic sulphate (as NH4HSO4)	57	IPCC, 2001
Biogenic carbonaceous aerosol (sizes>1 μm)	56	IPCC, 2001
Biogenic primary organic aerosol	15-17	Andreae and Rosenfeld, 2008
Biogenic VOC compounds	16	IPCC, 2001
Secondary organic aerosol from biogenic VOC	11.2	Chung and Seinfeld, 2002
Secondary organic aerosol	2.5-83	Andreae and Rosenfeld, 2008
Sulphates (from all the natural primary and secondary sources)	107-374	Andreae and Rosenfeld, 2008
Nitrates (overall, from natural primary and	12-27	Andreae and Rosenfeld, 2008
Secondary sulphates from DMS	12.4 18.5	Liao *et al*., 2003 Tsigaridis *et al*., 2006
Carbonaceous aerosols from biomass burning (sizes<2 μm)	54	IPCC, 2001
Primary organic aerosol	44.4	Tsigaridis *et al*., 2006
Biomass burning organic	26-70	Andreae and Rosenfeld, 2008
Total natural particles over the whole size range	5 875 4 200-22 800	IPCC, 2001 Andreae and Rosenfeld, 2008

2.2.1 Soil dust

Soil dust is one of the major contributors to aerosol loading in the atmosphere (Kok *et al*., 2017). The turbulent air motion of speed as low as 0.5 m/s can pick up soil particles as large as 2 μm and can transport them over long distances to a destination far from the original location (Sathneesh *et al*., 2004). Global dust modelling suggests that the anthropogenic contribution to atmospheric dust loads today range between 10% and 60%, that is, between ∼90 and 2000 Mt. $year^{-1}$ (Mahowald *et al*., 2010; Shao *et al*., 2011).

Dust aerosols are divided into natural dust and anthropogenic dust according to their different dust source regions (Ginoux *et al*., 2001, Ginoux *et al*., 2012). The natural sources of dust are mainly deserts and open land, while anthropogenic dust emissions can be interpreted as soil particles that originate from soil conditions being altered or disrupted by human activity (Zheng *et al*., 2016; Chen *et al*., 2017; Luan *et al*., 2017). Mining operations and mine tailings are some of the anthropogenic activities that result in dust loading in the atmosphere due to soil surface disturbances. Dust deflations occur when the surface wind speed supersedes the velocity threshold resulting in the lifting of microscopic particles into the atmosphere. The velocity threshold is a function of surface roughness, size of the particle grain and moisture in the soil (Babikir, 2004).

The lifetime of dust in the atmosphere depends on particle size, with larger particles being the first to be removed through dry or wet deposition, while finer particles can remain suspended in the atmosphere for several weeks in the atmosphere (Lee *et al*., 2009).

2.2.2 Sea salt

Physical processes such as the bursting of air bubbles at the surface of the Ocean results in the emission of sea salt aerosols and this process is largely dependent on the wind speed (Blanchard, 1983; Monahan *et al*., 1986). Sea salt aerosols are mainly responsible for light scattering and cloud nuclei in marine regions particularly during high wind speeds and when there is weak loading of other aerosols particles into the atmosphere (O'Dowd *et al*., 1997; Murphy *et al*., 1998a; Quinn *et al*., 1998). Sea salt aerosols range in size from 0.05 to 10 μm, and in a typical urban atmosphere, measured mass size distributions of sodium and chloride

concentrations show a dominant peak around 4μm (Wall *et al*., 1988). Particles smaller than 1μm contribute significantly to cloud condensation nuclei concentrations (Pierce and Adams, 2006), while particles larger than 50μm are quickly removed from the atmosphere and play a negligible role in atmospheric chemistry (Lewis and Schwartz, 2004).

2.2.3 Industrial aerosols

Industrial activities such as mine smelting, coal combustion, cement manufacturing, stone crushing, mine haulage, waste incineration and brick manufacturing are responsible for the generation of primary aerosol particles into the atmosphere. It is estimated that the global aerosol emissions were about 100 Tg/yr in 1995 (Andreae, 1995) and doubled to about 200 Tg/yr in 1997 (Wolf and Hidy, 1997).

2.2.4 Carbonaceous aerosols

There are two major components of carbonaceous particles, black carbon and organic material, which make up a large but highly variable fraction of the atmospheric aerosols (Andreae *et al*., 1988). The organic particles emitted from biomass burning are also present in large quantities in the atmosphere (Andreae *et al*., 1988). Most of these organic aerosols are found in the upper troposphere (Murphy *et al*., 1998b). Many of these organic compounds in aerosols contain carboxylic and dicarboxylic acids which are water-soluble and allow them to form cloud nuclei (Sempéré and Kawamura, 1996) and consequently play a major role in indirect climate forcing (Rivera-Carpio *et al*., 1996). Elemental carbon (black carbon) refers to light-absorbing, combustion-generated carbonaceous materials that does not volatilise below temperatures of about 550°C and when suspended in the atmospheric boundary layer they can reduce surface albedo (Hansen *et al*., 1997; Schult *et al*., 1997).

2.3 Aerosol chemical composition

Aerosol particles in the troposphere contain sulphates, nitrates, sodium, chlorides, trace metals, carbonaceous material, crustal elements, and water. The sulphate fraction results from the oxidation of anthropogenic and natural sulphur-containing compounds such as sulphur dioxide (SO_2) and dimethyl sulphide. The crustal materials such as silicon, calcium, magnesium,

aluminium and iron, and biogenic particles are usually in the coarse aerosol fraction. The nitrates can be found in both the fine and coarse fraction. Fine nitrate usually results from the reaction of nitric acid and ammonia during the formation of ammonium nitrate, while the coarse nitrate is the product of reactions of coarse particles and nitric acid (Seinfeld and Pandis, 1998). The trace metal component of aerosol particles depends on the geology of the emission area. The major important trace metals are Al, Ca, Si, Fe, Ti, K, Mg, Co, Rb, Ba and Sr (Chester *et al*., 1996; Bonelli *et al*., 1996). The mineral components of aerosol particles are quartz (SiO_2), calcite ($CaCO_3$), dolomite ($CaMg(CO_3)2$) and clay minerals (Ávila *et al*., 1997). Particulate organic carbon is directly emitted into the atmosphere or can result from atmospheric condensation of low-volatile organic gases by either nucleation or gas-to-particle partitioning to pre-existing particles (Odum *et al*., 1996; Hoffmann *et.al*., 1997; Kamens *et al*., 1999).

Understanding the composition of atmospheric aerosol particles is necessary for profiling of air pollution sources such as vehicular emissions, wood burning fires and industrial processes (Fenger, 1999; Mayer, 1999). The pollution from these sources can lead to possible adverse health effects (Harrison and Yin, 2000; Pope *et al*., 2002)

2.4 Aerosol lifetime and sinks

Particles and trace gases are removed from the atmosphere through coagulation (for ultrafine particles), wet deposition (for fine and coarse particles) and dry deposition. The removal process depends on whether the substance is in the gaseous or solid phase, the solubility of the species in water, the amount of precipitation, the terrain and type of surface cover (Seinfeld and Pandis, 1998).

2.4.1 Coagulation

Coagulation is the removal of ultrafine particles from the atmosphere when particles collide and adhere to each other. The collision arises from the motion caused by forces acting on the particles. For ultrafine particles, the instantaneous momentum imparted to the particle varies randomly and causes the particle to move on an erratic path known as Brownian motion (Figure 2.6). The coagulation rate (J_{12}) is determined by the collision efficiency (Seinfeld and Pandis, 2006). The probability that two colliding particles will coagulate and form a new larger particle

is termed "collision efficiency" (α) (Roldin *et al*, 2011). The coagulation rate is determined by equation 15, where K_{12} is the Brownian coagulation coefficient between two number concentrations of the colliding particles (N_1 and N_2):

$$J_{12}=K_{12}\,N_1N_2 \qquad 2.15,$$

$$K_{12}=2\pi(D_1+D_2)(D_{p1}+D_{p2})\left[\left(\frac{Dp1+Dp2}{Dp1+Dp2+2\left(g_1^2+g_2^2\right)1/2}+\frac{1}{(\bar{c}_1^2+\bar{c}_2^2)1/2(Dp1+Dp2)}\right]^{-1}\right. \qquad 2.16,$$

With D_1 and D_2 denoting the diffusion coefficients of the two particles, D_{p1} and D_{p2} their diameters, $\bar{c}_1$ and $\bar{c}_2$ being the mean velocities of the particles and g_1 and g_2 are functions of the particle diameters and their mean free path in the air (Seinfeld and Pandis, 2006).

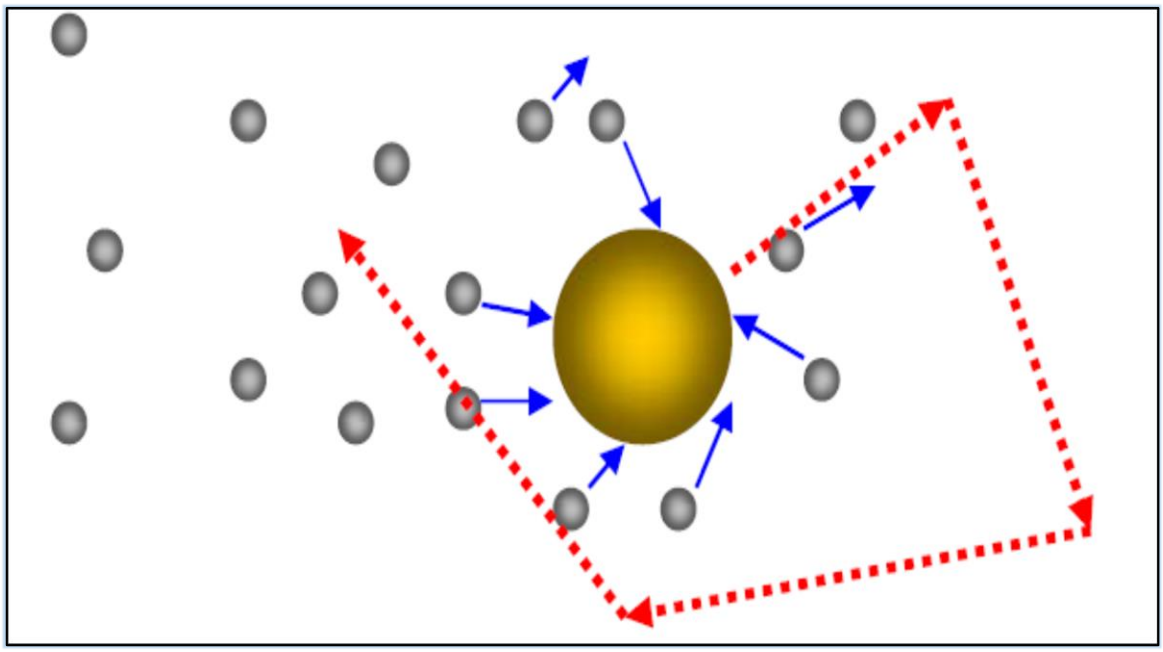

Figure 2.6: Schematics of a Brownian motion process (Abouali and Ahmandi, 2007).

2.4.2 Wet deposition

Wet deposition occurs when particles are removed from the atmosphere through dissolution of particles in atmospheric hydrometers such as clouds, fog, rain or snow, and is subsequently delivered to the Earth's surface (Finlayson-Pitts and Pitts, 1999). The scavenging of materials by atmospheric hydrometers sometimes results in compounds undergoing chemical

transformation. The removal of aerosols through wet deposition involve a number of physical phases and are influenced by a variety of physical scales as shown in Figure 2.7.

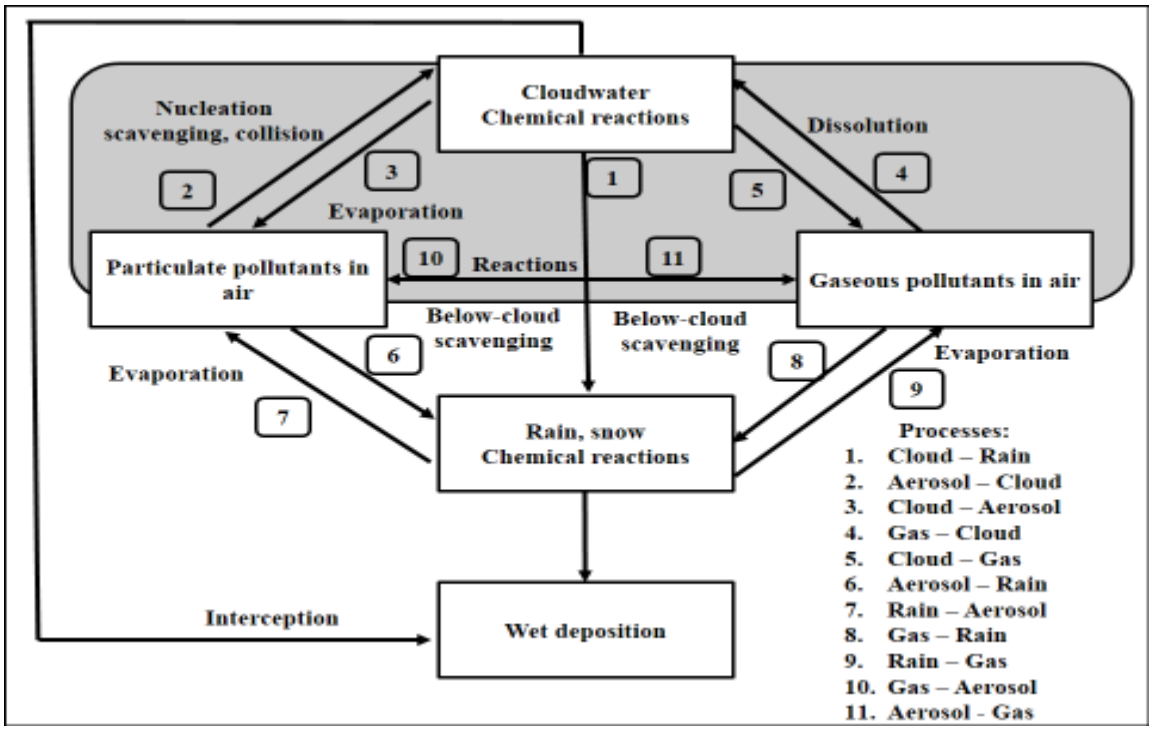

Figure 2.7: Conceptual framework of wet deposition process (Seinfeld and Pandis, 2006).

Wet deposition can be divided into two types of scavenging, namely in-cloud and below-cloud scavenging. Below-cloud scavenging is described as the collection efficiency between the hydrometeor and the aerosol particle, where collection efficiency is the product of a collision efficiency times a coagulation efficiency (Seinfeld and Pandis, 2006). In-cloud scavenging occurs either due to impaction of an aerosol particle with a cloud droplet or an ice crystal (Seinfeld and Pandis, 2006).

2.4.3 Dry deposition

Dry deposition is a process that occurs when gaseous particles are removed from the atmosphere onto the Earth's surface through adsorption and/ or absorption (Seinfeld and Pandis, 1998; Finlayson-Pitts and Pitts, 1999). Dry deposition is governed by atmospheric turbulence, the nature of the surface and the chemical properties of the species. Deposition velocity (*Vg*) is the proportionality constant that characterize dry deposition and is defined as

the flux (F) of the species (S) to the surface divided by the concentration [S] at a given reference height h:

$$Vg = F/([S]) \quad 2.17,$$

The deposition velocity can also be calculated in terms of the resistance (r) as shown in the formula:

$$Vg = 1/r \quad 2.18,$$

where the resistance can be broken further into surface resistance (rsurf) which depends on surface affinity to the species, and a gas phase resistance (rgas) which depends on the transportation of the gas to the surface by micrometeorology and the height above the Earth's surface:

$$r = rgas(h)) + rsurf \quad 2.19,$$

Where the deposition velocity can be given by:

$$Vg = \frac{1}{rgas(h)()} + \frac{1}{rsurf} \quad 2.20,$$

which is the deposition function of particles reciprocal of the gas and surface resistance.

2.5 Mining in the Bushveld Complex

Since the discovery of the platinum-bearing dunite pipes on the Eastern Limb of the Bushveld Complex, as described in this section, mining activities have been increasing at an alarming rate in the GTM (study area). To date, there are 27 mining activities taking place in the GTM with 15 operational mines and 12 which are in the prospecting stage. The mining of these ores in the eastern limb of the Bushveld complex may lead to PM emissions containing metal contaminants. High winds and mining activities, such as grinding, milling and mine tailings management, create coarse particles (≥1 μm diameter) through mechanical action and contribute to particle emissions (Zdanowicz *et al*., 2006).

The Bushveld Complex in South Africa (Figure 2.8) contains the world's largest layered mafic-ultramafic intrusion extending over an area of about 65 000 km^2 in the sub-surface outcrop.

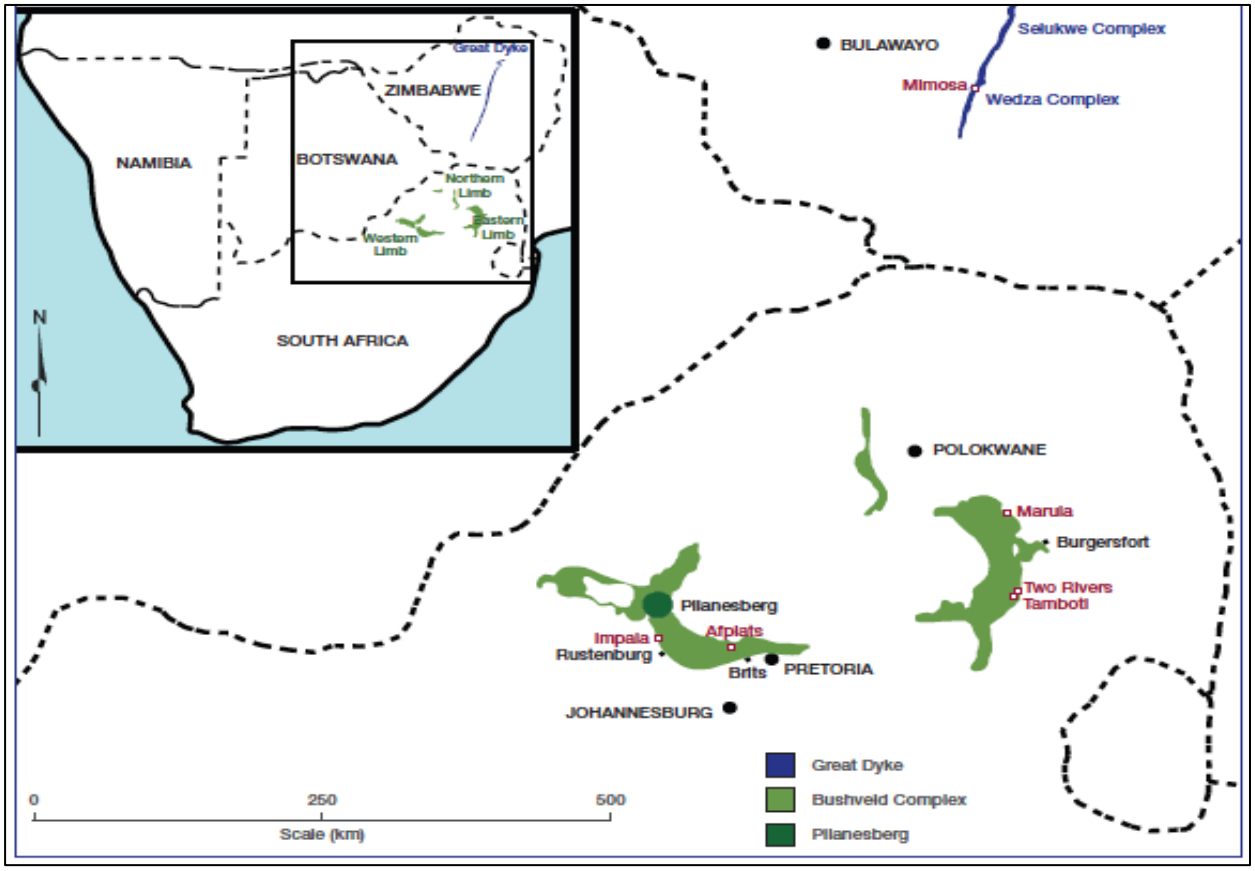

Figure 2.8: Map of the Bushveld Complex showing chrome, platinum, vanadium, tin and fluorspar mining sites (Viljoen and Schürmann, 1998; Cawthorn *et al*., 2006).

The Western Bushveld Complex comprises a great variety of rock strata ranging from dunite, pyroxenite, anorthosite and oxide layers in the ultramafic to mafic suite, and granophyres and granites of the felsic suites mainly found on the Eastern Bushveld Complex (Eales and Cawthorn, 1996; Cawthorn *et al.*, 2006). The complex is home to several important ore deposits such as chromium, the platinum-group elements (PGE), vanadium, iron, titanium, tin, fluorspar and andalusite (Wilson and Anhaeusser, 1998; Cawthorn *et al*., 2006). Dr. Hans Merensky discovered the platinum-rich pipes and the Merensky Reef in 1924 (Cawthorn, 1999; Scoon and Mitchell, 2004). According to Schouwstra *et al.* (2000), the Merensky Reef extends to about 300 km around the entire outcrop of the eastern and western limbs of the Bushveld Complex, and a depth of about 5 km. The reef varies in thickness, mineral composition as well

as position of the mineralization. The rock-forming minerals of the Merensky Reef comprise approximately equal amounts of dark iron-magnesium silicate minerals and lighter calcium-aluminium-sodium silicate minerals under and overlain by thin (5 to 15 mm) often discontinuous layers of chrorite concentrations. This zone, commonly known as the Merensky pegmatoid, contains the base metal sulphide grains and associated platinum group minerals.

Wagner (1929) discovered that the PGEs mineralization in the Merensky and the Upper Group Two (UG2) chromitite reefs is restricted to a very narrow vertical interval of rocks. The UG2 Reef consists primarily of chromite (60 -90% by volume), orthopyroxene (5-25%) and 5-15% of plagioclase (McLaren and De Villiers, 1982). Hence, in the UG2 chromitite there is essentially no PGE above or below the chromitite layer that rarely exceeds 1 m thick (Cawthorn, 2010). The most commonly found platinum group sulphide minerals found in the UG2 chromitites are laurite, cooperite, malanite and braggite (Penberthy *et al*., 2000). The secondary minerals forming part of the UG2 reef are listed in Table 2.2.

Table 2.2: Secondary mineral composition of the UG2 reef (modified from McDowell, 2011).

Minerals	**Composition**
Clinopyroxene	Ca, Mg, Fe, Na, Li silicates
Base metal sulphides and other sulphides	Chalcopyrite ($CuFeS_2$), Pyrrhotite (FeS), Pyrite (FeS_2), Pentlandite ((FeNi)S)
Oxides	Ilmenite ($FeTiO_3$), Magnetite (Fe_3O_4), Rutile (TiO_2)
Micas	K, Li substitution in $K_2O.Al_2O_3.6SiO_2.2H_2O$
Secondary quartz	SiO_2
Chlorite	(MgFe)5Al(SiAl)O10(OH)8
Serpentine	$Mg_3Si_2O_5(OH)4$
Laurite	Ru,S_2
Cooperite	PtS
Malanite	$(Pt,Rh,Ir)2CuS_4$
Braggite	(Pt,Pd)S

Kinloch and Peyerl (1990) have observed that “normal” reef is characterized by the Pt–Pd sulphides braggite and cooperite, with laurite (RuS2) commonly associated with chromitite layers, whereas in “pothole” reef, the predominant PGM are Pt–Fe alloys at the centre and Pt–Pd tellurides at the edge of potholes. The chromite-bearing rocks of the reef contain similar amounts of Ni, Cu, S, Au and Pd as the silicate rocks, but they contain 5 to 10 times more Os, Ir, Ru, Rh and Pt than the silicate rocks (Barnes and Maier, 2002).

2.6 Chromite smelting

Smelting operations in the GTM started in 1975 with the commissioning of the Tubatse Ferrochrome smelter owned by Samancor Chrome (Visser, 2006). This was followed (in 2003) by the commissioning of the Dilokong Smelter owned by ASA East Asia Metals Investment Co. Ltd. The third smelter (Lion Smelter) which was commissioned in 2014 is co-owned by Xstrata and Merafe Resources. According to Mining Watch Canada (2012), chromite ore is mined, crushed and processed to produce chromite concentrate (dry milling or grinding of chromite ore is now known to convert Cr(III) to Cr(VI) and efforts are required to avoid producing and spreading hexavalent chromium during mining activity). The chromite concentrate is then combined with a reductant (i.e. coke, coal, charcoal or quartzite) in a high temperature submerged arc furnace or direct current arc furnace to produce ferrochrome.

During ferrochrome production process, air pollutants such as nitrogen oxides, carbon oxides and sulphur oxides (NOx, COx, SOx) and particulate dusts that contain heavy metals such as chromium (Cr), zinc (Zn), lead (Pd), nickel (Ni) and cadmium (Cd) are emitted into the atmosphere. The high temperature smelting of chromite ore results in the conversion of Cr(III) to toxic Cr(VI) which contaminates the emitted dust.

Ferrochrome smelter operations are a potential source of aerosols containing toxic metals such as Cr-IV, lead, and cadmium which can have adverse health effects. Depending on atmospheric conditions, these metal-containing aerosols can find their way into river streams, human bodies and vegetation.

2.7 Heavy metals and their health effects

Metals occur naturally in the environment in varying concentrations and are mainly found in rocks, soil, animals, plants and water (Bielicka *et al.*, 2005). Metals occur in different forms such as ions in water, as vapours, salts, or mineral rock, sand and soil. Once emitted, metals can reside in the atmosphere for a lifetime (Bielicka *et al.*, 2005). Heavy metals are metallic elements with a relatively high density and tend to be toxic or poisonous at low concentrations (Lentech Water Treatment and Air Purification, 2004).

The heavy metals commonly found in the atmosphere are lead (Pb), cadmium (Cd), nickel (Ni), cobalt (Co), iron (Fe), zinc (Zn), chromium (Cr), arsenic (As), silver (Ag), mercury (Hg), and PGEs (GWRTAC, 1997; Nagajyoti *et al.*, 2010). Table 2.3 shows the important sources of heavy metals in geological material or rock.

Table 2.3: Heavy metal concentrations (ppm) in ingenious and sedimentary rocks (Cannon *et al*, 1978).

Metals	**Basaltic igneous**	**Granite igneous**	**Shales and clays**	**Black shales**	**Sandstone**
As	0.2 - 10	0.2 - 13.8	–	–	0.6-9.7
Cd	0.006 - 0.6	0.003 - 0.18	0.0-11	<0.3 - 8.4	–
Cr	40 - 600	2 - 90	30 - 590	26 - 1,000	–
Co	24 - 90	1 - 15	5 - 25	7 - 100	–
Cu	30 - 160	4 - 30	18 - 120	20 - 200	–
Pb	2 - 18	6 - 30	16 - 50	7 - 150	<1 - 31
Mo	0.9 - 7	1 - 6	–	1 - 300	–
Ni	45 - 410	2 - 20	20 - 250	10 - 500	–
Zn	48 - 280	5 - 140	18 - 180	34 - 1,500	2 - 41

These metals are emitted into the atmosphere as a result of human activities such as industrial operations, agriculture, motor transport and natural activities such as volcanic activities, soil erosion, forest fires, evaporation (Salomons and Forstner, 1984). Most metals in the atmosphere are in the form of particulates with the exception of mercury (Kvietkus *et al*., 2011). Most of these metals are soluble in water which makes it easy for them to enter the ecosystem

(Schwela, 2000). Some of the heavy metals such as Fe, Mn, Cu and Zn are essential elements for both plants and animals (Wintz *et al*., 2002), and their biochemical and physiochemical functions in plants and animals are in the form of redox reactions and in building blocks for enzymes (Nagajyoti *et al*., 2010). However, excess uptake of these metals results in toxic effects (Monni *et al*., 2000; Reeves and Baker 2000). These metals are removed from the atmosphere through dry and wet deposition processes (Shrivastav, 2001).

2.7.1 Arsenic

The source of arsenic is sulphide ores such as arsenopyrides FeAsS, realgar As_4S_4, and orpiment As_2S_3, and it also occurs in traces in other ores. Arsenic has a distinctive colour and mainly occurs as the As_2O_3 mineral produced as a by-product of non-ferrous metal processing of ores containing Cu, Pb, Zn, Ag and Au. It can also be found in ashes from coal combustion (Lee *et al.*, 1991; Wuana and Okieimen, 2011). Arsenic metal is mainly used to alloy with lead, as rat poison, in medicine to kill parasites and to prevent wood rot (Lee *et al*., 1991). The toxic As(III) oxides are absorbed through the lungs and intestines (Manahan, 2004) and it is associated with cancer and circulatory disorders (Hayes, 1997).

2.7.2 Cadmium

Cadmium is mainly found in the Earth's crust and is produced as a by-product in the extraction of Zn, Pd and Cu. It is mostly used in nickel-cadmium batteries, as pigment in paints, in coating and plating to prevent corrosion, as stabilizers for plastics and as an alloy (Lee *et al*., 1991; Hayes, 1997; Manahan, 2004). The major exposure to humans occurs through uptake into food, plants and tobacco. Cadmium has low excretion rates which causes it to accumulate in human bodies, in particular in the kidneys and liver. Cadmium causes renal damage, bone disease and when inhaled as dust or fumes it can lead to oedema and epithelium necrosis (Hayes, 1997; Manahan, 2004; Wuana and Okieimen, 2011).

2.7.3 Chromium

Chromium is the 24^{th} element on the periodic table of elements and is found in mineral ores such as chromite $FeCr_2O_4$ which is iron-black to brownish-black in colour. Chromite is formed

from cooling mafic magma or ultramafic magma (Lee *et al*., 1991; Wuana and Okieimen, 2011). Chromium is mainly used to produce ferrochrome alloy (containing Fe, Cr). This element has a high melting point and hence it is used to manufacture refractory bricks, in furnace linings and foundry sand (Tkachenko *et al*., 1995). Trace amounts of Cr are necessary in the diet of mammals. Cr(III) and insulin helps to maintain glucose levels in the blood. Both Cr(III) and Cr(VI) are mainly used for chrome plating, the manufacture of dyes and pigments, leather tanning and wood preserving (Lee *et al*., 1991; Hayes 1997). Cr(VI) can readily pass cell membranes and has been linked to various cancer (Hayes, 1997).

2.7.4 Cobalt

Cobalt (Co) is generally abundant and most stable in the oxidation states Co(II) and Co(III). Co has low abundance in the Earth's crust and occurs in ores such as cobaltide (CoAsS), smaltide (CoAs2), and linnaeite (Co3S4). Co ores exist with other ores such as Ni ores, Cu ores and Pb ores and hence Co is obtained as a by-product from the extraction of other metals. Co is used as pigment for the ceramic, glass and paint industries, and it forms high temperature alloys with steel, hard alloys such as stellite, and magnetic alloys such as alnico (containing Al, Ni, and Co). Co salts in fatty acids and naphthenic acids are used as drying agents in the paint industry (Lee *et al*., 1991). Industrial processing of Co ores such as mining and smelting, burning of fossil fuels and uses of cobalt containing phosphate fertilizers are the major anthropogenic sources of environmental cobalt (Linna *et al*., 2004). High exposure to cobalt causes haem oxidation (Yamatani *et al*., 1998; Bargagli, 2000).

2.7.5 Copper

Copper (Cu) is a transition metal and it is found in the Earth's crust as copper nuggets. The most common copper ores are chalcocite Cu_2S, basic copper carbonate CuCO3•Cu(OH)2, cuprous oxide Cu2O, bornite Cu5FeS4. Cu is the most abundant transition metal after Fe and Zn. Cu is an essential micronutrient required (4-5mg) in the growth of both plants and animals, and the deficiency of Cu in animals results in the inability to use Fe stored in the liver. However, excessive amounts of Cu in the body can lead to anaemia, liver and kidney damage, and irritation of the stomach and intestines (Lee, 1991; Wuana and Okieimen, 2011). Anthropogenic activities such as smelting, fossil fuel combustion, processing of crustal

material and waste burning are the major sources of copper in the atmosphere (Egodawatta *et al*. 2013; Lee, 1991).

2.7.6 Lead

Lead (Pb) is a transition metal and its main ore is galena PbS, which is black, shiny and very dense, and contains a number of metallic impurities such as copper (Cu), gold (Au), silver (Ag), tin (Sn), arsenic (As), antimony (Sb), bismuth (Bi) and zinc (Zn), and it ranges from 10 to 30 mg kg-1 in the Earth's crust (Lee, 1991; USDHHS, 2019). The majority of industrially-produced lead is used in the manufacture of lead/acid storage batteries. Lead is also used in solders, bearings, cable covers, ammunition, pigments, and as an additive (tetraethyl plumbane, PbEt4) to petrol (Lee, 1991; Manahan, 2004). Humans are typically exposed to lead through inhalation and ingestion. The use of lead-containing products has declined because of knowledge about lead toxicity (Lee, 1991). Accumulation of lead in body organs such as the brain, kidneys, the gastrointestinal tract and the central nervous system can lead to loss of memory, nausea, insomnia, anorexia, and weakness of joints or even death (Blaxter, 1950).

2.7.7 Molybdenum

Molybdenum (Mo) is a transition metal that does not occur naturally as a free metal on Earth, but rather in various oxidation states in minerals. It occurs as the mineral molybdenite MoS2, other minor commercial ores of molybdenum are powellite (Ca(MoW)O4) and wulfenite (PbMoO4). Mo is a silvery metal with a grey cast and has the melting point of 2,623 °C. It readily forms hard, stable carbides in alloys such as ferromolybdenum which can then be added to steel (Lee, 1991). It is also used for pollution controls in power plants. At 350 °C (662 °F) the element acts as a catalyst for NO_2/NOx to form only NO molecules for consistent readings by infrared light (Lal and Patil, 2001). Mo is an essential element occurring as a component of a pterin coenzyme essential for the activity of xanthine oxidase, sulphite oxidase, and aldehyde oxidase (Abumrad, 1984). Mo deficiency in infants may result in high levels of sulphite and urate, and neurological damage due to the inability of the body to use Mo in enzymes (Reiss, 2000). However, high levels of Mo in the body can interfere with the uptake of copper, leading to copper deficiency in the body and thus preventing plasma proteins from binding with copper.

The symptoms of high levels of Mo include diarrhoea, stunted growth, anaemia and achromotrichia (loss of pigment in hair) (Suttle, 1974).

2.7.8 Nickel

Nickel (Ni) is a silvery-white lustrous transition metal with a slight golden tinge and is the 22nd most abundant element by weight in the Earth's crust. The most important Ni ore is pentlandite (Fe,Ni)9S_8 with the ratio of 1:1 of Fe:Ni, while some commercially-available ores include sulphides mixed with Fe and Cu, and alluvial deposits of silicates and oxides or hydroxides such as garnierite (Mg,Ni)6Si_4O_{10}(OH)8 and nickeliferous limonite (Fe,Ni)O(OH)(H_2O)n.

Ni is mostly produced to make ferrous and non-ferrous alloys to increase the strength of steel and to alleviate chemical attack (Lee, 1991). Ni is the central metal in urease enzyme which acts as a catalyst in the hydrolysis of urea in plants (Sigel *et al*., 2008; Sydor *et al*., 2014). However, in humans the urease enzyme serves as a virulence factor and is responsible for pathogenesis (Sujoy and Aparna, 2013). This metal is released into the environment through mining or smelting, refining, waste-water production, fossil fuel combustion, and exposure to humans can occur through inhalation, ingestion and dermal contact (ATSDR, 2005). Chronic exposure of Ni to the skin can result in dermatitis (Butticè, 2015) while inhalation of Ni has been linked to respiratory illnesses (ATSDR, 2005). However, ingested Ni is excreted from the body through faeces, sweat and urine (Das *et al*., 2008).

2.7.9 Mercury

Mercury (Hg) exists as a red-coloured ore cinnabar HgS with a density of 8.1 g.cm^{-3}, melting point of 13.5 °C and boiling point of 357 °C (Lee, 1991; Smith *et al*., 1995). The major source of mercury into the atmosphere is mining, coal combustion, smelting of metal ores and oil refining (Smith *et al*, 1995; UNEP, 2013). It is mainly released into the atmosphere as elemental mercury (Hg^0), reactive gaseous mercury (Hg^{+2}), mercurous (Hg_2^{+2}) and particulate mercury [Hg(p)] (Smith *et al*, 1995; Cohen *et al*. 2004). Mercury in its insoluble state (Hg^0) has been estimated to have a lifetime of about one year and can be transported over long distances through global circulation systems (Euro Chlor, 2009). (Hg^{+2}) and [Hg(p)] have shorter atmospheric lifetimes and deposit more locally and regionally (Cohen *et al*. 2004).

Human exposure to mercury is through inhalation, ingestion and dermal contact. Once in the body, mercury can enter the blood stream and damage the brain and kidneys (ATSDR, 1999).

2.7.10 Platinum group metals

Platinum group metals (PGMs) such as platinum (Pt), palladium (Pd), rhodium (Rh), ruthenium (Ru), osmium (Os) and iridium (Ir) occur naturally in the Earth's crust as mafic-ultramafic ores and they have similar chemical and physical properties (Lee, 1991). Table 2.4 shows chemical properties of PGMs.

Table 2.4: Chemical properties of platinum group elements (British Geological Survey, 2009).

	Pt	**Pd**	**Rh**	**Ir**	**Ru**	**Os**	**Au**
Atomic weight	195.08	106.42	102.91	192.22	101.07	190.23	196.97
Atomic number	78	46	45	77	44	76	79
Density (gcm^{-3})	21.45	12.02	12.41	22.65	12.45	22.61	19.3
Melting point (°C)	1769	1554	1960	2443	2310	3060	1034
Electrical resistivity (micro-ohm cm at 0 °C)	9.85	9.93	4.33	4.71	6.8	8.12	2.15
Hardness (Mohs)	4-4.5	4.75	5.5	6.5	6.5	7	2.5-3

PGMs are released into the environment by human activities such as mining and smelting, medical institutions and motor vehicles (Sures *et al*., 2005; Rauch and Morrison, 2008). Human exposure to PGMs is through inhalation, dietary intake and dermal contact. There are no known health effects associated with the presence of PGMs in the environment due to the low levels found in the environment (Rauch and Morrison, 2008).

2.8 PM monitoring

The purpose of ambient monitoring is to collect data that will scientifically inform policy and strategy development for environmental management. An air quality monitoring plan must be developed to outline the monitoring objectives which in turn will determine the type of

parameters to be monitored, whether it should be continuous monitoring or passive sampling and the location of monitoring stations. The measurement of concentrations of PM in ambient air is not straight-forward. There are a variety of techniques available for measuring mass concentrations, but due to the complex nature of PM, the method that is selected can significantly influence the results. Meteorology plays an important role in air quality monitoring and must be collected simultaneously with ambient air pollution data.

2.8.1 PM continuous monitoring

There are several commercially-available technologies for automated, continuous monitoring of PM mass. These include opacity monitors, light-scattering technologies, beta gauges, acoustic-energy monitoring, tapered-element oscillating microbalance (TEOM), and turboelectric technology. These continuous monitors are automated to provide real-time data (Baron and Willeke, 2001).

2.8.2 Passive sampling

Originally, passive samplers were developed for personal exposure assessment, however, in recent years they have been increasingly used to monitor a broad range of pollutants due to their low cost and user friendliness (White 2014). The passive samplers have been tested as an alternate method to conventional air sampling methods, such as the University of North Carolina (UNC) passive samplers (used in this study) for monitoring PM. Passive samplers are ideal for assessing personal and environmental exposures over time frames generally ranging from one day to two weeks. Exposure times as short as 8-hours and as long as one month are achievable under requisite concentration conditions (U.S EPA, 2004). The passive sampling methods offer advantages in affordability and portability that allow more sites to be monitored. Weaknesses include the need for sampling over longer periods of time precluding gathering information on a short-term basis, e.g., hourly or daily peaks (MASSPORT, 2007).

Wagner and Leith (2001a; 2001b) introduced the University of North Carolina (UNC) passive samplers (Figure 2.9) as the cheapest way of measuring PM concentration. The passive sampler was designed to be small and lightweight and sturdy for easy deployment anywhere, and they

are convenient for microscopy analysis, and are resistant to sample contamination or resuspension (Wagner and Leith, 2001a).

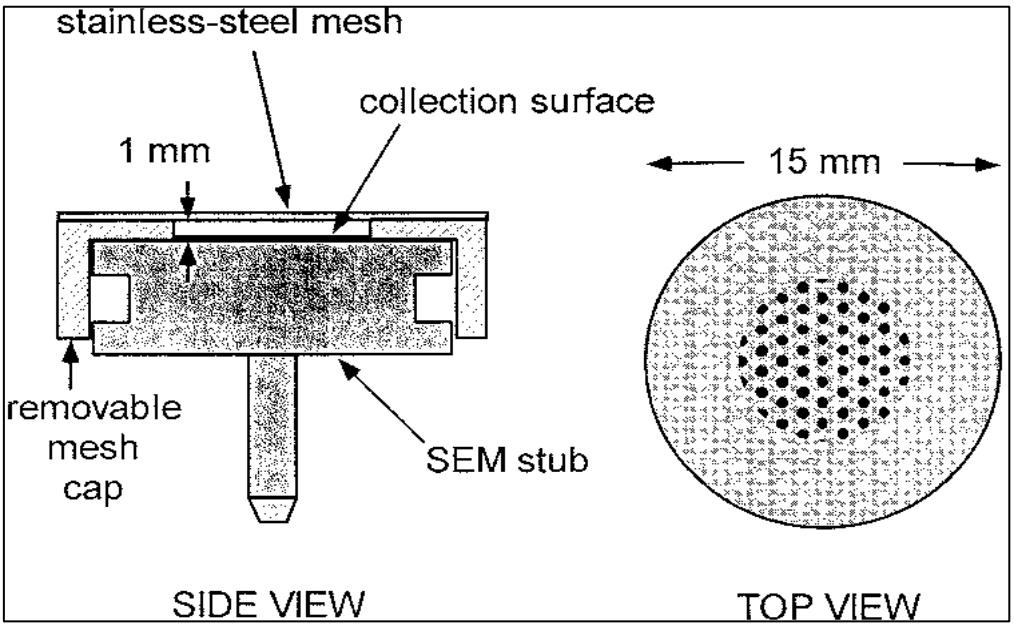

Figure 2.9: UNC passive sampler (Wagner and Leith, 2001a).

The sampler body is composed either of aluminium or a carbon Scanning Electron Microscopy (SEM) sample mount. Aluminium-based samplers are preferable for size distribution analyses because their high conductivity allows for good resolution. Carbon-based samplers are preferable when elemental analysis is important to minimise interference with the elemental spectra. The stainless-steel mesh cap prevents deposition of large particles such as sand, hair or other debris from collecting onto the sampler surface. The diameter of the mesh hole ranges from 160 µm to 225 µm from top to bottom. However, there are many commercially available mesh sizes that can be used depending on the sampling application (Wagner and Leith, 2001a).

The samplers collect particles onto the collection surface as shown in Figure 2.10. The particles settle out of the atmosphere through gravitational, diffusion and turbulent inertial forces onto the collection surface. The flux of particles deposited onto the collection surface during a given time is used to estimate the average mass concentration of airborne particles (Wagner and Leith, 2001b). Ott and Peters (2008) developed flat plate shelter (Figure 2.11) to protect the passive sampler designed by Wagner and Leith from precipitation and to minimize wind-induced turbulence and deposition velocity

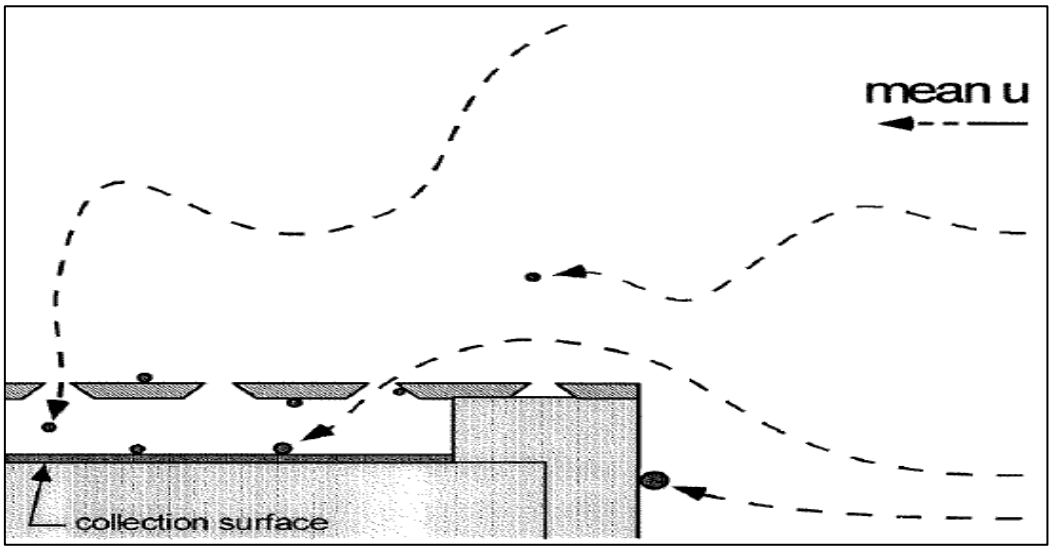

Figure 2.10: Schematic deposition into passive sampler with horizontal mean wind velocity (Wagner and Leith, 2001b).

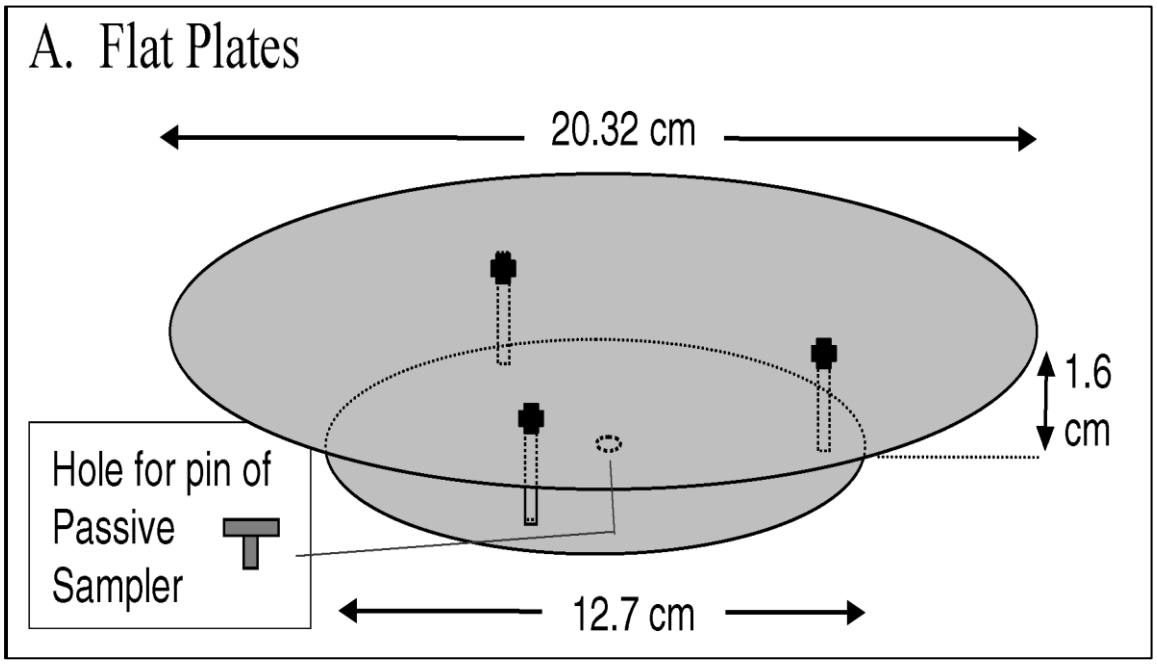

Figure 2.11: Shelter plates for passive sampler (Ott and Peters, 2008).

Wagner and Leith (2001a) gave a detailed description of the deposition velocity model to estimate airborne mass concentration from microscopic images of particles collected on a passive sampler. The contribution of a single particle *i* to mass concentration, *C*, is calculated as:

$$Ci = \frac{Fi}{Vdep,,\mathrm{i}} = \left(\frac{mi}{AT\ t}\right)\frac{1}{Vdep,i}, \quad 2.21,$$

where F is the mass flux of the particle to the deposition surface, V_{dep} is the deposition velocity of the particle, mi is the mass of the particle, A_T is the total area of the sample that was analyzed and t is the sample time. Deposition velocity, V_{dep}, is calculated as:

$$Vdep, i\ =\ Vambient\ \gamma mesh \quad 2.22,$$

where $V_{ambient}$ is the theoretical deposition velocity and γ_{mesh} is the mesh factor. The mesh factor accounts for the fact that the sampler's mesh cover reduces the deposition of particles to the substrate. The mesh factor is calculated as follows:

$$\gamma\mathrm{mesh} = 0.00595\left(\frac{da\ \tau g}{\upsilon}\right)^{-0.439} \quad 2.23,$$

where d_a is the particle's aerodynamic diameter, τ is its relaxation time, g is the gravitational constant, and ν is the kinematic viscosity of air.

Ott and Peters (2008) in their study accounted for turbulent inertial deposition and frictional velocity, u^*, that occurs when Wagner and Leith passive samplers are used without the shelter plate, where $V_{ambient}$ is then calculated as follows:

$$V_{ambient} = \frac{-Vt}{\left((1-0.67\tau^{0.49}\mathrm{u}^{*-0.02}\upsilon^{-0.49}\mathrm{Vt})\mathrm{e}^{-\mathrm{VtI}}\right)-1} \quad 2.24,$$

where,

$$\mathrm{I} = \frac{1}{\frac{3\sqrt{3}}{29\tau}(\upsilon/\mathrm{D})^{-2/3}+6.2\times10^{-4}(\tau\mathrm{u}^{*2}/\mathrm{v})2} \times \frac{1}{\mathrm{u}^*} \quad 2.25,$$

where $Vt\ =\ \tau g$ and D is the particle diffusion. The frictional velocity is estimated using the following equation:

$$u^* = k\frac{u}{ln(\frac{z}{z0})} \quad 2.26,$$

where k is von Karman's constant, u is the wind speed, z is the height above ground level at which wind is measured and z_0 is the surface roughness. When Ott and Peters (2008) shelter plates are used, the particle settling velocity, $V_{ambient}$, without turbulent inertial deposition is calculated as:

$$Vambient = \tau g \quad 2.27,$$

2.9 Computer Controlled Scanning Electron Microscopy

Microscopes have long been used in identifying the chemical and morphological characteristics of features too small to be identified with the naked eye. The microscope can analyze individual features to provide a resolution of sample constituents and their associations unobtainable by most gross or bulk analysis methods. The increased resolution, both light- (optical) and electron microscopy have often been employed in PM analysis. The manual microscopic analysis is tedious and laborious. The results obtained from manual microscopic analysis have usually been only qualitative because of the relatively small number of particles being characterized. A quantitative analysis requires reproducible sizing and identification of enough individual particles to satisfy statistical counting requirements. Hence, a computer-controlled scanning electron microscopy (CCSEM) is used to provide quantitative results within a reasonable analysis time. CCSEM permits comparison of microscopic results with those from bulk analysis while retaining the feature-specific resolution of manual microscopy (Casuccio *et al*., 1983).

CCSEM combines three analytical tools under computer control: 1) the scanning electron microscope, 2) the energy dispersive spectrometry X-ray analyzer, and 3) the digital scan generator for image processing. In the SEM, a finely focused electron beam impinges upon the sample surface. The interaction of the electron beam with the sample produces various effects that can be monitored with suitable detectors such as energy dispersive spectrometry (EDS) and wavelength-dispersive spectrometry (WDS). Some of these effects include the production of secondary, backscattered and Auger electrons; emission of characteristic X-rays; photo and cathodoluminescence; and electron channeling. Secondary and/or backscattered electrons are

used to create a viewing image, and the X-ray emission is monitored to determine the elementary chemistry and properties of an object (Casuccio *et al*., 1983). The SEM has been used in receptor modelling because of its ability to characterize the attributes of individual particles and thereby defining their sources (Husar and Wilson, 1989).

For PM analysis, the automated image analysis uses the backscattered electron mode, which is sensitive to differences in atomic number, to determine when the beam is on a particle. As the electron moves across the image, the image intensity at each point is compared with a threshold level. This comparison is used to determine whether the electron beam is "on" a particle (above threshold) or "off" a particle (below threshold). If the signal is below the threshold level, the computer selects a new coordinate and directs the beam to the new point. The distance between these "off points" is specified so that all particles larger than a selected size will be detected. When the coordinate is reached where the signal is above the threshold level, the computer switches to a subroutine that drives the beam across the particle in a preset pattern to determine the dimensions and shape of the detected feature. For each feature, the maximum, minimum, and average diameters are stored along with the centroid location. The centroid of each location is compared to those of previously detected particles to prevent double counting (Casuccio *et al*., 1983).

In the CCSEM, each particle is classified as a particle type based on its elementary chemistry. This is accomplished by characteristic X-rays which are fluoresced by the electron beam on the particle. The X-ray spectrum from each particle is processed to obtain relative concentrations for metal elements. Applying the chemistry and shape factor, each particle is then assigned to a defined particle type. If that particle's chemistry fits none of the predefined types, a new type will be created. In the absence of elemental peaks, or low peak to background ratios, the particle is then classified as carbon. The labels assigned to particle types are often descriptors of elemental composition and do not imply positive identification of a specific chemical compound (Casuccio *et al*., 1983). CCSEM can analyze many particles in a short period of time compared to manual microscopic methods (Lee *et al*., 1981). The use of computers to control SEM enables each particle to be tested against the same set of analysis parameters to assure uniformity of the analysis. CCSEM results are more precise and accurate than manual methods (Lee and Fisher, 1980).

2.10 Impacts of meteorology and topography on PM concentrations

Weather systems are distinguished by their characteristic scales (ranging from microscale to global-scale) and circulation patterns. The difference in weather patterns is caused by energy imbalances which produce temperature and therefore, pressure variations. Pressure gradients generate winds, which in turn are influenced by factors such as the Earth's rotation, frictional drag, temperature variations, moisture variations and mountain barriers. The wind systems occur at a variety of scales which are interdependent on each other (Tyson and Preston-Whyte, 2000). The physical and chemical properties of particulates are largely affected by meteorological conditions of the emission and deposition location. Meteorological parameters such as wind speed and direction, mixing height, relative humidity, temperature and rain can influence air pollutant concentrations (DeGaetano and Doherty, 2004).

During winter months in South Africa, the north-eastern parts are strongly dominated by anticyclonic systems throughout the troposphere in which airflows are associated with frequent subsidence within the atmosphere resulting in increased stability which in turn suppresses the vertical distribution of air (Tyson and Preston-Whyte, 2000). Stagnant wind conditions allow air pollutants to accumulate near the Earth's surface, resulting in elevated and localised concentrations of air pollutants (Chaloulakou *et al*., 2003).

During the months of May–October, Southern Hemisphere mid-latitude frontal systems influence the southern portions of the region. These frontal systems and the low cloudiness and fog associated with the Benguela Current are the only significant synoptic-scale weather phenomena which affect the region. Winds over most of the region are south-easterly throughout the year, with wind speeds varying from a low of 2.6-7.7 $m.s^{-1}$ in June to December to a high of 5-10 $m.s^{-1}$ in June to December (Potgieter, 2006). High wind speeds are generally associated with low levels of gaseous pollution due to dilution and dispersion of the pollutants. Conversely, fast near surface winds are linked with high levels of PM caused by resuspension of ground particles and long-range transport of particulates between regions (Wise and Comrie, 2005; Gietl and Klemm, 2009). The shape of the landscape plays an important role in trapping or dispersing pollutants. Air pollution concentrations in mountain valleys tend to be higher in colder months compared to warmer months (Ahrens, 2012).

2.10.1 Homogeneous and flat terrain

A homogeneous and flat terrain is one in which the vertical structure of the atmospheric boundary layer (ABL), and therefore the vertical profiles of meteorological variables, are mainly determined by the surface turbulent fluxes of momentum, heat and moisture, as described by the Monin-Obukhov similarity theory (Garratt, 1992; Kaimal and Finnigan, 1994). The wind flow in the homogeneous and flat terrain is influenced by synoptic circulations. Hence, pollution measured in this area can be transported over long distances before settling down (Stohl *et al*., 2002).

2.10.2 Complex and valley terrain

The interaction between the winds in the valley and winds above the valley influences the dispersion of pollutants released at the ground or from high stacks in the valley. The winds are dependent on the relation between valley circulations and synoptic circulation (Whiteman and Doran, 1993). Mechanisms responsible for valley winds, such as when the thermal forcing gives rise to the mountain/valley breeze system, have been described (Figure 2.12).

The forced channelling produces winds flowing along the valley axis and generates sudden reversal of the wind direction when geostrophic wind moves across a line normal to the valley axis. The downward turbulent transport of horizontal momentum produces wind directions within the valley that are similar to the geostrophic direction, with a slight turning near ground caused by friction. During pressure-driven channelling the winds inside the valley are driven by the component of geostrophic pressure gradients along the valley axis, and wind direction reversal occurs when the geostrophic wind shifts across the valley axis.

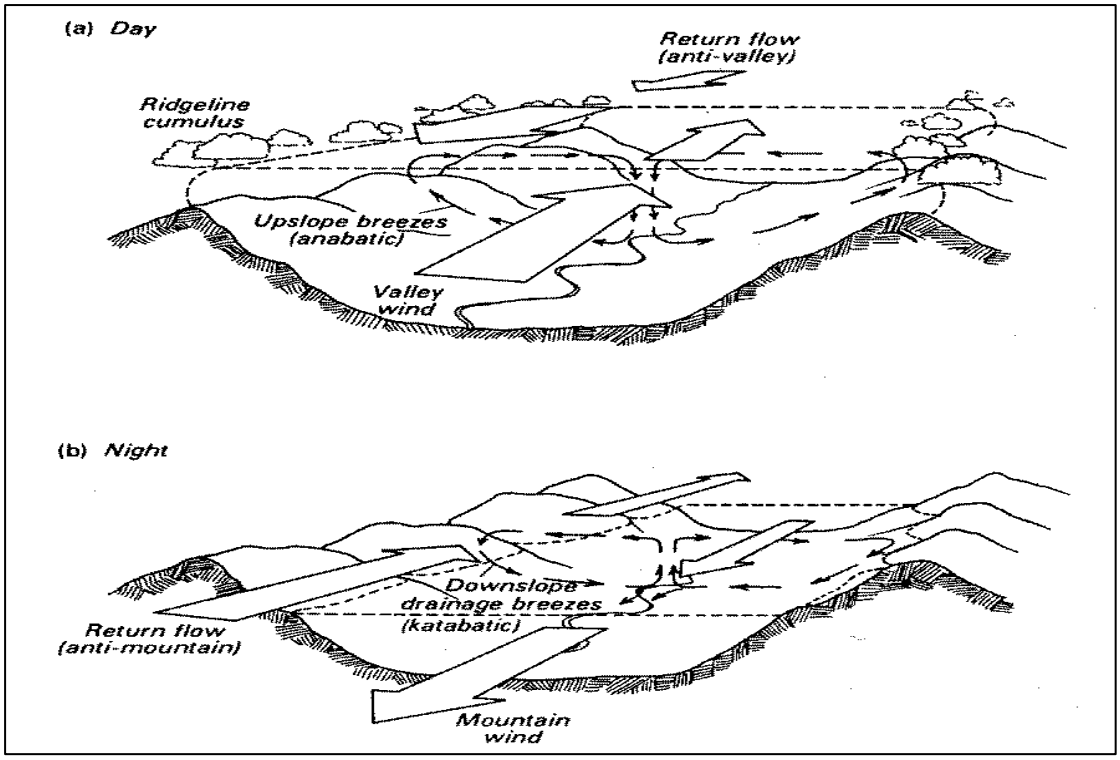

Figure 2.12: Mountain and valley wind system by day (a) and at night (b) (Oke, 1987).

The relative importance of the different flows depends on the size, depth and width of the valley. The first two mechanisms are more important in narrow and steep-sided valleys, while the last two are more relevant in large scale wide valleys of moderate depth. Therefore, there are few situations in which wind speed and direction inside the valley can be predicted from the overlying synoptic wind. Nonetheless for many practical applications the flow inside broad valleys characterized by a flat bottom is locally similar to flow over flat terrain, unless the site is located near a valley side-slope. The flow over small scale gentle valleys, where downward momentum transport is dominant, can be described by the linear theory. The air pollution associated with valley terrain will be discussed in the next paragraphs.

A complex terrain is a landscape with high mountains and steep inclinations. In that type of terrain, the wind flow is very hard to predict. However, the steep slopes give rise to thermally-induced circulations like mountain-valley breezes, generates mountain waves, and strongly modifies the characteristics of synoptic flow (Atkinson, 1981; Whiteman, 1990; Durran, 1990).

Zardi and Whiteman (2012) referred to mountain winds as slope winds or valley winds (shown by blue arrows in Figure 2.13). The slope winds are generated by buoyancy forces induced by

temperature differences between the air adjacent to the slope and the ambient air at the same height far from the slope. The slope winds blow up-slope during daytime and down-slope during night-time. To maintain continuity a closed circulation develops across the valley, involving air moving downward in the valley centre during the day and upward during the night.

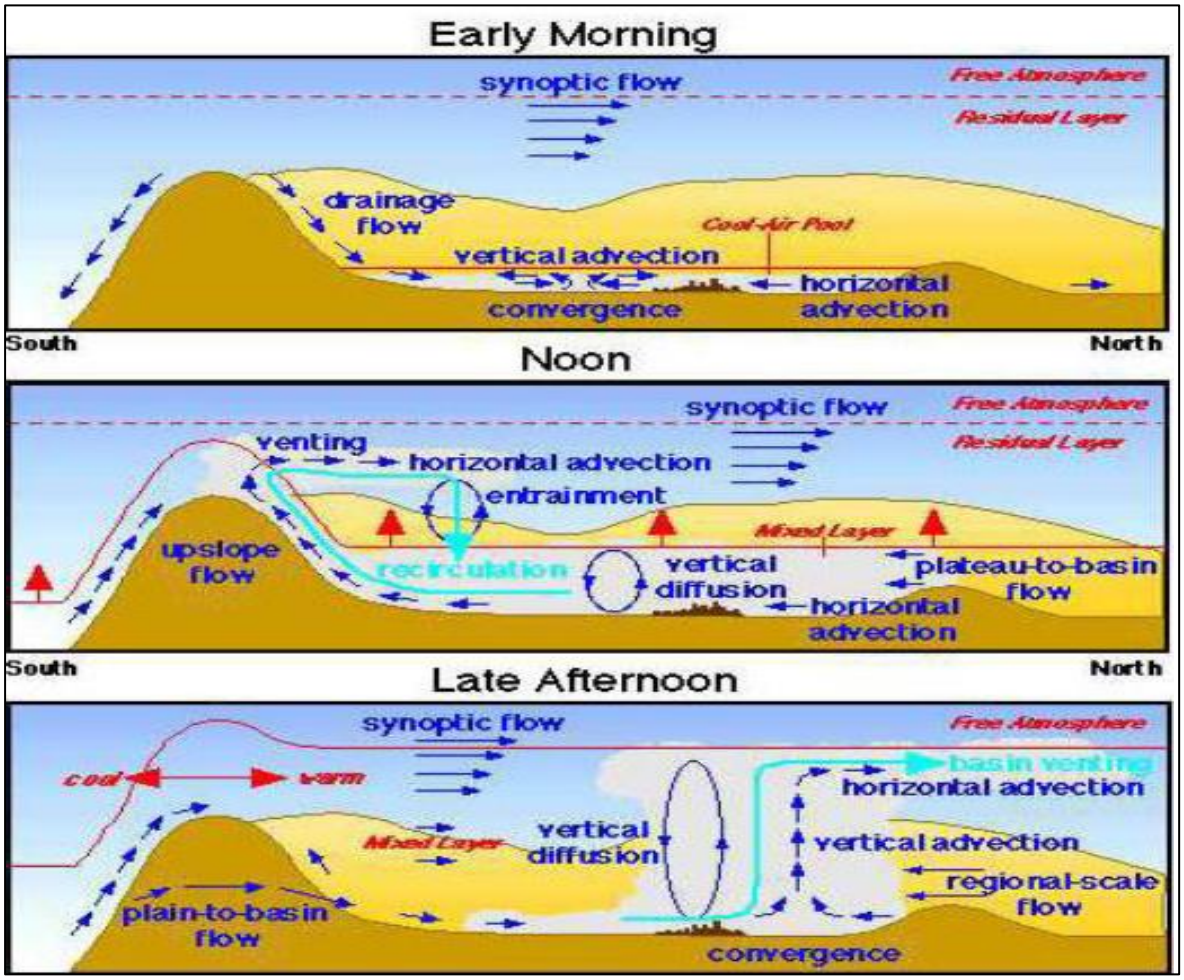

Figure 2.13: Mountain/valley winds (Edgerton *et al*., 1995).

The cross-valley circulation transports heat across the valley, heating (or cooling) the whole valley atmosphere, and therefore contributing to the development of valley winds. These winds are produced by horizontal pressure gradients that develop as a result of temperature differences between the air in the valley and the air at the same height over the adjacent plain. Valley winds blow parallel to the longitudinal axis of the valley, directed up-valley during daytime and down-valley during night-time (Figure 2.14). The circulation is closed above the mountain ridges by a return current flowing in the reverse direction. The actual development

of thermally-driven winds is often complicated by the presence of other wind systems developed on different scales. The mountain/valley breezes (Figure 2.14) have a significant impact on the dispersion of pollutants released inside the valleys.

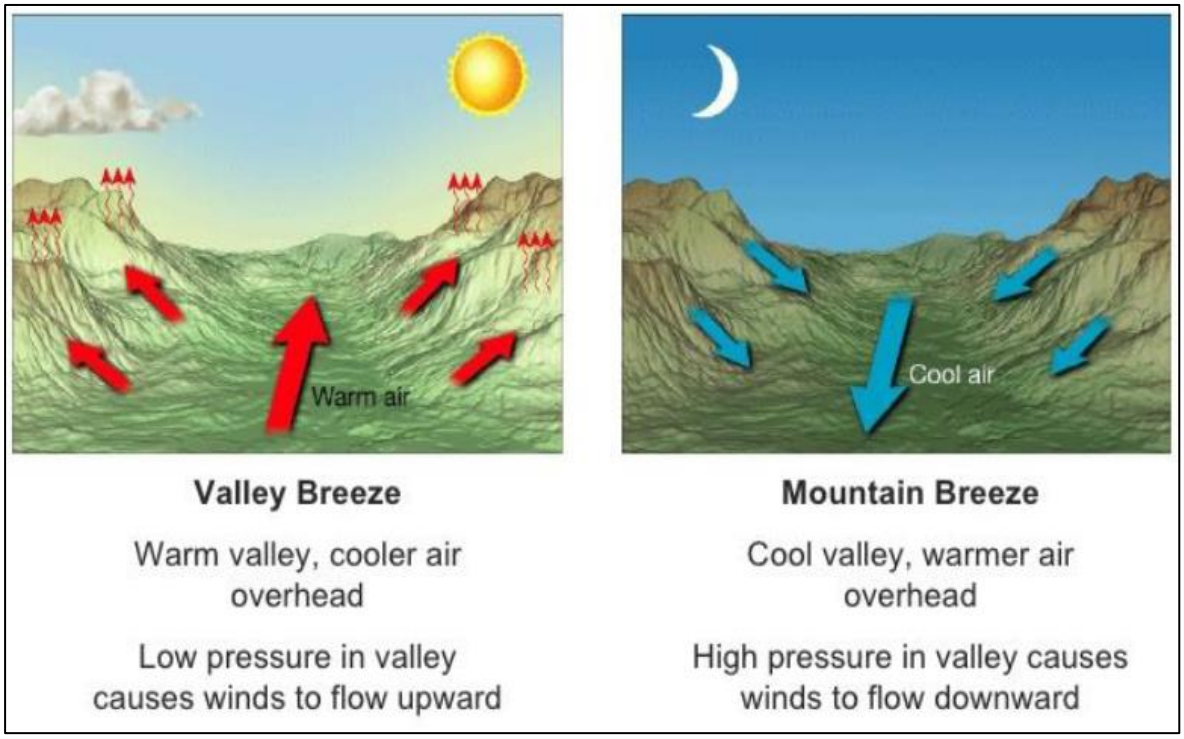

Figure 2.14: Mountain/valley winds blowing parallel to the longitudinal axis of the valley (Darrow, 2018).

Temperature inversions are most common in valleys where cool mountain air sweeps down into the valley at night, below the warm, polluted air. This inversion keeps the pollutants close to the ground instead of allowing it to disperse into the atmosphere. A flow of thermal or synoptic origin, channelled inside a valley, can transport plumes along the valley towards cities limiting the crosswind dispersion. Smoke stagnation in the bottom of the valleys can be favoured by the temperature inversion that develops inside the valley during the night and is destroyed by the growing convective boundary layer in the morning (Oke, 1987).

2.11 Literature review on international and local studies

Given the complex nature of PM which varies in size distribution, composition and morphology (Khlystov, 2001) there have been several studies indicating that PM contains

heavy metals as one of its constituents. There is a plethora of studies on source apportionment internationally with only a handful of studies undertaken in South Africa.

2.11.1 International and local chemical composition studies

Several studies on the composition of PM have been conducted around the world. Sharifi *et al*. (2008) did a study in Sheffield, United Kingdom, on the composition and physical/chemical properties of airborne PM in trying to make a connection between their impacts on the environment and human health. The samples in this study were collected using the tapered element oscillating microbalance technique (TEOM). The sample filters were then analysed for their morphology and elemental compositions using Scanning Electron Microscopy with Energy Dispersive X-Ray Spectrometer (SEM-EDS) and Laser Ablation Inductively Coupled Plasma Mass Spectrometry (LA-ICP-MS). The findings showed that most individual particles originated from high temperature sources and road transportation. Some metals and their elemental compositions detected in the samples were traced back to the common metallic elements widely used in the steel and metal industries.

A study on seasonal variation of heavy metals in ambient air was also conducted in Washington DC, USA (Melaku *et al*., 2008). Ambient air samples were isolated by drawing air through a quartz fibre filter which was placed in a home-built cyclone impactor. The samples were dissolved in acid before analysis with a Perkin-Elmer Model 800 Atomic Absorption Spectrometer (AAS) with an inverse longitudinal Zeeman-effect background correction system for the quantification of heavy metals. The results indicated that the heavy metal concentrations in ambient air followed the trend Cr~Pb > Cd > As. The peak values in the concentrations of the heavy metals were typically observed during the summer months, except for cadmium and chromium (in ambient air), regardless of the sample type. When the heavy metals data were compared to the meteorological variables temperature and precipitation, the results indicated a strong dependence on mean temperature and amount of precipitation. The spread in the heavy metal concentration over the observation period suggested a high seasonal variability for heavy metal content in ambient air.

Herrera *et al*. (2009) did a study in San Jose, Costa Rica, on composition of trace metals in PM in an effort to better the understanding of the origin of these trace metals. Samples were

collected with a Thermo Andersen high volume PM_{10} sampler on glass fibre and quartz filters and were analysed using an AAS with a graphite furnace attachment. It was found that Pb, V and Cu received a large contribution from the combustion of fossil fuels and metalworking industries located in the city of San Jose. Pb, Cr, Fe and Al concentrations were increased by the predominant winds that transport industrial and domestic emissions which pass through the city where the sampling stations were located.

Kothai *et al*. (2009) did a study on the characterization of atmospheric PM using the PIXE technique in the area of Vashi, Navi Mumbai, India. They found that high levels of zinc and sulphur were present in both particulate fractions. However, there was an enrichment of Cu, Cr and Mn in the fine fraction, suggesting their origin from anthropogenic sources. The analysis also identified other sources such as industrial, combustion and sea salt as contributing to elements' concentrations in the area.

In 2010, Razos and Christides published a study to determine the fine and coarse PM concentrations of heavy metals in the industrial area of Elefsis, Greece. The samples were collected using a stacked filter unit sampler and analysed by Anodic Stripping Voltammetry (ASV) and Inductively Coupled Plasma Atomic Emission Spectrometry (ICP-AES). The study found that although the levels of PM_{10} particulates were two times that of $PM_{2.5}$ particulates, the annual concentrations of elements (which are regulated by the European Union) namely lead (Pb), cadmium (Cd) and Nickel (Ni) were lower than the prospective assessment threshold. Furthermore, the Pb/Cd average ratio in coarse and fine airborne particulates suggested that Pb was mainly emitted by industrial sources as opposed to motor vehicles.

A study of the seasonal variation of metal composition of PM particles conducted in Warszawa, Poland (Majewski *et al*., 2011) collected and analysed sampled using AAS. The study found that although there were occasional occurrences of exceedances of PM_{10} levels in the area, the composition of PM_{10} particles confirmed that the target values of As, Cd and Ni were not exceeded as determined by the Poland Directive 2004/107/WE. However, analysis of data spanning five years in the area of Warszawa indicated that there was a risk of exceeding the limits set by the European Union.

Seasonal variation and sources of heavy metals and composition of particulates was assessed in Ulsan, Korea (Lee and Hieu, 2011). Samples were collected simultaneously using a high volume PM_{10} sampler (Model 6070, Tisch Environmental, Inc., USA) and a PQ 200 $PM_{2.5}$ sampler. The high-volume sampler (1.13 m^3/min) for PM_{10} measurements and PQ 200 (16.7 L/min) for $PM^{2.5}$ measurements were loaded with Whatman quartz fibre filters at a size of 203 × 254 mm and a diameter of 47 mm, respectively. The samples were then extracted by dissolving them with a mixture solution of 1.03 M HNO_3 and 2.03 M HCl (1:1) using an ultrasonic water bath at 90°C for two hours. Samples were kept in a refrigerator at 4°C until analysed. Extracted solutions were analysed by (ICP-AES). All of the metals in $PM_{2.5}$ and PM_{10} were found to have higher concentrations in spring than in summer, except Cr in PM_{10} which showed similar concentrations between spring and summer. Seasonal differences in the metal concentrations may have been attributed to differences in wind directions with some winds passing through industry or traffic areas. Principal component analysis for the heavy metals in $PM_{2.5}$ and PM_{10} identified industrial emissions and road dust (soil and traffic) as major sources at the sampling site.

Dubey *et al*. (2012) did a trace metal analysis of PM_{10} particulate in the mining and non-mining areas of Dhanbad region, Jharkhand, India. The samples were collected using the EPM 2000 filter papers and acid digested before analysis by AAS. The concentrations of trace metals were found in the order of Fe>Cu>Zn>Mn>Cd>Pb>Ni. The study found that the major sources of airborne trace metals identified were from mining and associated activities, Earth crust, biomass burning, oil combustion, and fugitive emissions. Similarly, Ogugbuaja and Barsisa (2001) did a study to determine the metal composition of suspended PM in Yola and Maiduguri areas in Nigeria. High levels of metal concentrations were observed in both areas with concentrations of Cd and Pb reaching a maximum of 83.1 ppb and 95 ppb, respectively. A number of industries were identified as the source of metals in this area in addition to dust from the desert during Harmattan season. The high values in Yola were also attributed to lack of air dispersion due to the area being situated in a valley.

Pumure *et al*. (2003) studied characterization of PM emissions from the Zimbabwe Mining and Smelting Company (ZIMASCO) in Kwekwe, Zimbabwe. The samples were collected and analysed using AAS. The study found that the highest concentrations of Cr and Fe occurred in the fine particulates of sizes less than 59 μm whilst that of Cu and Zn occurred in the coarse

particulates of size range 70-100 μm. Chromium and Iron where found to be metals in the largest amounts than any other metals.

Kgabi (2012) studied the composition of inhalable atmospheric particulates in Rustenburg, South Africa. In this study, inhalable PM was sampled using the TEOM series 1400a, the samples were then analysed using Scanning Electron Microscopy coupled with Energy Dispersive Spectrometer (SEM-EDS) to determine their elemental composition. Concentrations of nitrates and sulphates were determined using Ion Chromatography (IC). Analysis by SEM-EDS showed the presence of atmospheric particles of complex composition including S, Si, Al, Mg, Ca, Pb, Fe, Cr, Ni, V, and Pb. The sources which were identified as the possible contributors to elemental composition in the area were soil dust, industry, biomass burning and traffic.

In a study on characterization of PM_{10} samples in Vanderbijlpark, South Africa (Moja and Mnisi, 2013) samples were collected using a dual E-Sampler which combines the light scatter and the gravimetric filter methods. SEM-EDS and ICP 6000 were then used for elemental and physical characterization of the samples. The results concluded that the concentrations of evaluated heavy metals decreased in the following order: iron (Fe) > manganese (Mn) > zinc (Zn) > copper (Cu) > vanadium (V) > titanium (Ti) > nickel (Ni) > lead (Pb). It was also found that there was a positive correlation between Zn and Pb (r = 0.916); Zn and Mn (r =0.883); Zn and V (0.984); Zn and Ni (r = 0.877); Zn and Fe (r = 0.914), which suggests common anthropogenic sources such as the steel and metallurgical alloy-making processes, road transport, industrial chemical reactions, coal and oil burning activities and windblown dust.

Having considered the literature and techniques used, in this study the UNC passive samplers were used to collect PM samples and the chemical composition of particulate matter was determined using CCSEM. This introduced a new method (in South Africa and likely the whole of Africa) of identifying both natural and anthropogenic sources of PM with particle rich elements. Future studies using UNC passive samplers might consider using other spectroscopic techniques such as Ion Chromatography (IO), Inductively Coupled Plasma (ICP), and AAS for elemental analysis of PM samples. This will assist in determining individual elements rather than particle rich elements. This is to ensure that we build a database of PM chemical elements.

2.11.2 International and local source apportionment studies

Source apportionment of PM using receptor modelling has been studied across the globe by many researchers. Several international studies on source apportionment are mentioned in the introduction section of Manuscript 2. There is scarcity of articles on source apportionment in South Africa and the African continent as a whole where few studies have been undertaken, namely in South Africa (Engelbrecht *et al*., 2001; Kgabi, 2010), Ghana and Gambia (Zhou *et al*., 2013, Zhou *et al*., 2014), Nigeria (Oluyemi and Asubiojo, 2001), Tanzania (Bennet *et al*., 2005; Mkoma *et al*., 2010), Ethiopia (Etyemezian *et al*., 2005) and Benin (Fourn and Fayomi, 2006).

In this study, source apportionment was undertaken to determine the source profiles, apportion the sources and determine their contribution to the total PM in the GTM to add to the knowledge base within South Africa. To the best of the author's knowledge, there has never been a study in South Africa and Africa as a whole to determine source profiles and apportion the sources using a combination of UNC passive samplers (to collect the samples), CCSEM (for chemical composition), and PMF model.

2.12 Air quality legislation

Air quality management in South Africa began in 1965 through the promulgation of the Atmospheric Pollution Prevention Act (Act No 45 of 1965) (APPA). However, the APPA proved to be relatively ineffective in reducing pollution from the sources as intended. This resulted in emergence of pollution "hot-spots" across the country. Enshrined in the South African Constitution (Act No. 108 of 1996) is the right for everyone to live in an environment that is not harmful to their health or wellbeing (National Framework for Air Quality Management, 2012). Air quality monitoring and data analysis provides the scientific basis for the management of air quality through policy and legislation development. There are several legislations in place in South Africa to manage the environment. The National Environmental Management Act (Act No 107 of 1998) states that pollution and degradation of the environment must be avoided and if not they must be minimised or remedied.

The National Environmental Management Act: Air Quality Act (Act No.39) was established in 2004 to integrate the management of the environment from both the sources and the ambient environment. This was intended to monitor the impacts on the receiving environment by setting standards for pollutant levels in ambient air (for compliance monitoring) and setting emission standards to minimise the amount of pollution that enters the atmosphere. National Ambient Air Quality Standards were promulgated on the 24th of December 2009 and updated on the 29th of June 2012 for $PM_{2.5}$ (Table 2.5). These standards were developed using guidelines from the WHO and are based on evidence of the impacts of air pollution on health outcomes.

Table 2.5: South African Ambient Air Quality Standards (DEA, 2012).

Pollutant	Averaging period	Concentration	Frequency of Exceedance	Compliance Date
SO_2	10 minutes	500µg/m^3	526	Immediate
	1 hour	350µg/m^3	88	Immediate
	24 hours	125µg/m^3	4	Immediate
	1 year	50µg/m^3	0	Immediate
CO	1 hour	30µg/m^3	88	Immediate
	8 hour (calculated on 1 hourly averages)	10µg/m^3	11	Immediate
NO_2	1 hour	200µg/m^3	88	Immediate
	1 year	40µg/m^3	0	Immediate
PM_{10}	24 hours	120µg/m^3	4	Immediate – 31 December 2014
	24 hours	75µg/m^3	4	1 January 2015
	1 year	50µg/m^3	0	Immediate – 31 December 2014
	1 year	40µg/m^3	0	1 January 2015
O_3	8 hours (running)	120µg/m^3	11	Immediate
$PM_{2.5}$	24 hours	40 µg/m^3	4	1 January 2016 – 31 December 2029

	24 hours	25 µg/m^3	4	1 January 2030
	1 year	20 µg/m^3	0	1 January 2016 – 31 December 2029
	1 year	15 µg/m^3	0	1 January 2030

2.13 Geographic Information Systems and Modelling Applications

Geospatial analysis and modelling applications play a very important role in formulating air pollution control and management strategies by providing information about better and more efficient air quality planning. This section outlines the role of Geographic Information System (GIS) in air quality management through its ability to analyse the spatial distribution of PM and PM chemical components as outlined in manuscript 1. This statistical software is also used in manuscript 3 to display the spatial distribution of PM_{10} from industrial point sources. A detailed description of the HYSPLIT model is given below. This model is used in manuscript 2 to qualitatively identify the dominant transport pathways to receptor sites in the study area. Based on the chemical information from CCSEM, the PMF model (which is described in detail in section 2.13.3) was used to determine source profiles and identify PM_{10} sources in the GTM.

2.13.1 GIS

A GIS is designed to capture, store, manipulate, analyse, manage, and present all types of geographical data. This means that some portion of the data is spatial and referenced to locations on the Earth. Spatial interpolation refers to the estimation of values at un-sampled points based on known values of surrounding points in space (Waters, 1988). Spatial interpolation is mainly used in GIS to generate a continuous layer of data from a set of point data taken at sample locations. There are several spatial interpolations, for instance, extensions, such as inverse distance weighting (IDW) (Shepard, 1968) and Kriging (Krige, 1951). Tobler (1970) stated that the spatial interpolation methods assume a stronger correlation among points that are closer, with the correlation weakening as points move further apart. The major challenge in GIS is the required computational space for treating a large amount of data points for spatial interpolation. The spatiotemporal analysis in GIS integrate space and time simultaneously (Li, 2008).

Several studies have examined the performance of IDW and Kriging, and the findings of these studies had mixed results. Kravchenko and Bullock (1999) found that the performance of IDW was not as good as that of Kriging. However, Weber and Englund (1992) found that IDW outperformed Kriging. To predict a value for any unmeasured location, IDW uses the measured values surrounding the prediction location. The measured values closest to the prediction location have more influence on the predicted value than those farther away. IDW assumes that each measured point has a local influence that diminishes with distance. It gives greater weights to points closest to the prediction location, and the weights diminish as a function of distance (Li *et al*, 2014). However, in Kriging, the weights are based not only on the distance between the measured points and the prediction location, but also on the overall spatial arrangement among the measured points (Childs, 2004). According to Childs (2004) the Kriging method depends on a fitted model to the measured points, whereas IDW is a deterministic interpolator that depends solely on the distance to the prediction location to interpolate the unmeasured location. IDW is a more efficient tool to use when there are limited data points for spatial interpolation. Hoek *et al*. (2008) used IDW interpolation techniques to investigate the relationship between traffic-related air pollution and mortality. In this study, IDW was used to interpolate the spatial variability of PM_{10}, $PM_{2.5}$ and PM chemical components and the Kriging method was used for the simulation of PM_{10} emissions from point source emitters.

2.13.2 HYSPLIT model description

Trajectory models are widely used tools in studying source receptor relations (Collett and Dyuyemi, 1997; Zannetti and Puckett, 2004). Among them, the Hybrid Single-Particle Lagrangian Integrated Trajectory (HYSPLIT) model by Draxler and Hess (1998) is a commonly used air modelling programme that can calculate the air mass paths from one region to another and thus demonstrate whether the vector for air pollutant transport is indeed present.

The HYSPLIT model is a complete system that is designed to support a wide range of simulations related to the regional or long-range transport, dispersion, and deposition of air pollutants (Prapat and Nguyen, 2007). The output of the HYSPLIT model can vary from simple air parcel trajectories to complex dispersion and deposition simulations (NOAA, 1999). The trajectory calculation (which forms part of this study) is achieved by time integration of the

position of an air parcel as it is transported by the 3-D winds (Draxler and Hess, 1997). By moving backwards in time, the resulting back trajectory indicates air mass arriving at a receptor location at a time, and thus identifies the source region (Angelos *et al*., 2004).

Like most air transport models, the use of HYPSLIT can be a time-intensive and resource-intensive operation because air transport modelling remains a combination of human operator effort (e.g., manual model setup and input) and computer processing effort. In particular, the analysis of graphical trajectory plots generated by HYSPLIT's trajectory module is typically a manual operation. It is therefore of interest to investigate the modelling resolution (i.e., number of modelling runs) that is required to achieve satisfactory and statistically significant results; since a lower modelling resolution (i.e., fewer runs) translates directly into potential time and money savings.

An air mass trajectory can be thought of as a line that traces the path over time. On a map, this path can be represented as a series of points drawn either backwards or forwards in time, whose X and Y coordinates are longitude and latitude. HYSPLIT trajectory generation works by using a formula that calculates position based on wind velocity vectors and time. The meteorological data are interpolated from the meteorological grid to the internal HYSPLIT model grid using linear interpolation of the horizontal wind velocity components, the vertical wind velocity component, and time. The advection, or movement of the particle is calculated from the average of the three-dimensional velocity vectors for an initial position *P(t)* and the first-guess position *P'(t+Δt)* (Draxler and Hess, 1997; Draxler and Hess, 1998). The differential trajectory equation is:

$$dP/dt = V[P(t)]. \qquad 2.28,$$

where *V* is the velocity vector and *P(t)* is the initial position. A common solution to this equation is to expand *P(t)* in a Taylor series about $t = t_0$ evaluated at $t_1 = t_0 + \Delta t$; and about $t = t_1$ evaluated at $t = t_0$. The resulting first-guess position is:

$$P'(t + \Delta t) = P(t) + V(P, t)\,\Delta t \qquad 2.29,$$

where Δt is the integration time step and P is the pressure at initial time t. And the final position is given by:

$$P(t + \Delta t) = P(t) + 0.5[V(P, t) + V(P', t + \Delta t)]\,\Delta t \quad 2.30,$$

where P' is the surface pressure. Equation (30) is accurate to the second order, and higher order methods do not yield greater precision (Draxler and Hess, 1997; Draxler and Hess, 1998).

The HYSPLIT model uses Ward's method initially described by Romesburg (1984), Moody and Galloway (1988) and Stunder (1996) to cluster trajectories. Wang *et al*. (2006) expanded Ward's clustering to a three-dimensional trajectory position, while Sodemann (2000) normalized the three-dimensional trajectory position prior to clustering, and Eneroth *et al*. (2003) used the spherical distance between trajectory points. The end point trajectory data sets are used as input to Ward's clustering technique in HYSPLIT. In the application of cluster analysis, it is necessary to decide how many clusters are needed to adequately describe the data. The criteria for this decision depend on the analysis goal. When constructing long-range transport climatology, as in the present study, cluster analysis may be used as an exploratory analysis tool to provide a descriptive summary of a trajectory data set (Harris and Kahl, 1990). With this goal, a robust method for determining the optimal number of clusters is unnecessary. Therefore, the model run provides several clusters and the clusters that reveal meaningful structure (coherent patterns) in the data are then chosen.

Meteorological data used to force HYSPLIT is available at relatively coarse temporal resolution (of 1-6 hours) which can result in errors in rapidly changing conditions. The advantage of the HYSPLIT model is its ability to cluster several trajectories to provide meaningful transport pathways (Draxler and Hess, 1998).The main limitation of the HYSPLIT model is that the terrain is smoothed and inhibits the influence of terrain on wind flow modification. The other limitation is that the meteorological data available to run the model are at relatively coarse horizontal resolution which can result in errors in rapidly changing conditions such as mountain-valley circulations. Hence, the model should be run at high altitude.

2.13.3 PMF model description

Multivariate statistical techniques are important tools used extensively in environmental research to provide meaningful analysis on volumes of data sets (Kaplunovsky, 2005; Viana *et al*., 2008; Mostert *et al*., 2010). Gordon (1988) attributed the importance of multivariate statistical tools to their ability to reduce the dimensionality of examined data sets and their ability to point out any trend and/or correlation among variables. These techniques are also useful in profiling and identification of natural / anthropogenic sources impacting on the environment (Watson *et al*., 2008).

There are two types of source apportionment models (source-oriented models and receptor models (such as the PMF model used in this study)) used to identify sources of pollution in the environment (Schauer *et al*., 1996). Source-oriented (dispersion) models require knowledge of all emissions from the contributing sources (Pant and Harrison, 2012). Receptor models infer contributions from different source types using multivariate measurements taken at one or more receptor locations. These models use ambient data and the chemical components in source emissions to quantify contributions, unlike the source models that use emissions and meteorological parameters to estimate concentrations at the receiving environment (Watson, 2002).

PMF has been used widely in source apportionment of ambient PM because of its ability to account for uncertainty variables that are often associated with sample measurements, and ensures that the source profiles and mass concentrations are non-negative (Paatero and Tapper, 1993, 1994; Paatero, 1997; Reff *et al*., 2007). The key output of PMF is the percentage contributions of different sources of pollutant concentration (Pant and Harrison, 2012). USEPA (2014) defined the main objective of PMF as the identification of several factors – p, the species profile of each source – f, and the amount of mass contributed by each factor to each individual sample – g. These objectives are achieved by minimizing the weighted objective function (*Q*), based upon the data uncertainties (*U*) given by:

$$Q = \sum_{i=1}^{n} \sum_{i=1}^{m} \left[\frac{C_{ij} - \sum_{k=1}^{p} G_{ij} F_{ij}}{U_{ij}} \right]^2 \qquad 2.31,$$

where C_{ij} is the measured concentration values (in µg.m^{-3}) at the receptor locations, U_{ij} is the estimated uncertainty value (in µg.m^{-3}), G_{ik} is the factor score (source contribution) value, F_{kj} is the factor loading (source profile) value, n is the number of samples, m is the number of species and p is the number of sources included in the analysis (USEPA, 2014).

The factor loading value in the wind sector profile of the sources was used to estimate the average mass contribution of the sources using equation 2.32;

$$C_{kl} = F_k \, x \, F_{kl} / \sum_{l=1}^{n} F_{kl} \qquad 2.32,$$

where n is the number of wind sectors, C_{kl} is the average contribution of source k in wind sector l (in µg.m^{-3}), F_k is the factor loading of source k in aerosol mass (in mg m_3), and F_{kl} is the factor loading of source k in sector l (in µg.m^{-3}). The total contribution of all the identified sources due to wind in sector l can also be estimated by summing the contribution of all the source factors from sector l together (Chan *et al*., 2011).

The PMF model strengths and limitations have been considered (Watson *et al*., 2008). The strength of the TAPM model arises from its ability to calculate the uncertainty in the data, and the model can identify the source categories and their contribution without source chemistry and location. Coupled with back trajectory data (as in this study) the origin of sources can be traced to regional and trans-boundary sources. The limitations include the use of chemical speciation data from pollution measurements (which requires further analysis of measurements), the model cannot be used for reactive species (with short lifespan) and requires atmospheric experience and knowledge of the study area to verify the source profiles.

2.13.4 TAPM model description

TAPM is a three-dimensional, prognostic meteorological and air pollution model (Hurley, 2002). It uses predicted meteorology and turbulence from the meteorological component and consists of four modules. The Eulerian Grid Module (EGM) solves prognostic equations for the mean and variance of concentrations. The Lagrangian Particle Module (LPM) can be used to represent near-source dispersion more accurately. Wet and dry deposition effects are also included (Hurley *et al*., 2003).

Technical details of the model equations, parameterizations, and numerical methods are described by Hurley *et al.* (2005) as follows:

$$\frac{du}{dt} = \frac{du}{dt} + (u+v)\,.\nabla = \frac{\partial}{\partial x}[K_H\frac{\partial u}{\partial x}] + \frac{\partial}{\partial y}\left[K_H\frac{\partial u}{dy}\right] - \frac{\overline{\partial\acute{\omega}\acute{u}}}{\partial\sigma}\frac{\partial\sigma}{\partial z} - \theta_v[\frac{\partial P}{\partial y} + \frac{\partial P}{\partial\sigma}\frac{\partial\sigma}{\partial y}]$$
$$- f_u - N_S(v\text{-}v_S) \qquad 2.33,$$

$$\frac{\partial\dot{\sigma}}{\partial\sigma} = -\left[\frac{\partial u}{\partial x} + \frac{\partial v}{\partial y}\right] + u\frac{\partial}{\partial\sigma}\left[\frac{\partial\sigma}{\partial x}\right] + v\frac{\partial}{\partial\sigma}\left[\frac{\partial\sigma}{\partial y}\right] \qquad 2.34,$$

$$\sigma = Z_T[\frac{Z-Z_S}{Z_T-Z_S}] \qquad 2.35,$$

Where t is the time, (u, v) are horizontal winds, u_s and v_s are large-scale synoptic winds, σ is sigma-pressure, $\dot{\sigma}$ is vertical wind, Z_T is the height of the top of the model; Z_S is terrain height; K_H is the horizontal diffusion coefficient; $\overline{w'\varphi'}$ is the eddy term; f is the Coriolis parameter; θ_v is the potential virtual temperature. The turbulence terms in Eqs. (2.34), and (2.35) are derived by solving equations for the turbulent kinetic energy and the eddy dissipation rate. The governing equation for species concentration, χ, such as PM_{10} is given by:

$$\frac{d\chi}{dt} = \frac{\partial}{\partial x}\left[K_\chi\frac{\partial\chi}{\partial x}\right] + \frac{\partial}{\partial y}\left[K_\chi\frac{\partial\chi}{\partial y}\right]\chi - \left[\frac{\partial\sigma}{\partial z}\right]\frac{\partial}{\partial\sigma}\left[\overline{\acute{\omega}\acute{\chi}}\right] + R\chi + S \qquad 2.37,$$

where K_χ is the diffusion coefficient, $\overline{\acute{\omega}\acute{\chi}}$ is the eddy term; R_χ is the chemical reaction term; S_χ is the pollutant emission term. The diffusion coefficient used for pollutant concentration is K_χ = 2.5 K, where K is the diffusion coefficient for the turbulent kinetic energy (Hurley *et al.*, 2005).

Hurley (2002) described TAPM as a model consisting of coupled prognostic meteorological data and air pollution concentration components, eliminating the need to have site-specific meteorological observations. Instead, the model predicts the flows important to local-scale air pollution, such as sea breezes and terrain-induced flows, against a background of larger-scale meteorology provided by synoptic analyses. The model solves the momentum equations for horizontal wind components, the incompressible continuity equation for the vertical velocity

in a terrain following coordinate system, and scalar equations for potential virtual temperature, specific humidity of water vapours and cloud-rainwater. Pressure is determined from the sum of hydrostatic and optional non-hydrostatic components, and a Poisson equation is solved for the non-hydrostatic component.

Explicit cloud micro-physical processes are included. Wind observations can optionally be assimilated into the momentum equations as nudging terms. The turbulence closure terms in these mean equations use a gradient diffusion approach, including a counter-gradient term for the heat flux, with eddy diffusivity determined using prognostic equations for turbulence kinetic energy and eddy dissipation rate. A weighted vegetation canopy, soil and urban land-use scheme is used at the surface, while radiative fluxes, both at the surface and at upper levels, are also included.

Boundary conditions for the turbulent fluxes are determined by Monin-Obukhov surface-layer scaling variables and parameterizations for stomatal resistance. Luhar and Hurley (2003) indicated that the air pollution component of TAPM uses the predicted meteorology and turbulence from the meteorological component and consists of a Eulerian grid-based set of prognostic equations for pollutant concentration and an optional Lagrangian particle mode. This information is then used on the inner-most nest for pollution for selected point sources to allow a more detailed account of near-source effects, including gradual plume rise (Grigoras *et al.*, 2012).

As with most models, limitations in TAPM predictions arise from several reasons: approximations to the underlying physics; uncertainties in the input data; and problems of matching of the scale of the model to the observations. The main advantage of the TAPM model is that it eliminates the need to have site-specific meteorological observations to drive a pollution model but can assimilate observations if they are available (Hurley *et al*., 2005).

The following Chapter presents the Overview and then manuscript 1 which describes the work carried out to meet the requirements of research objectives 1, 2, 3 and 4 for this study.

2.14 References

Abouali, O. and Ahmadi, G., 2007: 3-D Simulation of Airflow and Nanoparticle Beam Focusing in Aerodynamic Lenses. *Int. J. Engineer*. 20: 45–54.

Abumrad, N.N., 1984: Molybdenum-is it an essential trace metal? Bulletin of the New York Academy of Medicine. 60(2): 163-71.

Adams, P. and Seinfeld, J., 2002: Predicting global aerosol size distributions in general circulation models. *J. Geophys. Res.-Atmos*.107: 4370.

Ahrens, C.D., 2012: Meteorology Today: An Introduction to Weather, Climate, and the Environment. 10th Edition, Canada: Thomas Brooks/Cole; 537p.

Andreae, M.O., 1995: Climatic effects of changing atmospheric aerosol levels. In: World Survey of Climatology. Vol. 16: Future Climates of the World, A. Henderson-Sellers (ed). Elsevier, Amsterdam, pp. 341-392.

Andreae, M.O., Browell, E.V., Garstang, M., Gregory, G.L., Harris, R.C., Hill, G.F., Jacob, D. J., Pereira, M.C., Sachse, G.W., Setzer, A.W., Dias, P.L.S., Talbot, R.W., Torres, A.L. and Wofsy, S.C., 1988: Biomass-burning emissions and associated haze layers over Amazonia. *J. Geophys. Res*. 93: 1509-1527.

Andreae, M.O. and Rosenfeld, D. 2008: Aerosol-cloud-precipitation interactions. Part 1. The nature and sources of cloud active aerosols. *Earth Sci. Rev*. 89 (1-2): 13–41. doi: 10.1016/j.earscirev.2008.03.001.

Angelos, A., Son, N. and Xiaohong, X., 2004: On the use of HYSPLIT model to study air quality in Windsor, Ontario, Canada. *Environ. Inform. Arch*. 2: 517-525.

Aitchison, J. and Brown, J.A.C., 1957: The Log-normal Distribution, Cambridge University Press, Cambridge, London. pp xviii, 176.

Atkinson, B.W., 1981: Mesoscale atmospheric circulation, Academic Press, London. pp xvii, 595.

Agency for Toxic Substances and Disease Registry (ATSDR), 1999: Agency for Toxic Substances and Disease Registry. Toxicological Profile for Mercury. Atlanta: U.S. Department of Health and Human Services. Available from:
https://www.atsdr.cdc.gov/toxprofiles/tp46.pdf

Agency for Toxic Substances and Disease Registry (ATSDR), 2005: Toxicological Profile for Nickel. Atlanta, GA: US Public Health Service, Agency for Toxic Substances and Disease Registry. Available from:
https://www.atsdr.cdc.gov/toxprofiles/tp15.pdf

Avila, A., Queralt-Mitjans, I. and Alacón, M., 1997: Mineralogical composition of African dust delivered by red rains over north-eastern Spain. *J. Geophys. Res*. 102: 21977–21996.

Babikir, A.A A., 2004: Some aspects of climate and economic activities in the Arab Gulf States, *Geo. J.* 13(3): 211-222.

Bargagli, R., 2000: Trace metals in Antarctica related to climate changes and increasing human impact. *Rev. Environ. Contam. Toxicol*. 166: 129-173.

Barnes, S.J. and Maier, W.D., 2002: Platinum-group elements and microstructures of normal Merensky Reef from Impala Platinum mines, Bushveld complex. *J. Petrol*. 43: 103-128.

Baron, P.A. and Willeke, K., 2001: Aerosol Measurement: Principles, Techniques and Applications. 2nd Edition, John Wiley & Sons: New York, NY. Pp xviii, 1131.

Bennet, C., Jonsson, P. and Lingren, E.S., 2005: Concentrations and sources of trace elements in particulate air pollution, Dar es Salaam, Tanzania, studied by EDXRF. X-Ray Spectrometry. 34; 1–6.

Bielicka, A., Bojanowska, I. and Wiśniewski, A., 2005: Two Faces of Chromium - Pollutant and Bioelement. *Polish J. Environ. Stud.* 14(1): 5-10.

Blanchard, D.C., 1983: The Production Distribution and Bacterial Enrichment of the Sea Salt Aerosol. Air-Sea Exchange of Gases and Particles. P. Liss and W. Stum. Dordrecht, Holland, Kluwer Academic Publishers: 407-454.

Blaxter, K.L., 1950: Lead as nutritional hazard to form livestock. 111. Factors influencing the distribution of lead in the tissues. *J. Comp. Pathol. Ther.* 60: 177.

Bonelli, P., Marcazzan, G.M. and Cereda, E., 1996: Elemental composition and air trajectories of African dust transported in northern Italy. The impact of African dust across the Mediterranean. Edited by R. Chester, and S. Guerzoni, pp. 275 - 283, Kluwer Academic publishers, Dordrecht, Netherlands.

British Geological Survey, 2009: Platinum. Available from: https://www.bgs.ac.uk/downloads/start.cfm?id=1401

Buttice, C., 2015: Nickel compounds. In: Colditz GA. The SAGE encyclopaedia of cancer and society, 2nd Edition, SAGE publications, Inc., pp: 828-831.

Cannon, H.L., Connally, G.G., Epstein, J.B., Parker, J.G., Thornton, I. and Wixson, G., 1978: Rocks: geological sources of most trace elements. In: report to the workshop at south coast plantation Captiva Island, FL, US. *Geochem. Environ*. 3: 17–31.

Casuccio, G.S., Janocko, P.B., Lee, R.J., Kelly, J.F., Dattner, S.L., and Mgebroff, J.S., 1983: "The Use of Computer Controlled Scanning Electron Microscopy in Environmental Studies." *J. Air Poll. Control Ass.* 33(10): 937-943. doi:10.1080/00022470.1983.10465674.

Cawthorn, R.G., 1999: The discovery of the platiniferous Marensky Reef in 1924. *S Afr. J Geol*. 102:178–183.

Cawthorn, G.R., Eales, H.V., Walraven, F., Uken, R. and Watkeys, M.K., 2006: The Bushveld complex. In: Johnson M.R., Anhaeusser C. R. and Thomas R.J. (Eds.), the Geology of South Africa. Geological Society of South Africa, Johannesburg/Council for Geoscience, Pretoria, 261-279.

Cawthorn, G.R., 2010: The platinum Group Elements Deposits of the Bushveld Complex in South Africa. *Platinum Metals Rev*. 54(4): 205-215.

Chaloulakou, A., Kassomenos, P., Spyrellis, N., Demokritou, P. and Koutrakis, P., 2003: Measurements of PM10 and PM2.5 particle concentrations in Athens, Greece. *Atmos. Environ*. 37(5): 649-660.

Chan, Y., Hawas, O., Hawker, D., Vowles, P., Cohen, D.D., Stelcer, E., Simpson, R., Golding, G. and Christensen, E., 2011: Using multiple type composition data and wind data in PMF analysis to apportion and locate sources of air pollutants. *Atmos. Environ*. 45: 439-449. doi:10.1016/j.atmosenv.2010.09.060

Chen, S.Y., Huang, J.P., Qian, Y., Zhao, C., Kang, L.T., Yang, B., Wang, Y., Liu, Y.Z., Yuan, T.G., Wang, T.H., Ma, X.J., Zhang, G.L., 2017: An overview of mineral dust modelling over East Asia. *J. Meteor. Res*. 31: 633-653, doi:10.1007/s13351-017-6142-2

Chester, R., Nimmo, M. and Keyse, S., 1996: The influence of Saharan and Middle Eastern desert-derived dust on the trace metal composition of Mediterranean aerosols and rainwaters: An overview, in The Impact of Desert Dust across the Mediterranean, edited by S. Guerzoni and R. Chester, pp. 253, Kluwer Academic Publishers.

Childs, C., 2004: Interpolating surfaces in ArcGIS spatial analyst. *ArcUser*. c2004 [2018 February13]. Available from: https://www.esri.com/news/arcuser/0704/files/interpolating.pdf

Chung, S.H. and Seinfeld, J.H., 2002: Global distribution and climate forcing of carbonaceous aerosols. *J. Geophys. Res*. 107, D19: AAC 14-1–AAC 14-33. doi: 10.1029/2001JD001397.

Cohen, M., Artz, R., Draxler, R., Miller, P., Poissant, L., Niemi, D., Ratte, D., Deslauriers, M., Duval, R., Laurin, R., Slotnik, J., Nettesheim, T. and McDonald, J., 2004: Modelling the atmospheric transport and deposition of mercury to the Great Lakes. *Environmental Research*, 95, 247-265.

Collett, R.S. and Dyuyemi, K., 1997: Air quality modelling; a technical review of mathematical approaches. *Meteor. Appl*. 4: 235-246.

Darrow, R., 2018: Clovis online school, accessed 25 September 2018, Available from: http://cosscience1.pbworks.com/w/page/8286085/Lesson7-06 Regional Wind Systems

Das, K.K., Das, S.N. and Dhundasi, S.A., 2008: Nickel, its adverse health effects and oxidative stress. *Indian J. Medical Res.* 128: 412-425.

DeGaetano, A.T. and Doherty, O.M., 2004: Temporal, spatial and meteorological variations in hourly PM2.5 concentration extremes in New York City. *Atmos. Environ*. 38: 1547-1558.

de Leeuw, G., Andreas, E.L., Anguelova, M.D., Fairall, C.W., Lewis, E.R., O'Dowd, C., Schulz, M. and Schwartz, S.E., 2011:. Production flux of sea spray aerosol, *Rev. Geophys*. 49(2): 1-39.

Draxler, R.R. and Hess, G.D. 1997: Description of HYSPLIT_4 modelling system. NOAA technical memorandum ERL ARL-224, 24pp.

Draxler, R.R. and Hess, G.D. 1998: An overview of the HUSPLIT_4 modelling system for trajectories, dispersion and deposition. Australian Meteorological Magazine, **47**, 295-308.

Dubey, B., Pal, A.K. and Singh, G. 2012: Trace metal composition of airborne particulate matter in the coal mining and non–mining areas of Dhanbad Region, Jharkhand, India. *Atmos. Poll. Res*. 3: 238-246.

Durran, D.R., 1990: Mountain waves and downslope winds. *Meteorol. Monolog*. 23(45). American Meteorological Society, Boston.

Eales, H.V. and Cawthorn, R.G., 1996: The Bushveld Complex. In: Cawthorn, R. G. (ed.) Layered Intrusions. Amsterdam: Elsevier, pp. 181–229.

Edgerton, S.A., Malone, E.L., Bian, X. and Shaw, W.J., 1995: Particulate air pollution in Mexico City. A collaborative research project. *J. Air & Waste Manage. Ass*. 49: 1221-1229. DOI: 10.1080/10473289.1999.10463915.

Egodawatta, P., Ziyath, A.M. and Goonetilleke, A., 2013: Characterising metal build-up on urban road surfaces. *Environ. Pollut*. 176: 87–91.

Engelbrecht, J.P., Swanepoel, L., Chow, J.C., Watson, J.G. and Egami, R.T., 2001: PM2.5 and PM10 concentrations from the Qalabotjha low-smoke fuels macro-scale experiment in South Africa. *Environ. Monit. Assess*. 69: 1-15.

Eneroth, K., Kjellström, E. and Holmén, K., 2003: Interannual and seasonal variations in transport to a measuring site in western Siberia and their impact on the observed atmospheric CO_2 mixing ratio. *J. Geophys. Res*. 108: 4660-4673.

Etyemezian, V., Tesfaye, M., Yimer, A., Chow, J.C. Mesfin, D. and Nega, T., *et al*. 2005: Results from a pilot-scale air quality study in Addis Ababa, Ethiopia. *Atmos. Environ*. 39: 7849-7860.

EURO Chlor, 2009: The origin and fate of mercury species in the environment. Science Dossier. Available from: http://www.eurochlor.org/media/14966/sd14-mercuryenvironment-final.pdf.

Fenger, J., 1999: "Urban Air Quality." *Atmos. Environ*. 33(29): 4877-4900.

Finlayson-Pitts, B.J. and Pitts, Jr, J.N., 1999: *Chemistry of the Upper and Lower Atmosphere: theory, Experiments, And Applications* Academic press (1999).

Fourn, L. and Fayomi, E.B. 2006: Air pollution in urban area in Cotonou and Lokossa, Benin. *Bull. Soc. Pathol. Exot*. 99: 264-268.

Gardner, C.S., Liu, A.Z., Marsh, D.R., Feng, W. and Plane, J.M.C., 2014: Inferring the global cosmic dust influx to the Earth's atmosphere from lidar observations of the vertical flux of mesospheric Na. *J. Geophys. Res*. 119 (9): 7870–7879. doi: 10.1002/2014JA020383.

Garratt, J.R., 1992: The atmospheric boundary layer, Cambridge University Press, Cambridge, 316 pp.

Gaydos, T.M., Stanier, C.O. and Pandis, S.N., 2005: Modelling of in situ ultrafine atmospheric particle formation in the eastern United States. *J. Geophys. Res. Atmos*. 110(7): D07S12.

Gietl, J.K. and Klemm, O., 2009: Source identification of size-segregated aerosol in Munster, Germany, by factor analysis. *Aerosol Sci. Tech*. 43: 828–837.

Ginoux, P., Chin, M., Tegen, I., Prospero, J.M., Holben, B., Dubovik, O. and Lin, S.J., 2001: Sources and distributions of dust aerosols simulated with the GOCART model *J. Geophys. Res*., 106 (17): 20255-20273, 10.1029/2000JD000053.

Ginoux, P., Prospero, J.M., Gill, T.E., Christina, N.H. and Zhao, M,. 2012: Global with the GOCART model, J. el, J. l, J. le aerosol. *Rev. Geophys*. 50(3): 3005, 10.1029/2012RG000388.

Gong, S.L., Barrie, L.A. and Lazare, M., 2002: Canadian Aerosol Module (CAM): a size-segregated simulation of atmospheric aerosol processes for climate and air quality models. 2. Global sea-salt aerosol and its budgets. *J. Geophys. Res*. 107 (D24): 4779. doi: 10.1029/2001JD002004.

Gordon, G.E., 1988: Receptor models. *Environ. Sci. Tech*. 22: 1132-1142.

Gray, H.A., Cass, G.R., Huntzicker, J.J., Heyerdahl, E.K. and Rau, J.A., 1986: Characteristics of atmospheric organic and elemental carbon particle concentrations in Los Angeles, *Environ. Sci. Technol*. 20: 580-589.

Grigoras, G., Cucumeanu, V., Ene, G., Mocioaca, G. and Deneanu, A., 2012: Air pollution dispersion modelling in a polluted industrial area of a complex terrain from Romania. *Environ. Phys*. 64(1): 173-186.

GWRTAC, 1997: Remediation of metals-contaminated soils and groundwater. *Tech. Rep*. TE-97-01, GWRTAC, Pittsburgh, PA.

Hansen, J.E., Sato, M. and Ruedy, R., 1997: Radiative forcing and climate response. *J. Geophys. Res*. 102: 6831-6864.

Harris, J.M. and Kahl, J.D. 1990: A descriptive atmospheric climatology for the Mauna Loa Observatory, using clustered trajectories. J. *Geophys. Res*. 95: 13651-13677.

Harrison, R.M. and Yin, J., 2000: Particulate matter in the atmosphere: which particle properties are important for its effect on health? *Sci. Total Environ*. **249:** 85-101.

Hayes, B., 1997: The carcinogenicity of metals in humans. Cancer Causes Control, 8: 371-385.

Herrera, J., Rodriguez, S. and Baez, A.P., 2009: Chemical Composition and Sources of PM10 Particulate Matter Collected in San José, Costa Rica. *Atmos. Sci. J.* 3: 124-130.

Hildemann, L.M., Cass, G.R., Mazurek, M.A. and Simoneit, B.R.T., 1994: Seasonal trends in Los Angeles ambient organic aerosol observed by high-resolution gas chromatography, *Aerosol Sci. Technol*. 20: 303-317.

Hind, W.C., 1999: Aerosol technology: properties, behaviour, and measurement of airborne particles. Wiley, New York, pp 111–170.

Hobbs, P.V., 2000: Introduction to Atmospheric Chemistry, Cambridge University Press, New York, p. 182.

Hoffmann, T., Odum, J.R., Bowman, F., Collins, D., Klockow, D., Flagan, R.C. and Seinfeld, J.H., 1997: Formation of organic aerosols from the oxidation of biogenic hydrocarbons. *J. Atmos. Chem*. 26: 189–222.

Hoek, G., Beelen, R., de Hoogh, K., Vienneau, D., Gulliver, J., Fischer, P. and Briggs, D., 2008: A review of land-use regression models to assess spatial variation of outdoor air pollution. *Atmos. Environ.* 42(33): 7561-7578.

Hurley, P., 2002: The Air Pollution Model (TAPM) Version 2. Part 1: Technical description, CSIRO Atmospheric Research Technical Paper No. 55.

Hurley, P., Physick, W., Cope, M., Borgas, M. and Brace, P., 2003: 'An evaluation of TAPM for photochemical smog applications in the Pilbara region of WA', Proceedings of the National Clean Air Conference of CASANZ, Newcastle, Australia, 23-27 November 2003.

Hurley, P., Physick, W., Luhar, A. and Edwards, M., 2005: 'The Air Pollution Model (TAPM) Version 3. Part 2: Summary of some verification studies', CSIRO Atmospheric Research Technical Paper No. 72. pp36.

Husar, R.B. and Wilson, W.E., 1989: Trends of seasonal haziness and sulphur emissions over the eastern United States. In: Mathai, C.V., ed. Transactions: Visibility and Fine Particles, An

Intergovernmental Panel on Climate Change (IPCC), 2001: Climate Change: The scientific basis, Contribution of Working Group I to the Third Assessment Report of the Inter-governmental Panel on Climate Change, Cambridge University Press, pp 881.

Jaenicke, R., 1993: Tropospheric aerosols; In: Aerosol-Cloud-Climate Interactions, P V Hobbs (ed.) Academic Press Inc., pp 1–31.

Jaenicke, R., 2005: Abundance of cellular material and proteins in the atmosphere. *Science*, 308: 73. doi: 10.1126/science.1106335.

Kaimal, J.C. and Finnigan, J.J., 1994: Atmospheric boundary layer flows. Their structure and measurements, Oxford University Press, Oxford, 289 pp.

Kamens, R.M., Jang, M., Chien, C.J. and Leach, K., 1999: Aerosol formation from the reaction of α-pinene and ozone using a gas-phase kinetics-aerosol partitioning model. *Environ. Sci. Tech*. 33: 1430–1438.

Kaplunovsky, A.S., 2005: Factor analysis in environmental studies. *HAIT J. Sci. Eng*. 2: 54-94.

Kgabi, N., 2010: An assessment of common atmospheric particulate matter sampling and toxic metal analysis methods. *African J. Environ. Sc. Tech*. 4(11): 718–728.

Kgabi, A.N., 2012: Composition of Inhalable Atmospheric Particulates in Rustenburg, South Africa. *British J. Eviron. & CC*. 2(1): 58-72.

Khlystov, A., 2001: Quality Assurance Project Plan for Pittsburgh Air Quality Study (PAQS), Department of Chemical Engineering. Carnegie Mellon University.

Kinloch, E.D. and Peyerl, W., 1990: Platinum-group minerals in various rock types of the Merensky Reef: genetic implications. *Econ. Geol*.85: 537-555.

Kok, J.F., Ridley, D.A., Zhou, Q., Miller, R.L., Zhao, C., Heald, C.L., Ward, D.S., Albani, S. and Haustein, K., 2017: Smaller desert dust cooling effect estimated from analysis of dust size and abundance. *Nature Geosci*. 10 (4): 274-278, doi:10.1038/ngeo2912

Kothai, P., Prathibha, P., Saradhi, I.V., Pandit, G.G. and Puranik, V.D., 2009: Characterization of Atmospheric Particulate Matter using PIXE Technique. *Int. J. Civil and Environ. Eng.* 1(1): 27-30.

Kravchenko, A. and Bullock, D.G., 1999: A comparative study of interpolation methods for mapping soil properties. *Agronomy J.* 91: 393-400. http://dx.doi.org/10.2134/agronj1999.00021962009100030007x

Krige, D.G., 1951: A Statistical Approach to Some Mine Valuations and Allied Problems at the Witwatersrand. Master's Thesis, University of Witwatersrand, Johannesburg, South Africa.

Kumar, A., Shunquan Wu, M.F. and Weise, M.F., 2013: Free troposphere ozone and carbon monoxide over the North Atlantic for 2001-2011. *Atmos. Chem. Phys*. 13(6): 15377-15407.

Kvietkus, K., Šakalys, J. and Valiulis, D., 2011: Trends of atmospheric heavy metal deposition in Lithuania. *Lith. J. Phys*. 51(4): 359-369.

Lagzi, I., Mészáros, R., Gelybó, G. and Leelössy, Á., 2013: Atmospheric Chemistry. A book, being part of the project entitled "E-learning scientific content development in ELTE TTK" with number TÁMOP-4.1.2.A/1-11/1-2011-0073, Eötvös Loránd University.

Lal, S. and Patil, R.S., 2001: Monitoring of atmospheric behaviour of NO_x from vehicular traffic. *Environ. Monit. Assess.* 68(1): 37–50.

Lee, R.J. and Fisher, R.M., 1980: "Quantitative Characterization of Particulates by Scanning and High Voltage Electron Microscopy," National Bureau of Standards Special Publication 533.

Lee, B.K. and Hieu, N.T., 2011: Seasonal Variation of Heavy Metals in Atmospheric Aerosols in a Residential Area of Ulsan, Korea. *Aeros. AQ Res.* 11: 679-688.

Lee, R.J., Spitzig, W.A., Kelly, J.F. and Fisher, R.M., 1981: "Quantitative metallography by computer-controlled scanning electron microscopy," *J. Metals*, 33:3.

Lee, J.D., 1991: Concise Inorganic Chemistry. Chapman and Hall, 4th Edition, London, UK.

Lee, C.K., Low, K. S. and Hew, N.S., 1991: Accumulation of arsenic by aquatic plants. *Sci. Total Environ*. 103: 215-227.

Lee, Y.H., Chen, K. and Adams, P.J. 2009: Development of a global model of mineral dust aerosol microphysics. *Atmos. Chem. Phys*. 9: 2441–2458.

Lenntech Water Treatment and Air Purification.: Water Treatment. Published by Lenntech, Rotterdamseweg, Netherlands. 2004.

Lewis, E.R. and Schwartz, S.E.: Sea Salt Aerosol Production: Mechanisms, Methods, Measurements, and Models: A Critical Review, American Geophysical Union, Washington, DC, 2004.

Li, L., 2008 Constraint Databases and Data Interpolation. In *Encyclopaedia of Geographic Information System*; Shekhar, S., Xiong, H., Eds.; Springer: Berlin/Heidelberg, Germany. pp. 144–153.

Li, L., Losser, T., Yorke, C. and Piltner, R., 2014: Fast Inverse Distance Weighting-based spatiotemporal interpolation: a web-based application of interpolating daily fine particulate matter PM2.5 in the Contiguous U.S. using parallel programming and k-d tree. *Int. J. Environ. Res and Public Health*. 11(9): 9101-9141.

Liao, H., Adams, P.J., Seinfeld, J.H., Mickley, L.J. and Jacob, D.J., 2003: Interactions between tropospheric chemistry and aerosols in a unified GCM simulation. *J. Geophys. Res*. 108 (D1): 4001. doi: 10.1029/2001JD001260.

Linna, A., Oksa, P. and Groundstroem, K., 2004: Exposure to cobalt in the production of cobalt and cobalt compounds and its effect on the heart. *J. Occup. Environ. Med*. 61: 877-885.

Manahan S. E. 2004. Environmental chemistry, 8th edition. Boca Raton: CRC Press LLC, 816 pp.

Luan, Z.P., Han, Y.X., Zhao, T.L., Liu, F. and Liu, C., 2017: Dust opacities inside the dust devil column in the Taklimakan Desert. *Atmos. Meas. Tech*. 10 (1): 273-279, doi:10.5194/amt-2016-231.

Luhar, A. and Hurley, P., 2003: *Evaluation of TAPM, a prognostic meteorological and air Pollution model, using urban and rural point source data*, *Atmos. Environ*. 37: 2795-2810.

Mahowald, N.M., Kloster, S., Engelstaedter, S., Moore, J.K., Mukhopadhyay, S. and McConnell, J.R., 2010: Observed 20th century desert dust variability: Impact on climate and biogeochemistry. *Atmospheric Chemistry and Physics*, 10: 10875–10893. https://doi.org/10.5194/acp-10-10875-2010

Mahowald, N., Albani, S., Engelstaedter, S., Winckler, G. and Goman, M., 2011: Model insight into glacial-interglacial paleo dust records. *Quat. Sci. Rev*., 30 (7–8): 832-854.

Majewski, G., Kleniewska, M. and Brandyk, A., 2011: Seasonal Variation of Particulate Matter Mass Concentration and Content of Metals. *Polish J. Environ. Stud*. 20 (2): 417-427.

Mahlman, J.D., 1997: Uncertainties in Projections of Human-Caused Climate Warming. *Science*, 278(5342): 1416-1417. DOI: 10.1126/science.278.5342.1416

Manahan, S.E., 2004. Environmental Chemistry, 7th Edition, CRC Press, Boca Raton, FL.

Massachusetts Port Authority Logan International Airport (MASSPORT), 2007: Air Quality Monitoring Study Passive Monitoring Program Final Quality Assurance Project Plan. Available from:
https://www.massport.com/media/2167/final_quality_assurance_projplanpassmonitoring.pdf

Mayer, H., 1999: "Air Pollution in Cities." *Atmos. Environ*. 33(24-25): 4029-4037.

Mazurek, M.A., Cass, G.R. and Simoneit, B.R.T., 1989: Interpretation of high-resolution gas chromatography and high-resolution gas chromatography/mass spectrometry data acquired from atmospheric organic aerosol samples. *Aerosol Sci. Technol*. 10: 408-420.

McDowell, A.C.M., 2011: Investigating non-disclosing precious metal components in the UG2 reef. Wired Space, Wits Institutional Repository environment on DSpace. http://hdl.handle.net/10539/9161

McLaren, C.H. and De Villiers, J.P.R: 1982. The platinum-group chemistry and mineralogy of the UG-2 chromitite layer of the Bushveld Complex. *Economic Geology*, 77: 1348-1366.

Melaku, S., Morris, V., Raghavan, D. and Hosten, C., 2008: Seasonal variation of heavy metals in ambient air and precipitation at a single site in Washington, DC. *Environ. Poll*. 155: 88-98.

Mining Watch Canada, 2012: Potential environmental impacts of mining and processing: An overview of chromium, chromite and toxicity. Available from: https://miningwatch.ca/sites/default/files/PotentialEnvironmental.pdf

Mkoma, S.L., Tungaraza, C., Maenhaut, W. and Raes, N., 2010: Elemental Composition and Sources of Atmospheric Particulate Matter in Dar es Salaam, Tanzania. *Ethiopian J. Environ. Studies and Manag.* 3(1): 20–29.

Moja, S.J and Mnisi, J.S., 2013: Seasonal variation in airborne heavy metals in Vanderbijlpark. *S. A. Journ. Environ. Chem. and Toxicol.* 5(9): 227-233.

Monahan, E.C., Spiel, D.E. and Davidson, K.L., 1986: A model of marine aerosol generation via whitecaps and wave disruption, in Oceanic Whitecaps, edited by E. C. Monahan and G. Mac Niocail, pp. 167–174, Reidel, D., Norwell, Mass.

Monni, S., Salemma, M. and Millar, N., 2000: The tolerance of Empetrum nigrum to copper and nickel. *Environ. Pollut*. 109: 221–229.

Moody, J.L. and Galloway, J.N., 1988: Quantifying the relationship between atmospheric transport and the chemical composition of precipitation on Bermuda. *Tellus*, 40: 463-479.

Mostert, M.M.R., Ayoko, G.A. and Kokot, S., 2010: Application of chemometrics to analysis of soil pollutants. *Trends in Analytical Chemistry*, 29(5): 439-445.

Murphy, D.M., Anderson, J.R., Quinn, P.K., McInnes, L.M., Brechtel, F.J., Kreidenweis, S.M., Middlebrook, A.M., Posfai, M., Thomson, D.S. and Buseck, P.R. 1998a: Influence of sea-salt on aerosol radiative properties in the Southern Ocean marine boundary layer. Nature, 392: 62–65.

Murphy, D.M., Thomson, D.S. and Mahoney, T.M.J., 1998b: In situ measurements of organics, meteoritic material, mercury, and other elements in aerosols at 5 to 19 kilometres. Science, 282, 1664-1669.

Nagajyoti, P.C., Lee, K.D. and Sreekanth, T.V.M., 2010: Heavy metals, occurrence and toxicity for plants: a review. *Environ. Chem. Lett*. 8(3):199-216.

National Oceanic and Atmospheric Administration (NOAA), 1999: NOAA Technical Memorandum ERL ARL-230, pp. 35.

O'Dowd, C.D., Smith, M.H., Consterdine, I.E. and Lowe, J.A., 1997: Marine aerosol, sea-salt and the marine sulphur cycle: a short review, *Atmos. Environ*. 31: 73–80.

Odum, J.R., Hoffmann, T., Bowman, F., Collins, D., Flagan, R. and Seinfeld, J.H., 1996: Gas/particle partitioning and secondary organic aerosol yields. *Environ. Sci. Technol*. 30: 2580–2585.

Ogugbuaja, V.O. and Barsia, L.Z., 2001: Atmospheric pollution in north-east Nigeria: Measurement and Analysis of suspended particulate matter. *Bull. Chem. Soc. Ethiopia*, 15(2): 109-117.

Oke, T.R., 1987: Boundary Layer Climates, Methuen & Co., London, 435 pp.

Oluyemi, E.A. and Asubiojo, O.I., 2001: Ambient air particulate matter in Lagos, Nigeria: a study using receptor modelling with X-ray fluorescence analysis. *Bull. Chemical Soc. of Ethiopia*. 15, 97-108.

Ott, D. and Peters, T., 2008: "A Shelter to Protect a Passive Sampler for Coarse Particulate Matter, PM10-2.5." *Aeros. Sci. Technol.* 42(4): 299–309.

Paatero, P. and Tapper, U., 1993: Analysis of different modes of factor analysis as least squares fit problems. Chemometrics and Intelligent Laboratory System, 18: 183-194.

Paatero, P. and Tapper, U., 1994: Positive matrix factorization: a non-negative factor model with optimal utilization of error estimates of data values. *Environmetrics* 5, 111-126.

Paatero, P., 1997: Least squares formulation of robust non-negative factor analysis. *Chemometrics and Intelligent Laboratory Systems* 37, 23-35.

Pant, P. and Harrison, R.M., 2012: Critical review of receptor modelling for particulate matter: A case study of India. *Atmos. Environ*. 49: 1-12.

Penberthy, C.J., Oosthuyzen, E.J. and Merkle, R.K.W. 2000: The recovery of platinum group elements from the UG-2 chromitite, Bushveld complex - a mineralogical perspective. *Mineralogy and Petrology*, 68: 213-222.

Pierce, J.R. and Adams, P.J., 2006: Global evaluation of CCN formation by direct emission of sea salt and growth of ultrafine sea salt. *J. Geophys. Res. Atmos*. 111, D06203, doi:10.1029/2005JD006186, 2006.

Plane, J.M.C., 2012: Cosmic dust in the earth's atmosphere. *Chem. Soc. Rev*. 41(19): 6507-6518. doi: 10.1039/C2CS35132C.

Pope, C.A., Burnett, R.T., Thun, M.J., Calle, E.E., Krewski, D., Ito, K. and Thurston, G.D., 2002: "Lung Cancer, Cardiopulmonary Mortality, and Long-Term Exposure to Fine Particulate Air Pollution." *J. Amer. Med. Ass*. 287(9): 1132-1141.

Potgieter, C.J., 2006: Accuracy and skill of the conformal-cubic atmospheric model in short-range weather forecasting over southern Africa. Unpublished MSc. Thesis, University of Pretoria.

Prapat, P. and Nguyen, T.K.O., 2007: Assessment of potential long-range transport of particulate air pollution using trajectory modelling and monitoring data. *Atmos. Res*. 85: 3-17.

Pumere, I., Sithole, S.D. and Kahwai, S.G.T., 2003: Characterisation of particulate matter emissions from the Zimbabwean mining and smelting company (ZIMASCO) Kwekwe division: A Ferrochrome smelter. *Environ. Mon. and Ass*. 3: 111-121.

Quinn, P.K., Coffman, D.J., Kapustin, V.N., Bates, T.S. and Covert, D.S., 1998: Aerosol optical properties of marine boundary layer during ACE 1 and underlaying chemical and physical aerosol properties. *J. Geophys. Res*. 103 (16): 547–16 563.

Rauch, S. and Morrison, G.M., 2008: Environmental relevance of the platinum-group elements. *Elements,* 4(4), 259–263.

Razos, P. and Christides, A., 2010: An Investigation on Heavy Metals in an Industrial Area in Greece. *Int. J. Environ. Res*. 4 (4): 58-65.

Reff, A., Eberly, S.I. and Bhave, P.V., 2007: Receptor modelling of ambient particulate matter data using positive matrix factorization: review of existing methods. *JAPCA J. Air Waste Manag*. 57: 146–154.

Reeves, R.D. and Baker, A.J.M., 2000: Metal-accumulating plants. In: Raskin I, Ensley BD (eds) Phytoremediation of toxic metals: using plants to clean up the environment. Wiley, New York, pp 193–22.

Reiss, J. 2000: Genetics of molybdenum cofactor deficiency. *Human Genetics*, 106(2): 157–63.

Rivera-Carpio, C.A., Corrigan, C.E., Novakov, T., Penner, J.E., Rogers, C.F. and Chow, J.C., 1996: Derivation of contributions of sulphate and carbonaceous aerosols to cloud condensation nuclei from mass size distributions. *J. Geophys. Res. Atmos*. 101: 19483-19493.

Roldin, P., Swietlicki, E., Schurgers, G., Arneth, A., Lehtinen, K.E.J., Boy, M. and Kulmala, M., 2011: Development and evaluation of the aerosol dynamics and gas phase chemistry model ADCHEM. *Atmos. Chem. Phys*. 11: 5867–5896.

Romesburg, H.C., 1984: Cluster analysis for researchers. Lifetime Learning, Belmont, Calif., 334pp.

Salomons, W. and Förstner, U., 1984: Metals in the Hydrocycle. Heidelberg: Springer.

Sathneesh, S.K., Moothy, K.K. and Srinivasan, J., 2004: Introduction to aerosols and impact on atmosphere: Basic Concepts, ISRO-GBP Scientific Report SR 05.

Schauer, J.J., Rogge, W.F., Hildemann, L.M., Mazurek, M.A., Cass, G.R. and Simoneit, B.R.T., 1996: Source apportionment of airborne particulate matter using organic compounds as tracers. *Atmos. Environ.* 30: 3837–55.

Schouwstra, R.P., Kinloch, E.D. and Lee, C.A. 2000: `A short geological review of the Bushveld Complex', Platinum Metals Review 44(1): 33-39.

Schult, I., Feichter, J. and Cooke, W.F., 1997: Effect of black carbon and sulphate aerosols on the Global Radiation Budget. *J. Geophys. Res. Atmos*. 102: 30107-30117.

Schwela, D., 2000: Air pollution and health in urban areas. *Reviews on Environmental Health, 15*(1-2): 13-42.

Scoon, R.N. and Mitchell, A.A., 2004: The platiniferous dunite pipes in the eastern limb of the Bushveld Complex: review and comparison with unmineralized discordant ultramafic bodies. *S Afr. J Geol.* 107: 505–520.

Seinfeld, J.H. and Pandis, S.N., 1998: Atmospheric Chemistry and Physics: From air pollution to climate change. New York. John Wiley and Sons, Incorporated.

Seinfeld, J.H. and Pandis, S.N., 2006: Atmospheric Chemistry and Physics: From Air Pollution to Climate Change. 2nd Edition, John Wiley & Sons, New York. pp xxvii, 1203.

Sempéré, R. and Kawamura, K., 1996: Low molecular weight dicarboxylic acids and related polar compounds in the remote marine rain samples collected from western Pacific. *Atmos. Environ.* 30: 1609-1619.

Shepard, D., 1968: A two-dimensional interpolation function for irregularly spaced data. In Proceedings of the 23nd National Conference ACM, Las Vegas, NV, USA, 27–29; ACM: New York, USA, pp. 517–524.

Shao, Y., Wyrwoll, K.H., Chappell, A., Huang, J., Lin, Z. and McTainsh, G.H., 2011: Dust cycle: An emerging core theme in earth system science. *Aeolian Res.* 2: 181–204. https://doi.org/10.1016/j.aeolia.2011.02.001

Sharifi, V.N., Swithenbank, J., Osammor, O. and Nolan, A., 2008: Characterisation of Airborne Particulate Matter in a City Environment. *Modern Applied Science* 3(4): 17-32.

Shrivastav, R., 2001: Atmospheric Heavy Metal Pollution: Development of Chronological Records and Geochemical Monitoring. Resonance, 62-68.

Sigel, A., Sigel, H. and Sigel, R.K.O., 2008: Nickel and Its Surprising Impact in Nature. In: Metal Ions in Life Sciences 2 (Eds) Sigel A., Sigel H. John Wiley & Sons, Ltd. Chichester, U.S.A.

Smith, L.A., Means, J.L., Chen, A., Alleman, B., Chapman, C.C., Tixier, J.S. Jr., Brauning, S.E., Gavaskar, A.R. and Royer, M.D. 1995: Remedial Options for Metals-Contaminated Sites, Lewis Publishers, Boca Raton, FL.

Sodemann, H., 2000: Relationships between the origin of air masses and Carbon Monoxide measurements at the Cape Point Trace Gas Monitoring Station, Honours Thesis, Department of Environmental and Geographical Science, University of Cape Town, South Africa, 75 pp.

South African Department of Justice and Constitutional Development (DOJ&CD).: The Constitution of the Republic of South Africa, 1996. Available from: http://www.justice.gov.za/legislation/constitution/SAConstitution-web-eng.pdf.

South African Department of Environmental Affairs (DEA).: National Environmental Management (*Act* No.107), 1998. Available from: https://www.environment.co.za/documents/legislation/NEMA-National-Environmental-Management-Act-107-1998-G-19519.pdf.

South African Department of Environmental Affairs (DEA). National ambient air quality standards [document on the Internet]. c2012 [cited 2018 June29]. Available from: https://www.environment.gov.za/content/national-environmental-management-air-quality-act-2004-act-no-39-2004-national-ambient-air-q.

South African Government.: National Framework for Air Quality Management in the Republic of South Africa, 2012. Available from: https://www.environment.gov.za/sites/default/files/gazetted_notices/nema_national_framework_aqm_gn115_0.pdf.

Stohl, A., Eckhardt, S., Forster, C., James, P. and Spichtinger, N., 2002: On the pathways and timescales of intercontinental air pollution transport, *J. Geophys. Res.*, 107: 4684, doi:10.1029/2001JD001396.

Stunder, B.J.B., 1996: An assessment of the quality of forecast trajectories. *J. Appl. Meteor*. 35: 1319-1331.

Sujoy, B. and Aparna, A: 2013. Enzymology, Immobilization and Applications of Urease Enzyme. *Int. Res. J. Biological Sci*. 2(6): 51-56.

Sures, B., Zimmermann, S., Messerschmidt, J., von Bohlen, A., Thielen, F. and Baska, F., 2005: The intestinal parasite *Pomphorhynchus laevis* as a sensitive accumulation indicator for the platinum group metals Pt, Pd, and Rh. *Environ. Res.* 98: 83–88.

Suttle, N.F., 1974: Recent studies of the copper-molybdenum antagonism. Proceedings of the Nutrition Society. CABI Publishing. 33(3): 299–305.

Sydor, A.M., Lebrette, H., Ariyakumaran, R., Cavazza, C. and Zamble, D.B., 2014: Relationship between Ni(II) and Zn(II) coordination and nucleotide binding by the Helicobacter pylori [NiFe]-hydrogenase and urease maturation factor HypB. *J. Biol. Chem*. 289: 3828-3841.

Tkachenko, F.K., Efremenko, V.G., Tikhonyuk, L.S. and Gogol, A.B., 1995: Heat resistance of chromium cast iron for lining of blast-furnace equipment. *Metal Science and Heat Treatment,* 37(12): 23-25.

Tobler, W.R., 1974: A computer movie simulating urban growth in the Detroit region. *Econ. Geogr*. ***46***: 234–240.

Tomasi, C. and Lupi, A., 2017: Atmospheric Aerosols: Life Cycles and Effects on Air Quality and Climate, First Edition. Edited by Claudio Tomasi, Sandro Fuzzi, and Alexander Kokhanovsky. pp 1-86.

Tsigaridis, K., Krol, M., Dentener, F.J., Balkanski, Y., Lathière, J., Metzger, S., Hauglustaine, D.A. and Kanakidou, M., 2006: Change in global aerosol composition since preindustrial times. *Atmos. Chem. Phys*. 6 (12): 5143–5162. doi: 10.5194/acp-6-5143-2006.

Tyson, P.D. and Preston-Whyte, R.A., 2000: Atmospheric circulation and weather over southern Africa, Oxford University Press, Cape Town, pp 176.

United Nations Environment Programme (UNEP), 2013: Global Mercury Assessment. Sources, Emissions, Releases and Environmental Transport. UNEP Chemicals Branch, Geneva, Switzerland.

United States Environmental Protection Agency (US EPA), 2014: EPA PMF v5.0, User Guide. Available from:
https://www.epa.gov/sites/production/files/2015-02/documents/pmf_5.0_user_guide.pdf

United States Environmental Protection Agency (US EPA), 2014: Air Quality Criteria for Particulate Matter. National Centre for Environmental Assessment, Office of Research and Development, US Environmental Protection Agency, Research Triangle Park, NC 27711. Report No. EPA/600/P-99/002aF and EPA/600/P-99/002bF. Washington, DC.

United States Department of Health and Human Services (USDHHS), 1999: Toxicological profile for lead, United States Department of Health and Human Services, Atlanta, Ga, USA. Available from: https://www.atsdr.cdc.gov/toxprofiles/tp13.pdf

University of Pretoria (UP).: Atmospheric Air Pollution Prevention Act (*Act* No.45), 1965. Available from:
https://www.up.ac.za/media/shared/600/LAS%20Legislation/air-pollution-prevention-act_17-april-1965.zp53523.pdf.

Viana, M., Kuhlbusch, T.A.J., Querol, X., Alastuey, A., Harrison, R.M., Hopke, P.K., Winiwarter, W., Vallius, M., Szidat, S., Prevot, A.S.H., Hueglin, C., Bloemen, H., Wahlin, P., Vecchi, R., Miranda, A.I., Kasper-Giebl, A., Maenhaut, W. and Hitzenberger, R., 2008: Source apportionment of particulate matter in Europe: A review of methods and results. *Aerosol Sci.* 39: 827–849.

Viljoen, M.J. and Schurmann, L.W., 1998: Platinum-group metals. In the Mineral Resources of South Africa (M.G.C. Wilson & C.R. Anhaeusser, eds.). Council for Geoscience, Pretoria, South Africa (532-568).

Visser, M., 2006: An Overview of the History and Current Operational Facilities of Samancor Chrome. *Southern African Pyrometallurgy* 2006, Edited by R.T. Jones, South African Institute of Mining and Metallurgy, Johannesburg.

Wagner, P.A., 1929: The Platinum Deposits and Mines of South Africa. Oliver and Boyd, Edinburgh. pp xv, 326.

Wagner, J. and Leith, D., 2001a: "Passive Aerosol Sampler. Part I: Principle of Operation." Aerosol Science & Technology 34 (2): 186–192.

Wagner, J. and Leith, D., 2001b: "Passive Aerosol Sampler. Part II: Wind Tunnel Experiments." Aerosol Science & Technology 34 (2): 193–201.

Wall, S.M., John, W. and Ondo, J.L., 1988: Measurement of aerosol size distributions for nitrate and major ionic species. *Atmos. Environ*. 22: 1649–1656.

Wang, Y.Q., Zhang, X.Y. and Arimoto, R., 2006: The Contribution from Distant Dust Sources to the Atmospheric Particulate Matter Loadings at XiAn, China during spring. *Science of the Total Environment*, 368(2-3), 875-883.

Waters, N.M., 1988: "Expert Systems and Systems of Experts," Chapter 12 in W.J. Coffey, ed., Geographical Systems and Systems of Geography: Essays in Honour of William Warntz, Department of Geography, University of Western Ontario, London, Ontario.

Watson, J.G., 2002: Visibility: science and regulation. *J. Air and Waste Manag. Ass.* 52: 628-713.

Watson, J.G., Chen, L.W.A., Chow, J.C., Doraiswamy, P. and Lowenthal, D.H., 2008: Source Apportionment: findings from the U.S. Supersite Program. Technical paper *Air &Waste Manage. Assoc*. 58: 265-288.

Weber, D. and Englund, E., 1992: Evaluation and comparison of spatial interpolators. *Math. Geol*. 24: 381–391.

Whitby, K.T., 1978: The physical characteristics of sulphur aerosols. *Atmos. Environ*. 12: 135-159.

Whitby, K.T. and Sverdrup, G.M., 1980: California aerosols: Their physical and chemical characteristics, in The Character and Origins of Smog Aerosols, edited by Hidy G.M. *et.al*., pp. 477-521, John Wiley, New York.

White, P. 2014: Passive Sampling for Quality Monitoring of Irish Marine Waters. Doctoral Thesis. Dublin Institute of Technology.

Whiteman, C.D., 1990: Observations of thermally developed wind systems in mountainous terrain. Atmospheric processes over complex terrain. *Meteor. Monogr., Amer. Meteor. Soc*. 45: 5-42.

Whiteman, C.D. and Doran, J.C., 1993: The relationship between overlying synoptic-scale flows and winds within a valley. *J. Appl. Meteor.* 32: 1669-1682.

Wilson, M.G.C. and Anhaeusser, C.R., 1998: The mineral resources of South Africa. Handbook 16, Council for Geoscience, Pretoria, 740pp.

Wintz, H., Fox, T. and Vulpe, C., 2002: Responses of plants to iron, zinc and copper deficiencies. *Biochem. Soc. Trans*. 30:766–768.

Wise, E.K. and Comrie, A.C., 2005: Meteorologically Adjusted Urban Air Quality Trends in the South-western United States. *Atmos. Environ*. 39: 2969–2980.

Wolf, M.E. and Hidy, G.M., 1997: Aerosols and climate: anthropogenic emissions and trends for 50 years. *J. Geo. Res*. 102(D10): 11 113–11 121.

Wuana,, R.A. and Okieimen, F.E., 2011: Heavy metals in contaminated soils: A review of sources, chemistry, risks and best available strategies for remediation. *Int Scholarly Res*. Network ISRN Ecology, 1–20.

Yamatani, K., Saito, K., Ikezawa, Y., Ohnuma, H., Sugiyama, K., Manaka, H., Takahashi, K. and Sasaki H., 1998: Relative contribution of Ca^{2+} dependent mechanism in glucagon-induced glucose output from the liver. *Arch. Biochem. Biophy*. 355: 175-180.

Zannetti, P. and Puckett, K., 2004: Air Quality Modelling: Theories, Methodologies, Computational Techniques, and Available Databases and Software-Volume I-Fundamentals, *A&WMA and the Enviro Comp Institute*, pp. 430.

Zardi, D. and Whiteman, D., 2012: Diurnal mountain wind systems. In Mountain Weather Research and Forecasting: Recent Progress and Current Challenges; Chow, F., De Wekker, S., Snyder, B., Eds.; Springer Atmospheric Sciences; Springer: Dordrecht, The Netherlands: 35–119.

Zdanowicz, C.M., Banic, C.M. and Paktunc, D.A., 2006: Metal emissions from a Cu smelter, Rouyn-Noranda, Québec: characterization of particles sampled in air and snow. Geochemistry: Exploration, Environment, Analysis. 6(6):147–162.

Zender, C.S., Brian, H. and Newman, D., 2003: Mineral Dust Entrainment And Deposition (DEAD) model: description and 1990s dust climatology. *J. Geophys. Res*. 107 (D24): 4416. doi: 10.1029/2002JD002775.

Zheng, Y., Zhao, T.L., Che, H.Z., Liu, Y., Han, Y.X., Liu, C., Xiong, J., Liu, J.H. and Zhou, Y.K., 2016: A20-year simulated climatology of global dust aerosol deposition. *Sci. Total Environ*. 557: 861-868, Doi:10.1016/j.scitotenv.2016.03.086

Zhou, Z., Dionisio, K.L., Verissimo, T.G., Kerr, A.S., Coull, B., Arku, R.E., Koutrakis, P., Spengler, J.D., Hughes, A.F., Vallarino, J., Agyei-Mensah, S. and Ezzati, M., 2013: Chemical composition and Sources of Particle Pollution in Affluent and Poor Neighbourhoods of Accra, Ghana. *Environ. Res. Letters*, (8). doi:10.1088/1748-9326/8/4/044025.

Zhou, Z., Dionisio, K.L., Verissimo, T.G., Kerr, A.S., Coull, B., Howie, S., Arku, R.E., Koutrakis, P., Spengler, J.D., Fornance, K., Hughes, A.F., Vallarino, J., Agyei-Mensah, S. and Ezzati, M., 2014: Chemical Characterization and Source Apportionment of Household Fine Particulate Matter in Rural, Peri-urban, and Urban West Africa. *Environ. Sc. & Techn*. 48 (2): 1343-1351.

CHAPTER 3

Results: Spatial variability of PM_{10}, $PM_{2.5}$ and PM chemical components in an industrialized rural area within a mountainous terrain

3.1 Paper overview

There has been growing interest in the exposure and health implications of PM. Many studies have focused on the acute respiratory effects (WMO, 2013) and more recently, studies have examined the long-term and chronic effects of air pollution on the cardiovascular and respiratory systems (Thurston, 2017). An increasing body of evidence suggests that PM also has an adverse effect on pregnancy outcomes (Woodruff *et al*., 2009). Therefore, it is important to know whether some locations have higher PM concentrations than others. Characterisation of the spatial variation of PM and PM components is crucial to enable a thorough understanding of the formation, transport and accumulation of PM in the atmosphere; such knowledge will aid in air quality monitoring and management (Zheng *et al*., 2013).

3.1.1 Layout of the study area

The GTM is mainly rural but there has been an increase in the number of urban areas such as Steelpoort and Burgersfort. The municipality encompasses several potential pollution sources such as mines, crusher plants, agricultural farms, brick manufacturing, and smelters. Figure 3.1a shows the location of the GTM in South Africa and Figure 3.1b show residential areas (names in black) and potential pollution sources in the study area located in the GTM. Site 1 is located on an agricultural farm about 2.5 km west south-west of X-Strata smelter, and 1.4 km east of a residential area. Site 2 is in a residential are about 7.9 km north north-east of X-Strata smelter and 4 km west south-west of Samancor smelter. Site 3 is in a residential area (closer to

the main road) about 2 km north north-east of Samancor smelter and north of Silicone mine. Site 4 is in a residential area (closer to the main road) about 7 km south-east of ASA smelter and 4 km north-east of platinum mine. Site 5 is in a residential area about 1.3 km north north-east of ASA smelter and 3.5 km north north-east of a chrome mine. Site 6 is in a residential area about 10 km north-west of ASA smelter and 1.4 km west north-west of a platinum mine.

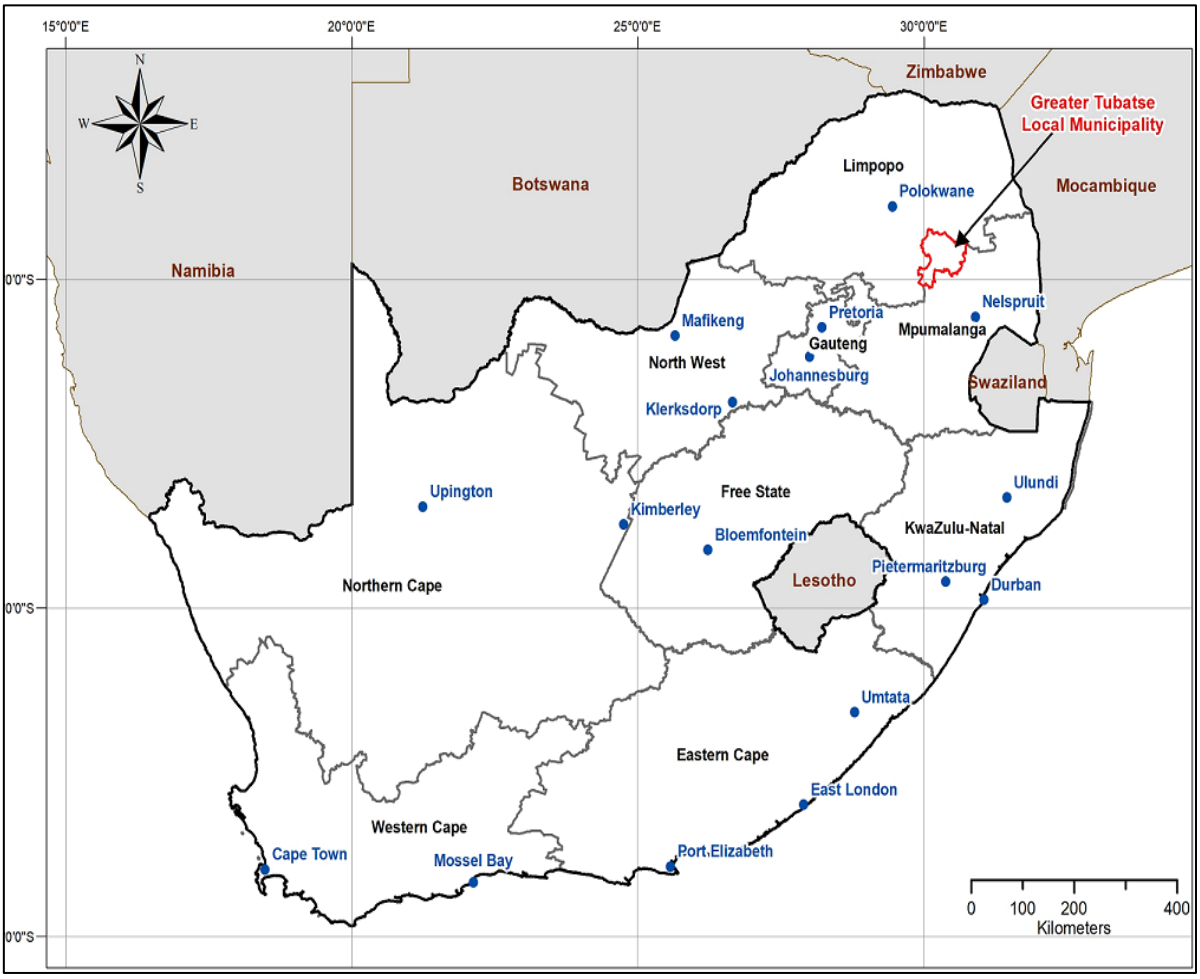

Figure 3.1. Location of the Greater Tubatse Municipality in Limpopo, South Africa.

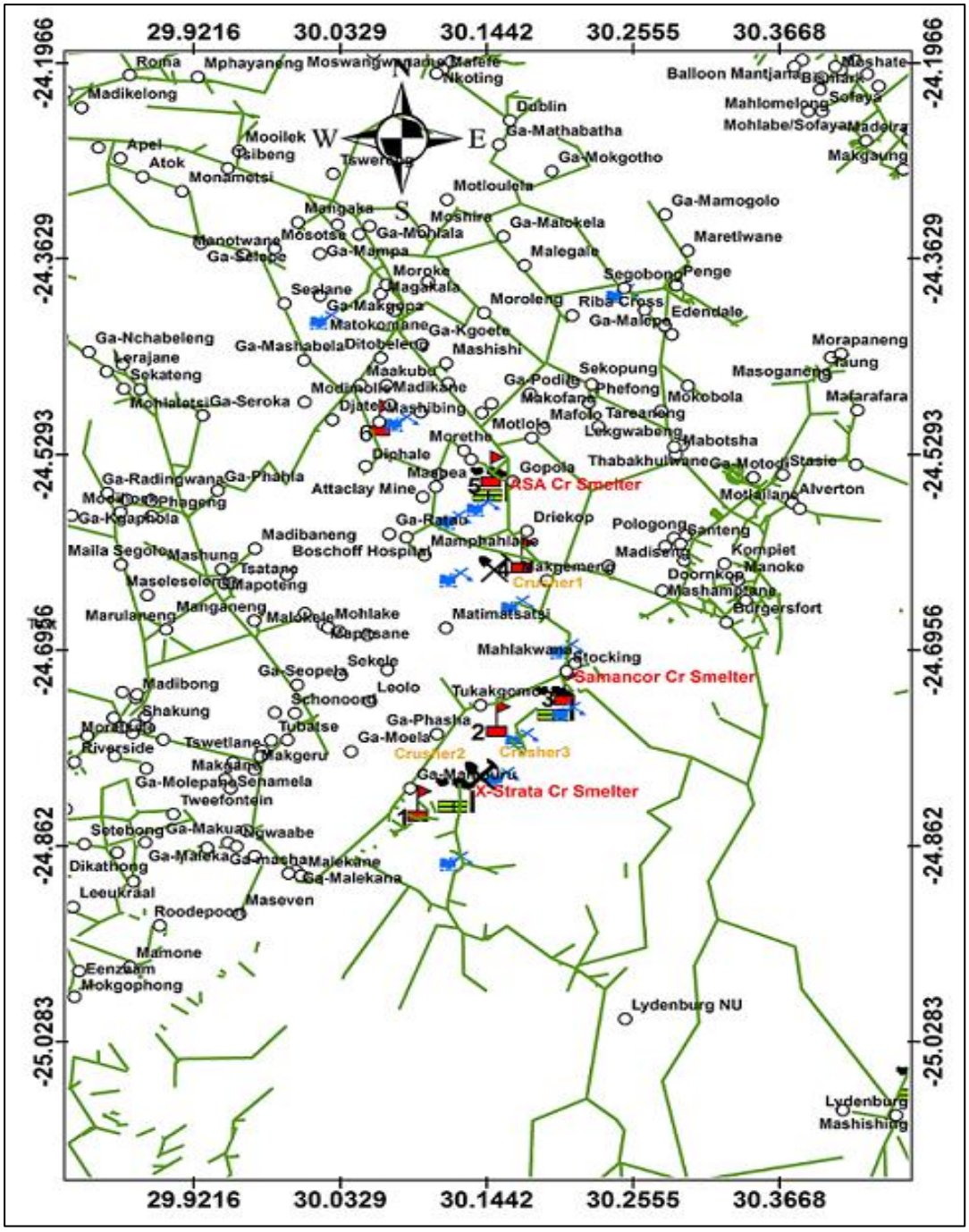

Figure 3.2. Air pollution sources in the Greater Tubatse Municipality. Smelters (green), mines (blue), road network (green lines), crusher plants (black cross), and sampling sites (red flags). Residential settlement names are given in black.

3.1.2 Wind profile of the stud area

Wind is an atmospheric factor that affects air pollution. Windy conditions disperse atmospheric pollutants and dilute them with distance. Strong winds may cause pollution problems farthest

downwind from the pollution source (Rohli and Vega, 2015). Figure 3.2 shows the horizontal annual wind profile for the GTM study area. The white arrows (direction from which the wind is blowing) indicate that strong winds (long tail from the arrow) are easterly to north-easterly with moderate winds coming from the north. Therefore, easterly and north-easterly winds will be effective in distributing pollutants to the west and south-west of the study area.

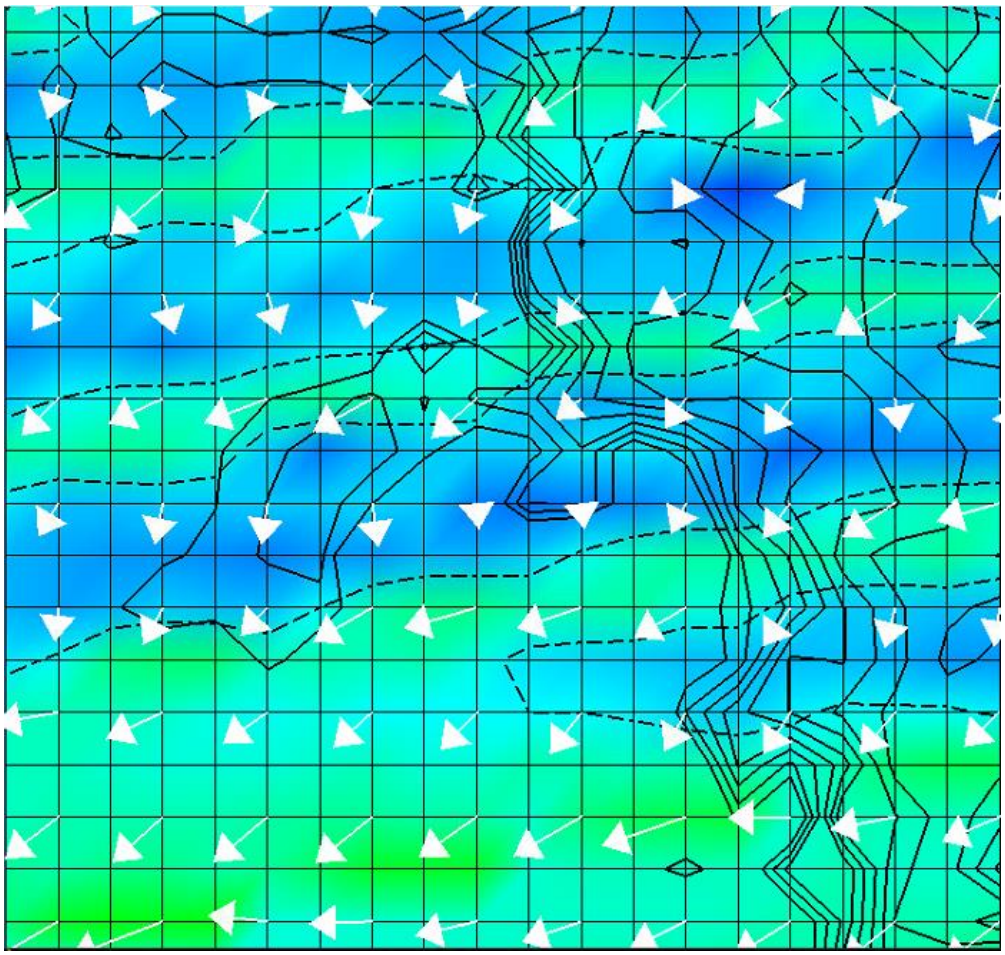

Figure 3.3. Horizontal annual wind pattern of the study area with high wind speed indicated by green colour and low wind speed indicated by blue colour.

3.1.3 Methodology used in the research article

This research article considers the use of passive sampling as a method of collecting PM data in remote rural areas without adequate electricity supply. It further uses Computer Controlled Electron Microscopy with energy-dispersive X-ray spectroscopy (CCSEM-EDS) to analyse the chemical composition of the collected PM samples. The spatial variation of $PM_{2.5}$, PM_{10} and

PM chemical components was determined using the Inverse Distance Weighing (IDW) tool in Geographic Information System (GIS) and the coefficient of divergence statistical tools. The relationship between PM_{10} and meteorological parameters was tested using monthly averaged data.

Although several studies have been done locally on the spatial variation of PM_{10} and $PM_{2.5}$, there has never been (to the best of the author's knowledge) a study on the spatial variability of PM chemical components. Therefore, this study sheds light on how PM toxicity varies spatially and assists in understanding possible PM health effects. The study also introduces UNC passive samplers as an alternative to collecting PM data for assessing pollution levels in areas without active monitoring equipment.

3.1.4 Suggested improvements to the research article

Several improvements could be made to this work. For example, by using the hourly data in determining the relationship between PM_{10} and meteorological parameters. Secondly, by including the annual wind profiles of the area to help in the discussion on PM_{10} distribution, and also to mention that the UNC passive samplers collect total suspended particles from which the concentrations PM_{10}, $PM_{2.5}$ and PM chemical components were determined using CCSEM. Other improvements include the use of more recent data on the climate of the GTM that could be obtained from Mpandeli *et al*. (2015) and also to states the accuracy of UNC passive samplers on PM measurements was discussed in other studies such as Shirdel *et al*. (2018).

3.2 Contribution to the thesis

This manuscript contributes to the thesis by pursuing four objectives: objective 1 'To collect particulate matter samples using UNC gravimetric passive samplers' that seeks to find a simple and cost-effective way of monitoring air pollution particularly in remote areas with lack of electricity supply in South Africa. The passive samplers proved to be useful tools to monitor PM in particular PM with aerodynamic diameter > 2.5 $\mu g.cm^{-3}$. The UNC passive samplers show limitations in providing reliable $PM_{2.5}$ concentration measurements when samplers are deployed for a longer period due to evaporation of species such as nitrates and sulphates.

Therefore, this finding provides a platform to increase the network of PM monitoring (especially ≥ $PM_{2.5}$) for assessment purposes in addition to compliance monitoring using continuous monitors.

The second objective 2 'to characterize the chemical composition of PM using Computer Controlled Scanning Electron Microscopy (CCSEM)' was pursued. The results show that PM in the GTM is dominated by Carbon-rich (C-rich), Cr-rich, Iron-rich (Fe), FeCr-rich, Silicon (Si-rich), Calcium-rich (Ca-rich), Silicon/Aluminium/Iron-rich (SiAlFe-rich), Silicon/Magnesium-rich (SiMg-rich) and Silicon/Aluminium-rich (SiAl-rich). Monitoring of the individual species which make up PM is still an emerging field in South Africa and needs to be intensified to develop the best speciation network. This will assist in classification of airsheds into groups with similar PM composition and concentration and will also be useful for source apportionment studies.

The third objective 3 'to characterize the spatial distribution of $PM_{2.5}$, PM_{10}, and PM chemical components' was undertaken to determine the extent to which these particles vary spatially within the GTM airshed. The results showed that the concentrations of $PM_{2.5}$, PM_{10} and PM chemical components were spatially heterogeneous with high heterogeneity observed near the industrial sources for Iron/Chromium-rich (FeCr-rich) and Chromium-rich (Cr-rich) particles and Si containing particles. The statistical coefficient of divergence values also showed that the highest heterogeneity was near the industrial sources. The study showed a need to monitor PM at sites located near big traffic congestion, residential areas, and near industrial facilities (i.e. mines, smelters and crusher plants). These findings also show an important need to gain an understanding of characterisation of the aerosols spatially. This will ensure that limited resources are adequately used in monitoring and managing environmental sensitive areas.

The fourth objective 4 'to determine the relationship between calculated mixing height, Monin-Obukhov length, ventilation coefficient and air pollution potential and the PM_{10} distribution' was pursued to determine whether the average monthly data will be useful in evaluating the effect of meteorological parameters on the distribution of PM_{10} in a complex terrain. The evidence from the study indicated that there was little or no correlation between PM_{10} and meteorological parameters such as the mixing height, Monin-Obukhov length, air pollution potential, and coefficient of divergence. However, the ventilation coefficient (VC) was able to

predict the areas for high PM_{10} concentrations at the valley openings where the VC is possibly influenced by the impact of pressure gradient on the wind strength. Lack of hourly PM_{10} data and the use of synoptic data from model data (without hourly ground level data) could be the reason for the observed relations. Therefore, for future research studies on the behaviour of pollutants in a complex terrain, the emission source strength and hourly data from a network of meteorological surface stations and balloon soundings within the valley floor and adjacent slopes must be used in the analysis. The findings suggest that investment in ground meteorological and air pollution monitoring equipment in areas with complex terrain is of high importance.

In conclusion, findings of the spatial variation of PM may assist in identifying optimal locations for monitoring PM pollution for future impact assessment studies. These findings provide scientific input for government policies directed to reduce or eliminate the particulate matter pollution. An important policy implication of this study is to extend a network of passive samplers to determine the level of pollution in areas with no continuous monitoring to assist in environmental planning and health impact assessment.

3.3 Role of the candidate

Cheledi E. Tshehla performed all the sampling and shipping of the samples to RJ Lee laboratories. The laboratory analysis of PM chemical components was performed by RJ Lee group. Cheledi E. Tshehla also processed all data sets, performed the GIS and statistical analysis of all the data and wrote the first draft of the manuscript. The evaluation and interpretation of the results were performed in close cooperation with the Dr C.Y. Wright (co-author).

3.4 Publication status

Tshehla C. E, and Wright C.Y. 2019. Spatial variability of PM_{10}, $PM_{2.5}$ and PM chemical components in an industrialized rural area within a mountainous terrain. *S. Afr. J Sci.* 115(9/10): 1-10. DOI: https://doi.org/10.17159/sajs.2019/6174

3.5 References

Mpandeli, S., Nesamvuni, E. and Maponya, P., 2015: Adapting to the Impacts of Drought by Smallholder Farmers in Sekhukhune District in Limpopo Province, South Africa. *J. Agr. Sci.* 7(2): 1916 – 9760.

Rohli, R.V. and Vega, A.J., 2015: Climatology, 3rd Edition. Jones & Bartlett Learning, Burlington, pg 310 – 311.

Shirdel, M., Andersson, B.M., Bergdahl, I.A., Sommar, J.N., Wingfors, H. and Liljelind, I.E., 2018: Improving the UNC Passive Aerosol Sampler Model Based on Comparison with Commonly Used Aerosol Sampling Methods. *Annals of Work Exposures and Health*, 62 (3): 328 – 338. https://doi.org/10.1093/annweh/wxx110

Thurston, G.D., Kipen, H., Annesi-Maesano, I., *et al*., 2016: A joint ERS/ATS policy statement: what constitutes an adverse health effect of air pollution? An analytical framework. *Eur. Respir. J.* 49:1600419. https://doi.org/10.1183/13993003.00419-2016.

World Meteorological Organization (WMO), 2013: Health effects of particulate matter: Policy implications for countries in Eastern Europe, Caucasus and central Asia. Available from: http://www.euro.who.int/__data/assets/pdf_file/0006/189051/Health-effects-of-particulate-matter-final-Eng.pdf?ua=1

Woodruff, T.J., Parker, J.D., Darrow, L.A., Slama, R., Bell, M.L., Choi, H., Glinianaia, S., Hoggatt, K.J. Karr, C.J., Lobdell, D.T. and Wilhelm, M., 2009: Methodological issues in studies of air pollution and reproductive health. *Environ. Res.* 109: 311-320.

Zheng, J., Che, W., Zheng, Z., Chen L. and Zhong L., 2013: Analysis of Spatial and Temporal Variability of PM10 Concentrations Using MODIS Aerosol Optical Thickness in the Pearl River Delta Region, China. *Aerosol and Air Quality Research*, 13(3):862-876.

Manuscript 1

AUTHORS:
Cheledi Tshehla[1,2]
Caradee Y. Wright[1,3]

AFFILIATIONS:
[1]Department of Geography, Geoinformatics and Meteorology, University of Pretoria, Pretoria, South Africa
[2]South African Weather Service, Pretoria, South Africa
[3]Environment and Health Research Unit, South African Medical Research Council, Pretoria, South Africa

CORRESPONDENCE TO:
Cheledi Tshehla

EMAIL:
Cheledi.Tshehla@weathersa.co.za

DATES:
Received: 28 Mar. 2019
Revised: 14 May 2019
Accepted: 05 June 2019
Published: 26 Sep. 2019

HOW TO CITE:
Tshehla C, Wright CY. Spatial variability of PM_{10}, $PM_{2.5}$ and PM chemical components in an industrialised rural area within a mountainous terrain. S Afr J Sci. 2019;115(9/10), Art. #6174, 10 pages. https://doi.org/10.17159/sajs.2019/6174

ARTICLE INCLUDES:
☒ Peer review
☐ Supplementary material

DATA AVAILABILITY:
☐ Open data set
☐ All data included
☒ On request from author(s)
☐ Not available
☐ Not applicable

EDITOR:
Priscilla Baker

KEYWORDS:
complex terrain, passive samplers, mixing height, air pollution potential

FUNDING:
None

Spatial variability of PM_{10}, $PM_{2.5}$ and PM chemical components in an industrialised rural area within a mountainous terrain

We describe the measurement and spatial variability of particulate matter (PM) chemical composition, PM_{10} and $PM_{2.5}$ in the Greater Tubatse Municipality, South Africa. Monthly samples were collected over 12 months (July 2015 to June 2016) using the inexpensive and easy to operate passive samplers of the University of North Carolina. Sites for sample collection were located at private residences, a church, a hospital and a school. Concentrations of PM_{10}, $PM_{2.5}$ and PM chemical components were determined using computer-controlled scanning electron microscopy with energy-dispersive X-ray spectroscopy. The annual observed concentrations at all sites were below the South African National Ambient Air Quality Standards of 40 $\mu g/m^3$ for PM_{10} and 25 $\mu g/m^3$ for $PM_{2.5}$. The Cr-rich and CrFe-rich particles showed substantial heterogeneity with high concentrations observed near the chrome smelters, and Si-rich particles were highest near the silicon mine. SiAl-rich particles were highest at sites close to busy roads, while SiAlFe-rich particles were less spatially distributed. The low spatial variability of SiAlFe-rich particles indicates that these elements are mainly found in crustal material. Using the synoptic meteorological parameters of The Air Pollution Model, we were unable to effectively determine correlations between PM_{10} and mixing height, Monin–Obukhov length, air pollution potential, or coefficient of divergence.

Significance:

- We have shown that the use of University of North Carolina passive samplers coupled with computer-controlled scanning electron microscopy is effective in determining the chemical composition of PM.
- The use of passive samplers is a cheap and effective method to collect data in remote areas of South Africa which have limited or no electricity supply.
- Assessment of the spatial distribution of PM and PM chemical components can assist in the development of effective air quality management strategies.

Introduction

Airborne particulate matter (PM) is a term used to describe solid particles or a mixture of solid and liquid droplets suspended in the air.[1] The particle mixture may vary in size distribution, composition and morphology and may be in the form of sulfates, nitrates, ammonium and hydrogen ions, trace elements (including toxic and transition metals), organic material, elemental carbon (or soot) and crustal components.[2,3] PM may originate from either primary or secondary sources. Primary particles are those directly emitted into the atmosphere from sources such as road vehicles, coal burning, industry, windblown soil, dust and sea spray. Secondary particles are particles formed within the atmosphere by chemical reactions or condensation of gases. The major contributors of secondary particles are sulfate and nitrate salts formed from the oxidation of sulfur dioxide and nitrogen oxides, respectively.[4] Ambient PM has long been associated with adverse effects on respiratory, cardiovascular and cardiopulmonary health.[5-7] The severity of such health effects depends largely on the size, concentration and composition of inhaled particles.[8] PM pollution emanating from industrialisation has serious environmental impacts mainly because of the release of toxic substances and trace metals into the atmosphere.[9]

Industrialisation and urbanisation of rural areas can lead to the emission of large amounts of PM and chemical elements into the atmosphere. These emissions result in widespread air pollution problems[10], and these problems have proved to be more regional and complex with time[11]. The Greater Tubatse Municipality (GTM) in South Africa is home to a large number of people and a variety of anthropogenic pollution sources such as chrome smelters, mines (for chrome, silicon and platinum), agricultural operations, biomass combustion, brick manufacturing, vehicles and unpaved roads, which can contribute to PM emissions. Differences in the composition of particles emitted by these sources may lead to spatial heterogeneity in the composition of the atmospheric aerosols. Hence, understanding the spatial variability of PM is of great importance for environmental planning and management purposes by both the industries and governing authorities. Therefore, this study will lay a foundation for developing effective intervention strategies to reduce PM emissions in the GTM. In South Africa, PM is only regulated in two size fractions (PM_{10} and $PM_{2.5}$). However, to date, there are no ambient air quality standards for elemental particles. The list of metals regulated under the *National Environmental Management: Act No. 39 of 2004* should be expanded to include metals such as chromium, iron, arsenic, copper, cobalt, manganese and other metals that have been identified[12] to have the potential to cause environmental health threats.

Apart from air pollution challenges due to anthropogenic activities, South Africa has a varying topography ranging from flat to complex terrain that can have differing effects on the dispersion of air pollutants. The shape of the landscape plays an important role in trapping or dispersing pollutants. Air pollution in mountain valleys tends to be higher in colder months than in warmer months.[13] The distribution of pollutants depends largely on the meteorology and the landscape of the area. Surface heterogeneity plays a major role in the interaction between the atmosphere and the underlying surface, and it affects moist convection, and systematically produces responses in both local circulation and regional climate.[14-18] Complex terrain such as that of the GTM is characterised by high mountains and steep inclinations. In this

type of terrain, the wind flow is very hard to predict. However, the steep slopes give rise to thermally induced circulations like mountain valley breezes which strongly modify the characteristics of synoptic flow.[19-22] The ability of the atmosphere to disperse pollutants depends on the local circulations, mixing height, stability of the atmosphere and wind strength. However, the complex nature of the terrain in the GTM and the lack of electricity supply in some areas of the municipality, makes it impossible to rely only on a network of continuous ambient air pollution monitoring.

A number of methods have been developed over the years to collect and analyse air pollutant samples, using both active and passive techniques. The passive sampling techniques involve non-active means such as gravitational settling to collect air samples onto the substrate. This method of sampling is cheaper than active sampling and allows for the deployment of more samplers to evaluate air pollution spatially.[23] The GTM has only one air quality monitoring station that is not sufficiently well maintained to produce good quality data. As a result, a network of passive samplers was used to determine the spatial variation of $PM_{2.5}$ and PM_{10}, which in future can be used as a baseline for the deployment of active samplers in the area.

Mountain winds

Wind circulations in the free atmosphere above the mountains and valleys are governed by pressure gradients between large circulation systems.[24] The lower troposphere interacts with mountains, valleys and vegetation that in turn alter the circulation patterns. Mountainous terrain has a high degree of topographical variation and land-cover heterogeneity.[25] This variation in topography influences the atmosphere in two ways.[26] The first is in the form of momentum exchange between the atmosphere and the surface that occurs as a result of flow modification by mountains in the form of mountain lee waves, flow channelling and flow blocking.[27] The second effect involves energy exchange between the terrain and the atmosphere. The thermally induced winds depend on the temperature differences along the mountain plains systems and the strength of the synoptic systems and the cloud cover, with weak synoptic systems and cloud-free atmosphere producing more pronounced winds.[20,28] Mountain winds blow parallel to the longitudinal axis of the valley, directed up-valley during daytime and down-valley during night time. The circulation is closed above the mountain ridges by a return current flowing in the reverse direction. The actual development of thermally driven winds is often complicated by the presence of other wind systems developed on different scales.[22,28] Anabatic flows are more temporally limited during wintertime than summertime due to the shorter exposure period to sunlight.[29]

Mixing height

Mixing height (MH) is the height to which relatively vigorous mixing occurs in the lower troposphere. Temperature inversions are most common in mountainous terrain where cool mountain air sweeps down into the valley at night, below the warm, polluted air. This inversion keeps the emitted pollutants close to the ground instead of allowing them to disperse into the atmosphere. A flow of thermal or synoptic origin channelled inside a mountain valley can transport plumes along the valley floor, thus limiting crosswind dispersion. Pollution stagnation in the bottom of the valleys can be favoured by the temperature inversion that develops inside the valley during the night and is destroyed by the growing convective boundary layer in the morning.[30] The thermally induced MH influences the concentration and transport of pollutants[31], and is used in air quality models to determine atmospheric pollutant dispersion[32-34]. However, in mountainous terrain, processes such as MH and mountain slope winds are coupled together[35] to transport air pollutants across mesoscales to synoptic scales[36]. Research by De Wekker and Kossmann[27] has illustrated that the dispersion of pollutants in mountainous terrain does not depend on the boundary layer but rather on the thermally induced mountain slope winds.

Monin–Obukhov length

The Monin–Obukhov (MO) similarity theory has been applied in air pollution modelling for determining the dispersion of air pollutants. The MO measures the stability of the atmosphere, with stable atmospheric conditions favouring higher pollutant concentrations and unstable conditions allowing the dispersion of pollutants and hence lowering pollutant concentrations.[37] However, the MO is restricted to horizontal homogeneous terrains where there are no sudden roughness changes (such as in forested area, hilly or mountainous terrain) to modify the velocity profile and turbulent transport of heat and momentum.[38] Figueroa-Esspinoza and Salles[38] and Grisogono et al.[39] reported that MO theory is unable to account for the transport of pollutants in mountain valleys because the flow dynamics of the valleys are governed by anabatic and katabatic flows. These flows are generated by the mountain slopes and are normally decoupled from the synoptic flows above.

Ventilation coefficient

Gross[40] defined the ventilation coefficient (VC) as the product of the MH and the average wind speed, which can also be defined as a measure of the volume rate of horizontal transport of air within the MH per unit distance normal to the wind. Iyer and Raj[41] describe the VC as a measure of the atmospheric condition that gives an indication of the air quality and air pollution potential. When the coefficient is higher, it is an indication that the atmosphere is able to disperse air pollutants effectively, resulting in a better state of air quality, whereas low ventilation indicates poor pollutant dispersion resulting in high pollution levels. The VC varies diurnally during summer and winter with high coefficients observed in the late afternoon and low values in the early mornings. Winter coefficients are also lower than those in summer due to low MH and reduced wind speeds in winter,[42,43] and the influence of the dominant anti-cyclones that are experienced over southern Africa during the winter months.

Air pollution potential

Gross[40] and Nath and Patil[44] describe air pollution potential (APP) as the measure of the inability of the atmosphere to adequately dilute and disperse pollutants emitted into it. The APP depends on meteorological conditions such as the MH, wind speed, atmospheric stability and solar radiation.[45] Once the pollutants are emitted into the atmosphere, their transportation is dependent on the mean wind speed which carries the pollutants away from the source to their sinks, and their convective mixing is dependent on the vertical temperature gradient.[44] The higher values of APP indicate that the atmosphere is unfavourable for the dilution and dispersion of pollutants[46] and indicate high concentrations of observed pollutants at the receiving environment. The low values of APP indicate that the atmosphere is conducive for the dispersion of pollutants which will result in low concentrations on the receiving environment.[44] The APP can be used as a management tool for siting of ambient air quality monitoring stations and for land-use planning in the development of new residential areas and zoning of new industrial sites.

The aim of this work was to determine the spatial variability of PM_{10}, $PM_{2.5}$ and PM chemical composition. Further analysis of the MO theory, MH, VC and the atmospheric pollution potential was performed to determine whether these factors have any influence on the PM_{10} concentrations in the study area.

Methods

Study area

Sampling of PM was undertaken in a rural area of the GTM in Limpopo Province, South Africa (Figure 1). The main towns in the area are Steelpoort and Burgersfort which are sustained through economic activities such as mining and smelting of chromium ores. Furthermore, there are agricultural and forestry activities and transportation that also add to the economic activities in the area. Most of the households in the area are dependent on wood burning for space heating and cooking. The GTM has a complex terrain with high mountains and steep inclinations. The elevation of the surface area is approximately 740 m above sea level with the surrounding mountains extending to a height of approximately 1200–1900 m above sea level. The area is located in the subtropical climate zone where the maximum and minimum average temperatures are 35 °C and 18 °C, respectively in summer, and 22 °C and 4 °C, respectively in winter.[46] The annual rainfall for the area ranges between 500 mm and 600 mm.[47]

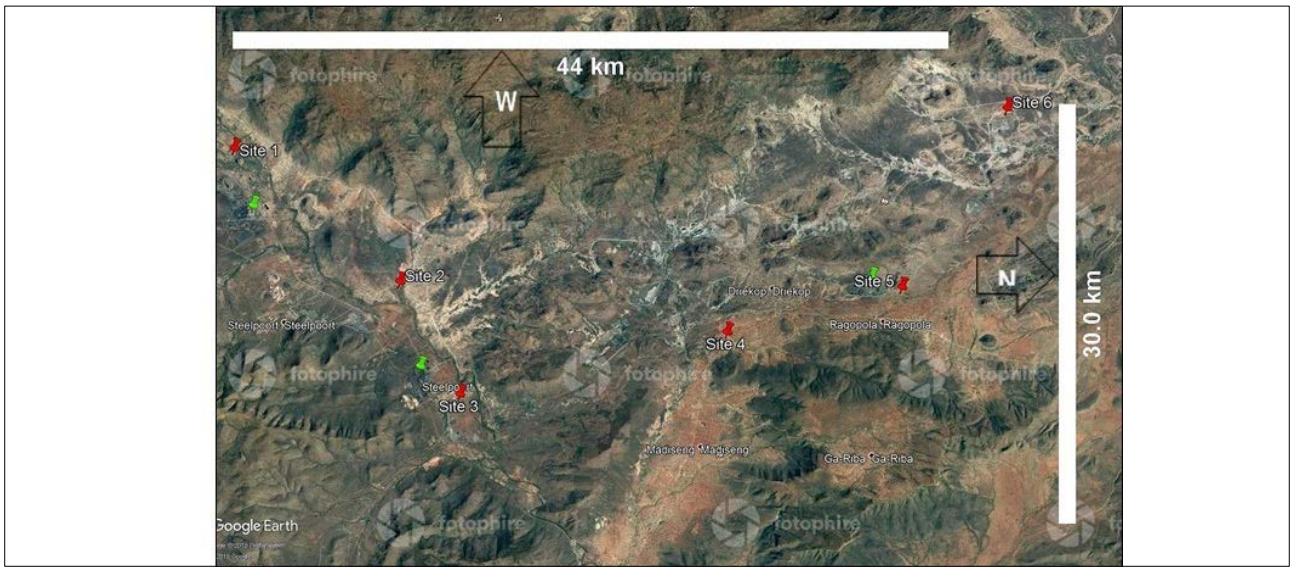

Figure 1: Google Earth map of the study area showing passive sampler locations (indicated by red pins) and smelters (indicated by green pins).

Site selection

The locations of the monitoring sites were selected to optimise spatial sampling for exposure assessment. A sequential sampling technique[48,49] was used to design an optimal sampling network of six sites in the GTM. This technique is based on extended knowledge of the area to be sampled and factors controlling the distribution of pollutants. These factors could be the terrain and various phenomena like meteorological conditions and the chemistry of pollutants.[50] The number of sites selected was influenced by budgetary constraints due to costs associated with laboratory analysis of samples. The sites were located at private residences, a church, a hospital and a school, to ensure a secure area with easy access for site visits.

Sampling and sample analysis

The University of North Carolina passive samplers designed by Wagner and Leith[23] and housed in a protective shelter designed by Ott et al.[51] were deployed at six sites for PM sampling. Ott et al.[51] designed the shelter to shield the passive sampler from precipitation and to minimise the influence of wind speed on particle deposition.[52] The samplers consist of a scanning electron microscopy stub, a collection substrate and a protective mesh cap.[53] The samplers were deployed for a period of ±30 days from July 2015 to June 2016, except for the months of August–September and September–November for which they were deployed for a period of >35 days. The longer sampling periods were selected to ensure that there was sufficient particle loading on the samplers.[52]

The $PM_{2.5}$ and PM_{10} concentrations and the elemental composition of individual particles deposited on the passive sampler were determined by computer-controlled scanning electron microscopy with energy-dispersive X-ray spectroscopy (CCSEM-EDS). Before sample analysis by photoemission electron microscopy (according to the method of Hopke and Casuccio[54]), the samples were coated with a thin layer of graphitic carbon under vacuum to bleed off the charges induced by the electron beam in the SEM. The photoemission electron microscopy was operated at 20 kV.[52] We used the method of Lagudu et al.[53] to determine the chemical composition of PM using CCSEM analysis. Briefly, CCSEM scans the collection substrate of the SEM stub for individual particles and provides fluoresced X-ray spectra and an image of each particle. The method involves rastering the electron beam over the sample while monitoring the resultant backscattered signal. At each point, the image intensity is compared to a pre-set threshold level. Once a coordinate is reached at which the signal is above the threshold level, the electron beam is driven across the particle in a pre-set pattern to determine the size of the particle. Upon measurement of the particle size, the elemental composition of the particle is then determined by collection of characteristic X-rays using EDS techniques. Individual particles characterised during CCSEM analysis are then grouped into particle classes based on their elemental composition. The individual particle masses are finally calculated by multiplying the assigned density of the particle by its volume. Each particle is assigned a density based on common oxide in proportion to the elements present as determined by the EDS analyses.[53] The particle classes obtained from the analysis include carbon-rich (C-rich), chromium-rich (Cr-rich), iron-rich (Fe-rich), iron/chromium-rich (FeCr-rich), silicon-rich (Si-rich), calcium-rich (Ca-rich), silicon/aluminium/iron-rich (SiAlFe-rich), silicon/magnesium-rich (SiMg-rich) and silicon/aluminium-rich (SiAl-rich).

Data analysis

The coefficient of divergence (COD) was used to characterise the spatial variation of PM_{10}, $PM_{2.5}$ and PM chemical components. The COD is defined as:

$$\mathrm{COD} = \sqrt{1/p \sum_{i=1}^{p} \left(\frac{x_{ij} - x_{ik}}{x_{ij} + x_{ik}}\right)^2} \qquad \text{Equation 1}$$

where x_{ij} and x_{ik} are the concentration for sampling interval *i* at sites *j* and *k,* respectively, and *p* is the number of sampling intervals. In terms of spatial distribution, a COD of 0 means that there are no differences between the observed concentrations at the two sites, while a value approaching 1 indicates that the two sampling sites are different.[53,55] Graphical analysis was also used in determining spatial variation. The inverse distance weighted (IDW) interpolation within the mapping software (ArcMap version 10.0) was applied to the annual and monthly concentrations of PM_{10}, $PM_{2.5}$ and the PM chemical components given that the number of sites was restricted by the cost. When data are sparse, the underlying assumptions about the variation among samples may differ and the use of a spatial interpolation method and parameters may become critical.[56,57] The performance of the spatial interpolation method is better when the sample density is higher.[58-60] However, the accuracy of regression modelling is not really dependent on the sampling density, but rather on how well the data are sampled and how significant the correlation is between the primary variable and secondary variable(s).[61] To predict a value for any unmeasured location, IDW uses the measured values surrounding the prediction location. The measured values closest to the prediction location have a greater influence on the predicted value than those farther away. IDW assumes that each measured point has a local influence that diminishes with distance. It gives greater weight to points closest to the prediction location, and the weight diminishes as a function of distance.[62]

APP calculation

The Air Pollution Model (TAPM) was used in the calculation of parameters needed to determine the APP. The dynamic parameters that were calculated included the MO length, wind velocity, planetary boundary layer height and turbulence parameters. The APP was determined according to the method of Swart[63] using Equation 2:

$$P(APP) = P(|\bar{V}|)P(H)P(L) \quad \text{Equation 2}$$

where P(APP) is the air pollution potential index, $P(|\bar{V}|)$ is the wind speed, P(H) is the planetary boundary layer and P(L) is the atmospheric stability. The APP index for a specific area can be classified as being favourable, moderate or unfavourable depending on the conditions set out for the parameters that are the driving force behind the APP calculation, as shown in Table 1.

Table 1: Parameters and limits for air pollution potential (APP) calculation

Parameter	Unfavourable	Moderate	Favourable
Wind speed	0–2 m/s	2–5 m/s	>5 m/s
Mixing height	0–400 m	400–1000 m	>1000 m
Monin–Obukhov length	0 to 200 m	>1000 m	0 to -200 m

In this study, APP, MO, MH and VC values were calculated and correlated with the PM measurement values collected during the sampling campaign.

Results and discussion

Figure 2 shows the annual concentrations of PM_{10}, $PM_{2.5}$ and PM chemical components. The annual concentrations of PM_{10} were 38.11 μg/cm^3 at Site 3, 31.28 μg/cm^3 at Site 2, 31.02 μg/cm^3 at Site 1, 24.65 μg/cm^3 at Site 5, 24.10 μg/cm^3 at Site 4, and 20.98 μg/cm^3 at Site 6. Annual PM_{10} concentrations were below the South African National Ambient Air Quality Standard of 40 μg/cm^3. The $PM_{2.5}$ concentrations are on average lower than the concentrations of SiAl-rich and SiAlFe-rich particles. This finding can be attributed to the fact that some $PM_{2.5}$ particles may have evaporated during the 3–5 week period during which the samplers were deployed in the field. The Fe-rich particles were the least abundant, with an annual average below 1 μg/cm^3 across all sites. The C-rich particles had the same signature as $PM_{2.5}$, with the lowest concentration being around Site 6. The highest concentrations for Ca-rich particles were observed around sampling Site 6 which is located about 1.6 km west-northwest of Marula Platinum Mine, with the lowest concentrations around Site 4 and Site 5. The highest Si-rich, SiMg-rich, SiAl-rich and SiAlFe-rich particle concentrations were observed around sampling Site 3 which is about 1.7 km from the Samancor chrome smelter and 1.9 km from the silicone mine, with the lowest concentrations being observed at Site 6. The highest observed concentrations for FeCr-rich particles were at sampling Sites 3 and 5, and Site 5 is about 2 km from the ASA chrome smelter. The Cr-rich particles were highest at Site 1 and Site 3; Site 1 is about 2.5 km from the Glencore chrome smelter. The annual concentrations of Cr-rich particles across all the sites were above the 0.11 μg/m^3 annual limit set by the New Zealand Ministry of Environment.[64] The highest PM_{10} concentrations were measured during the winter months (May–July) except at Site 6 (Mashegoane) where the highest concentrations were observed during the month of November when there was soil tillage in preparation for crop sowing just before the rainy season. SiAl-rich and SiAlFe-rich particles were the most abundant particles with Fe-rich particles being less abundant. Si-rich, Cr-rich and CrFe-rich particles were more abundant closer to their sources.

Spatial variation

The annual spatial concentration map was generated using geographic information system software (Figure 3). The number of sampling sites was limited due to budgetary constraints, so IDW was used because it does not require a threshold for number of points. The choice of the IDW statistical method proved to be useful as it was able to predict the spatial variation of PM_{10}, $PM_{2.5}$ and PM chemical components in the study area. This output is very important for cash-strapped local authorities that are tasked with the responsibility of managing air quality in their jurisdiction because they can perform this analysis with limited resources. The maps in Figure 3 indicate that there is a distinct spatial heterogeneity in the study area with variability in both low and elevated concentrations being observed at different sites for PM_{10}, $PM_{2.5}$ and PM chemical components. This difference can be attributed to the vast distribution of sources in the area. The highest concentrations for annual PM_{10}, Cr-rich, Fe-rich, Si-rich, SiAl-rich, SiAlFe-rich and SiMg-rich particles were observed around Site 3, which is about 1.7 km from the Samancor chrome smelter and 1.9 km from the Silicone mine, which are located south-southeasterly of the sampling site. The highest Fe-rich, Si-rich and SiMg-rich concentrations were sparsely distributed. Lowest concentrations for the same particles were observed around Site 6. The highest concentrations for $PM_{2.5}$ and C-rich particles were observed around Site 1, and they have similar distribution patterns. The lowest concentrations of PM_{10}, $PM_{2.5}$ and PM chemical components were observed around Site 6, extending to Site 5 and Site 4. The only exception was SiAlFe-rich particles for which the lowest concentrations were observed to the northeast (Site 6) and southeast (Site 1) of the study area. FeCr-rich particles showed highest concentrations closer to the smelters around Site 3 and Site 5.

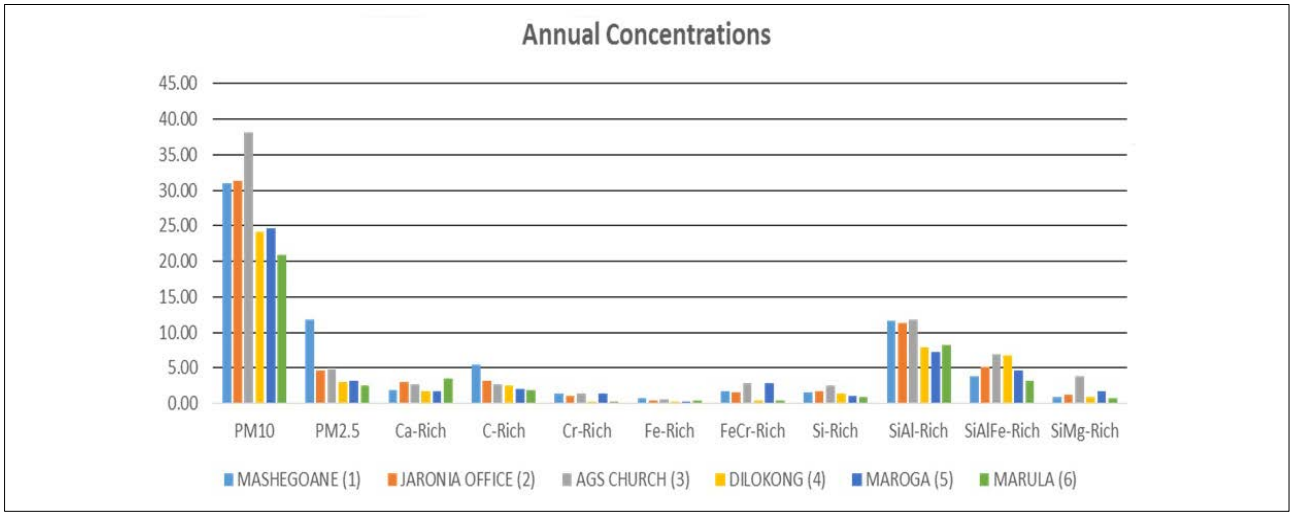

Figure 2: Annual concentrations (μg/cm^3) of PM_{10}, $PM_{2.5}$ and PM chemical components (site number in parentheses).

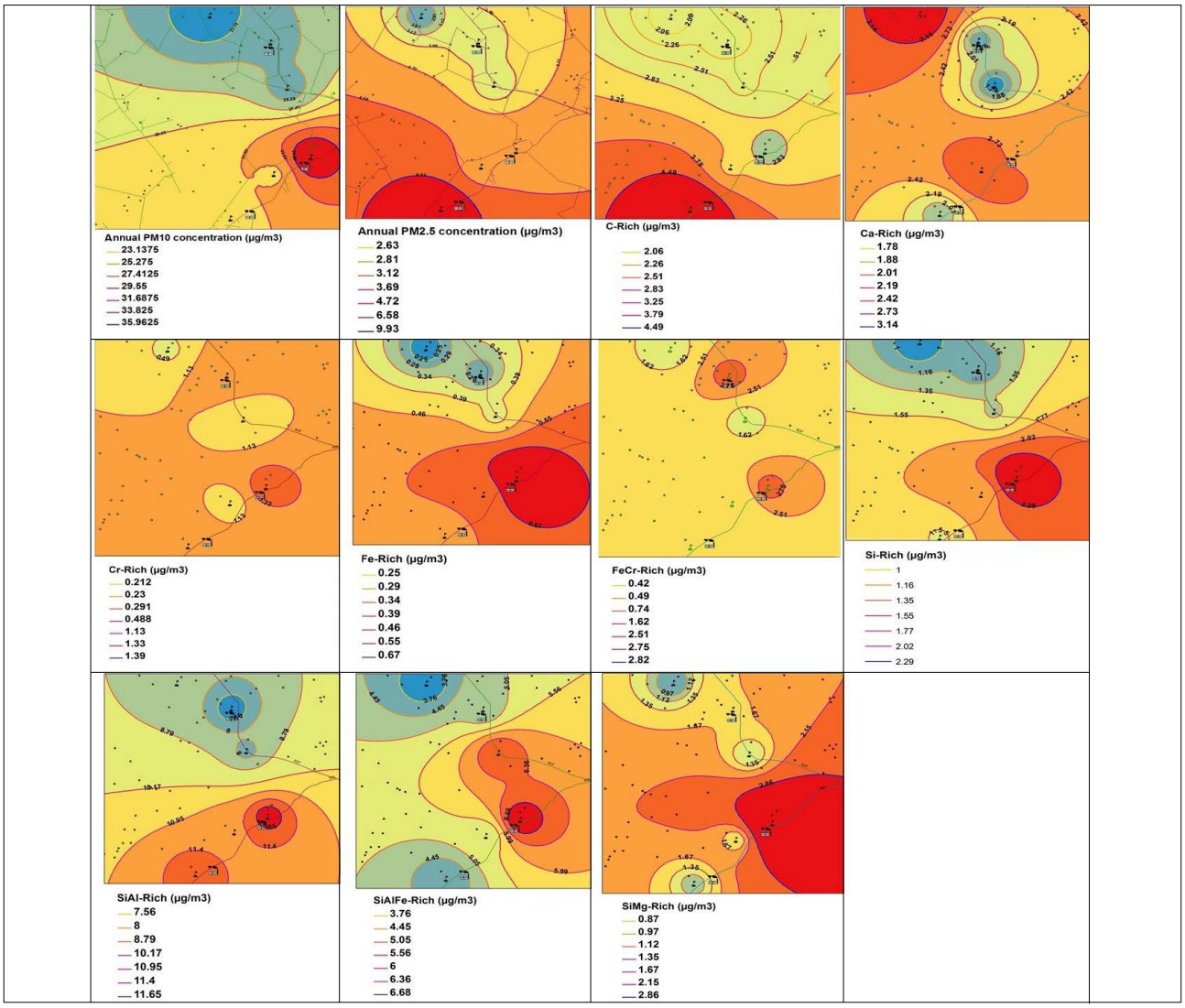

Figure 3: Maps of annual spatial variation for PM_{10}, $PM_{2.5}$, and C-rich, Ca-rich, Cr-rich, Fe-rich, FeCr-rich, Si-rich, SiAl-rich, SiAlFe-rich and SiMg-rich particles. High concentrations are shown in dark red and low concentrations are depicted in blue.

The highest Ca-rich concentrations were observed around Site 6, which is located in an area with black cotton soil. However, because the sites were not equally spaced in the study area, other methods such as the COD and *r* were used to confirm and validate the results of the spatial analysis determined using the geographic information system.

The COD values were calculated (Table 2) to characterise the spatial heterogeneity of PM_{10}, $PM_{2.5}$ and PM chemical components.

Table 2: Results of coefficient of divergence (COD) analysis for Greater Tubatse Municipality

Species	COD
PM_{10}	0.24
$PM_{2.5}$	0.29
C	0.25
Ca	0.38
Cr	0.6
Fe	0.41
FeCr	0.59
Si	0.35
SiAl	0.3
SiAlFe	0.28
SiMg	0.42

COD values higher than 0.2 indicate spatial heterogeneity, while COD values less than 0.1 indicate homogeneity of concentrations. All components in the study area had COD values greater than 0.2, which is an indication that there was a heterogeneous relation observed between the sites in the study area, and is in agreement with the observations in Figure 3. The lowest heterogeneity values for COD ranged from 0.24 to 0.4 and were observed for PM_{10} (0.24), C-rich (0.25), SiAlFe-rich (0.28), $PM_{2.5}$ (0.29), SiAl-rich (0.3), Si-rich (0.35) and Ca-rich (0.38) particles. The moderate to highest COD values were observed for Fe-rich (0.41), SiMg-rich (0.42), FeCr-rich (0.59) and Cr-rich (0.6) particles. The highest COD values were observed for sites located in the vicinity of point source emitters, which indicates that the communities residing in the vicinity of these point sources are more vulnerable to the exposure of these particles than those living further downwind.

Influence of APP, MO, MH and VC on the distribution of PM_{10}

The annual influence of APP, MH, MO and VC on the distribution of PM_{10} concentrations is shown in Figure 4a–d. The highest annual PM_{10} concentrations are centred on Site 3 and distributed more to the east of the sampling site. The highest values for APP (Figure 4a) are centred to the south of the study area around Site 1, which is in contrast to the high APP values which are an indication of low dilution and poor dispersion of concentrations. The distribution of high concentrations to the east of Site 3 suggests that these concentrations move over the mountain

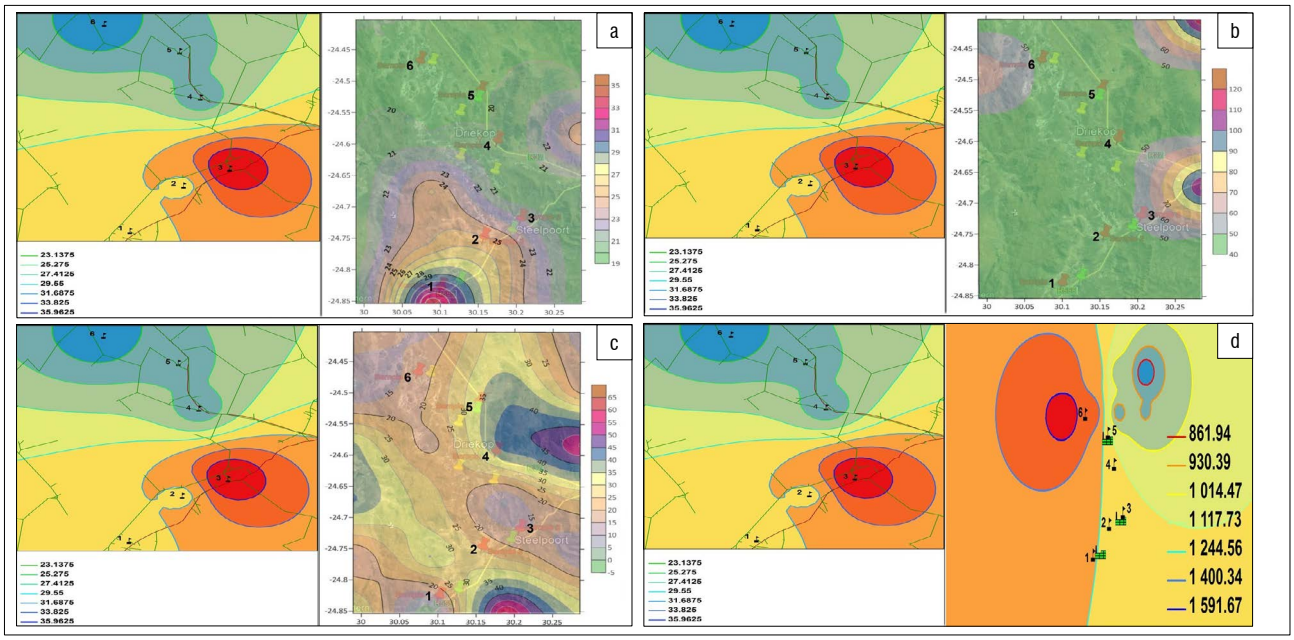

Figure 4: Spatial distribution of PM_{10} and (a) air pollution potential, (b) mixing height, (c) Monin–Obukhov length and (d) ventilation coefficient.

slope to the east of Site 3, which is an indication that mountain winds may be responsible for this flow pattern. The lowest concentrations are centred on Site 6 and extend to Site 5 and Site 4. The lowest APP values are also encountered in the same area as that of the low PM_{10} concentrations which is in contrast to the APP definition. Site 1 and Site 2 have moderate PM_{10} concentrations, which could be attributed to the fact that the area from Site 4 to Site 6 is within a broader mountain valley floor base, compared to the area from Site 1 to Site 3 which has a narrow mountain valley floor base.

Figure 4b shows the comparison between PM_{10} and MH. There is no correlation between PM_{10} and MH. The highest MH was observed to the northeast of Site 3 which is supposed to be an area of low PM_{10} concentrations; however, high PM_{10} concentrations were observed in this region of high MH. The lowest PM_{10} concentrations were observed where there was generally low MH, which is in contrast to the notion that low MH values are associated with poor dilution and dispersion resulting in accumulation of pollutants.

The relationship between PM_{10} and MO is shown in Figure 4c. The area indicated by light green is an area with MO values below 0 and indicates favourable conditions for pollution dispersion. However, the lowest PM_{10} concentrations were observed in an area with moderate stability values, with high PM_{10} concentrations observed in an area of moderate MO. Therefore, MO was unable to correctly indicate the locations of high and low PM_{10} concentrations. This anomaly between PM_{10} concentrations and MO in a complex terrain is because MO is dependent on horizontal wind flows and local equilibrium.[39,65] However, these conditions do not hold in a complex terrain.[39] The MO was derived from synoptic circulations and showed stable conditions in areas where high and low PM_{10} concentrations were observed. The model's inability to account for discontinuities in steep terrain suggests that the PM_{10} concentrations within the valley floor were influenced by the thermal circulations within the valley, with upslope winds due to thermal heating favouring low PM_{10} concentrations and downwind flows due to thermal cooling leading to stagnation and a possible increase in PM_{10} concentrations. However, this hypothesis needs to be further tested in future studies with continuous ambient monitoring in the GTM.

Figure 4d shows the relationship between PM_{10} and the VC. The VC shows moderate to high values to the west of the study area with moderate to low values spreading to the east of the study area. The highest VC values are observed around Site 6 with moderate values across all sites and low values observed to the northeast of Site 6. The observations show that there is a slight correlation between low PM_{10} concentrations and high VC values, and poor correlation between high PM_{10} concentrations and VC values.

The seasonal influence of APP, MH, MO and VC on the distribution of PM_{10} concentrations is shown in Figure 5 and Figure 6, for winter and summer, respectively. The highest PM_{10} concentrations during the winter month of July were observed around sampling Site 5 which is located to the northeast of ASA chrome smelter. The lowest PM_{10} concentrations were observed around Site 1 and Site 6, with moderate concentrations distributed across Site 2, Site 3 and Site 4. The highest APP values were concentrated around Site 1. Moderate APP values were observed to the northeast of Site 5 which is where high PM_{10} concentrations were observed, and to the east of the study area. Low APP values were observed in areas with moderate PM_{10} concentrations. The winter APP was unable to clearly identify areas with high and low PM_{10} concentrations. The highest winter MH was observed to the southeast of the study area with moderate values spreading from southwest to northeast of Site 5. All other sites are located in regions with low MH, which is in contrast to the expected relation between MH and the expected dispersion ability of the atmosphere. The most favourable areas ($MO \leq 0$) for the dispersion of pollutants are indicated in Figures 5 and 6 by light green around Site 1 and Site 2. These areas are where the lowest PM_{10} concentrations were observed. The most stable MO values were spatially distributed across Site 2, Site 3 and Site 4, which are areas where the highest pollution was expected. However, the highest concentrations were observed in an area of moderate MO values. This finding is an indication that the MO cannot clearly identify areas of high PM_{10} concentrations in winter. Strong ventilation (VC) was observed to the west of the mountain valley and weak ventilation to the east of the mountain valley with moderate VC observed within the valley floor. This indicates that the winds within the valley were decoupled from winds outside the valley, and as a result, the VC cannot adequately predict the dispersion of pollutants in the study area.

During the summer month of December (Figure 6), the highest PM_{10} concentrations were distributed around Site 1 and lowest concentrations observed around Site 4, Site 5 and Site 6, with moderate concentrations observed around Site 2 and Site 3. The high APP was distributed around Site 1 with moderate values distributed across Site 2, Site 3 and Site 4, and lower values around Site 5 and Site 6. The PM_{10} concentrations are in agreement with the observed APP for all sites except Site 4 which is supposed to lie within a similar APP to that of Site 5 and Site 6. High MH values were observed to the southeast of the study area with

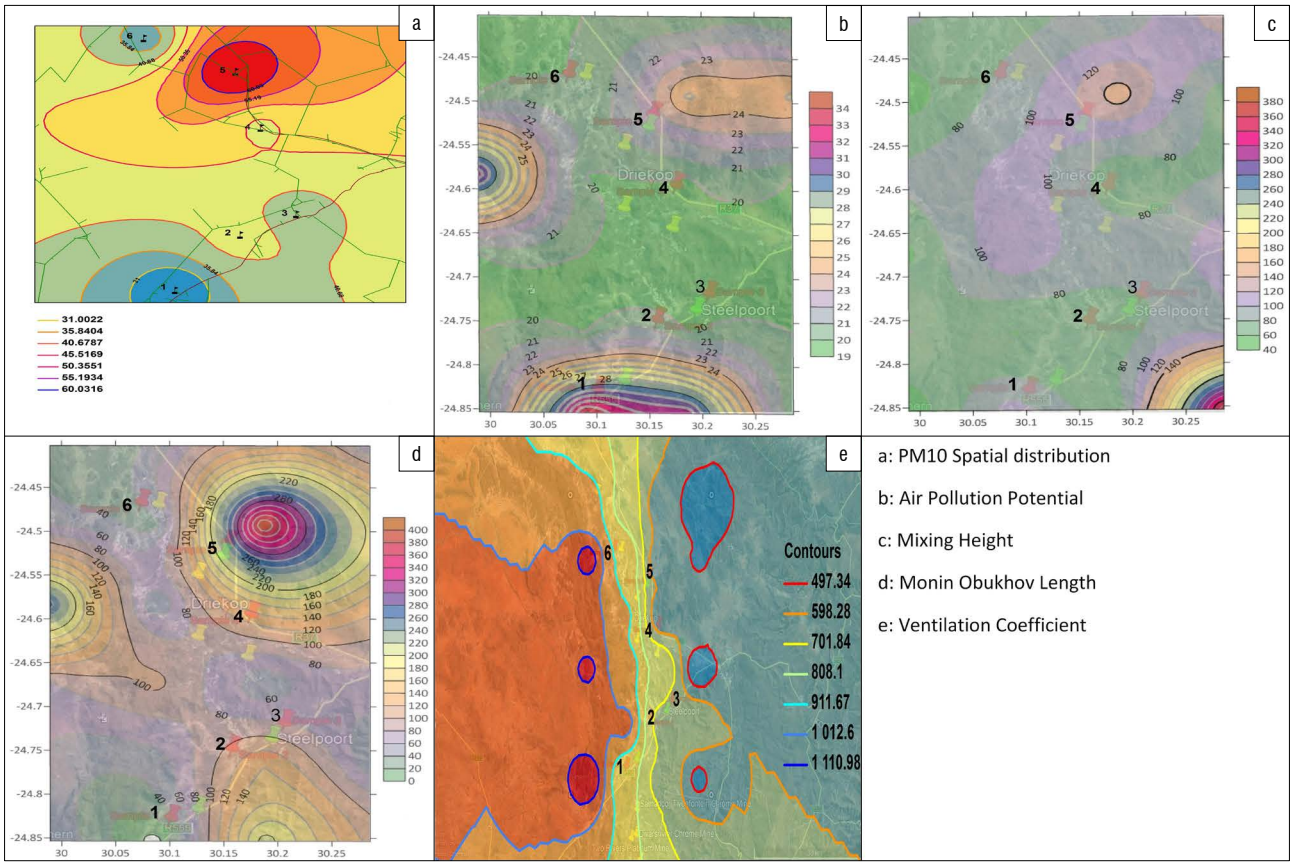

Figure 5: Influence of air pollution potential (APP), mixing height (MH), Monin–Obukhov length (MO) and ventilation coefficient on PM_{10} concentrations in winter.

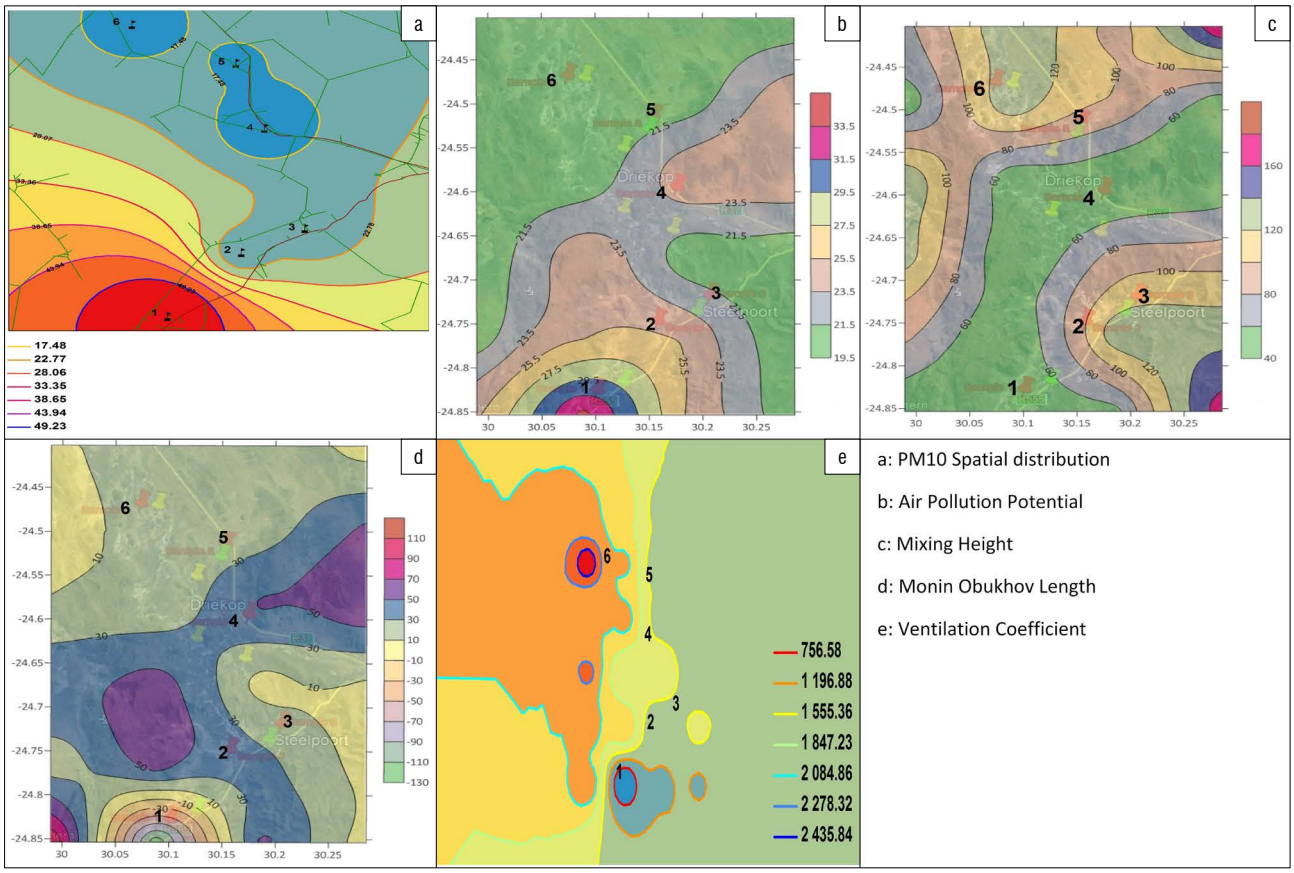

Figure 6: Influence of air pollution potential (APP), mixing height (MH), Monin–Obukhov length (MO) and ventilation coefficient on PM_{10} concentrations in summer.

moderate values distributed across Site 2, Site 3, Site 5 and Site 6. The lowest MH values were observed across Site 1 and Site 4. The PM_{10} concentration was therefore expected to be highest around Site 1 and Site 4 in accordance with the definition of MH, with moderate PM_{10} expected across all other sites. However, only results from Site 1 were in agreement with the observed MH. The most favourable conditions (with respect to MO) for the dispersal of pollutants were observed around Site 1, with unfavourable conditions observed around Site 2 and Site 4, and moderate conditions around Site 3, Site 5 and Site 6. The lowest VC values were observed around Site 1 and the highest VC values were observed around Site 6, with moderate values distributed across the remaining sites. Therefore, the VC was able to predict the areas for high PM_{10} concentrations (Site 1) and low PM_{10} concentrations (Site 6). Site 1 and Site 6 are located in the valley openings with Site 1 being in an area with a narrow valley opening and Site 2 being in an area with a wide valley opening. The strength of the valley flows depends on the valley volume. Wind speeds are often larger near the valley head where valley volume is small and the pressure gradient is high relative to distance from ridge top to ridge top. Wind speed weakens near the valley opening where the valley volume is larger and the pressure gradient is low relative to the distance between ridge tops.[66] Therefore, wind erosion may have played a major role in the observed high PM_{10} concentrations at Site 1 and, similarly, calm conditions may have been responsible for the observed low PM_{10} concentrations at Site 6. However, the VC did not have the same influence on the other sites which are situated in the middle of the valley floor. The reason could be that the TAPM model inputs terrain following coordinate systems and was unable to account for discontinuities in the steep terrain of the study area.

Conclusion

The University of North Carolina passive samplers coupled with CCSEM_EDS were used to determine spatial heterogeneity of PM chemical components. The concentrations of $PM_{2.5}$, PM_{10} and PM chemical components were spatially heterogeneous with high heterogeneity observed near the industrial sources for FeCr-rich and Cr-rich particles and Si-containing particles. The COD values also showed that the highest heterogeneity was observed near the industrial sources. Findings showed little or no correlation between PM_{10} and the meteorological parameters MH, MO length, APP and COD.

The findings highlight a very important point: passive samplers can be used (particularly in developing world contexts) as a substitute to more expensive continuous samplers to determine the spatial variation of PMs and their chemical components for effective environmental planning. The IDW interpolation within the mapping software (ArcMap version 10.0) was able to predict the spatial variation of PM_{10}, $PM_{2.5}$ and PM chemical components that indicated the existence of different conditions within the air shed, and therefore this variation may require different control strategies to mitigate the impacts of pollution within the air shed. The second finding was that synoptic winds used by the TAMP model were unsuccessful in determining the influence of APP, MO, MH and VC on the distribution of PM_{10} concentrations in a complex terrain. This finding clearly indicates that these parameters are dependent largely on winds generated by temperature changes and mountain slopes in mountainous terrain. However, the VC was able to predict the areas for high PM_{10} concentrations at the valley openings where the VC is influenced by the impact of pressure gradient on the wind strength. Therefore, for future analysis of the behaviour of pollutants in a complex terrain, a network of meteorological station balloon soundings within the valley floor and adjacent slopes needs to be set up in order to capture the actual meteorological parameters that influence the behaviour of air pollution. The ambient air quality should be monitored continuously to verify the findings of this study.

Acknowledgements

C.Y.W. receives research funding support from the South African Medical Research Council and the National Research Foundation (South Africa). C.T. thanks the South African Weather Service for provision of resources, space and time for conducting this research.

Authors' contributions

C.T. conceptualised the study, collected the samples, performed the GIS analysis, interpreted the data, wrote the initial draft of the manuscript and the revised version of the manuscript. C.Y.W. provided critical feedback and helped to shape the manuscript.

References

1. Gautam S, Prusty BK, Patra AK. Pollution due to particulate matter from mining activities. Reciklaža i održivi razvoj. 2012;5:53–58. Available from: https://www.rsd.tfbor.bg.ac.rs/download/arhiva_radova/2012/6_SnehaGAUTAM_ST.pdf
2. Seinfeld JH, Pandis SN. Atmospheric chemistry and physics from air pollution to climate change. New York: John Wiley and Sons; 1998.
3. Khlystov A, edited by Wittig B, Davidson C. Quality assurance project plan for Pittsburgh Air Quality Study (PAQS) [document on the Internet]. c2001 [cited 2018 Jun 15]. Available from: https://www3.epa.gov/ttnamti1/files/ambient/super/pittqapp.pdf
4. Quality of Urban Air Review Group (AQUARG). Airborne particulate matter in the United Kingdom. Third report of the Quality of Urban Air Review Group [document on the Internet]. c1996 [cited 2018 Jun 10]. Available from: https://uk-air.defra.gov.uk/assets/documents/reports/empire/quarg/quarg_11.pdf
5. Pope CA, Dockery W. Health effects of fine particulate air pollution: Lines that connect. J Air Waste Manag Assoc. 2006;56:709–742. ttps://doi.org/10.1080/10473289.2006.10464485
6. Brook RD, Rajagopalan S, Pope CA, Brook JR, Bhatnagar A, Diez-Roux AV, et al. Particulate matter air pollution and cardiovascular disease: An update to the scientific statement from the American Heart Association. Circulation. 2010;121(21):2331–2378. https://doi.org/10.1161/CIR.0b013e3181dbece1
7. World Health Organization (WHO). Health effects of particulate matter: Policy implications for countries in eastern Europe: Policy implications for countries in eastern Europe, Caucasus and central Asia. Copenhagen: WHO; 2013. Available from: http://www.euro.who.int/__data/assets/pdf_file/0006/189051/Health-effects-of-particulate-matter-final-Eng.pdf
8. Hinds WC. Aerosol technology, properties, behavior, and measurements of airborne particles. 2nd ed. New York: John Wiley and Sons; 1999.
9. Shah MH, Shaheen N, Jaffar M, Khalique A, Tariq SR, Manzoor S. Spatial variations in selected metal contents and particle size distribution in an urban and rural atmosphere of Islamabad, Pakistan. J Environ Manage. 2006;78:128–137. https://doi.org/10.1016/j.jenvman.2005.04.011
10. Wang Y, Eliot MN, Koutrakis P, Gryparis A, Schwartz JD, Coull BA. Ambient air pollution and depressive symptoms in older adults: Results from the MOBILIZE Boston study. Environ Health Perspect. 2014;122(6):553–558. https://doi.org/10.1289/ehp.1205909
11. Chan CK, Yao X. Air pollution in mega cities in China. Atmos Environ. 2008;42:1–42. https://doi.org/10.1016/j.atmosenv.2007.09.003
12. Environmental Protection Agency (EPA). Technology Transfer Network (TTN). National air toxics assessments [webpage on the Internet]. c2010 [cited 2018 Jun 14]. Available from: https://www.epa.gov/national-air-toxics-assessment
13. Ahrens CD. Meteorology today. 9th ed. Belmont, CA: Thomas Brooks/Cole; 2007. Available from: https://epdf.tips/meteorology-today-9th-edition.html
14. Courault D, Drobinski P, Brunet Y, Lacarrere P, Talbot C. Impact of surface heterogeneity on a buoyancy-driven convective boundary layer in light winds. Bound Layer Meteorol. 2007;124:383–403. https://doi.org/10.1007/s10546-007-9172-y
15. Reen BP, Stauffer DR, Davis KJ, Desai AR. A case study on the effects of heterogeneous soil moisture on mesoscale boundary layer structure in the southern Great Plains, USA. Part II: Mesoscale modelling. Bound Layer Meteorol. 2006;120:275–314. https://doi.org/10.1007/s10546-006-9056-6
16. Yuan X, Xie Z, Zheng J, Tian X, Yang Z. Effects of water table dynamics on regional climate: A case 10 study over East Asian Monsoon Area. J Geophys Res. 2008;113, D21112, 16 pages. https://doi.org/10.1029/2008JD010180
17. Yates DN, Chen F, Nagai H. Land surface heterogeneity in the Cooperative Atmosphere Surface Exchange Study (C 5 ASES-97). Part II: Analysis of spatial heterogeneity and its scaling. J Hydrometeorol. 2003;4:219–234. https://doi.org/10.1175/1525-7541(2003)4<219:LSHITC>2.0.CO;2
18. Zhang N, Williams Q, Liu H. Effects of land-surface heterogeneity on numerical simulations of mesoscale atmospheric boundary layer processes. Theoret Appl Climatol. 2010;102:307–317. https://doi.org/10.1007/s00704-010-0268-9

19. Atkinson BW. Mesoscale atmospheric circulation. London: Academic Press; 1981.

20. Whiteman CD. Observations of thermally developed wind systems in mountainous terrain. In: Blumen W, editor. Atmospheric processes over complex terrain. Meteorological Monographs vol. 23. Boston, MA: American Meteorological Society; 1990. p. 5–42. https://doi.org/10.1007/978-1-935704-25-6_2

21. Durran DR. Mountain waves and downslope winds. In: Blumen W, editor. Atmospheric processes over complex terrain. Meteorological Monographs vol. 23. Boston, MA: American Meteorological Society; 1990. p. 59–81. https://doi.org/10.1007/978-1-935704-25-6_4

22. Whiteman CD, Doran JC. The relationship between overlying synoptic-scale flows and winds within a valley. J Appl Meteorol. 1993;32:1669–1682. https://doi.org/10.1175/1520-0450(1993)032<1669:TRBOSS>2.0.CO;2

23. Wagner J, Leith D. Passive aerosol sampler. Part I: Principle of operation. Aerosol Sci Technol. 2001;34(2):186–192. https://doi.org/10.1080/027868-201300034808

24. Jiménez PA, González-Rouco JF, Montávez JP, Navarro E, García-Bustamante E, Valero F. Surface wind regionalization in complex terrain. J Appl Meteorol Climatol. 2007;47:308–324. https://doi.org/10.1175/2007JAMC1483.1

25. Helgason W, Pomeroy JW. Characteristics of the near surface boundary layer within a mountain valley during winter. J Appl Meteorol Climatol. 2012;51:583–597. https://doi.org/10.1175/JAMC-D-11-058.1

26. Geiger R. Das Klima der bodennahen Luftschicht**.** Ein Lehrbuch der Mikroklimatologie. 4. neubearbeitete und erweiterte Auflage mit 281 Abb., 646 S [The climate of ground-level air-layer. A textbook of microclimatology 4. New and expanded edition with 281 Abb.,646 S]. Brunswick: Verlag Friedrich Vieweg & Sohn; 1961. German. https://doi.org/10.1002/jpln.19620960108

27. De Wekker SFJ, Kossmann M. Convective boundary layer heights over mountainous terrain: A review of concepts. Front Earth Sci. 2015;3(77):1–22. https://doi.org/10.3389/feart.2015.00077

28. Zardi D, Whiteman D. Diurnal mountain wind systems. In: Chow F, De Wekker S, Snyder B, editors. Mountain weather research and forecasting: Recent progress and current challenges.: Dordrecht: Springer; 2013. p. 35–119. https://doi.org/10.1007/978-94-007-4098-3_2

29. Bianco L, Djalaova IV, King CW, Wilczak JM. Diurnal evolution and annual variability of boundary-layer height and its correlation to other meteorological variables in California's Central Valley. Bound Layer Meteorol. 2011;140:491–511. https://doi.org/10.1007/s10546-011-9622-4

30. Working Group 4 (WG4). COST 710: Pre-processing of meteorological data for dispersion models. Wind flow models over complex terrain for dispersion calculations [document on the Internet]. c1997 [cited 2018 Mar 11]. Available from: https://www2.dmu.dk/atmosphericenvironment/cost/docs/COST710-4.pdf

31. Coulter RL. A comparison of three methods for measuring mixing-layer height. J Appl Meteorol. 1979;8:1495–1499. https://doi.org/10.1175/1520-0450(1979)018<1495:ACOTMF>2.0.CO;2

32. Saurez MJ, Arakawa A, Randall DA. The parameterization of the planetary boundary layer in the UCLA general circulation model: Formulation and results. Mon Weather Rev. 1983;111:2224–2243. https://doi.org/10.1175/1520-0493(1983)111<2224:TPOTPB>2.0.CO;2

33. Wesely ML, Cook DR, Hart RL, Speer RE. Measurements and parameterization of particulate sulfur dry deposition over grass. J Geophys Res. 1985;90:2131–2143. https://doi.org/10.1029/JD090iD01p02131

34. Konor CS, Boezio GC, Mechoso CR, Arakawa A. Parametrization of PBL process in an atmospheric general circulation model: Description and preliminary assessment. Mon Weather Rev. 2009;37:1061–1082. https://doi.org/10.1175/2008MWR2464.1

35. Rotach A, Gohm MN, Lang D, Leukauf I, Stiperski, Wagner JS. On the vertical exchange of heat, mass and momentum over complex, mountainous terrain. Front Earth Sci. 2015;3:76. Available from: https://www.frontiersin.org/articles/10.3389/feart.2015.00076/full

36. Steyn DG, De Wekker SFJ, Kossmann M, Martilli A. Boundary layers and air quality in mountainous terrain. In: Chow FK, De Wekker SFJ, Snyder B, editors. Mountain weather research and forecasting: Recent progress and current challenges. Berlin: Springer; 2013. p. 261–289. https://doi.org/10.1007/978-94-007-4098-3_5

37. Faiz A, Sinha K, Walsh M, Varma A. Automotive air pollution: Issues and options for developing countries. Washington DC: Infrastructure and Urban Development, World Bank; 1990. Available from: http://documents.worldbank.org/curated/en/743671468739209497/pdf/multi-page.pdf

38. Figueroa-Esspinoza B, Salles P. Local Monin–Obukhov similarity in heterogeneous terrain. Atmos Sci Lett. 2014;15:299–306. https://doi.org/10.1002/asl2.503

39. Grisogono B, Kraljevic L, Jericevic A. Notes and correspondence the low-level katabatic jet height versus Monin-Obukhov height. Q J R Meteorol Soc. 2007;133:2133–2136. https://doi.org/10.1002/qj.190

40. Gross E. The National Air Pollution Potential Forecast Program: ESSA technical memorandum WBTM NMC 47 [document on the Internet]. c1970 [cited 2018 Mar 03]. Available from: https://apps.dtic.mil/dtic/tr/fulltext/u2/714568.pdf

41. Iyer US, Raj P. Ventilation coefficient trends in the recent decades over four major Indian metropolitan cities. J Earth System Sci. 2013;122:537–549. https://doi.org/10.1007/s12040-013-0270-6

42. Devara PCS, Raj PE. Lidar measurements of aerosols in the tropical atmosphere. Adv Atmos Sci. 1993;10:365–378. https://doi.org/10.1007/BF02658142

43. Krishnan P, Kunhikrishnan PK. Temporal variations of ventilation coefficient at a tropical Indian station using UHF wind profiler. Curr Sci. 2004;86(3):447–451. Available from: https://www.currentscience.ac.in/Downloads/article_id_086_03_0447_0451_0.pdf

44. Nath P, Patil RS. Climatological analysis to determine air pollution potential for different zones in India. In: Brebbia CA, Power H, Longhurst JWS, editors. Air pollution VIII [document on the Internet]. c2000 [cited 2018 Apr 15]. Available from: https://www.witpress.com/Secure/elibrary/papers/AIR00/AIR-00048FU.pdf

45. Anil Kumar KG. Air pollution climatology of Cochin for pollution management and abatement planning. Mausam. 1999;50:383–390. Available from: http://metnet.imd.gov.in/mausamdocs/15046.pdf

46. Schulze BR. Climate of South Africa. Part 8: General survey WB28. Pretoria: SA Weather Bureau; 1986.

47. South African Department of Water Affairs and Forestry (DWAF). Water Services Planning Reference Framework, Sekhukhune District Municipality [document on the Internet]. c2005 [cited 2018 Jun 13]. Available from: http://www.sekhukhunedistrict.gov.za/sdm-admin/documents/Sekhukhune%202011-12%20IDP.pdf

48. Goovaerts P. Kriging vs stochastic simulation for risk analysis in soil contamination. In: Soares A, Gomez-Hernandez J, Froidevaux R, editors. geo-ENV I – Geostatistics for environmental applications. Dordrecht: Kluwer Academic Publishers; 1997. p. 247–258. https://doi.org/10.1007/978-94-017-1675-8_21

49. Van Groenigen JW, Stein A, Zuurbier R. Optimization of environmental sampling using interactive GIS. Soil Tech. 1997;10:83–97. https://doi.org/10.1016/S0933-3630(96)00122-5

50. Fraczek W, Bytnerowicz A, Legge A. Optimizing a monitoring network for assessing ambient air quality in the Athabasca oil sands region of Alberta, Canada. Alpine Space – Man Environ. 2009;48:127–142. Available from: https://www.researchgate.net/publication/313609727_Optimizing_a_monitoring_network_for_assessing_ambient_air_quality_in_the_Athabasca_oil_sands_region_of_Alberta_Canada

51. Ott DK, Cyrs W, Peters TM. Passive measurement of coarse particulate matter, PM10-2.5. J Aerosol Sci. 2008;39(2):156–167. https://doi.org/10.1016/j.jaerosci.2007.11.002

52. Sawvel EJ, Willis R, West RR, Casuccio GS, Norris G, Kumar N, et al. Passive sampling to capture the spatial variability of coarse particles by composition in Cleveland, OH. Atmos Environ. 2015;105:61–69. https://doi.org/10.1016/j.atmosenv.2015.01.030

53. Lagudu URK, Raja S, Hopke PK, Chalupa DC, Utell MJ, Casuccio G, et al. Heterogeneity of coarse particles in an urban area. Environ Sci Technol. 2011;45:3288–3296. https://doi.org/10.1021/es103831w

54. Hopke PK, Casuccio G. Scanning electron microscopy. In: Receptor modeling for air quality management vol. 7. Amsterdam: Elsevier; 1991; p. 149–212. https://doi.org/10.1016/S0922-3487(08)70129-1

55. Wongphatarakul V, Friedlander SK, Pinto JP. A comparative study of $PM_{2.5}$ ambient aerosol chemical databases. Environ Sci Technol. 1998;32:3926–3934. https://doi.org/10.1021/es9800582

56. Burrough PA, McDonnell RA. Principles of Geographical Information Systems. New York: Oxford; 1998.

57. Hartkamp AD, White JW, Hoogenboom G. Interfacing GIS with agronomic modeling: A review. Agron J. 1999;91:917–928. https://doi.org/10.2134/agronj1999.915761x

58. Webber D, Englund E. Evaluation and comparison of spatial interpolators. Math Geol. 1992;24(4):381–391. https://doi.org/10.1007/BF00891270

59. Isaaks H, Srivastava MR. An introduction to applied geostatistics. New York: Oxford University Press; 1989. p. 561. Available from: https://www.scribd.com/document/266290280/An-Introduction-to-Applied-GEOostatistics-Isaaks-and-Srivastava-1989-Oxford

60. Stahl K, Moore RD, Floyer JA, Asplin MG, McKendry IG. Comparison of approaches for spatial interpolation of daily air temperature in a large region with complex topography and highly variable station density. Agric Forest Meteorol. 2006;139:224–236. https://doi.org/10.1016/j.agrformet.2006.07.004

61. Hengl T. A practical guide to geostatistical mapping of environmental variables. EUR 229404 EN. Luxembourg: Office for Official Publications of the European Communities; 2007. Available from: https://www.lu.lv/materiali/biblioteka/es/pilnieteksti/vide/A%20Practical%20Guide%20to%20Geostatistical%20Mapping%20of%20Environmental%20Variables.pdf

62. Li L, Losser T, Yorke C, Piltner R. Fast inverse distance weighting-based spatiotemporal interpolation: A web-based application of interpolating daily fine particulate matter $PM_{2.5}$ in the contiguous U.S. using parallel programming and k-d tree. Int J Environ Res Public Health. 2004;11:9101–9141. https://doi.org/10.3390/ijerph110909101

63. Swart A. An analysis of the air dispersion potential over Uubvlei, Oranjemund, Namibia [dissertation]. Pretoria: University of Pretoria; 2015. Available from: https://repository.up.ac.za/bitstream/handle/2263/60862/Swart_Assessment_2017.pdf?sequence=1&isAllowed=y

64. Fisher G, Metcalfe J. Good practice guide for assessing discharges to air from industry. Wellington: NZ Ministry for the Environment; 2016. https://doi.org/10.13140/RG.2.1.3803.4162

65. Monin AS, Obukhov AM. Basic laws of turbulent mixing in the surface layer of the atmosphere [translation]. Tr Akad Nauk SSSR Geophiz Inst. 1954;24(151):163–187. Available from: https://mcnaughty.com/keith/papers/Monin_and_Obukhov_1954.pdf

66. Whiteman CD. Mountain meteorology: Fundamentals and applications. New York: Oxford University Press; 2000. p. 355. Available from: https://www.amazon.com/Mountain-Meteorology-Fundamentals-David-Whiteman/dp/0195132718#reader_0195132718

CHAPTER 4

Results: Source profiling, source apportionment and cluster transport analysis to identify the sources of PM and the origin of air masses to an industrialised rural area in Limpopo

4.1 Paper overview

Source apportionment of PM is important to identify the sources responsible for ambient concentrations observed in a particular area. In the field of atmospheric sciences, source apportionment models aim to re-construct the impacts of emissions from different sources of atmospheric pollutants (Viana *et al*., 2008).

A few studies have been done on source apportionment locally and in Africa. However, none of these studies have applied the top-down method for source apportionment using PMF model and PM chemical composition data derived from UNC passive samplers and the CCSEM analytical tool. Therefore, this work is unique in that it introduces a cost-effective method for source apportionment as an alternative to the bottom-up method (dispersion modelling) that requires emissions data, which are normally not readily available in South Africa, particularly point source data which industries are normally not willing to share with researchers.

This manuscript covers the source profiling and source apportionment based on the statistical evaluation of PM chemical data acquired at receptor sites. The paper assesses the contributions from various sources based on the observations at the sampling sites. The underlying principle of receptor modelling is that mass and species conservation can be assumed, and a mass balance analysis can be used to identify and apportion sources of airborne PM in the atmosphere (Hopke, 2016). The first section of the manuscript looks at mining as an economic activity that sustains the economy of the GTM. This activity, however, has led to the increase in the number

of households, vehicles, and domestic waste production in the GTM. The increase of these activities is likely to have resulted in environmental pollution due to heavy metals emissions. Heavy metals have been associated with adverse health (Zayed and Terry 2003; Ravindra *et al*., 2004). The manuscript also considers the role of the three spheres of government in implementing the National Environmental Management: Air Quality Act, 2004 (Act No. 39 of 2004) and the inability of the Act to cater for ambient elemental standards with the exception of lead. The third part of the manuscript defines source apportionment and gives a full description of the two source apportionment models, i.e. source-oriented models and receptor models. The two models used in the study namely Positive Matrix Factorization (PMF) and Hybrid Single Particle Lagrangian Integrated Trajectory (HYSPLIT) are described in detail, and the results from these two models are discussed thoroughly. The layout of the study area, the site selection and the sampling and sample analysis methodology are described in detail.

The Candidate acknowledges that though an effort was made in the manuscript to explain how the source profiles were determined, a full description of the steps undertaken to select the profiles generated from the model run should have been included in the discussion of the results. In summary, for each model run the PMF model lists a number of possible source fingerprints (F-matrix). Statistical tools within the model were used to determine how well the model fitted each species, and evaluated if a species should be accepted, down-weighted or excluded from the model. The user then interpreted the profiles using atmospheric science experience coupled with knowledge of sources in the study area. This information was then supported by literature for measured PM source profiles with characteristics similar to the factor profiles in the F-matrix.

4.2 Contribution to the thesis

This manuscript contributes to the thesis by pursuing two research objectives. The first objective 5 ‘to determine source profiles of PM, the number of sources, and the contribution of each source using Positive Matrix Factorization (PMF) model’ was achieved. The results from PMF analysis identified a mixture of tracer elements as markers for source identification. However, differentiating these markers for different sources in the area proved to be difficult because some of the chemical components that are solely industrial can find their way into other source categories such soil and road dust through deposition, and wood and agricultural

plantation through absorption from the soil. This difficulty was overcome by knowledge of the geographical layout of the study area. The major source contributions in the area were identified as crustal/road dust > agricultural/wood burning > ferrochrome smelters > industrial coal burning > vehicle emissions. The contribution of these sources varied across the study area with chromium pollution being concentrated closer to the sources. These results showed that the composition and levels of PM in the GTM varied significantly among the six study sites. Therefore, systematic sampling and characterization of PM is needed to increase the sampling numbers and improve PMF results.

The impacts of regional and trans-boundary air transport to the GTM were investigated by pursuing objective 6. The HYSPLIT model was used to track the air masses and analyse the dominant transport pathways, while a k-means clustering algorithm within the model was applied to group various air mass trajectories into different transport pathways. Five air pollutant transport pathways were identified and were represented by five air mass trajectory clusters. The cluster transport pathways indicated both regional and trans-boundary transport of air masses from the North-West, Province in South Africa, Zimbabwe (passing over Limpopo Province), Mozambique and the Indian Ocean (passing over Northern KwaZulu-Natal Province and Swaziland). The proposed modelling approach in this study has the potential to be applied to other regional air pollutant emission investigations and policy development studies.

This study will add value for future assessment of the impact of sources on ambient air quality under different management / interventions / control options and inform a roadmap of short-term and long-term measures as considered appropriate and cost-effective to ensure compliance with ambient air quality standards.

4.3 Role of the candidate

Cheledi E. Tshehla set up and performed the PMF analysis and the HYSPLIT model trajectory analysis and wrote the paper. The evaluation and interpretation of the results were performed in close cooperation with the Prof. G. Djolov (co-author).

4.4 Publication status

Tshehla C.E and Djolov G. 2018. Source profiling, source apportionment and cluster transport analysis to identify the sources of PM and the origin of air masses to an industrialized rural area in Limpopo. *Clean Air Journal.* 28(2): 54-66. DOI: http://dx.doi.org/10.17159/2410-972X/2018/v28n2a18

4.5 References

Hopke, P.K., 2016: Review of receptor modelling methods for source apportionment. *J. Air & Waste Manag. Assoc*. 66(3): 237-259.

Ravindra, K., Bencs, L. and Van Grieken, R., 2004: Platinum group elements in the environment and their health risk. *The Science of the Total Environment*, 318: 1-43.

South African Department of Environmental Affairs (DEA).: National Environmental Management: Air Quality Act (*Act* No.39), 2004. Available from: https://www.environment.gov.za/sites/default/files/legislations/nema_amendment_act39.pdf.

Viana, M., Kuhlbusch, T.A.J., Querol, X., Alastuey, A., Harrison, R.M., Hopke, P.K., Winiwarter, W., Vallius, M., Szidat, S., Prévôt, A.S.H., 2008: Source apportionment of particulate matter in Europe: A review of methods and results. *Journ. Aeros. Sci.* 39(10): 827-849.

Zayed, A.M. and Terry, M., 2003: Chromium in the environment: factors affecting biological remediation. *Plant and Soil*, 249: 139–156.

Manuscript 2

Research article

Source profiling, source apportionment and cluster transport analysis to identify the sources of PM and the origin of air masses to an industrialised rural area in Limpopo

Cheledi Tshehla[1,2] and George Djolov[1†]

[1]Department of Geography, Geoinformatics and Meteorology, University of Pretoria, Pretoria, South Africa
[2]South African Weather Service, Centurion, Gauteng, South Africa, cheledi.tshehla@weathersa.co.za

Received: 2 August 2018 - **Reviewed:** 13 September 2018 - **Accepted:** 23 November 2018
http://dx.doi.org/10.17159/2410-972X/2018/v28n2a18

Abstract

The Greater Tubatse Municipality in Limpopo is home to three ferrochrome smelters and over fifteen operational mines which are mining chromium, platinum or silica. Source apportionment in this study was performed by combining air mass back trajectories and receptor modelling. The particulate matter (PM) samples at six sites were collected using the University of North Carolina Passive Samplers. The monthly samples were collected for a period of 4-5 weeks, except for August-September and September-October 2015 where the samples were collected for up to 6 weeks. The sampling was carried out from July 2015 to June 2016. PM chemical analysis was performed using Computer Controlled Scanning Electron Microscopy coupled with Energy-Dispersive X-ray Spectroscopy (CCSEM-EDS). The PM chemical analysis indicated the presence of elements such as carbon (C), calcium (Ca), chromium (Cr), iron (Fe), aluminium (Al), silicon (Si), magnesium (Mg) and lead (Pb). All the six sites except site 1 exceeded the WHO annual guidelines for PM_{10} concentration of 20 µg/m^3. The annual chromium concentrations exceeded the New Zealand limits of 0.0001 µg/m^3 and 0.11µg/m^3 Cr (VI) and Cr (III), respectively. The back trajectory clusters computed by the HYSPLIT model identified 5 transport clusters for each site. The main transport patterns were northerly to north-easterly, easterly to south-easterly, and south-westerly to north-westerly. The US EPA PMF model version 5.0 used in source profiling and source apportionment identified agriculture/wood combustion, coal combustion, crustal/road dust, ferrochrome smelters, and vehicle emissions as the main sources in the area. The source contributions varied across all sites indicating the existence of different microenvironments within the airshed and that the pollution can originate from either local or regional sources as indicated by back trajectory clusters.

Keywords

source apportionment, back trajectories, particulate matter, chemical characterization

Introduction

South Africa is one of the developing countries in the world, and as such the country has considered economic growth, social and educational development and industrialization as key development priorities. In the Greater-Tubatse Municipality (GTM) in Limpopo Province, South Africa, mining is viewed as one of the important economic activities which has the potential of contributing to the development of the area's economy (Community Empowerment Impact Assessment Report, 2007). Though the contribution of mining activities to economic development of GTM is well acknowledged, this might be achieved at a significant environmental, health and social costs to the region due to urbanization, high traffic volumes and higher industrial and domestic waste production.

Environmental pollution due to heavy metals from mining activities, vehicular emissions, agricultural and biomass burning are a major concern in many parts of the world (UNEP, 2006). Extensive mining of chromite, platinum and silica in the GTM mining belt may pose a serious threat to the environment. Mining of these ores may release toxic metals such as hexavalent chromium and platinum group metals which are carcinogenic and mutagenic to human health (Zayed and Terry, 2003; Ravindra et al., 2001). Studies worldwide have found that ambient levels of PM_{10} are associated with adverse health effects including increase in premature deaths, hospital admissions and emergency attendances for respiratory and cardiovascular disease and exacerbation of asthma (Pope III, 2000; Dockery, 2001). $PM_{2.5}$ which is smaller in aerodynamic diameter than PM_{10},

[†] Deceased on 7 November 2017

can penetrate deeper into the lungs and reach the blood system and it can also impact on visibility and climate change (Chen et al., 2014) The potential of adverse health effects of particulate pollution has triggered extensive research on PM chemical composition and source apportionment in many countries over the past decade (Liu et al., 2018). Understanding the chemical components of PM is crucial to adequately assess the impacts of these chemicals on the receiving environment. A number of ferrochrome smelters are found in the GTM. Ferrochrome is a major chromium source used as raw material for the production of stainless steel and ferro-metal alloys. The morphology of the chromite spinel ore can be described stoichiometrically as (Fe, Mg)(Cr, Al, Fe)$_2$O$_4$ and they often contain gangue compounds of SiO_2 and MgO. Submerged-arc furnaces are commonly used to smelt chromite ores by using carbonaceous reductants such as coke, bituminous coal and char. The ferrochrome slag created during the smelting process mainly consists of SiO_2, Al_2O_3 and MgO in different proportions but also smaller amounts of CaO, chromium and iron oxides (Nkohla, 2006; Hockaday and Bisaka, 2010). These elements may find their way into the atmosphere during the smelting operations and they can cause serious harm to human health.

In South Africa, the National Environmental Management: Air Quality Act (AQA, Act No. 39 of 2004) was promulgated in 2005 as an approach to manage air quality in the country. The Act requires national, provincial and local authorities to identify substances or mixtures of substances in ambient air which may reasonably be anticipated to endanger public health, and to establish air quality standards to limit emission of such substances. However, to date no ambient metal standards (with the exception of Pb) have been promulgated to define the level of air quality that is necessary to protect the public welfare from known or anticipated adverse effects of these pollutants on the receiving environment in South Africa. There is also little information on PM source apportionment studies to assist in developing effective policies to mitigate the impacts of PM in South Africa.

Numerous methods have been developed over the years to collect and analyze air pollutant samples, using both active and passive techniques. Easy to use passive samplers are available in the market and are less expensive than conventional samplers. Therefore, a large number of passive samplers can be deployed at a given time to capture representative spatial measurements in an airshed (Lagudu et al., 2011).

There are two types of models (source-oriented models and receptor models) used to identify sources of pollution in the environment (Schauer et al., 1996). Source-oriented (dispersion) models require knowledge of all emissions from the contributing sources (Pant and Harrison, 2012). Receptor modes are statistical analysis tools used to identify contributions from different sources using multivariate measurements from different receptor locations. These models use ambient data and the chemical components in source emissions to quantify contributions, unlike the source models that use emissions and meteorological parameters to estimate concentrations at the receiving environment (Watson, 2002). Positive Matrix Factorization (PMF) is one of the recent models developed by the United State (U.S) Environmental Protection Agency (EPA). PMF has been used widely in source apportionment of ambient PM because of its ability to account for the uncertainty variables that are often associated with sample measurements and also the output values in the solution profiles and contributions are nonnegative (Reff and Eberly, 2007). The key output of PMF is the percentage contributions of different sources to ambient pollutant concentration at specific receptors (Pant and Harrison, 2012). The PMF model has been used by many researchers across the world for source identification and profiling. A study by Harris and Davidson (2005) characterized Ca, Al, Mg, Si, K, Fe, Mn and Zn as elements emitted from metal smelters. Soil was found to contain elements such as Fe, Al, K, Ca, Ti in a study by Watson and Chow (2001a; 2001b), while road dust contributed to Fe, Al, K, Ca, Si, Mg, P, S, Na and BC (Bhave et al., 2001; Ho et al., 2003). However, these profiles can vary from one area to the other due to varying soil types. A source profiling study by Kim et al., (2003b) and Begum et al., (2004) identified motor vehicle emissions as the source of Mg, Al, Fe, Si, S and BC (black carbon). Biomass burning emissions are a mixture of both organic carbon and elemental carbon and their ratio depends on the type of fuel used (Karanasiou et al., 2015).

The quantitative assessment of sources contributing to the ambient PM on the receiving environment is required to develop sound and effective control strategies to address the scourge of PM pollution in South Africa. However, the bottom-up approach based on emission inventories is hindered by poor availability of the emissions data particularly from industries. The objective of this study is to identify sources of PM in a mountainous terrain in Limpopo, South Africa and estimate their contributions through receptor modeling (PMF) application. The sampling data obtained during the sampling campaign from July 2015 to June 2016 will be used.

Methods

Study area

Ambient PM sampling was undertaken in a rural area of the Greater Tubatse Municipality (GTM) in Limpopo Province, South Africa (Fig. A1). The main towns in the area are Steelpoort and Burgersfort which are sustained through economic activities such as mining and smelting of chromium ores. Furthermore there are agricultural and forestry activities and transportation that also add to the economic activities in the area. Most of the households in the area are dependent on wood burning for space heating and cooking (Community Empowerment Impact Assessment Report, 2007). The GTM has a complex terrain with high mountains and steep inclinations. The elevation of the surface area is approximately 740 m above sea level with the surrounding mountains extending to a height of approximately 1200-1900 m above sea level. The area is located in the subtropical climate zone where the maximum average

temperature reaches 35 °C with minimum average temperature of 18 °C in summer. In winter the maximum average temperature reaches 22 °C with average minimum of 4 °C (Schulze, 1986). The annual rainfall for the area ranges between 500 and 600mm (DWAF, 2005). Figure A1 in appendix should the map of the study area showing passive sampler locations (red place-marks) with smelter locations shown as green place-marks.

Site selection

The location of the monitoring sites was selected to optimize spatial sampling for exposure assessment. A sequential sampling technique (Goovaerts, 1997; Van Groenigen et al., 1997) was used to design an optimal sampling network of 6 sites in the GTM. This technique is based on extended knowledge of the area to be sampled and factors controlling the distribution of pollutants. These factors amongst others were terrain and various phenomena like meteorological conditions and the chemistry of pollutants (Frączek et al, 2009). The sites were located at private residences, a church, a hospital and a school for security reasons and easy access during site visits.

Sampling and sample analysis

The University of North Carolina (UNC) passive samplers designed by Wagner and Leith (2001) and housed in a protective shelter designed by Ott and Peters (2008) were deployed at six sites for PM sampling. Ott and Peters (2008) designed the shelter to shield the passive sampler from precipitation and to minimize the influence of wind speed on particle deposition (Sawvel, 2015). The samplers consist of a scanning electron microscopy (SEM) stub, a collection substrate, and a protective mesh cap (Lagudu et al., 2011). The samplers were deployed for sequential periods of approximately 30 days from July 2015 to June 2016, except for the month of August and September when they were deployed for a period of approximately 40 days. The longer sampling periods of 3-4 weeks were selected to ensure that there was sufficient particle loading on the samplers as suggested by Sawvel (2015).

The $PM_{2.5}$, PM_{10} concentrations and the elemental composition of individual particles deposited on the passive sampler were determined by CCSEM-EDS (Tescan Vega 3 model). Before sample analysis with Personal Scanning Electron Microscopy (PSEM) (method by Hopke and Casuccio, 1991), the samples were coated with a thin layer of graphitic carbon under vacuum to bleed off the charges induced by the electron beam in the SEM. The PSEM was operated with a 20-kV beam (Sawvel 2015). Lagudu et al., (2011) gave a brief description of the CCSEM analysis. The elements obtained from the analysis were Carbon (C), Chromium (Cr), Calcium (Ca), Iron (Fe), Silicon (Si), Aluminium (Al), Magnesium (Mg), Lead (Pb), and other miscellaneous elements. Pb and miscellaneous elements were not included in further analysis due to their insignificant weight. The concentrations of $PM_{2.5}$, PM_{10} and each particle was determined using the method outlined in Ott and Peters (2008). Data obtained from CCSEM is semi-quantitative, and therefore, in order to use the data in PMF for source contributions the particles needs to be classified into homogenous groups by applying cluster analysis (Song and Hopke, 1996b; Kim and Hopke, 2008; Lagudu et al., 2011).

Cluster analysis

Buhot et al., (1999) described cluster analysis in detail. In this study, hierarchical cluster analysis was performed on single particle data from CCSEM using the open source clustering software (Cluster 3) developed by the Institute of Medical Science (IDS) at the University of Tokyo. Once the analyses were completed, all the cluster groups with less than 4 (excluding Pb and miscellaneous elements) particles were chosen as potential homogenous classes. This is because as the number of classes created for each source sample increases, the number of particles assigned to each class decreases (Kim and Hopke, 1988). The particle classes obtained from cluster analysis include Carbon-rich (C-rich), Chromium-rich (Cr-rich), Iron-rich (Fe-rich), Iron/Chromium-rich (FeCr-rich), Silicon (Si-rich), Silicon/Aluminium/Iron-rich (SiAlFe-rich), Calcium-rich (Ca-rich), Silicon/Magnesium-rich (SiMg-rich) and Silicon/Aluminium-rich (SiAl-rich).

Positive matrix factorization

PMF 5.0 (USEPA, 2014) was used to apportion the contribution from emission sources (Lee et al., 1999; Reff et al., 2007). The guidelines specified in the user manual were closely followed in this study. Two input files are required by the model: the sample species concentration values and the sample species uncertainty values or parameters for calculating uncertainty. In this study, the sample species uncertainties were obtained during CCSEM analysis of samples.

The receptor modelling in principle relies on the observed concentrations of chemical species in the atmosphere and these species must be conserved during transport between the source and the receptor. The conserved mass is then used during the analysis in the identification and apportionment of these species (Pant and Harrison, 2012). The PMF model identifies the sources by applying the following mass balance equation:

$$X_{ij} = \sum_{k=1}^{p} g_{ik} f_{kj} + e_{ij} \quad (1)$$

Where x_{ij} is the concentration of the j^{th} species in the i^{th} sample, g_{ik} the contribution of k^{th} source to the i^{th} sample, f^{kj} the concentration of the j^{th} species in the k^{th} source, and e_{ij} is the difference between the measured and fitted value. If the number and sources in the area being modelled are known, (f_{kj}), then the mass contribution of each source to each sample, g_{ik}, in equation (1) is known (European Commission, 2014). However, the objective is to calculate values of g_{ik}, f_{kj}, and p that can reproduce x_{ij}. An adjustment is then made to g_{ik} and $f_{k}j$ until the minimum value of Q for a given *p* is found. Q is defined as:

Where σ_{ij} is the uncertainty of the j^{th} species concentration in sample I, *n* is the number of samples, and *m* is the number

$$Q = \sum_{i=1}^{n} \sum_{j=1}^{m} \left(\frac{e_{ij}}{\sigma_{ij}}\right) 2 \quad (2)$$

of species (Reff et al., 2007). In most cases, a given chemical

constituent will have multiple sources and the program performs correlation analysis to generate chemical profiles of 'factors' characteristic of the sources. Past knowledge of source chemical profiles is then used to assign factors to sources (Pant and Harrison, 2012). However, in South Africa there are few source chemical profiles available. Therefore, the international source chemical profiles (Central Pollution Control Board Parivesh Bhawan, East Arjun Nagar Delhi; Pant and Harrison, 2012; Barrera et al., 2012) were used as a guide.

HYSPLIT model

Backward air trajectories arriving at the six sampling sites were calculated using the Windows PC version of the Hybrid Single Particle Integrated Trajectory (HYSPLIT-4) model. This model is a system for computing air mass trajectories and complex dispersion and deposition simulations (Draxler and Hess, 1997; 1998). Meteorological data fields to run the model are available from routine archives. In this study, 24-hour back trajectories were calculated at a height 500 meters above ground level using reanalysis data from National Centre for Environmental Prediction (NCEP) and National Centre for Atmospheric Research (NCAR) available from the National Oceanic and Atmospheric Administration's (NOAA) Air Resources Laboratory (ARL) archives. The reanalysis data covers the globe from 1948 to the present with a horizontal resolution of about 2.5 x 2.5 degrees latitude-longitude and with an output every 6- hours.

Table 1: *Model parameters used for all runs.*

Model parameter	Setting
Meteorological dataset	NCEP/NCAR Reanalysis, 2.5 degree latitude-longitude
Trajectory direction	Backward
Trajectory duration	24hr
Site 1	(-24.825222, 30.093418)
Site 2	(-24.753453, 30.153452)
Site 3	(-24.726582, 30.205004)
Site 4	(-24.614130, 30.172281)
Site 5	(-24.541220, 30.149056)
Site 6	(-24.497841, 30.064537)
Start time	00:00 UTC
Start height1	500m AGL

The isosigma vertical motion method was selected for computing trajectories. This method follows the internal terrain following coordinates systems. A review on computation and applications of trajectories was provided by Stohl (1998). The length of the back trajectories is restricted in many ways by the distances between source regions and the destination zone. The choice of 24-hour back trajectory duration is a compromise between the objective to identify local and distant sources and sink regions and to limit the uncertainties in the trajectories. Stohl (1998) affirmed that errors of 20% of the distance travelled seem to be typical for trajectories computed from analysed wind fields.

Trajectory cluster analysis

In this study trajectory cluster analysis was performed using the HYSPLIT_4 model. The model uses Ward's method described by Romesburg (1984), Moody and Galloway (1988) and Stunder (1996). The HYSPLIT clustering method is described in detail by Draxler et al., (2018). Five clusters were chosen for each set of trajectory end point files because this number was sufficient to identify all major flow patterns, as well as several less common but nonetheless important patterns. Once the number of clusters has been decided, 'Special Runs' was chosen as the technique to produce standard clusters for all trajectory end points for the period starting from July 2015 to June 2016. A practical advantage of 'Special Runs' it's its ability to accommodate large volumes of data. The variables clustered were the latitude and longitude of trajectory segment endpoints at 1-hour intervals along each 24-hour back trajectory. Individual trajectories were further averaged to produce "cluster-mean" trajectories. Thus, our large data base (annual trajectories) was reduced to a number of cluster-mean plots that can be interpreted in terms of known mesoscale and synoptic features. For each cluster, ensemble plots of all individual trajectories belonging to that cluster were produced. These ensembles or "cluster membership" plots were used to validate the mean and to assess the variability within the cluster (HYSPLIT4, 2018).

Results and discussion

The mean annual concentrations and the range between minimum and maximum concentrations for $PM_{2.5}$, PM_{10}, and particle classes obtained through cluster analysis are shown in Table 2. The $PM_{2.5}$ and PM_{10} annual mean concentrations were below the South Africa National Ambient Air Quality Standard (NAAQS) of 20 µg/m^3 and 40 µg/m^3, respectively. However, all the sites exceeded the WHO annual guideline of 20 µg/m^3 for PM_{10} and only site 1 exceeded the WHO annual guideline of 10 µg/m^3 for $PM_{2.5}$ (WHO, 2017). All the sites with the exception of site 4 and 6 recorded highest maximum PM_{10} concentration above 50 µg/m^3 with the minimum concentration of 10.3 µg/m^3 recorded at site 5. For chromium, all sites exceeded the New Zealand annual chromium limits (Ministry for the Environment, 2009) of 0.0011 µg/m^3 and 0.11 µg/m^3 for Cr (VI) and Cr (III), respectively. This is an indication that the area may experience negative impact on human health, and because the pollutants' toxicity differs so should be the environmental regulation strategies to mitigate their impacts. The existence of SiAl-rich particles with concentrations ranging between 3.3 µg/m^3 and 42.9 µg/m^3 in the study area may result in cardio metabolic effects on animals and humans (Sun et al., 2012) because they contribute 15%-55% of the total PM in the study area.

Table 2: *Species mean concentrations and range.*

	Mean						Range					
Species	Site1	Site2	Site3	Site4	Site5	Site6	Site1	Site2	Site3	Site4	Site5	Site6
PM_{10}	32.02	31.28	38.11	24.10	24.65	20.98	14.9-71.2	16.3-56.6	18.2-53.9	12.2-44.7	10.3-64.9	12.5-33.5
$PM_{2.5}$	11.8	4.7	4.8	3.0	3.2	2.5	2.3-65.6	2.1-8.3	2.4-9.4	1.8-3.8	1.2-7.5	1.4-3.2
Ca-Rich	1.9	3.1	2.7	1.7	1.8	3.4	0.4-3.5	0.9-6.3	0.8-4.4	0.7-5.6	0.3-9.9	0.9-6.3
C-Rich	5.4	3.2	2.6	2.5	2.1	1.9	2-16.1	2-4.6	1.6-4.8	1.6-4.5	1.3-2.9	0.9-6.3
Cr-Rich	1.3	1.0	1.4	0.2	1.3	0.2	0.8-1.9	0.3-2.5	0.4-3.4	0-0.7	0-6.9	0-1.2
Fe-Rich	0.8	0.4	0.6	0.3	0.2	0.5	0.1-1.1	0.2-1.1	0.4-1.2	0.1-1.4	0.1-0.5	0.1-0.6
FeCr-Rich	1.7	1.5	2.8	0.5	2.8	0.4	0-3.4	0.7-2.8	0.7-6.7	0.1-1	0.2-16.7	0-1.9
Si-Rich	1.5	1.8	2.6	1.3	1.0	0.9	0.8-2.5	1-3.1	1.1-4.1	0.5-3	0.4-2.6	0.2-1.5
SiAl-Rich	11.6	11.4	11.8	7.8	7.3	8.2	3.3-42.9	5-23	4.9-16.9	3.3-17.1	2.3-17.9	4-16.2
SiAlFe-Rich	3.8	5.1	7.0	6.7	4.6	3.2	1.3-7.8	2.7-10.2	3-12.6	3.1-13.8	2.4-7.5	1.2-5.4
SiMg-Rich	1.0	1.3	3.9	1.0	1.7	0.8	0.4-2.1	0.5-2.7	0.6-8.8	0.4-1.7	0.5-6.8	0.4-1.8

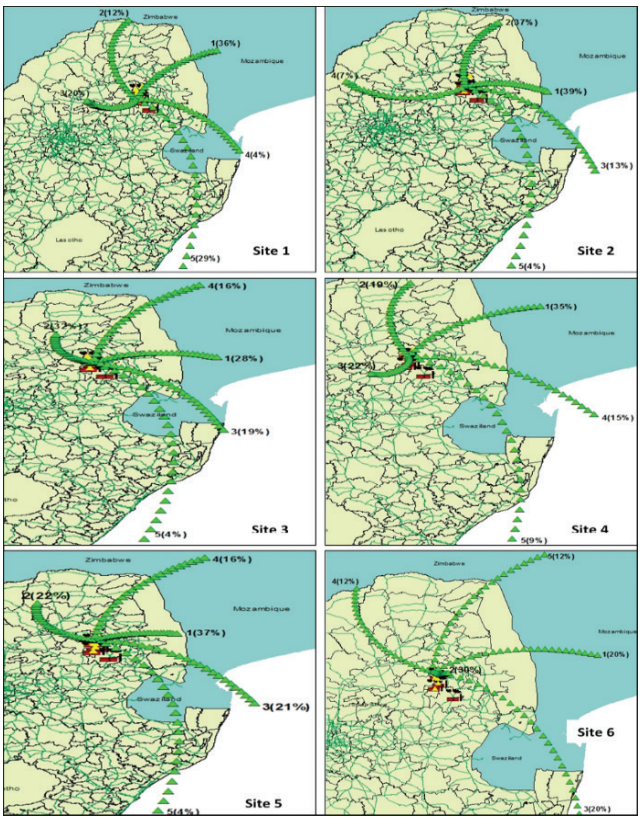

Figure 1: *Five transport pathways (clusters) arriving at the six sampling sites.*

HYSPLIT transport clusters

Figure 1 shows five clusters per receptor site. Clusters for site 1 to site 4 have similar pattern with varying trajectory percentage. For site 1, cluster 1 with 36% of trajectories originates from Mozambique and arrives at the receptor site by passing through mining areas and a smelter northeast of the sampling site. Cluster 2 with 12% of the trajectories originates from Zimbabwe and arrives at the receptor site from the northwest and away from the mines and smelters in the area. Cluster 3 with 20% of trajectories originates from the west while clusters 4 and 5 originate from the Indian Ocean. Only cluster 1, 4 and 5 pass through areas with mines and smelters within the study area. This makes them potential transporters of heavy metals to the receptor site. For site 2, all clusters with the exception of cluster 4 passes over the mines and smelters and as such have the potential of carrying elemental particles to the site. For site 3, all the clusters pass over the mining areas and only cluster 3 and 5 passes over the smelters. Hence all these clusters can transport elemental particles to the receptor. For site 4, all the clusters pass over mining areas and only cluster 2 and 3 pass over the smelters before arriving at the receptor site. For site 5, only cluster 1 is not passing over any industrial facility in the area. For site 6, only cluster 2, 3 and 5 pass over industrial facilities. Cluster 2 with 30% of trajectories is recirculating within the vicinity of the receptor site and this makes it the most likely contributor of local pollutants. However, it should be noted that even though some trajectories are not passing through the industrial facilities, they can also transport pollutants from a variety of sources such as transport, agriculture, domestic, crustal and oceans, and that these pollutants also contribute to the observed concentrations as shown in Table 2.

Source profiling by PMF

The most important step in PMF is to determine the number of factors which correspond to potential particle sources. After applying bootstrap and displacement tests on the data sets, three to five factors were deemed to be appropriate for a five source solution. The profile graph (Fig. A2.1-A2.6) displays the mass of each species apportioned to the factor (blue bar) and the percentage of each species apportioned to the factor (red bar). The factors were identified according to the type of elements dominating in percentage in that factor. Agricultural/ wood combustion was associated with the dominance of C as

Table 3: *Source contributions to the PM particles.*

		Vehicular emissions	Ferrochrome smeltering	Coal combustion	Agricultural/Wood combustion	Crustal/Road dust
Site 1	C-rich		35%		63%	2%
	Ca-rich			25%	44%	30%
	SiAl-rich		43%	21%	36%	
	Si-rich		21%	19%	26%	35%
	SiAlFe-rich		49%	32%		19%
	SiMg-rich		10%	61%	26%	3%
	Cr-rich		28%	13%	26%	33%
	Fe-rich		7%	40%	35%	19%
	CrFe-rich		2%	28%	36%	34%
Site 2	C-rich	45%	0%	18%	6%	31%
	Ca-rich	4%	3%	35%	50%	9%
	SiAl-rich	13%	10%	29%	33%	15%
	Si-rich	0%	28%	7%	15%	51%
	SiAlFe-rich	19%	25%	13%	23%	22%
	SiMg-rich		17%	11%	50%	22%
	Cr-rich	19%	55%	26%		
	Fe-rich		7%	38%	23%	32%
	CrFe-rich	34%	26%	30%	8%	2%
Site 3	C-rich	52%		45%	3%	
	Ca-rich	6%	21%	60%		14%
	SiAl-rich	18%	14%	26%	7%	36%
	Si-rich	13%	10%	20%	15%	42%
	SiAlFe-rich	36%		2%		62%
	SiMg-rich		1%	44%	41%	14%
	Cr-rich	1%	52%	31%	7%	9%
	Fe-rich	15%	6%	39%	6%	34%
	CrFe-rich	12%	40%	36%	12%	0%
Site 4	C-rich	55%	10%	6%	23%	7%
	Ca-rich	5%	7%	9%	45%	34%
	SiAl-rich		10%	28%	42%	21%
	Si-rich		6%	15%	23%	55%
	SiAlFe-rich	17%	3%	24%	16%	41%
	SiMg-rich	19%	28%	12%	38%	3%
	Cr-rich	7%	62%			31%
	Fe-rich	21%	27%	1%	24%	28%
	CrFe-rich	12%	35%	5%	13%	35%
Site 5	C-rich	17%	4%	13%	66%	
	Ca-rich	14%	10%	76%		
	SiAl-rich	15%	22%	30%	15%	19%
	Si-rich	23%	1%	14%	2%	61%
	SiAlFe-rich	19%	5%	15%	21%	41%
	SiMg-rich	3%	44%	13%	10%	30%
	Cr-rich	20%	65%	2%	6%	7%
	Fe-rich	12%	8%	23%	2%	55%
	CrFe-rich	2%	75%	4%	7%	13%
Site 6	C-rich	21%		4%	62%	13%
	Ca-rich	12%		8%	23%	57%
	SiAl-rich	16%	9%	8%	23%	44%
	Si-rich	25%	22%	23%	8%	22%
	SiAlFe-rich	9%	23%	22%	10%	37%
	SiMg-rich	32%	22%	5%	39%	3%
	Cr-rich		64%		36%	
	Fe-rich	45%	30%	3%	23%	
	CrFe-rich	20%	55%	11%		15%
Average contributions		18.61%	23.52%	22.00%	24.72%	26.33%

a primary species and Fe elements. Ferrochrome smelter was identified by the domination of Cr and Fe elements. Crustal/road dust factor was associated with Si, Al, Ca and Mg as the primary elemental species. Industrial coal combustion factor was identified by Ca, C, Al and Si as the dominating elements. Vehicular emission factor was associated with Fe as the primary species, C, Al, Si, and Ca. The most interesting outcome is that Cr was also associated with crustal/road dust and agricultural/wood burning which is an indication that once this element is emitted from the source it is then deposited on to the soil and water bodies before it is absorbed by plant material and released into the atmosphere during burning. Figures A2.1-2.6 in the appendix show the factors fingerprints for the species.

Source contributions to PM

PMF analysis determines the number of factors which correspond to potential particle sources. Source categories that potentially have contributed to ambient PM in the GTM rural area were identified as crustal/road dust, coal combustion fly ash, vehicle exhaust dust, agricultural/wood burning and industrial sources (Table 3). The average PM source contributions across all sites indicate that geological material (crustal/road dust) accounts for 26.33%. The crustal material could be mainly from resuspended dust from mine tailing in the area or transported from regional sources as indicated by the HYSPLIT transport pathways. Vehicular emissions are associated with tail pipe, emissions, tire and brake wear, road surface abrasion, wear and tear of other vehicle components such as the clutch, and resuspension of road surface dusts and accounted to 18.69% of the PM sources. Fly ash from industrial coal combustion contributed 22% to the PM in the study area. Most coal ash contain aluminium oxide (Al_2O_3), calcium oxide (CaO) and silicon dioxide (SiO_2) (Coal Ash, 2016). And regardless of the by-product produced, there are many toxic substances that are present in coal ash (such as arsenic, chromium, lead, mercury and uranium) that can cause major health problems in humans (Lockwood and Evans, 2016).

Agricultural and wood (cooking and space heating) burning accounts to 24.7% of the total PM emissions. The three ferrochrome smelters contributed 23.52% of the total PM in the airshed. The distribution of Cr elements across all source types indicate that ferrochrome smelters have a on the ambient air and have the potential to pollute the water bodies, which can impact on the human health since some of the communities in the area depend on water from the river streams for cooking and bathing.

Both PMF results and HYSPLIT clusters can be combined to make informed decisions on the sources and origin of PM sources. Crustal/road and soil dust can be transported by trajectories from both local and regional anthropogenic sources as shown in Fig. 1. However, it should be noted with caution that the trajectories are not accurately terrain following. Therefore, high-ending trajectories were chosen to represent more accurate boundary layer flow above the local terrain.

Emission reduction strategies

Source apportionment results can be useful for the review or development and implementation of strategies to reduce the impacts of pollution due to industrialization. Some of the immediate interventions to be considered in GTM are;

- Address fugitive emissions from industrial activities.
- Review of the separation process of silica and chrome from milling process.
- Review of the handling and transportation of milled chrome by road (as some of this material is spilled on the road).
- Effective enforcement of the Air Quality Act by authorities.
- Reduction of fugitive emissions from smelters during material handling.
- Electrification of households to reduce wood burning.
- Reduction of dust from mine tailings and haul roads.
- Re-look at the transportation of ground milled chromium to address the current scourge of spillages on the roads.
- Initiate waste collection from rural households to prevent waste burning.

These interventions can also be copied to other areas in South Africa.

Conclusion

The study investigated a selection of the chemical components of PM collected over a period of a year in the Greater Tubatse Municipality in Limpopo province of South Africa. The chemical components were used in PMF analysis for source profiling and source identification. HYSPLIT model was used in the identification of possible pollution source locations using backward clusters. The combination of the two models assisted in concluding that the sources can be either of local or regional origin.

These results show that the composition and levels of PM in GTM varied significantly among the six sites, however, systematic sampling and characterization of PM is needed in order to increase the sampling numbers and improve PMF results.

The PMF analysis identified a mixture of tracer elements as markers for source identification. However, differentiating these markers for different sources in the area has proved to be very difficult. This is because some of the chemical components that are solely industrial can find their way into other source categories such soil and road dust through deposition, and wood and agricultural plantation through absorption from the soil. The average source contributions were dominated by crustal/road dust, industrial activities such as ferrochrome smelters, and wood burning for space heating, with industrial coal burning, agricultural activities and vehicle emissions being other sources identified in the area. The contribution of this sources varied across the study area with chromium pollution being concentrated closer to the sources. These results show that the composition and levels of PM in GTM varied significantly

among the six sites indicating the existence of varying microenvironments within the airshed, however, systematic sampling and characterization of PM is needed in order to increase the sampling numbers and improve PMF results.

This study can serve as a base for siting of AQ monitoring stations to ensure harmonized AQ assessments throughout the GTM. It can also be used as a guiding document for strengthening intervention strategies in the industrialized areas across South Africa.

Acknowledgements

The author acknowledges the South African Weather Service for financial assistance during the sampling period. RJ Lee for chemical analysis, NOAA Air Resources Laboratory for providing the HYSPLIT model and NOAA/OAR/ESRL PSD, Boulder, Colorado, USA for the NCEP Reanalysis data. The author also acknowledges Prof. Phillip Hopke from Clarkson University for his advice on the treatment of CCSEM results before application of PMF, and Dr. Thomas M Peters from University of Iowa for providing the formula for calculating single particle concentrations.

References

Ault A., Moore M., Furutani H., and Prather K. 2009. Impact of emissions from the Los Angeles port region on San Diego air quality during regional transport events, *Environ. Sci. Technol.*, 43: 3500–3506.

Barrera, V. A., Miranda, J., Espionosa, A. A., Meinguer, J. N., Ceron, E., Morales, J. R., Miranda, P. A., and Dias., J. F. 2012. Contribution of Soil, Sulfate, Biomass Burning Sources to the Elemental Composition of PM10 from Mexico City. *Int. J. Environ. Res.*, 6(3): 597-612.

Begum, B.A., Kim, E., Biswas, S.K. and Hopke, P.K. 2004. Investigation of Sources of Atmospheric Aerosol at Urban and Semi-Urban Areas in Bangladesh. Atmos. *Environ*. 38: 3025-3038.

Bhave, P.V., Fergenson, D.P., Prather, K.A. and Cass, G.R. 2001. Source Apportionment of Fine Particle Matter by Clustering Single-Particle Data: Tests of Receptor Model Accuracy. *Environ. Sci. Technol*. 35: 2060-2072.

Buhot, A and W. Krauth. 1999. Phase separation in two dimensional additive mixtures. *Phys. Rev*. E 59: 2939-2941.

Casuccio, G. S., Janocko, P. B., Lee, R. J., Kelly, J. F., Dattner, S. L., and Mgebroff, J. S. 1983a. The Use of Computer Controlled Scanning Electron Microscopy in Environmental Studies, *J. Air Pollut. Control Assoc*. 33:937.

Central Pollution Control Board. Delhi, India (2010). Air quality monitoring, Emission Inventory and source apportionment study for Indian Cities – National Summary Report. http://moef.nic.in/downloads/public-information/Rpt-air-monitoring-17-01-2011.pdf

Chen, W.N., Chen, Y.C., Kuo, C.Y., Chou, C.H., Cheng, C.H., Huang, C.C., Chang, S.Y., Ramana, M.R., Shang, W.L., Chuang, T.Y. and Liue, S.C. 2014. The real-time method of assessing the contribution of individual sources on visibility degradation in Taichung. *Sci. Total Environ*. 497–498: 219–228.

Coal Ash: Characteristics, Management and Environmental Issues" (PDF). Electric Power Research Institute. Retrieved 3 March 2016.

Community Empowerment Impact Assessment Report: Phase 1. 2007. https://www.nra.co.za/content/Tubatse1.pdf

Dockery DW. 2001. Epidemiologic evidence of cardiovascular effects of particulate air pollution. *Environ. Health Perspect*. 109(4): 483–486.

Draxler, R. R. and G. D. Hess, 1997: Description of HYSPLIT_4 modelling system. NOAA technical memorandum ERL ARL-224: 24pp.

Draxler, R. R. and G. D. Hess, 1998: An overview of the HYSPLIT_4 modelling system for trajectories, dispersion and deposition. Australian Meteorological Magazine, 47: 295-308.

Draxler, R., Stunder, B., Rolph, G., and Stein, A. 2018. HYSPLIT4 USER's GUIDE. Version 4. NOAA Air Resources Laboratory.

European Commission. 2014. European Guide on with Receptor Models Air Pollution Source Apportionment. doi: 10.2788/9307.

Goovaerts, P. 1997. Kriging vs stochastic simulation for risk analysis in soil contamination. In: Soares, A., Gomez-Hernandez J., Froidevaux R. (Eds.), geo-ENV I - Geostatistics for Environmental Applications. Kluwer Academic Publishers, Dordrecht, 247-258.

DWAF, 2005. Water Services Planning Reference Framework, Sekhukhune District Municipality. DWAF, *Enviromap and GPM Consultants*, Pretoria, 124pp.

Harris, A.R. and Davidson, C.I. 2005. The Role of Resuspended Soil in Lead Flows in the California South Coast Air Basin. *Environ. Sci. Technol*. 39: 7410-7415.

Hockaday, S. and Bisaka, K. 2010. Some Aspects of the Production of Ferrochrome Alloys in Pilot DC Arc Furnaces At. In: The Twelfth International Ferroalloys Congress. 367-376.

Hopke, P.K., and Casuccio, G. 1991. Scanning Electron Microscopy. In: Receptor Modeling for Air Quality Management. *Elsevier*, p. 7.

Karanasiou A., Minguillón M. C., Viana M., Alastuey A., Putaud J. P., Maenhaut W., Panteliads P., Močnik G., Favez O., and Kuhlbusch T. A.J. 2015. Thermal-optical analysis for the measurement of elemental carbon (EC) and organic carbon (OC) in ambient air: a literature review. *Amos. Meas. Tech. Discuss*., 8: 9649-9712.

Kim, D.S., Hopke, P.K., 1988. The classification of individual particles based on computer-controlled scanning electron microscopy data. *Aerosol Sci. Technol*. 9: 133–151.

Kim, E., T.V. Larson, P.K. Hopke, C. Slaughter, L.E. Sheppardand Claiborne, C. 2003b. Source Identification of PM2.5 in an Arid Northwest U.S. City by Positive Matrix Factorization. *Atmos. Res*. 66: 291-305.

Kim, E. and Hopke, P. K. 2008: Source characterization of ambient fine particles at multiple sites in the Seattle area, *Atmos. Environ*., 42: 6047–6056.

Lagudu U.R.K, Raja S, Hopke P.K, Chalupa D.C, Utell M.J, Casuccio G, Lersch T.L, and West R.R., 2011. Heterogeneity of Coarse Particles in an Urban Area. *Environ. Sci. Technol*. 45: 3288–3296.

Lee, E., Chan, C.K., Paatero, P., 1999. Application of positive matrix factorization in source apportionment of particulate pollutants in Hong Kong. *Atmos. Environ*. 33 (19): 3201– 3212.

Liu, Y., Zhang W., Yang W., Bai Z., and Zhao X., 2018. Chemical Compositions of PM2.5 Emitted from Diesel Trucks and Construction Equipment. *Aer. Sci. & Eng* 2:51–60.

Lockwood, A. H., and Evans, L. "How Breathing Coal Ash Is Hazardous To Your Health". Physicians for Social Responsibility. Retrieved 3 March 2016

Mamane Y., Willis R., and Conner T., 2001. Evaluation of Computer-Controlled Scanning Electron 381 Microscopy Applied to an Ambient Urban Aerosol Sample. Aerosol Science and Technology: The 382 J*ourn. Amer. Ass. Aer. Res*., 34(1): 97.

Moody, J. L. and Galloway, J. N. 1988. Quantifying the relationship between atmospheric transport and the chemical composition of precipitation on Bermuda. *Tellus* 40B, 463—479.

Nkohla, M.A., 2006. Characterization of Ferrochrome Smelter Slag and its Implications in Metal Accounting, Cape Peninsula University of Technology, Cape Town, South Africa. 1-10.

Ott, D. K., Cyrs, W, and Peters T.M. 2008. "Passive Measurement of Coarse Particulate Matter, $PM_{10-2.5}$." *J. of Aeros. Sc*. 39 (2): 156–167.

Pant P. and Harrison R. M. 2012. Critical review of receptor modelling for particulate matter: A case study of India. *Atmos. Environ*. 49: 1-12.

Pope CA III. 2000. What do epidemiologic findings tell us about health effects of environmental aerosols? *Aerosol Med*. 13(4):335–354.

Ravindra, K., Bencs, L., Wauters, E., de Hoog, J., Deutsch, F., Roekens, E., Bleux, N., Bergmans, P. and Van Grieken, R. 2001. Seasonal and site specific variation in vapor and aerosol phase PAHs over Flanders (Belgium) and their relation with anthropogenic activities. *Atmos. Environ*, 40: 771–785.

Reff, A., Eberly, S. I., and Bhave, P. V. 2007. Receptor modeling of ambient particulate matter data using positive matrix factorization: review of existing methods. JAPCA *J. Air Waste Manag*. 57: 146–154.

Romesburg, H. C. 1984: Cluster analysis for researchers. Lifetime Learning, Belmont, Calif., 334pp.

Sawvel, E.J., Willis, R., West, R.R., Casuccio, G.S., Norris, G., Kumar, N., Hammond, D., and Peters T.M. 2015. Passive sampling to capture the spatial variability of coarse particles by composition in Cleveland, OH. *Atmos. Environ*., 105: 61-69.

Schauer, J.J., W.F. Rogge, L.M. Hildemann, M.A. Mazurek, G. R. Cass, and B.R.T. Simoneit. 1996. Source apportionment of airborne particulate matter using organic compounds as tracers. *Atmos. Environ*. 30:3837–55. doi:10.1016/1352-2310(96)00085-4.

Schulze B. R. 1986. Climate of South Africa. Part 8. General Survey, WB 28, Weather Bureau, Department of Transport, Pretoria, 330 pp.

Song, X.H., Hopke, P.K., 1996b. Solving the chemical mass balance problem using an artificial neural network. *Environ. Sci. Technol*. 30 (2): 531–535.

Stohl, A. 1998. Computation, accuracy and applications of trajectories - a review and bibliography, *Atmos. Environ*., 32: 947–966.

Stunder, B. J. B. 1996. An assessment of the quality of forecast trajectories. *J. of Appl. Meteor.* 35: 1319—1331.

Sun H, Shamy M, Kluz T. 2012. Gene expression profiling and pathway analysis of human bronchial epithelial cells exposed to airborne particulate matter collected from Saudi Arabia. *Toxicol. Appl. Pharmacol*. 265:147–57.

UNEP, 2006. African Regional Implementation Review for the 14th Session of the Commission on Sustainable Development.

Van Groenigen, J.W., Stein, A. and Zuurbier, R. 1997. Optimization of environmental sampling using Interactive GIS. *Soil Technology* 10: 83-97.

Wagner, Jeff, and David Leith. 2001b. "Passive Aerosol Sampler. Part II: Wind Tunnel Experiments." *Aeros. Sc. & Tech*. 34 (2): 193–201.

Watson, J.G. and Chow, J.C. 2001a. PM2.5 Chemical Source Profiles for Vehicular Exhaust, Vegetation Burning, Geological Materials and Coal Burning in Northwestern Colorado during 1995. *Chemosphere*. 43: 1141-1151.

Watson, J.G. and Chow, J.C. 2001b. Source Characterization of Major Emission Source in the Imperial and Maxicali Valleys along the US/Mexico Boarder. *Sci. Total Environ*. 276: 33-47.

Watson, J.G. 2002. Visibility: science and regulation. *J. of Air and Waste Manag. Ass*. 52: 628–713.

Zayed A.M and Terry M., 2003. Chromium in the environment: factors affecting biological remediation. *Plant and Soil* 249: 139–156.

Appendix A

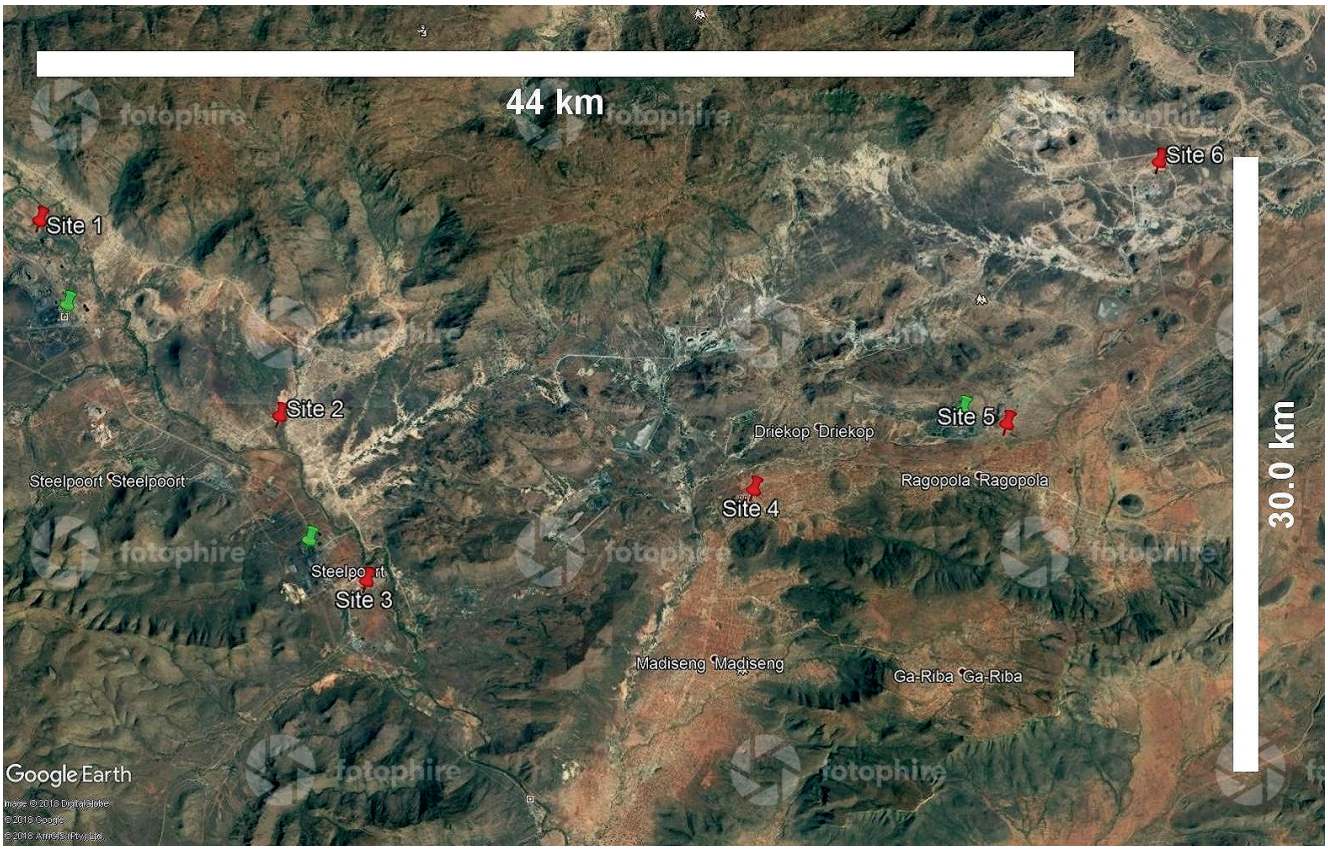

Figure A1: *Map of the study area showing passive sampler locations (red place-marks on Google map), with smelters shown as green place-marks.*

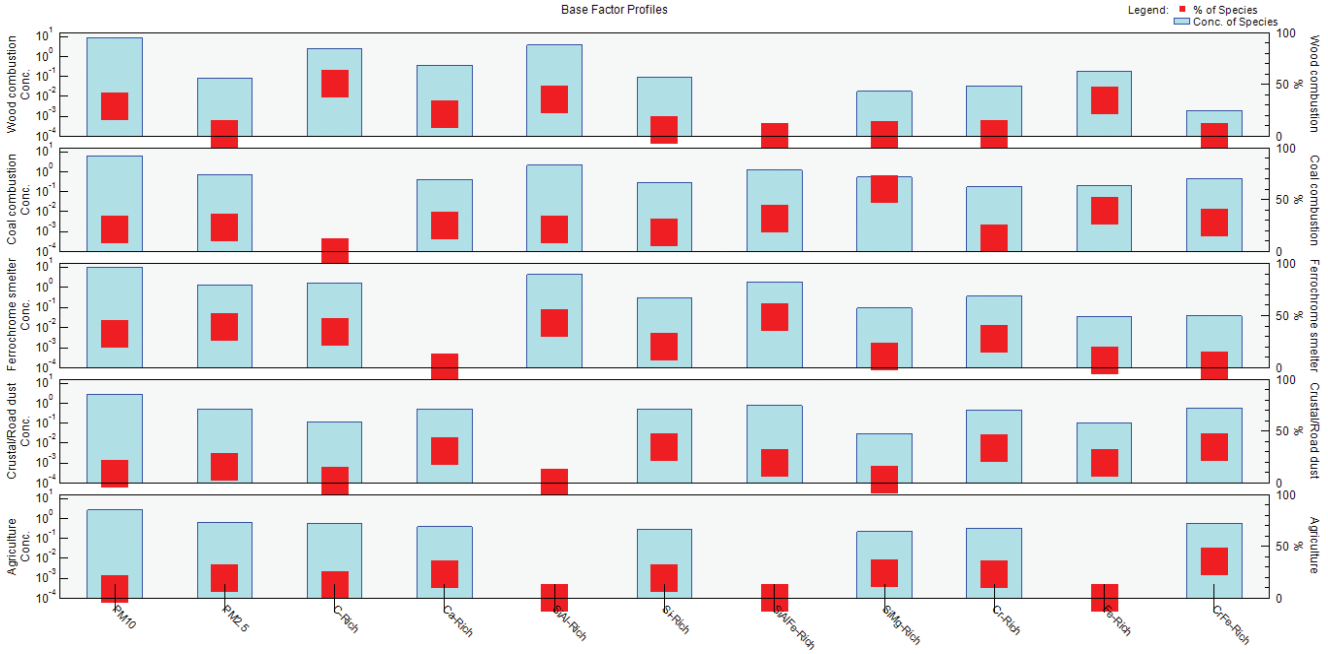

Figure A2.1: *Factor fingerprints for species at site 1.*

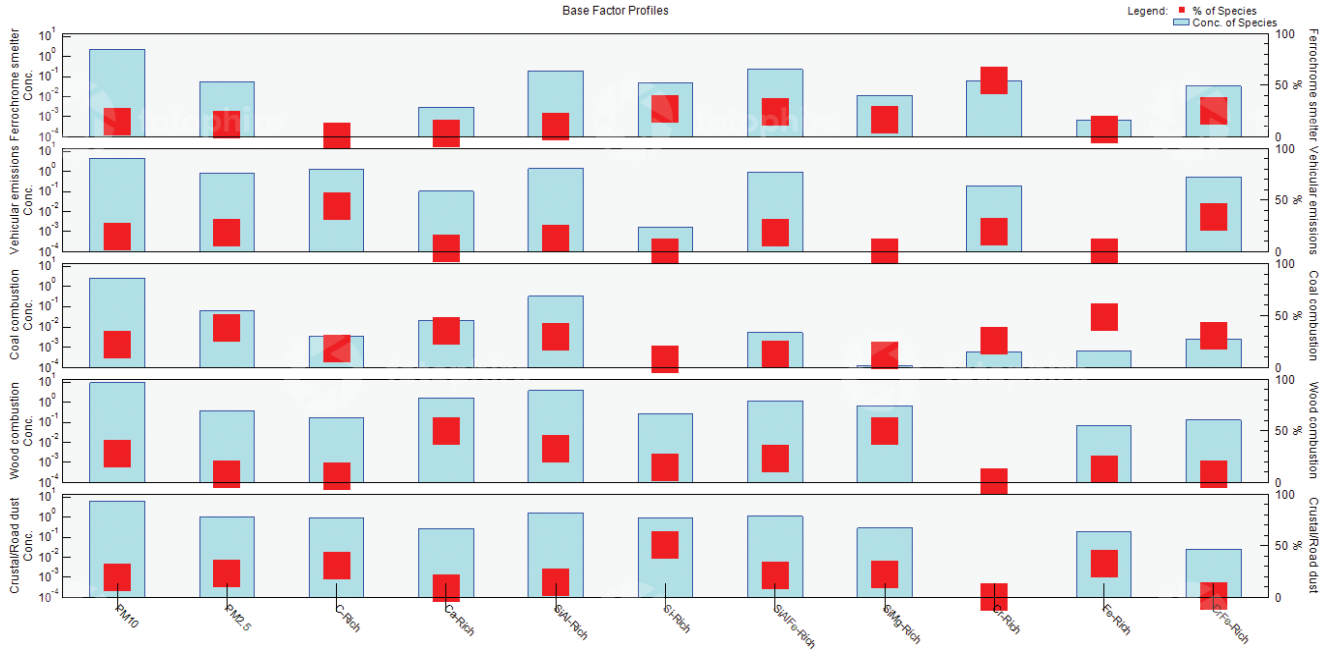

Figure A2.2: *Factor fingerprints for species at site 2.*

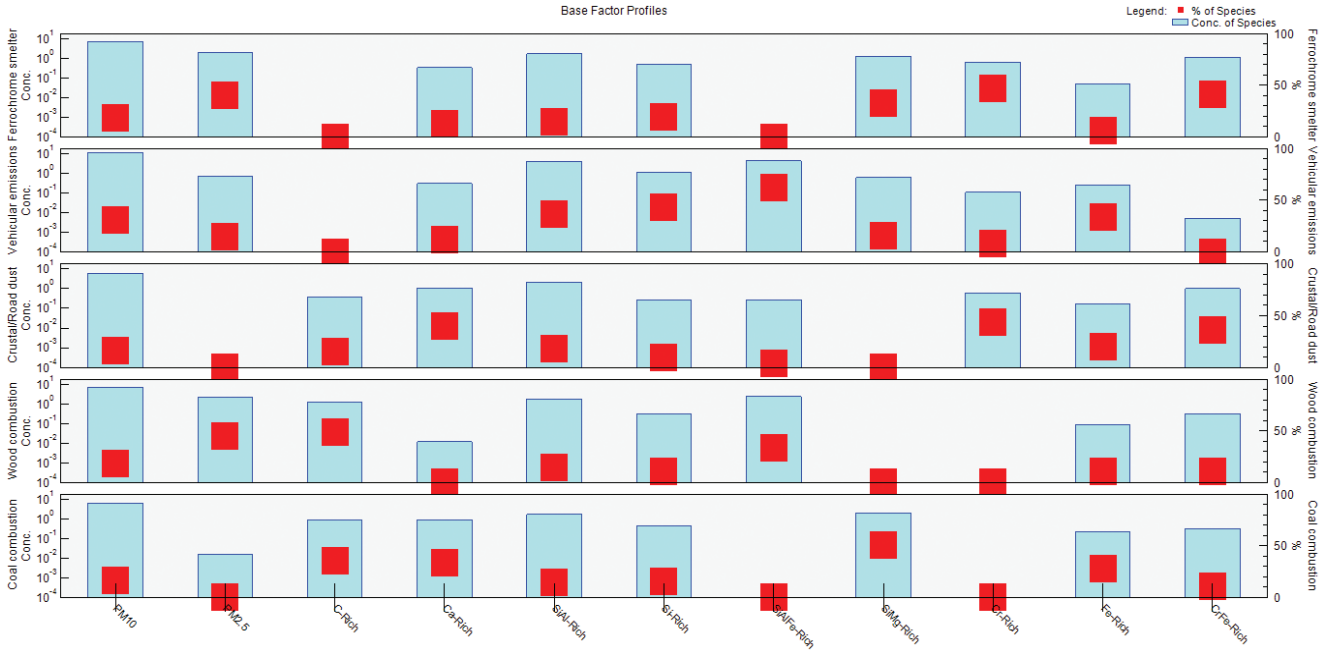

Figure A2.3: *Factor fingerprints for species at site 3.*

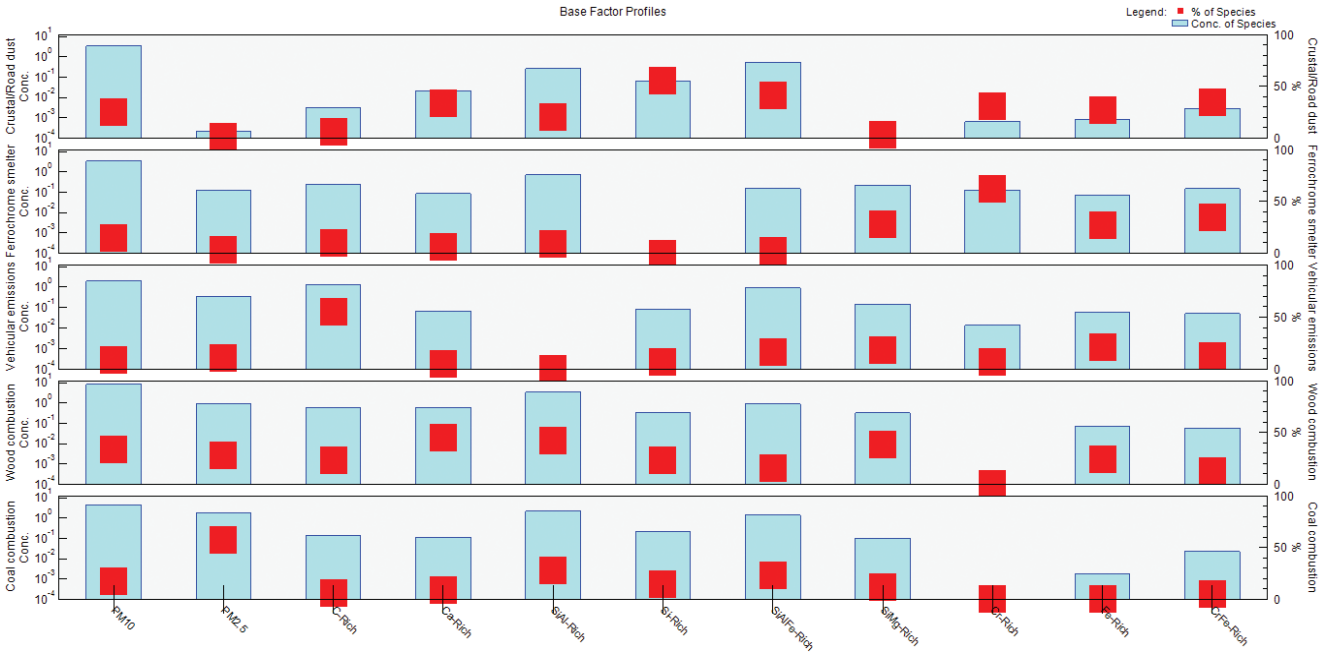

Figure A2.4: *Factor fingerprints for species at site 4.*

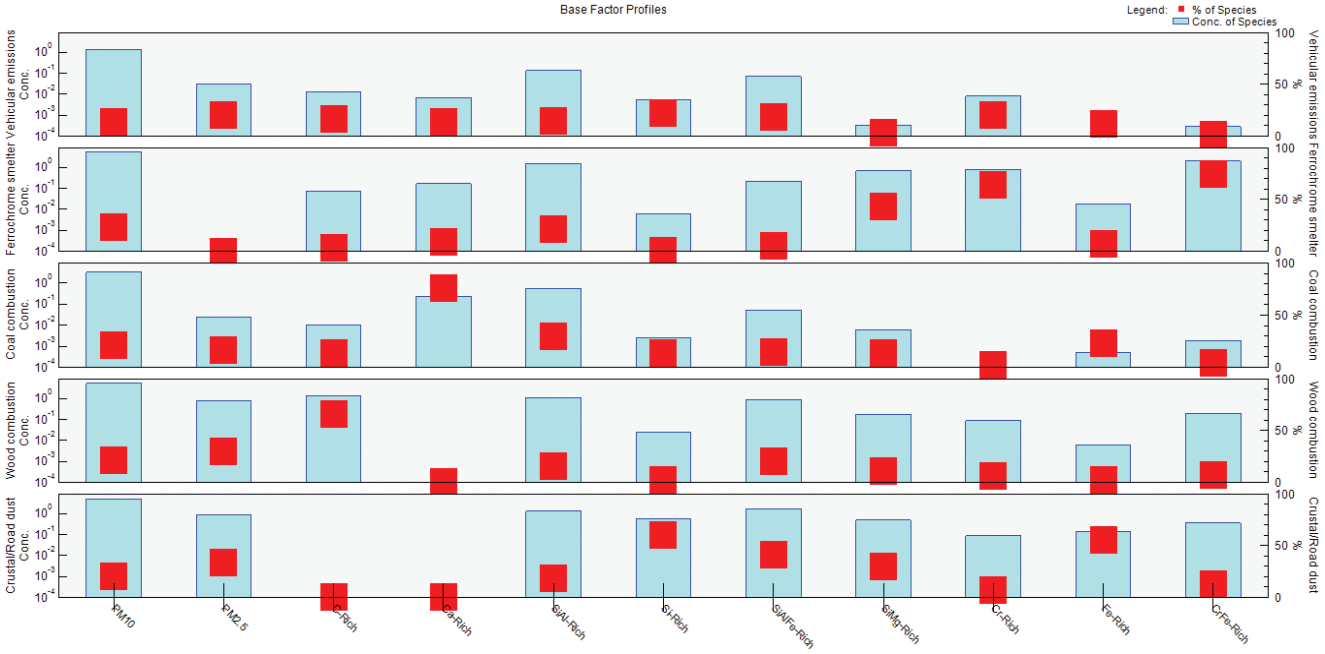

Figure A2.5: *Factor fingerprints for species at site 5.*

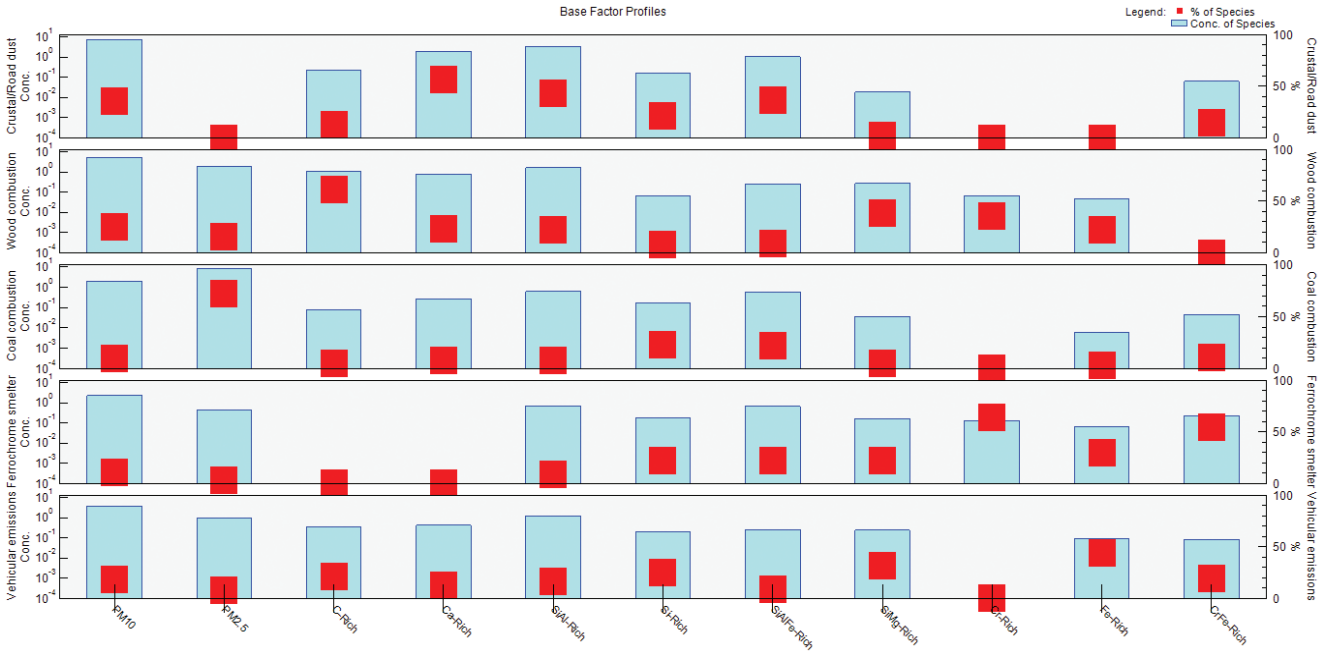

Figure A2.6: *Factor fingerprints for species at site 6.*

CHAPTER 5

Results: Spatial and Temporal Variation of PM_{10} from Industrial Point Sources in a Rural Area in Limpopo, South Africa

5.1 Paper overview

This manuscript describes the influence of meteorology on the spatio-temporal variation of PM from industrial point sources and identifies the possible areas in which to locate future ambient monitoring stations. The terrain of the GTM and the number of point sources in the area are discussed. The population statistics of the GTM are given from Statistics South Africa and the dispersion modelling processes are discussed using The Air Pollution Model (TAPM). The annual and seasonal variations of PM_{10} are evaluated, and the day-time and night-time PM_{10} distribution patterns are discussed to evaluate how they may impact on the environment and possibly on human health. The relation between PM_{10} distribution and meteorological parameters such as temperature, relative humidity, mixing height and solar radiation, are also discussed.

The relationship between PM_{10} and temperature depicts a bell-shape with high PM_{10} concentration occurring in the mid temperatures and low concentrations occurring during minimum and high temperatures. The relationship between PM_{10} and mixing height is influenced by solar radiation. This happens when less solar radiation heats the Earth's surface in autumn and winter (which causes shallow mixing height) and more radiating heating heats the surface during spring and summer (which result in elevated mixing height) due to longer day hours.

The GTM is home to several sources that were identified by Tshehla and Djolov (2018). Figure 3.1a (see Chapter 3, page 87) identifies the location of the GTM in South Africa and Figure 3.1b shows the location of the sources and monitoring sites in the GTM. These sources are the

result of industrialization in this rural local municipality. The gas emissions from ferro-alloy smelting furnaces contain large size particles of dirt, dust and incomplete combustion of coal and coke in addition to fine particles. The gas may contain harmful sulphurous products, toxic metal oxide vapours, carbon monoxide and other organic gases. Techniques have been developed for ferroalloy emission control, but the costs are high (Holappa, 2010). Therefore, to reduce pollution from ferrochrome processed in the GTM will require stringent measures such as production of ferro-alloy in closed furnaces to allow re-use of carbon monoxide in electricity co-generation, reduction of fugitive dust from material handling, continuous monitoring of emissions from the stacks, metal recovery from the slag dumps, and recycling of furnace off-gas dust to the furnace.

Wind was also considered. The seasonal winds in Figure 5.1 (overleaf) did not provide a clear picture of the wind patterns. There was a mix of strong and light winds in all seasons. The distribution of pollution in all seasons could be attributed to both the winds and the orientation of the valleys.

Dispersion modelling uses mathematical formulations to quantify the atmospheric processes that disperse a pollutant emitted by a source (Grigoras *et al*., 2010). Based on emissions and meteorological inputs, dispersion models can be used to predict concentrations at selected downwind receptor locations. Such models are widely used in the management of the impact of pollutant emissions on environment (Zannetti, 1990). There has been extensive modelling exercises that were undertaken in South Africa to assess and estimate the impacts of proposed or existing regulated industries. However, the requirement for impact assessment studies for a new activity (plant) or altering the existing emission license does not requires modelling the cumulative impact of all the point sources in the area. This may render measures already put in place to reduce pollution ineffective. Therefore, this study sought to show how cumulative impacts of point sources can lead to high pollution levels within an airshed and also helps in identifying optimal locations for monitoring the impacts of point sources.

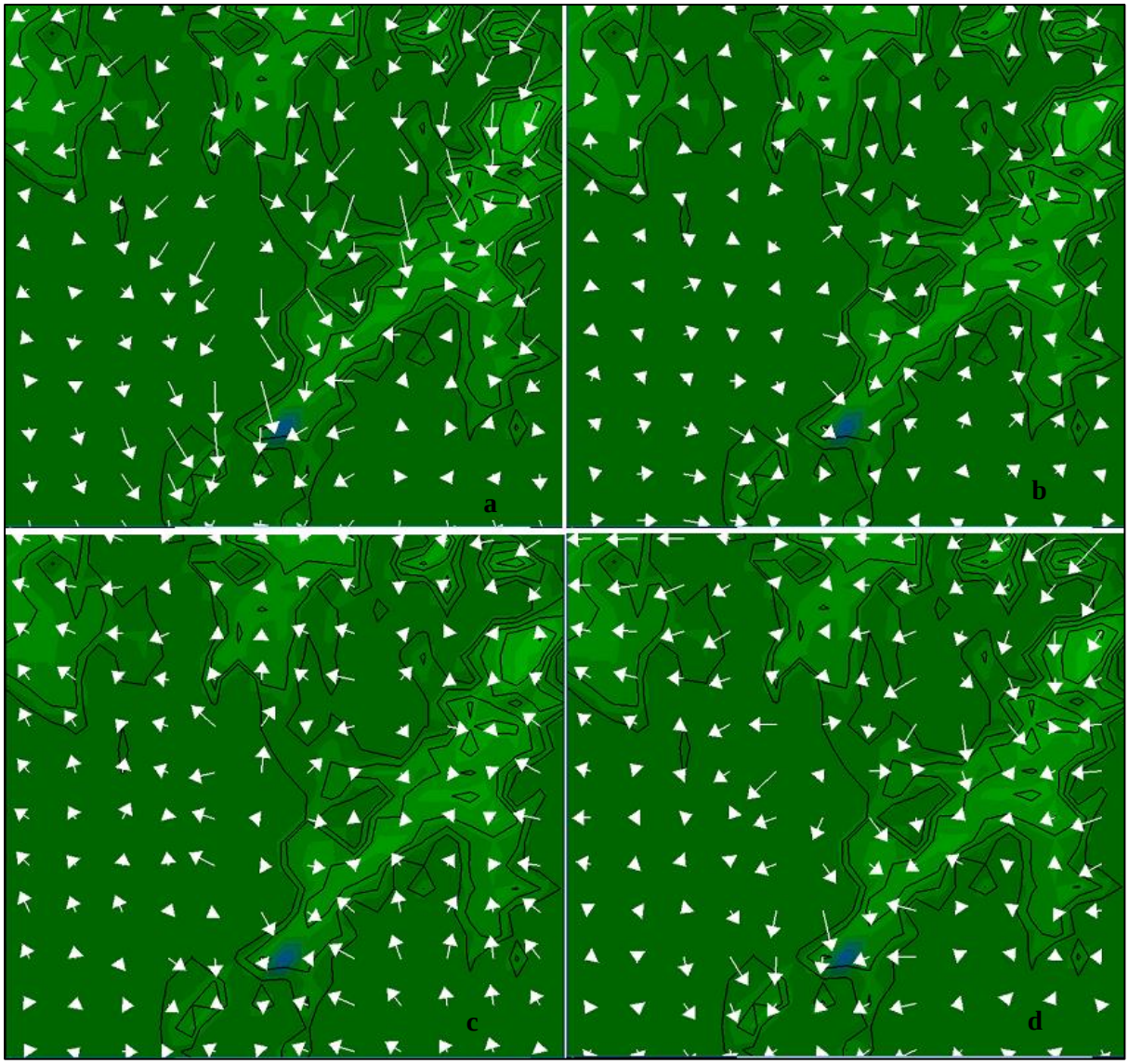

Figure 5.1. Horizontal seasonal wind patterns ((a) summer, (b) autumn, (c) winter, (d) spring) in the study area.

Several shortcomings of the publication were identified post-publication. While mention is made in the manuscript to indicate that the area has been increasingly urbanized, this information was not supported with a reference in the manuscript. However, it is mentioned in the GTM's 2016/2017 – 2020/2021 final integrated Development Plan (GTM, 2016). Although an effort was made to discuss the pollution distribution in terms of wind patterns, the seasonal variation in terms of source strengths was not considered in the study, and this was considered a shortcoming in the model set up by the Candidate. The inclusion of the seasonal source strength could have made the discussion more robust.

5.2 Contribution to the thesis

Industrial sources were identified in the previous paper as one of the major sources of PM. This paper addressed objective 7 'to determine the distribution of PM_{10} from industrial point sources and evaluate their possible impacts on human health using modelled hourly data from the TAPM model and GIS software'. The annual PM_{10} concentrations indicated that the highest concentrations (27.3 µg.cm^{-3}) were distributed to the southwest of Smelter 2 and northwest of Smelter 1. Though this value was below the South African annual PM_{10} National Ambient Air Quality Standard (NAAQS) of 40 µg.cm-3 (see Table 2.5), it was above the WHO annual guideline of 20 µg.cm^{-3}. Tshehla and Djolov (2018) indicated that industrial point sources contribute 23.52% of the total pollution in the GTM. Therefore, the annual value of 27.3 µg.cm^{-3} from industrial point sources may pose a serious environmental threat and cause health problems in the area.

The results also showed that there were distinct seasonal and day and night variations in the wind patterns in the area which distributes PM_{10} concentrations to the north-westerly, westerly and south-westerly of the airshed. Figure 4a shows higher night-time concentrations ranging from 14 – 16.5 µg.cm^{-3} and covering a number of residential areas (indicated by green dots), while Figure 5b shows high day-time concentrations ranging from 11.1 – 15.9 µg.cm^{-3} which covers a small area. During the night, the atmosphere is stable and vertical motion in the atmosphere is suppressed. Air pollution is distributed through a shallow layer causing high concentration over a larger area due to stagnation. Dispersion of pollution occurs more easily when the atmosphere is unstable during the day which leads to high concentrations near the sources. Therefore, a large number of settlements will be impacted by high concentrations at night compared to day-time. The settlements identified as the possible impact hot-spots from industrial pollution will require continuous ambient monitoring to assess future health impacts from industrial pollution.

5.3 Role of the candidate

Cheledi E. Tshehla set up and performed TAPM analysis and the GIS spatial interpolation of the TAPM output and wrote the first draft of the manuscript. The evaluation and interpretation of the results were performed in close cooperation with the Dr C.Y. Wright (co-author).

5.4 Publication status

Tshehla C.E., and Wright C.Y. 2019. Spatial and temporal variation of PM_{10} from industrial point sources in a rural area in Limpopo, South Africa. *Int. J. Environ. Res. Public Health* 16: 1-14. Doi: https://doi.org/10.3390/ijerph16183455

5.5 References

Greater Tubatse Municipality (GTM), 2016: FINALINTEGRATED DEVELOPMENT PLAN 2016/17-2020/21. Available from: http://www.tubatse.gov.za/docs/idp/Final%202016-17%20IDP%202.pdf.

Grigoras, G., Cuculeanu, V., Ene, G., Mocioaca, G. and Deneanu, A., 2010: Air pollution dispersion modelling in a polluted industrial area of complex terrain from Romania. *Romanian Reports in Physics*, 64(1): 173-186.

Holappa, L., 2010: Towards sustainability in ferroalloy production. *The Southern African Institute of Mining and Metallurgy. Infacon 2010 Congress*, 6–9 June 2010, Helsinki, Finland.

South African Department of Environmental Affairs (DEA). National ambient air quality standards [document on the Internet]. c2012 [cited 2018 June29]. Available from: https://www.environment.gov.za/content/national-environmental-management-air-quality-act-2004-act-no-39-2004-national-ambient-air-q.

Tshehla, C.E and Djolov, G., 2018: Source profiling, source apportionment and cluster transport analysis to identify the sources of PM and the origin of air masses to an industrialized rural area in Limpopo. *Clean Air Journal*, 28(2): 54-66.

Zannetti, P., 1990: Air Pollution Modelling: Theories, Computational Methods and Available Software, Van Nostrand Reinhold, New York.

Manuscript 3

International Journal of
Environmental Research and Public Health

MDPI

Article

Spatial and Temporal Variation of PM_{10} from Industrial Point Sources in a Rural Area in Limpopo, South Africa

Cheledi E. Tshehla [1,*] and Caradee Y. Wright [2]

[1] Department of Geography, Geoinformatics and Meteorology, University of Pretoria, Pretoria 0002, South Africa
[2] Environment and Health Research Unit, South African Medical Research Council, Pretoria 0084, South Africa; Caradee.Wright@mrc.ac.za
* Correspondence: cheledi.tshehla@weathersa.co.za; Tel.: +27123676076

Received: 21 June 2019; Accepted: 26 July 2019; Published: 17 September 2019

Abstract: Air pollution from industrial point sources accounts for a large proportion of air pollution issues affecting many communities around the world. However, emissions from these sources are technically controllable by putting in place abatement technologies with feasible and stringent regulatory conditions in the operation licenses. Pollution from other sources such as soil erosion, forest fires, road dust, and biomass burning, are subject to several unpredictable natural or economic factors. In this study, findings from dispersion modelling and spatial analysis of pollution were presented to evaluate the potential impacts of PM_{10} concentrations from point sources in the Greater Tubatse Municipality of Limpopo, South Africa. The Air Pollution Model (TAPM) was used to model nested horizontal grids down to 10 km for meteorology and 4 km resolution for air pollution was used for simulation of PM_{10}. An analysis of annual and seasonal variations of PM_{10} concentrations from point sources was undertaken to demonstrate their impact on the environment and the surrounding communities based on 2016 emissions data. A simple Kriging method was used to generate interpolation surfaces for PM_{10} concentrations from industrial sources with the purpose of identifying their areas of impact. The results suggest that valley wind channeling is responsible for the distribution of pollutants in a complex terrain. The results revealed that PM_{10} concentrations were higher closer to the sources during the day and distributed over a wide area during the night.

Keywords: air pollution; point sources; population distribution; particulate matter; TAPM

1. Introduction

Particulate matter (PM) is a complex mixture of solid particles and liquid droplets suspended in the air that vary in size, composition and concentration. PM with aerodynamic diameter of less than 10 μm (PM_{10}) can stay in the air for minutes to hours and can travel for up to 50 km, while $PM_{2.5}$ (fine) particles are lighter and can stay in the air for days or weeks and travel longer distances than coarser PM_{10} particles [1]. PM exposure has been a growing public concern and it is associated with severe health impacts [2]. Studies worldwide have linked exposure to PM air pollution with a range of cardiovascular, respiratory diseases, stroke, chronic obstructive pulmonary disease, childhood pneumonia, asthma and diabetes [3–9]. It should be noted, however, that the evidence for the hazardous nature of combustion-related PM (from both mobile and stationary sources) is more consistent than that for PM from other sources [10]. Ref. [11] estimated that approximately 3% of cardiopulmonary and 5% of lung cancer deaths are attributable to PM exposure globally.

The Greater Tubatse Municipality (GTM) in Limpopo, South Africa, is home to three ferrochrome smelters. The main pollutants emitted from the smelters in the GTM, PM_{10} and PM_{10} chemical

components are discussed in [12]. The area has a complex terrain (Figure 1) with terrain height ranging from 850 m to 1850 m above sea level. Mountainous terrain has a high degree of topographical variation and land cover heterogeneity [13].

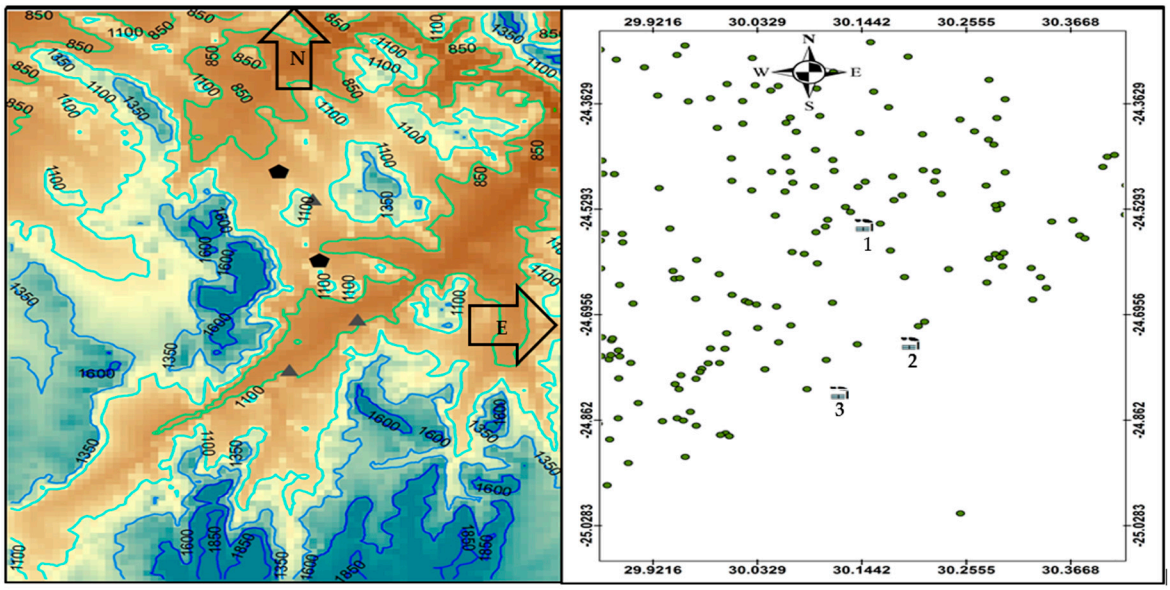

(a) **(b)**

Figure 1. (**a**) Terrain map of the study area showing smelters as black triangles and mine tailings as black pentagons. (**b**) Study area showing location of smelters (1–3) and residential areas in green dots.

The GTM has an area of approximately 4550 km^2 in size and a population size of 335,676 [14]. (Table 1) which comprises 115,809 children (0–14) and 17,119 elderlies (65+). These age groups are classified as being prone to the health impacts of PM pollution [15]. The GTM is largely rural with the majority of people being low-income earners and relying on river streams for water and vegetables from informal farming.

Table 1. Population statistics by age from the 2011 census for the GTM (statistics South Africa).

Age Group	Population *N* (%)
0–14	115,809 (34.5%)
15–64	202,748 (60%)
65+	17,119 (5.5%)
Total	335,676 (100%)

Due to intensive industrialization, the area has seen an increase in traffic activities and possibly in waste disposal due to urbanization of this rural area. Due to a lack of ambient air quality data and ground-level meteorological monitoring data in the area, it is vital to investigate how pollution from the industrial point sources impact on the environment. PM is mainly emitted into the atmosphere by anthropogenic sources such as industries, vehicles, combustion sources, road dust and open burnings, and natural sources such as wildfires due to lightning strikes and wind-blown dust from open un-vegetated surfaces.

The emissions alone cannot determine the type and intensity of air pollution of any area. Meteorology and the climate, as well as the topography of the site, all have a major influence on the dispersion and transformation of pollutants [16]. The concentration of pollutants in the lower layers of the atmosphere depends on the atmospheric pressure, the wind and the temperature [17]. The dispersion of pollutants increases with the wind speed and turbulence, and its direction orients the plumes emitted from the stacks. The vertical temperature gradient helps the ascending movement

of air pollutants. However, in cases of temperature inversion, pollutants are blocked in the low layers of the atmosphere, which creates episodes of pollution [18].

The topography variation such as the one found in the GTM influences the atmosphere in two ways [19]. The first is in the form of momentum exchange between the atmosphere and the surface that occurs because of flow modification by mountains in the form of mountain lee waves, flow channeling and flow blocking [20]. The second effect involves energy exchange between the terrain and the atmosphere. The thermally induced winds depend on the temperature differences along the mountain plain systems and the strength of the synoptic systems and the cloud cover, with weak synoptic systems and cloud-free atmospheres producing more pronounced winds [21,22]. Mountain winds blow parallel to the longitudinal axis of the valley and are directed up-valley during daytime and down-valley during night-time. The circulation is closed above the mountain ridges by a return current flowing in the reverse direction. The development of thermally driven winds is often complicated by the presence of other wind systems developed on different scales [22,23]. The anabatic flows are limited in time during wintertime as compared to during the summer due to the shorter exposure period to sunlight [24].

Dispersion modelling is a mathematical tool that includes simplified algorithms used to quantify the atmospheric processes that disperse pollutants emitted by a source. Dispersion models can be used to predict concentrations at selected downwind receptor locations depending on the emissions, topographical and meteorological inputs. These models can be used in the development of strategies for the management of pollution impacts on the environment and the assessment of air quality [25]. To effectively manage the PM pollution from industrial sources and to mitigate the impact of this pollutant on human health, it is important to provide information on the spatio-temporal pattern of PM emissions. However, emissions data is not readily available in South Africa.

Ref. [12] identified ferrochrome smelters as one the major contributors of PM_{10} (contributing 23.52% of the total PM_{10} in the GTM). Therefore, an air quality assessment in a highly industrialized rural area of Limpopo, South Africa was performed by means of The Air Pollution Model (TAPM) as a predictive (meteorological) modelling tool. The model output was imported into Geographic Information System to spatially display the seasonal and annual impact of PM concentrations from ferrochrome smelters in the region. The meteorological parameters such as wind, humidity, radiation, mixing height and temperature, were examined to evaluate potential influences on the PM_{10} concentrations.

2. Materials and Methods

2.1. Data

The annual PM_{10} emissions data (Table 2) for 2016 were provided by the Department of Environmental Affairs' National Emissions Inventory System (DEA, NAEIS). The annual data in kilograms per annum (kg/yr) were converted to grams per second for input into the TAPM model.

Table 2. 2016 industrial emissions in the GTM.

Source	PM_{10} Emissions (kg/yr)	Stack Height (m)	Stack Diameter (m)	Exit Velocity (m/s)	Exit Temperature (°C)	Gas Flow Rate	Operating Hours
Smelter 3 (Stack 1)	1598	56.5	0.78	21.55	75	6.24	8760
Smelter 3 (Stack 2)	365	64.45	0.78	21.55	75	3.48	8760
Smelter 3 (Stack 3)	10,231.	64.45	0.78	21.55	75	3.96	8760
Smelter 2 (Stack 1)	11,416	32.0	1.6	24.13	137	5.2	8760

Table 2. *Cont.*

Source	PM_{10} Emissions (kg/yr)	Stack Height (m)	Stack Diameter (m)	Exit Velocity (m/s)	Exit Temperature (°C)	Gas Flow Rate	Operating Hours
Smelter 2 (Stack 2)	2611	30.0	1.2	25.93	118	2.9	8760
Smelter 2 (Stack 3)	7308	30.0	1.7	25.18	110	3.3	8760
Smelter 1 (Stack 1)	13,699	50.3	1	24.13	160	5.72	8760
Smelter 1 (Stack 2)	3133	61.5	0.8	32.96	66	3.19	8760
Smelter 1 (Stack 3)	8769	60.6	1	30.59	50	3.63	8760

The population distribution (Table 1) for the GTM was obtained from the Statistics South Africa website [14].

2.2. Model Configuration

TAPM (version 4) was run for the period of July 2015 to June 2016. Four grids with nested domains of 25 × 25 horizontal grid points at 30 km (Figure 2a), 20 km (Figure 2b), 10 km (Figure 2c) spacing for the meteorology and 4 km (smaller grid in white) for pollution simulation were used. A total of 49 discrete receptor points were used for calculating pollution concentration fields. The model uses a default database of soil properties, topography, and deep soil parameters were used. The global terrain height data on a longitude/latitude grid at 30-second grid spacing (approximately 1 km) based on public domain data used in the model is available from the US Geological Survey, Earth Resources Observation Systems (EROS) Data Center Distributed Active Archive Center (EDC DAAC). The database for global soil texture types on a longitude/latitude grid at 2-degree grid spacing (approximately 4 km) was obtained from the Food and Agriculture Organization of the United Nation website. The global deep soil parameters data on a longitude/latitude grid at 30-second grid spacing (approximately 1 km) is available from the US Geological Survey, Earth Resources Observation Systems (EROS) Data Center Distributed Active Archive Center (EDC DAAC).

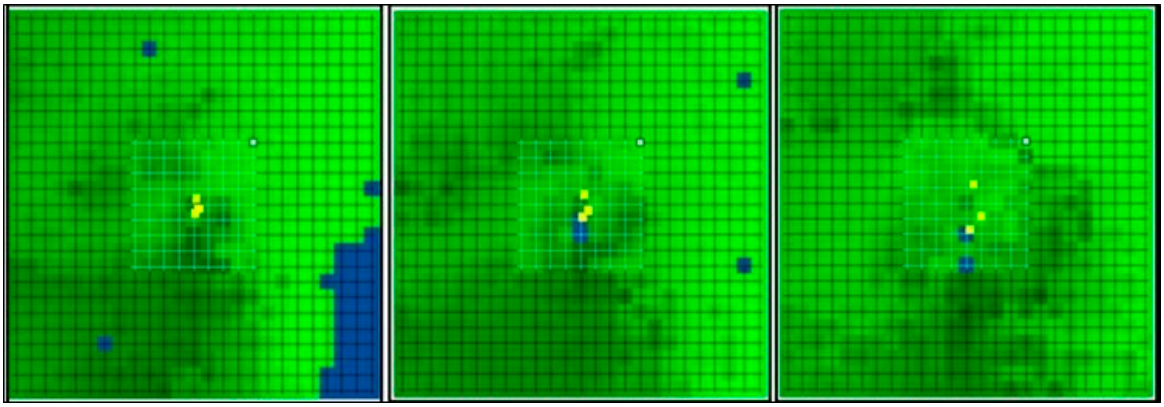

(**a**) (**b**) (**c**)

Figure 2. The horizontal grid domain used by TAPM for meteorology and the smaller grid for PM_{10} predictions (25 × 25). These domains were simulated at horizontal grid resolutions of (**a**) 30 km, (**b**) 20 km, (**c**) 10 km and 4 km for PM_{10} emissions.

TAPM has several characteristics: it is three-dimensional, prognostic, Eulerian, incompressible, and non-hydrostatic. It is a primitive equation model in terrain-following coordinates for simulating atmospheric motion and pollutant transport using nested grids [26]. The model comes with databases containing terrain height data, type of soil and vegetation, sea surface temperature and synoptic scale meteorology supplied by the model developer CSIRO Atmospheric Research Australia. Global terrain and land use datasets have a spatial resolution of 1 km. Sea surface temperature data used are monthly averages and have a spatial resolution of 100 km. Meteorological datasets contain six-hourly synoptic scale analyses on a longitude/latitude grid at 0.75- or 1.0-degree grid spacing (approximately 75 km or 100 km). TAPM then 'zooms-in' from the 100 km data to model local scales at a finer resolution using a one-way nested approach to improve the efficiency and resolution, predicting local-scale meteorology (typically down to a resolution of 1 km) [27].

TAPM uses the predicted meteorology and turbulence from the meteorological component and consists of four modules. The Eulerian Grid Module (EGM) solves prognostic equations for the mean and variance of concentration. The Lagrangian Particle Module (LPM) can be used to represent near-source dispersion more accurately. Wet and dry deposition effects are also included [27]. In this study the LPM was used for dispersion modelling in the GTM. The model was run in observation mode without data assimilation due to non-availability of meteorological data in the area to assimilate PM exposure.

3. Results and Discussion

The simple Kriging method was used to plot the spatial variation of PM_{10} concentrations from the industrial point sources. The method assumes that the mean and variance remain constant and are known in all locations [28]. The meteorological data predicted by the model were extracted at the grid points nearest to the centre of the study area. The annual wind rose (generated by OpenAir statistical software [29]) and spatial variation of PM_{10} concentrations at receptor points were plotted in Figure 3. The annual wind rose shown in Figure 3b indicates that the dominant wind direction is south-westerly, north-easterly and westerly with wind speed reaching 5.7–8.8 m.s^{-1}.

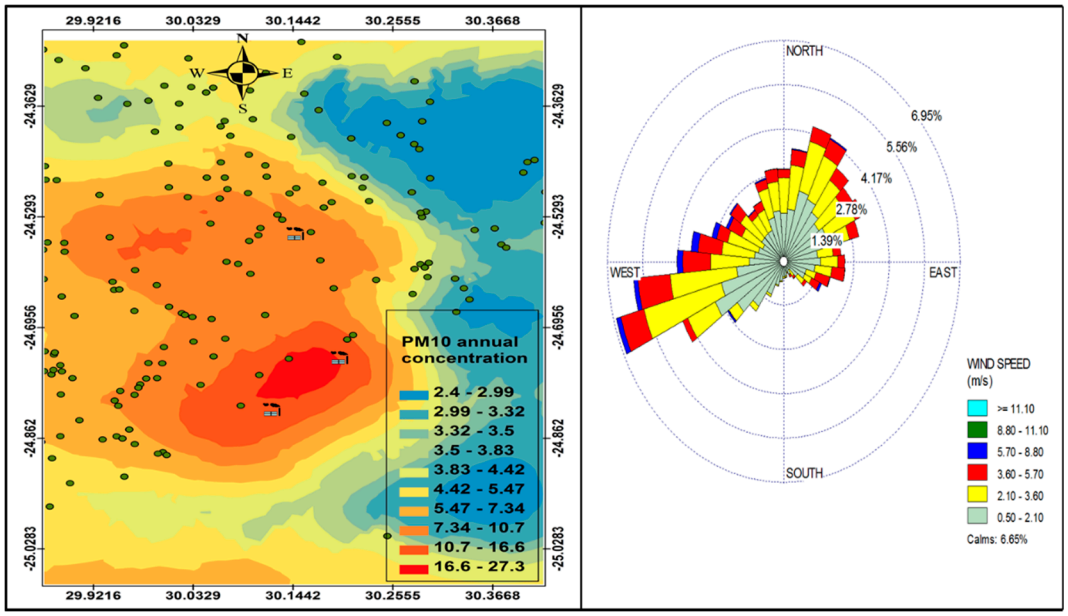

(a) **(b)**

Figure 3. Annual variation in PM_{10} (μg.cm^{-3}) ambient concentration (**a**) and annual wind rose (**b**).

The annual PM_{10} spatial analysis (Figure 3a) indicates that the highest PM_{10} concentration (27.3 μg.m^{-3}) was between Smelter 1 and Smelter 2, spreading to the west of Smelter 1 and south-west

of Smelter 2. The highest annual concentration was lower than the 40 μg.m^{-3} of the South African PM_{10} National Ambient Air Quality Standards (NAAQS), however, it was higher than the WHO annual mean guideline of 20 μg.m^{-3}. Even though the industrial point sources constitute less than a quarter of the total sources in the GTM, they may pose a danger to human health based on the WHO ambient air quality guidelines. The residential areas (indicated in Figure 1b) show areas that are potentially most vulnerable to the impacts of these pollutants from the smelters, given their proximity to the industrial facilities. Prevailing wind speed and direction (Figure 3b) play an important role in determining which areas may be affected by PM_{10} pollution from the point sources, with higher wind speeds dispersing pollutants furthest away from the source and low wind speeds depositing pollutants closest to the sources. The west south-westerly winds are responsible for transporting pollutants to the east north-easterly direction between Smelter 1 and Smelter 2, while the north-easterly and easterly winds are responsible for dispersing pollutants from Smelter 3 to the south-westerly and westerly direction.

Figures 4a and 5a indicate a variation in ambient concentrations during the night-time and day-time, respectively, which is caused by varying meteorological conditions during day time and night time, with night time conditions favouring recirculation of air due to the nocturnal inversion layer, plume impingement on high terrain and persistent wind channeling inside valleys, and the daytime conditions occur mainly when there is vertical mixing when the surface inversion breaks and the winds travel up the slopes and the valley disperse pollutants as a function of time and space, with concentration being higher closer to the sources and lower further away from the sources. The evidence of this is the nonexistence of dark red colours to indicate high concentrations on Figure 4a. However, there is wide spread of higher concentrations during the night that covers large residential areas as compared to high concentration of PM_{10} during the day that are localized closer to the sources. This is a clear indication that there is less mixing during the night compared to the day-time. Therefore, pollution episodes often occur more during the night than during the day. This makes communities more vulnerable to pollution at night than during the day, except those communities residing near the industries. Figure 4a shows re-circulation of PM_{10} during the night, which is distributed west of Smelter 1, north-west of Smelter 2 and west of Smelter 3. The wind profile (Figures 4b and 5b) shows that the easterly winds are the most effective winds that could potentially disperse pollutants to the west of Smelter 1 and Smelter 2.

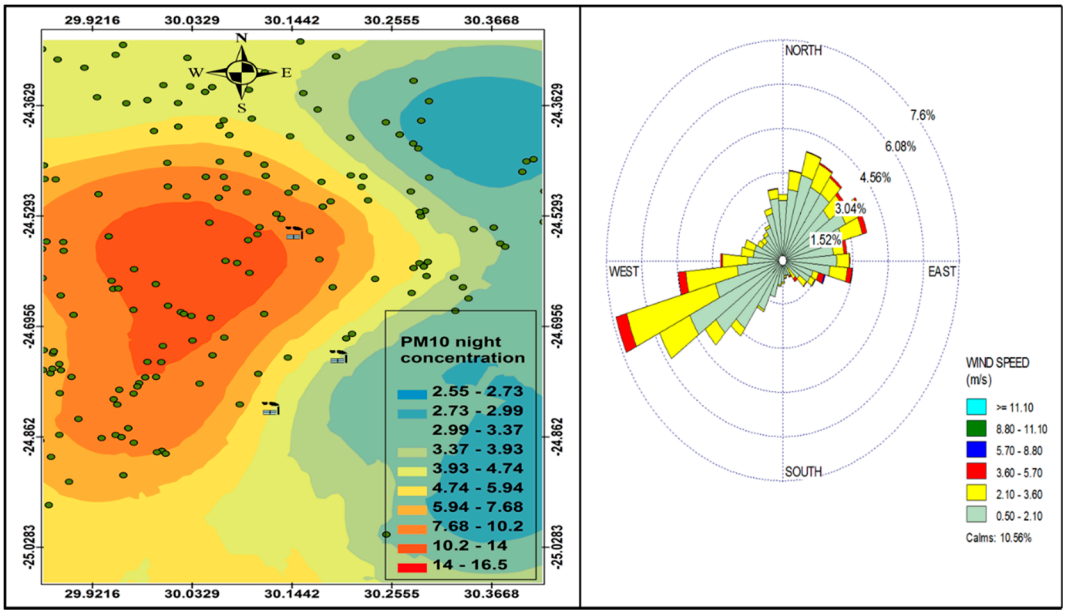

(a) **(b)**

Figure 4. Annual variation in PM_{10} (μg.cm^{-3}) concentration at night (**a**), wind rose during the night (**b**).

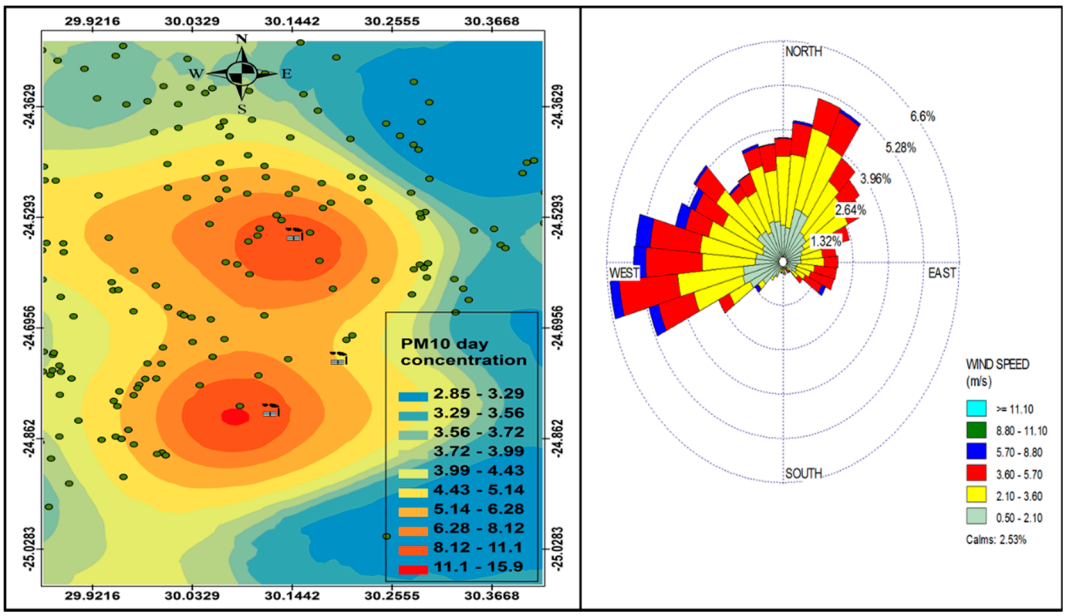

(a) **(b)**

Figure 5. Annual variation in PM_{10} ($\mu g.cm^{-3}$) concentration during day-time (**a**), wind rose during the day (**b**).

Figures 6–9 show the seasonal distribution of PM_{10} concentrations and wind profiles. The wind profiles show that the dominant wind is west to south-westerly during autumn (Figure 6a,b). These winds are responsible for the distribution of pollutants in a north-easterly direction in the south of the study area. The winds are then channeled in a north-westerly direction toward the north of the study area by following the valley axis. The winter season (Figure 7a,b) is dominated by south-westerly winds. However, the easterly and south-easterly winds are the ones dispersing pollutants to the west and southwest of the facilities. During spring (Figure 8a,b) and summer (Figure 9a,b), the north north-easterly to easterly winds are the dominant winds responsible for the dispersion of pollutants to the west and south-west of the facilities in the area. The south-westerly and north-easterly flows are parallel to the valley axis, particularly near Smelter 1 and Smelter 2. There is little or no wind coming from the southerly sector during all seasons. This could be due to the orientation of the valley axis in a south-westerly and north-easterly direction in the south of the study area and the north-west and south-east in the north of the study area. The lack of winds from the south limits the transport of pollution to the north of the facilities in the area. The seasonal patterns on the PM_{10} concentration distributions show that the north-easterly to easterly winds are responsible for dispersing pollutants to the west and south-west. The seasonal distribution also shows that the highest PM_{10} concentrations varies from 15.2 $\mu g.m^{-3}$ to 27.3 $\mu g.m^{-3}$ in the GTM, which constitutes 23.52% of the total PM_{10} sources. These areas likely experience high PM_{10} concentration from industrial point sources and should be considered for passive ambient air quality measurements. This will assist in determining whether there should be further investment in continuous monitoring in these areas.

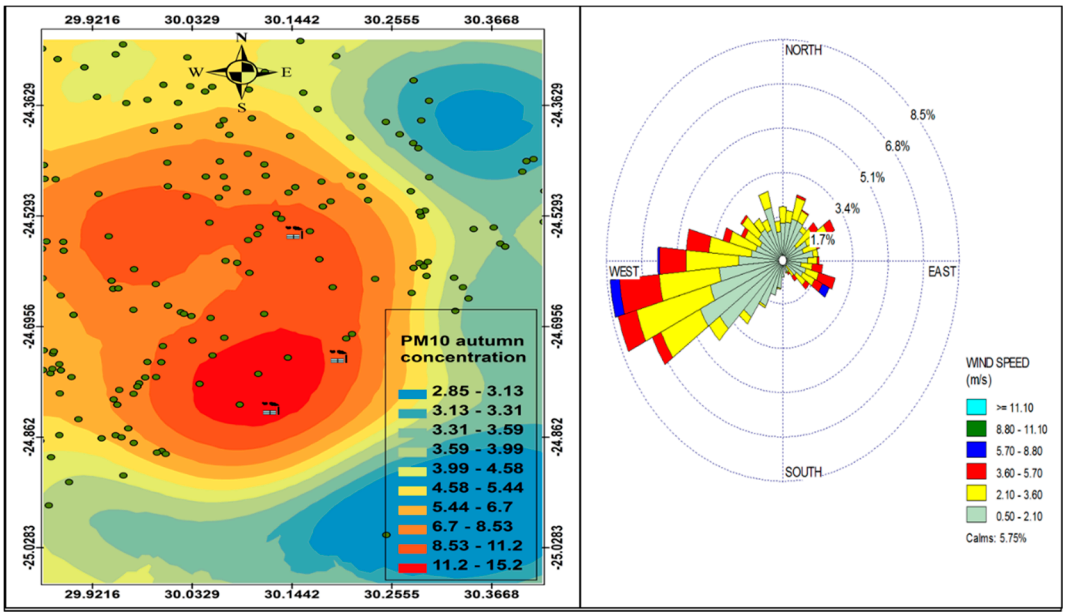

(a) **(b)**

Figure 6. Autumn variation in PM_{10} ($\mu g.cm^{-3}$) ambient concentration (**a**) and wind roses (**b**).

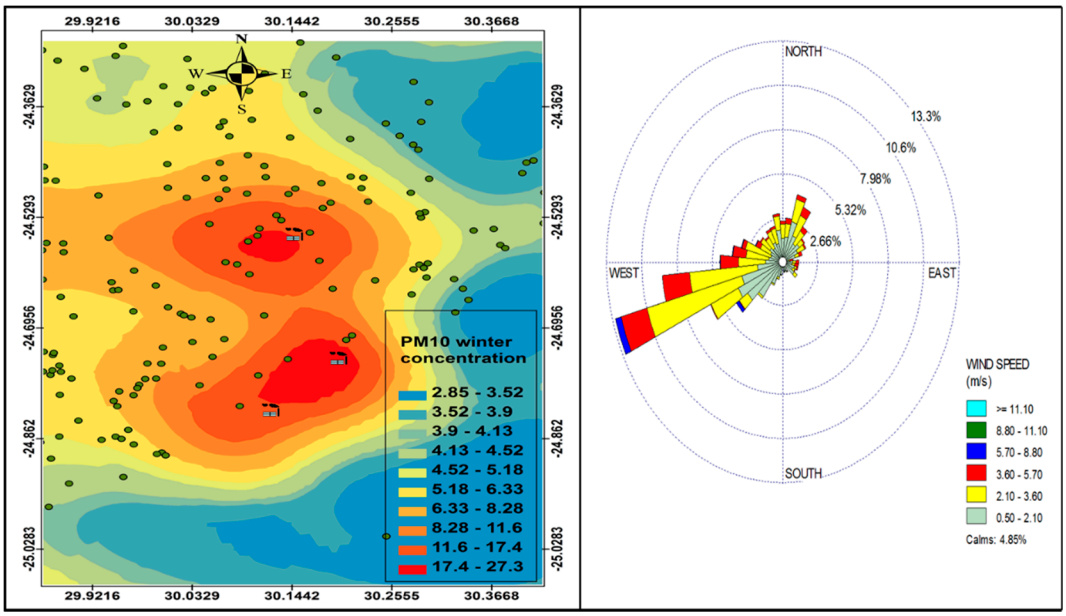

(a) **(b)**

Figure 7. Winter variation in PM_{10} ($\mu g.cm^{-3}$) ambient concentration (**a**) and wind roses (**b**).

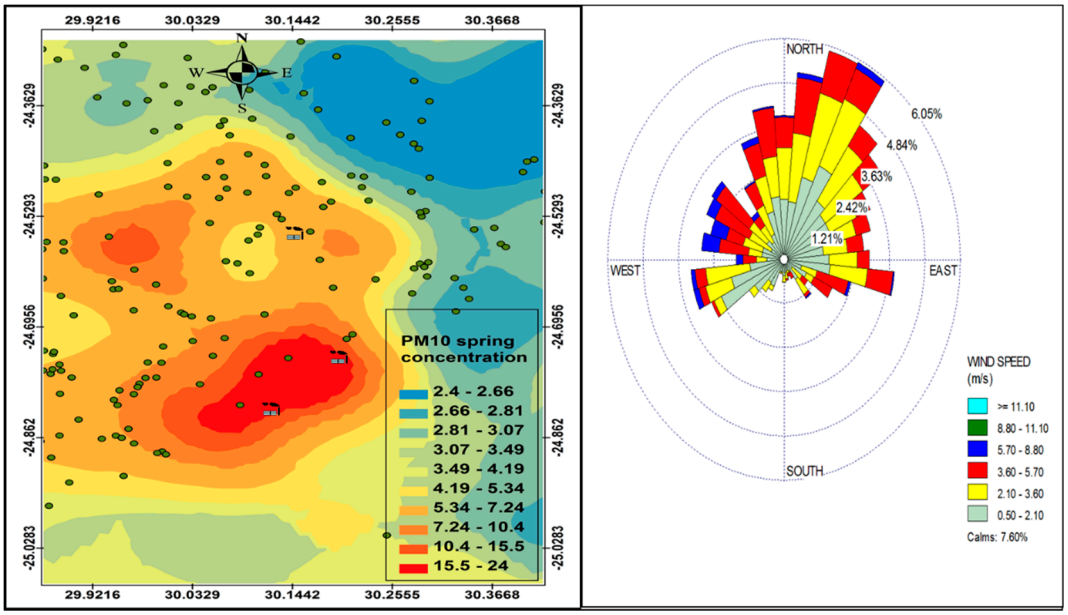

(a) **(b)**

Figure 8. Spring variation in PM_{10} ($\mu g.cm^{-3}$) ambient concentration (**a**) and wind roses (**b**).

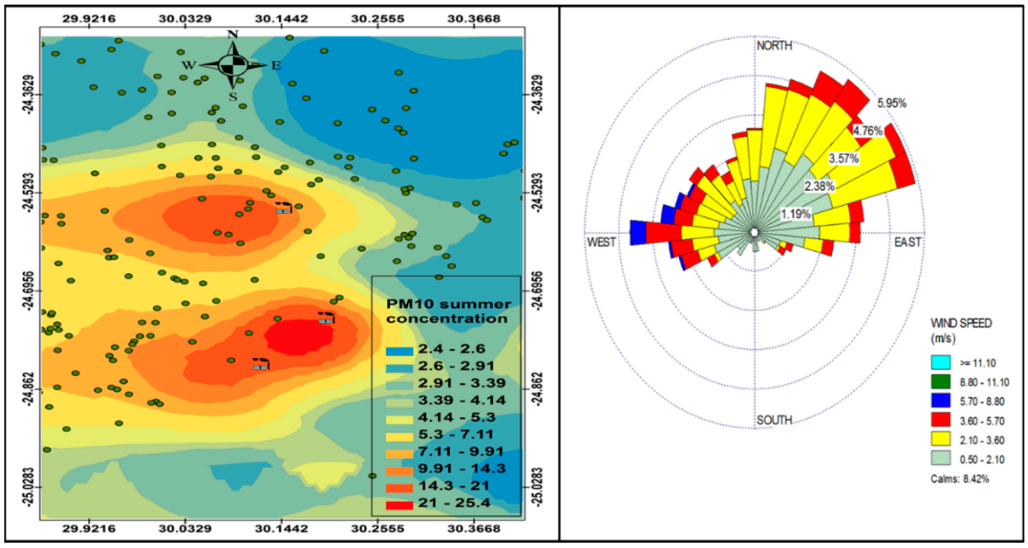

(a) **(b)**

Figure 9. Summer variation in PM_{10} ($\mu g.cm^{-3}$) ambient concentration (**a**) and wind roses (**b**).

The relation between PM_{10}, temperature, relative humidity, solar radiation and mixing height were tested using the Openair statistical software in R (Environmental Research Group, King's College London, Wareloo, England, United Kingdom) [29]. Figure 10 shows the seasonal relationship between PM_{10} and temperature. The autumn, winter and spring PM_{10} and temperature graphs show a D-shape plot with highest temperatures occurring during the day and the lowest concentration occurring in the morning and late afternoon. The winter temperatures reached a minimum of just above 5 °C with a maximum of around 28 °C. The autumn and spring seasons had similar lowest temperature of around 8 °C, however, the spring maximum temperatures were higher than those in autumn. The D-shaped plot indicates that during these seasons, the temperature correlates with PM_{10} concentrations in the GMT. During the summer months, there was a negative correlation between temperature and PM_{10} concentration; the highest PM_{10} concentrations occurred in the morning with minimum concentrations

occurring in the evening. These graphs also show that there was a decrease in concentrations when the surface inversion—which normally breaks up early during summer and later during the other seasons—broke. Hence, we see that the PM_{10} concentrations started to decrease at almost the same temperature of about 20 °C in all seasons. The minimum temperatures for summer were around 15 °C, with maximum temperatures reaching up to 36 °C.

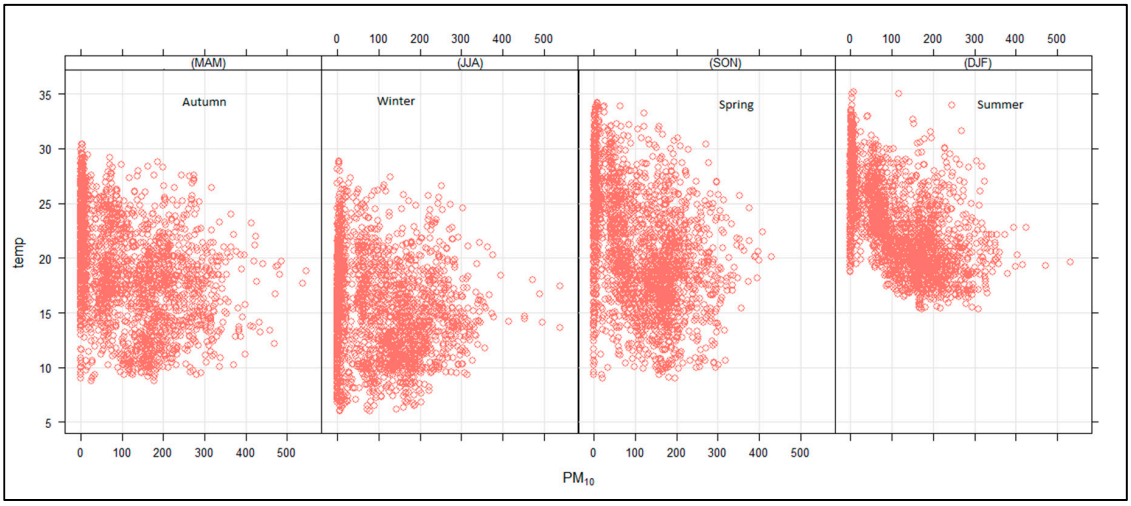

Figure 10. Relationship between PM_{10} (μg.cm^{-3}) and ambient temperature (°C) for autumn, winter, spring and summer.

The relation between PM_{10} and relative humidity (Figure 11) indicates that the PM_{10} concentrations increased with increasing humidity, particularly during autumn and summer. During winter and spring, there were high PM_{10} concentrations observed when humidity was low, though this was not as prevalent compared to when humidity was high, as was the case in other seasons. Therefore, humidity conditions positively affected the PM_{10} concentration, whereby moisture particles adhered to PM_{10}, accumulating atmospheric PM_{10} concentration.

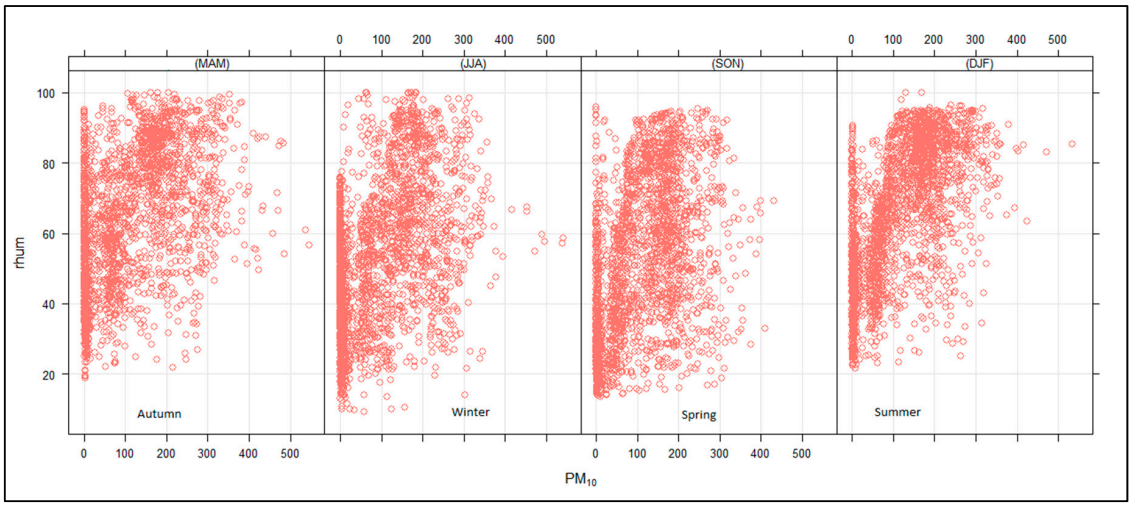

Figure 11. Relationship between PM_{10} (μg.cm^{-3}) and relative humidity (%) for autumn, winter, spring and summer.

Figure 12 shows that high PM_{10} concentrations were observed when the mixing height was shallow and decreased with an increasing mixing height. A similar trend was observed for PM_{10} and radiation. This is an indication that the mixing height was dependent on solar radiation. The PM_{10}

vertical distribution (Figure 13) was higher in spring and summer and lowest during autumn and winter. This was due to the reduction in the solar radiation that heats the earth's surface in autumn and winter and more radiating heating reaching the surface during spring and summer due to longer day hours. There is also vertical mixing during spring/summer seasons due to atmospheric instability, while during autumn/winter seasons, there are dominant high-pressure systems prevailing in the southern hemisphere that suppress the mixing height and lead to high concentrations at the surface. The surface inversion during autumn/winter is lower compared to the surface inversion in spring/summer seasons due to higher minimum temperatures in spring/summer compared to autumn/winter minimum temperatures Figure 13 also shows that the maximum PM_{10} concentrations were observed to a depth of up to 500 m above ground level, which is the indication of the boundary layer height in the study area, which therefore implies that the industrial stacks in the area should be raised to a height higher than their current height of less than 100 m to prevent build-up of pollution at the surface. The surface meteorological parameters were not considered in this study due to the non-availability of ground–based monitoring stations. It should be noted that the steep slopes found in the study area can give rise to thermally induced circulations, like mountain–valley breezes, that strongly modify the characteristics of synoptic flow [21,23,30,31].

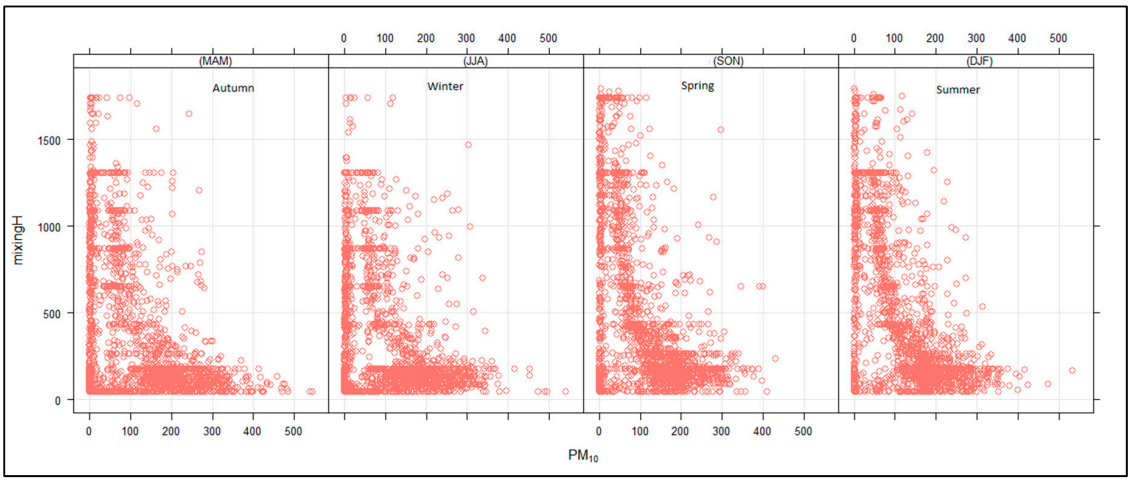

Figure 12. Relationship between PM_{10} (μg.cm^{-3}) and mixing height (m) for autumn, winter, spring and summer.

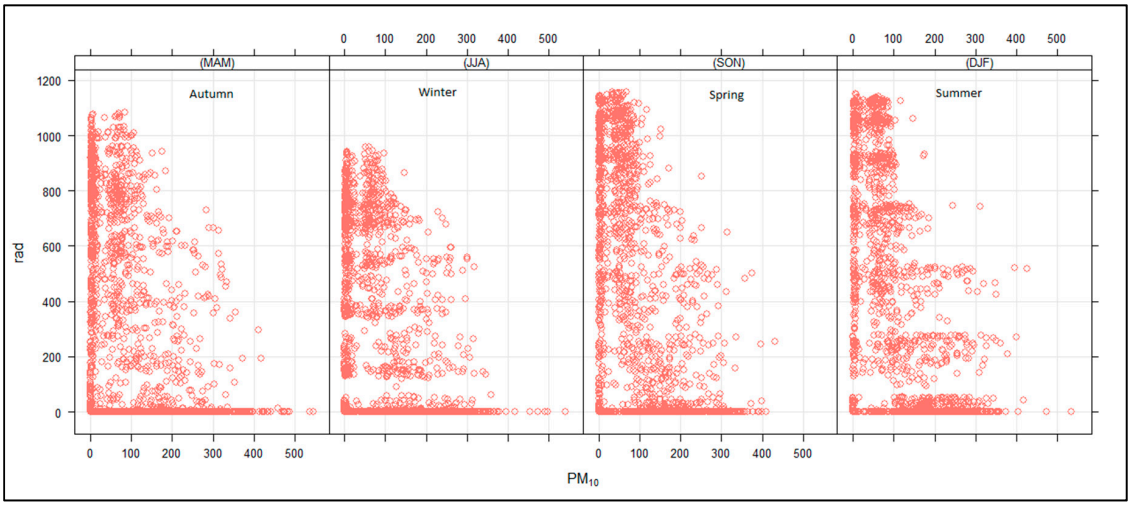

Figure 13. Relationship between PM_{10} (μg.cm^{-3}) and solar radiation (KWh/m^2) for autumn, winter, spring and summer.

PM Seasonl Varaiation

The average PM_{10} concentrations for the different seasons showed maximum values of 15.2 $\mu g.m^{-3}$ (autumn), 27.3 $\mu g.m^{-3}$ (winter), 24 $\mu g.m^{-3}$ (spring), and 25.3 $\mu g.m^{-3}$ (summer). These results suggest that the potential health risks associated with PM_{10} is low in autumn and high in winter. Although there are no standards for seasonal concentrations, the winter, spring and summer concentrations are high enough to warrant consideration of possible health effects in the GTM, given that these concentrations are from sources that constitute less than a quarter of the total sources in the area.

4. Conclusions

PM is a widespread air pollutant that lingers in the atmosphere depending on their size fraction. Pollutants emitted from point sources can be deposited closer to or at a further distance from the sources depending on the wind strength, the atmospheric stability and particle size. This study shows that meteorology played a major role in the distribution of PM_{10} in the study area. The orientation of the valley axis also had an influence on the distribution of pollutants by channelling the wind within the valley axis. The results of the PM_{10} distribution indicate that the concentrations were higher closer to the sources and lower further away from the sources during the day, while higher concentrations were distributed over a wide area during the night. These findings also show that during the day, the communities most likely to be impacted by pollution from the industrial point sources in the study area were those residing closer to the industrial facilities and during the night, the recirculation of pollution will likely impact a number of villages further away from the industries. Depending on the chemical composition, the PM_{10} emitted from the ferrochrome smelters could also carry heavy metals that could potentially impact human health, either directly through inhalation or indirectly through ingestion from water and food harvested from farms in the area depending on the extent of concentrations, given the fact that the simulated annual concentration of 27.3 $\mu g.m^{-3}$ only constituted 23.52% of the total sources in the area, and was higher than the WHO annual guidelines of 20 $\mu g.m^{-3}$ [10], though it is lower than the South African annual PM_{10} NAAQS of 40 $\mu g.m^{-3}$. This finding suggests that South Africa should revise the PM_{10} standards (and implement measures to comply with the set limits) to be comparable to the WHO guidelines in order to provide adequate protection of human health and well-being. Approximately 40% of the population of the GTM falls within the category of vulnerable individuals that are more likely to be impacted by exposure to PM_{10} concentration from the point sources because PM_{10} is a consistent pollutant [10]. It is therefore possible for regulating authorities to put in place stringent measures to reduce pollution from point sources (which are easily regulated compared to other sources of PM pollution). The monitoring of PM_{10} and $PM_{2.5}$ needs to be improved in GTM and South Africa as a whole to assess population exposure and to assist authorities in establishing plans for improving air quality. The results of this study and a study by [12] have been shared with the Limpopo Provincial authorities and the Sekhukhune district municipality authorities. As a result, we have seen both authorities commissioning the ambient air quality monitoring stations in the area. There is also a recommendation to establish an environmental forum that will involve all stakeholders in the area to better manage air pollution sources.

The study used the TAPM model to identify the areas that are most likely to be impacted by emissions from point sources in a complex terrain. Therefore, future studies should consider using meteorological models to simulate wind profiles in a complex terrain and compare the output with the analysis of ground measured meteorological parameters to verify the model simulations. This will help in analyse the statistically relevant dispersion conditions and search for critical situations with regards to the type of model to be used and the pollutant sources concerned. It would therefore be proper for South African regulations regarding dispersion modelling to be amended to include a requirement to perform wind field modelling using mass consistent models in complex terrain prior to performing a dispersion modelling, and to recommend the use of non-hydrostatic models (such as TAPM) on complex terrain.

Recommendations

TAPM should be considered as a regulating dispersion modelling tool in South Africa because it is now included in the EPA's list of recommended air dispersion models. There is a need for the DEA to partner with the South African Weather Service to identify areas where there is a need to monitor surface meteorology, particularly in complex terrain. This data will be useful as input when modelling a pollution in complex terrain. Furthermore, both wet and dry deposition of PM_{10} using the TAPM model need to be undertaken to check what the model predicts and compare with the measurements from the new commissioned ambient air quality monitoring stations. Future modelling studies in the area should also involve emissions data from sources identified by [12] which are omitted in this study due to non-availability of emissions data in the area.

Author Contributions: Conceptualization, C.E.T.; methodology, C.E.T.; software, C.E.T.; validation, C.E.T.; formal analysis, C.E.T.; investigation, C.E.T.; writing—original draft preparation, C.E.T.; writing—review and editing, C.Y.W.; supervision, C.Y.W.

Funding: This research was funded by the South African Weather Service as part of the personal development plan for employees.

Acknowledgments: The author acknowledges the Department of Environmental Affairs in South Africa for the provision of emissions data. The author would also like to acknowledge the laboratory for Atmospheric Studies at the University of Pretoria for the TAPM model.

Conflicts of Interest: The authors declare no conflict of interest.

References

1. Nel, A. Air pollution-related illness: Effects of particles. *Science* **2005**, *308*, 804–806. [CrossRef] [PubMed]
2. Dockery, D.W.; Pope, C.A. Acute Respiratory Effects of Particulate Air Pollution. *Annu. Rev. Public Health* **1994**, *15*, 107–132. [CrossRef] [PubMed]
3. Gehring, U.; Gruzieva, O.; Agius, R.M.; Beelen, R.; Custovic, A.; Cyrys, J.; Eeftens, M.; Flexeder, C.; Fuertes, E.; Heinrich, J. Air pollution exposure and lung function in children: The ESCAPE Project. *Environ. Health Perspect.* **2013**, *2*, 1357–1364. [CrossRef] [PubMed]
4. Kodama, K.; Tojjar, D.; Yamada, S.; Toda, K.; Patel, C.J.; Butte, A.J. Ethnic differences in the relationship between insulin sensitivity and insulin response: A systematic review and meta-analysis. *Diabetes Care* **2013**, *36*, 1789–1796. [CrossRef] [PubMed]
5. MacIntyre, E.A.; Gehring, U.; Molter, A.; Fuertes, E.; Klumper, C.; Kramer, U.; Quass, U.; Hoffmann, B.; Gascon, M.; Brunekreef, B. Air pollution and respiratory infections during early childhood: An analysis of 10 European birth cohorts within the ESCAPE Project. *Environ. Health Perspect.* **2014**, *22*, 107–113. [CrossRef] [PubMed]
6. Schikowski, T.; Adam, M.; Marcon, A.; Cai, Y.; Vierkotter, A.; Carsin, A.E.; Jacquemin, B.; Al Kanani, Z.; Beelen, R.; Birk, M. Association of ambient air pollution with the prevalence and incidence of COPD. *Eur. Respir. J.* **2014**, *44*, 614–626. [CrossRef] [PubMed]
7. Adam, M.; Schikowski, T.; Carsin, A.E.; Cai, Y.; Jacquemin, B.; Sanchez, M.; Vierkotter, A.; Marcon, A.; Keidel, D.; Sugiri, D. Adult lung function and long-term air pollution. ESCAPE: A multicentre cohort study and meta-analysis. *Eur. Respir. J.* **2015**, *45*, 38–50. [CrossRef] [PubMed]
8. Rice, M.B.; Ljungman, P.L.; Wilker, E.H.; Dorans, K.S.; Gold, D.R.; Schwartz, J.; Koutrakis, P.; Washko, G.R.; O'Connor, G.T.; Mittleman, M.A. Long-term exposure to traffic emissions and fine particulate matter and lung function decline in the Framingham heart study. *Am. J. Respir. Crit. Care Med.* **2015**, *191*, 656–664. [CrossRef] [PubMed]
9. Hu, C.; Jia, W. Diabetes in China: Epidemiology and genetic risk factors and their clinical utility in personalized medication. *Diabetes* **2018**, *67*, 3–11. [CrossRef] [PubMed]
10. The World Health Organization (WHO). Health Relevance of Particulate Matter from Various Sources. In *Report of a WHO Workshop*; WHO Regional Office for Europe: Copenhagen, Denmark, 2012; Available online: www.euro.who.int/document/E90672 (accessed on 30 March 2019).

11. Cohen, A.J.; Anderson, H.R.; Ostro, B.; Pandey, K.D.; Krzyzanowski, M.; Künzli, N.; Gutschmidt, K.; Pope, C.A., III; Romieu, I.; Samet, J.M. *Urban Air Pollution, Comparative Quantification of Health Risks*; World Health Organization: Geneva, Switzerland, 2001; Volume 2, pp. 1353–1433.
12. Tshehla, C.; Djolov, G. Source profiling, source apportionment and cluster transport analysis to identify the sources of PM and the origin of air masses to an industrialised rural area in Limpopo. *Clean Air J.* **2018**, *28*, 54–66. [CrossRef]
13. Helgason, A.B.; Pomeroy, J.W. Characteristics of the Near-Surface Boundary Layer within a Mountain Valley during winter. *J. Appl. Meteorol. Climatol.* **2012**, *51*, 583–597. [CrossRef]
14. Statistics South Africa. Available online: http://www.statssa.gov.za/?page_id=993&id=greater-tubatse-municipality (accessed on 2 May 2019).
15. Braga, A.L.F.; Conceição, G.M.S.; Pereira, L.A.A.; Kishi, H.S.; Pereira, J.C.R.; Andrade, M.F.; Goncealves, F.L.T.; Saldiva, P.H.N.; Latorre, M.R.D.O. Air pollution and paediatric respiratory hospital admissions in Sao Paulo, Brazil. *J. Environ. Med.* **1999**, *46*, 95–102. [CrossRef]
16. Chang, T.Y.; Norbeck, J.M. Vehicular CO emission factors in cold weather. *J. Air Pollut. Control Assoc.* **1983**, *33*, 1188–1189. [CrossRef]
17. Stull, R.B. *An Introduction to Boundary Layer Meteorology*; Kluwer Academic Publishers: Dortrecht, The Netherlands, 1991.
18. Salvador, R.; Millan, M.M.; Mantilla, E.; Baldasano, J.M. Mesoscale modelling of atmospheric processes over the western Mediterranean area during summer. *Int. J. Environ. Pollut.* **1997**, *8*, 513–529.
19. Geiger, R. *Das Klima der bodemnahen Luftschicht, Friedr*; Vieweg & Sohn: Braunschweig, Germany, 1961; p. 646.
20. De Wekker, S.F.J.; Kossmann, M. Convective Boundary Layer Heights Over Mountainous Terrain—A Review of Concepts. *Front. Earth Sci.* **2015**, *3*, 77. [CrossRef]
21. Whiteman, C.D. Observations of thermally developed wind systems in mountainous terrain. In *Atmospheric Processes over Complex Terrain*; American Meteorological Society: Boston, MA, USA, 1990; Volume 45, pp. 5–42.
22. Zardi, D.; Whiteman, D. Diurnal mountain wind systems. In *Mountain Weather Research and Forecasting: Recent Progress and Current Challenges*; Chow, F., De Wekker, S., Snyder, B., Eds.; Springer Atmospheric Sciences; Springer: Dordrecht, The Netherlands, 2013; pp. 35–119.
23. Whiteman, C.D.; Doran, J.C. The relationship between overlying synoptic-scale flows and winds within a valley. *J. Appl. Met.* **1993**, *32*, 1669–1682. [CrossRef]
24. Bianco, L.; Djalaova, I.V.; King, C.W.; Wilczak, J.M. Diurnal evolution and annual variability of boundary-layer height and its correlation to other meteorological variables in California's Central Valley. *Bound. Layer Meteorol.* **2011**, *140*, 491–511. [CrossRef]
25. Zannetti, P. *Air Pollution Modelling: Theories, Computational Methods and Available Software, Computational Mechanics*; Southampton and Van Nostrand Reinhold: New York, NY, USA, 1990. [CrossRef]
26. Hurley, P.; Physick, W.; Cope, M.; Borgas, M.; Brace, P. An evaluation of TAPM for photochemical smog applications in the Pilbara region of WA. In Proceedings of the 17th International Clean Air and Environment Conference, Newcastle, Australia, 23–27 November 2003.
27. Hurley, P.; Edwards, M.; Luhar, A. TAPM V4. Part 2: Summary of some verification studies. In *CSIRO Marine and Atmospheric Research Paper*; No. 26; CSIRO: Canberra, Australia, 2008; pp. 1–31.
28. Goovaerts, P. Kriging vs stochastic simulation for risk analysis in soil contamination. In *Geo-ENV I—Geostatistics for Environmental Applications*; Soares, A., Gomez-Hernandez, J., Froidevaux, R., Eds.; Kluwer Academic Publishers: Dordrecht, The Netherlands, 1997; pp. 247–258.
29. Carslaw, D. *The OpenaAir Manual Open-Source Tools for Analysing Air Pollution Data*; King's College London: London, UK, 2015; pp. 1–284.
30. Atkinson, B.W. *Mesoscale Atmospheric Circulation*; London Academic Press: London, UK, 1981.
31. Durran, D.R. *Mountain Waves and Downslope Winds*; American Meteorological Society: Boston, MA, USA, 1990; pp. 59–81.

CHAPTER 6

Results: 15 years after the National Environmental Management Air Quality Act: Is legislation failing to reduce air pollution in South Africa?

6.1 Commentary overview

The commentary suggests evidence that that the National Environmental Management Act: Air Quality Act, Act No. 39 of 2004 has the goal to reduce air pollution to acceptable levels, however, the implementation mechanisms and processes are unable to achieve the objectives of the Act. South Africa's National Department of Environmental Affairs (DEA) is mandated to develop, review and revise systems and procedures for attaining compliance with Air Quality Standards in South Africa. The provincial departments must monitor ambient air quality in their provinces as well as the performance of municipalities in implementing the Air Quality Act. Local authorities are required, in terms of the Air Quality Act (Section 8(a)) to monitor ambient air quality and emissions from point, non-point and mobile sources. Section 36 (1) charges the metropolitan and district municipalities with the responsibility of being the licensing authority. If these authorities are unable to perform this function, the provincial organ of state must be delegated to perform this function I terms of section 238 of the South African Constitution. Therefore, authorities must ensure that emissions reports from licensed emitters are scrutinised to ensure that they comply with the conditions of their licenses. The municipal by-laws should also be structured in such a way that they address emissions from small industries that are not regulated by atmospheric emission licences.

This commentary highlights the steps that have been undertaken to implement the Air Quality Act and identifies the bottlenecks that are impeding successful implementation. It also points to the need for scientific research to support the development of effective air quality management systems.

6.2 Contribution to the thesis

This commentary contributes to the thesis by identifying gaps and challenges in the implementation of Air Quality Act in South Africa. The findings of the six study objectives were used to inform recommendations for closing the identified gaps in the current implementation of the Air Quality Act. Institutional collaborations were recommended for effective implementation of the Act to reduce the levels of air pollution in the country.

6.4 Role of the candidate

Cheledi E. Tshehla performed the analysis of the requirements outlined in the Air Quality Act for implementation by all stakeholders to manage air pollution levels and wrote the first draft of the commentary. A review of the commentary was done in cooperation with Dr C. Y. Wright (co-author).

6.5 Publication status

Tshehla C. E. and Wright C.Y. 2019. 15 Years after the National Environmental Management Air Quality Act: Is legislation failing to reduce air pollution in South Africa. *S Afr J Sci* 115(9/10): 1-4. DOI: https://doi.org/10.17159/sajs.2019/6100

Manuscript 4

AUTHORS:
Cheledi Tshehla[1,2]
Caradee Y. Wright[1,3]

AFFILIATIONS:
[1]Department of Geography, Geoinformatics and Meteorology, University of Pretoria, Pretoria, South Africa
[2]South African Weather Service, Pretoria, South Africa
[3]Environment and Health Research Unit, South African Medical Research Council, Pretoria, South Africa

CORRESPONDENCE TO:
Cheledi Tshehla

EMAIL:
Cheledi.Tshehla@weathersa.co.za

HOW TO CITE:
Tshehla C, Wright CY. 15 Years after the *National Environmental Management Air Quality Act*: Is legislation failing to reduce air pollution in South Africa? S Afr J Sci. 2019;115(9/10), Art. #6100, 4 pages. https://doi.org/10.17159/sajs.2019/6100

ARTICLE INCLUDES:
☐ Peer review
☒ Supplementary material

KEYWORDS:
human health, environmental health, regulation, guidelines

PUBLISHED:
26 September 2019

15 Years after the *National Environmental Management Air Quality Act*: Is legislation failing to reduce air pollution in South Africa?

Air pollution is characterised by the presence of chemicals or compounds in the air which are usually not present or are present at levels higher than those considered to be safe for human health.[1] Air pollution is the main cause of environmental effects such as acid rain (formed primarily by nitrogen oxides and sulfur oxides in the atmosphere) which can acidify soil and water bodies leading to a threat on food security; and ground-level ozone which is responsible for destruction of agricultural crops and commercial forests.[2] Air pollution can cause detrimental changes to the quality of life. According to the World Health Organization, air pollution is one of the greatest environmental threats to human health that can lead to increased mortality and morbidity. Pollutants mostly associated with health effects are particulate matter, ozone, sulfur dioxide and nitrogen dioxide.[3]

Efforts have been made locally through the transition in legislation from the *Atmospheric Pollution Prevention Act (APPA) Number 45 of 1965* (focused on air pollution emitters) to the *National Environmental Management Air Quality Act (NEMAQA) No. 39 of 2004* to not only reduce emissions of air pollutants but also to monitor effects of air pollution on the environment. National Ambient Air Quality Standards for pollutants such as particulate matter (PM_{10}), lead (Pb), sulfur dioxide (SO_2), nitrogen dioxide (NO_2), carbon monoxide (CO), ozone (O_3), and benzene (C_6H_6) were gazetted in 2009[4], with $PM_{2.5}$ gazetted in June 2012[5]. However, the problems associated with air pollution are far from being solved, particularly with the observed levels of particulate matter and ozone in areas declared as hotspots (Priority Areas) in South Africa. The main sources of particulate matter in these areas have been identified as industry, mining, motor vehicles, and biomass and domestic burning.[6-8] Ground-level ozone is formed as a result of photochemical reactions in the atmosphere in the presence of sunlight.[9] The current approach to implementation of air quality legislation to reduce air pollution may be inadequate considering evidence of negative impacts and risks.[10,11]

Effective management of air quality in South Africa will require sound policy implementation, air quality monitoring and the enforcement of legislation and standards. Cooperation between government departments, economic sectors, research institutions and the public is of great importance in the battle against air pollution. The political buy-in of all spheres of government (municipal, provincial and national) is needed to ensure that environmental issues are at the top of the agenda in every sitting of the legislator to ensure that environmental programmes are allocated enough attention and appropriate resources. A published study has shown that a direct positive effect of democratic institutions on environment quality is higher in developed countries than in developing countries.[12]

The aim of this Commentary is threefold: (1) to provide an overview of the current NEMAQA legislative instruments for air pollution prevention; (2) to consider the current state of NEMAQA implementation approaches; and (3) to reflect on future approaches for effective implementation of NEMAQA and ultimate reduction of air pollution in South Africa.

Air pollution and its management

Air pollutants are solid particles, gases and liquid droplets in the air that can adversely affect ecosystems and human health.[13] Major ambient air pollutants include toxic metals, volatile organic compounds, PM_{10}, $PM_{2.5}$, NOx, SO_2, O_3 and CO[3]. Air pollutants are classified according to the source of emission into two main groups: primary and secondary pollutants. Primary air pollutants are emitted directly into the air from sources. They can have effects both directly and as precursors of secondary air pollutants (such as O_3, NO_3^-, SO_4^{2-}, H_2SO_4) which are formed by chemical reactions in the atmosphere.[14] Air pollutants can be emitted by natural sources such as wildfires, volcanic activities and crustal materials as well as anthropogenic activities such as power plants, smelters, mines, vehicles and domestic wood and coal burning.[15] The distribution of these pollutants is dependent on meteorological conditions.[16]

NEMAQA specifies that to reduce and manage air quality there needs to be:

- decentralisation of air quality management among all spheres of government;
- identification and quantification of all sources;
- compliance monitoring and enforcement;
- setting of ambient and emissions standards;
- development of Air Quality Management Plans (AQMPs) by all spheres of government and emissions reductions and management plans by all source emitters;
- access to information and public consultation; and
- norms and standards for air quality monitoring and management.

South Africa's national Department of Environmental Affairs (DEA) is mandated to develop, review and revise systems and procedures for attaining compliance with Air Quality Standards in South Africa. The provincial DEAs must monitor ambient air quality in their provinces as well as the performance of municipalities in implementing the *Air Quality Act*. Local authorities are required, in terms of the *Air Quality Act* (Section 8(a)), to monitor ambient air quality and emissions from point, non-point and mobile sources. Therefore, authorities must study emissions reports from licensed emitters to ensure that they comply with the conditions of their licences. The municipal by-laws should

also be structured in such a way that they address emissions from small industries that are not regulated by atmospheric emission licences.

Consideration of progress to date

The evidence collected during the development of the Mpumalanga Provincial AQMP suggests that decentralisation of air quality management in South Africa is not effectively managed, with most local authorities not performing this function due to several constraints (Supplementary tables 1–4). The *Municipal Systems Act No. 32 of 2000* requires local authorities to include their AQMPs in their Integrated Development Plans for resource allocation. However, only a few district municipalities have AQMPs in place, as shown in Figure 1. All provinces have developed their AQMPs with the exception of KwaZulu-Natal and Mpumalanga which are still under development (Figure 2). For the three areas that have been declared Priority Areas (that is, areas where the ambient air quality standards are being, or may be, exceeded, or any other situation which is causing, or may cause, a significant negative impact on air quality in the area) in terms of Section 18(1) of the *Air Quality Act*, processes are underway to implement the Priority Area AQMPs. Given that the status quo has not changed, there could be underlying problems in the implementation of the AQMPs.

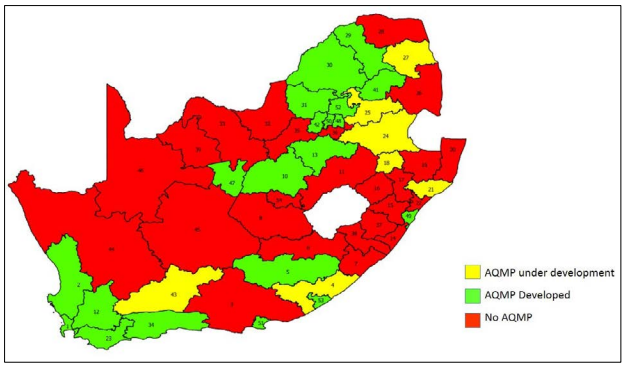

Source: South African Air Quality Information System[22]

Figure 1: Current development status of district municipality Air Quality Management Development Plans in South Africa.

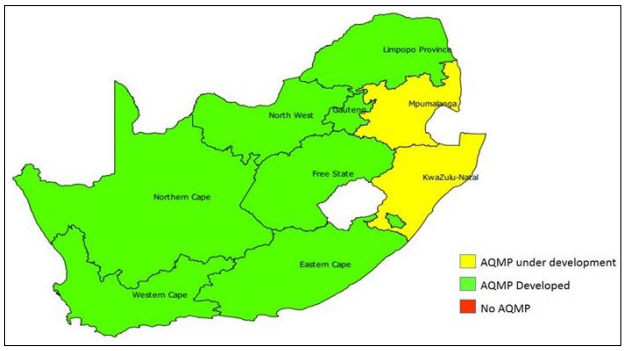

Source: South African Air Quality Information System[22]

Figure 2: Current development status of provincial Air Quality Management Development Plans in South Africa.

In terms of identification and quantification of sources of air pollutants, no formal study has been undertaken solely by any of the three spheres of government to identify and apportion sources of air pollutants. In 2016, a source apportionment study was commissioned by the DEA for the Vaal Triangle Airshed Priority Area (VTAPA).[17] This study was commissioned after the 2013 mid-term AQMP review revealed that there was no improvement in air quality in the VTAPA.[18] Given the unchanging status quo on air pollution levels in the Priority Areas, the source apportionment studies are necessary for effective implementation of abatement strategies. Air pollution has no boundaries; therefore, air pollution from the Priority Areas could also be transported to other regions in the country. As such, a directive should also have been issued to all provincial DEAs to commission source apportionment studies in their respective provinces for effective air quality management.

The establishment of the Environmental Management Inspectorate to monitor and enforce compliance with the *National Environmental Management Act* was to ensure that all those undertaking activities that may lead to detrimental effects on the environment are held accountable. However, the regulatory authorities either are not scrutinising the compliance reports from industries to look at the root-cause analyses, not following up on non-compliance or not doing trends analyses of the reports to check consistency. In a number of DEA Implementation Task Team meetings, industries have mentioned that they submit reports to regulatory authorities but their reports are not attended to nor do they receive feedback from authorities. The response from authorities was that there are not enough personnel to study the reports. This situation presents a potential loophole that industries may have identified within the regulatory framework and, as such, provides an opportunity for non-compliance with the minimum emissions standards by industries.

According to the South African Government website, there are 278 municipalities in South Africa.[19] Supplementary table 5 shows the 121 government-managed ambient air quality monitoring stations that have been reporting to the South African Air Quality Information System (SAAQIS) since 2009 when the system was launched. If all the municipalities were implementing Section 8(b) of the *Air Quality Act*, there would be 278 ambient air monitoring stations reporting to SAAQIS (i.e. one station per municipality) to ensure widespread spatial coverage necessary for effective compliance monitoring. The DEA and South African Weather Service have embarked on a project to revamp SAAQIS through the development and implementation of SAAQIS phase III. This improvement has led to live reporting of air quality monitoring stations. The DEA is in the process of reviving stranded municipal air quality monitoring stations to increase the number of stations reporting to SAAQIS. Privately owned stations are also targeted to report live on the SAAQIS system. New features on SAAQIS phase III include a mobile app to view live ambient data and the air quality index, and the ability to download data on the public page.

National norms and standards are required to ensure that there is standardised ambient air quality monitoring and management in the country. But to date, there is no document that outlines the national norms and standards for air quality management in South Africa that can be used as a directive to all regulating authorities and the source emitters. With a total of 164 monitoring stations reporting to SAAQIS, only a few are considered to have credible data that can be used for scientific research to inform policy development. As shown in Supplementary tables 2–4, the reason for non-credible data can be attributed to lack of funding and skilled personnel to perform air quality related functions. This situation is a matter of concern given the non-compliance with the National Ambient Air Quality Standards shown in Supplementary tables 6–8.

There has not been a cost–benefit analysis undertaken by the government since the promulgation of the *Air Quality Act* in 2004 to determine the impact of air pollution on the economy of South Africa. Some industries in South Africa have been applying for the postponement of minimum emissions standards for several years. Furthermore, there has not been projected cost–benefit analyses on how much will be saved by the country if air pollution was reduced to acceptable limits by complying with the minimum emissions standards and ambient air quality standards. Eskom undertook a cost–benefit analysis[20] of the offset (defined as an intervention to counterbalance an adverse environmental impact) project in the Highveld Priority Area. However, the focus of this analysis was on reducing pollution from households and compliance with the 2020 NEMAQA minimum emission standards was not considered. A report[21] by the Centre for Environmental Rights and groundWork indicates that the initiatives undertaken by Eskom to reduce household emissions from coal burning in Zamokuhle Township through air quality offset interventions did not bear positive results because of the high cost of electricity. The high cost of liquid petroleum gas in South Africa is also a negative factor in the proposed Eskom retrofit project and will lead to communities reverting to coal use for space heating and cooking.

In terms of mining, the Department of Mineral Resources is responsible for issuing Atmospheric Emission Licences and granting environmental authorisations. Environmental authorisations are a key tool in effective environmental management, including the management of air quality. However, the Department of Mineral Resources officials are not designated as Air Quality Officers and as such air quality related matters may not be fully explored during the authorisation process. This arrangement makes the management of mining-related air pollution very difficult in South Africa.

There is a gap between science and policy

Supplementary tables 6–8 show the 2018 National Ambient Air Quality Standards exceedance tables for the areas which have been declared pollution hotspots in South Africa: VTAPA declared in 2006, Highveld Priority Area declared in 2007 and Waterberg/Bojanala Priority Area declared in 2012. The VTAPA AQMP identified the main sources of air pollution in the area as biomass burning, domestic fuel burning, mining operations, petrochemical sector, power generation, transportation, waste burning, iron and steel and ferroalloy industries, and smaller industries. The Highveld and Waterberg/Bojanala Priority Area AQMPs identified the major sources of air pollution as residential fuel burning, coal mining, power generation, transport, biomass burning and burning coal mines and smouldering coal dumps, landfills, incinerators, waste treatment works, tyre burning, agricultural dust, and biogenic sources.[7,8] The variation in source categories in Priority Areas clearly shows that these sources will be complex to manage and will require multi-stakeholder partnership in implementation of abatement strategies. It is evident from the exceedance data that there is a problem with particulate matter and ozone in all the areas. However, there have not been any studies commissioned by the DEA to comprehensively identify sources of particulate matter and ozone (except in the VTAPA) and there are no known memoranda of understanding between DEA and research institutions to develop and fund programmes aimed at tackling this research gap.

The *Air Quality Act* requires new Atmospheric Emission Licence applicants to undertake an atmospheric emissions modelling study. Many air quality dispersion models rely on surface meteorological parameters to model air pollution dispersion, particularly in complex terrain. Section 4.2.1 of the draft regulations regarding Air Dispersion Modelling (Notice 1035 of 2012) in the *Air Quality Act* requires site-specific meteorological data for modelling purposes in complex terrain. However, there has not been any collaboration between the DEA and the South African Weather Service to ensure that there is a sufficient number of surface meteorological monitoring stations in remote areas with complex terrain. One such place is the Greater Tubatse Municipality which has several industrial facilities and a complex terrain but no meteorological stations. (A Research Article in this issue reports on air pollution in the Greater Tubatse Municipality). Institutional collaborations between government entities and research institutions may narrow the gap between science and strategic policy development and implementation for successful management of air quality. Air pollution reduction could be achieved by strengthening collaboration between government departments such as DEA and Department of Mineral Resources for better management of pollution from the mining sector; and allocating funding for environmental issues at all spheres of government to be centralised at DEA for better management of air quality. It could also entail developing a cost–benefit study for the implementation of the *Air Quality Act*; and making source apportionment a pre-requisite for the development of air quality management plans by authorities and for all industry applications for postponement of complying with the minimum emission standards by April 2020, and for atmospheric emission licence application for new facilities. The source apportionment and source quantification results will ensure that the contribution of major sources, as well as the impact that results from granting postponements and/or new licences, will be known. Establishing expert panels to identify research programmes aimed at addressing air pollution problems would also be beneficial, as it would ensure that resources are channelled to research studies that are relevant to air quality improvement. Lastly, air pollution programmes should be introduced from the foundation phase of basic education to build a nation that is conscious of and educated about air quality issues.

Conclusions

The *Air Quality Act* was passed in South Africa over 15 years ago, but it is evident that several of its strategic objectives have yet to be met. Even though emissions reduction is implemented by some industries, and there also are efforts by local authorities to develop and implement by-laws to reduce household emissions, the introduction of new small industries, and the failure to effectively reduce pollution from domestic burning, waste burning, biomass burning, vehicle emissions and mining activities within the air pollution hotspots makes it impossible to achieve the desired air pollution reduction. Particulate matter and ozone are two pollutants for which there is non-compliance with the National Ambient Air Quality Standards. Therefore a comprehensive study to look at the major precursors of ozone is necessary to develop abatement strategies for ozone. There is a need to relook at the drivers and factors influencing policy implementation such as political buy-in (by educating politicians on air quality matters) particularly in local authorities and reprioritisation of societal needs, especially with respect to housing and economic development in relation to protection of the environment and human health.

Acknowledgements

C.Y.W. receives research funding support from the South African Medical Research Council and the National Research Foundation (South Africa). C.T. thanks the South African Weather Service for provision of resources, space and time for conducting the research.

References

1. Sharma SB, Jain S, Khirwadka P, Kulkarni S. Effects of air pollution on the environment and human health. Indian J Res Pharm Biotechnol. 2013;1(3):391–396. Available from: http://www.ijrpb.com/issues/Volume%201_Issue%203/ijrpb%201(3)%2020%20page%20391-396.pdf
2. Ashfaq A, Sharma P. Environmental effects of air pollution and application of engineered methods to combat the problem. J Ind Pollut Control. 2013;29(1):19–29. Available from: http://www.icontrolpollution.com/articles/environmental-effects-of-air-pollution-and-application-of-engineered-methods-to-combat-the-problem-.php?aid=45739
3. World Health Organization (WHO). Ambient air pollution: A global assessment of exposure and burden of disease. Geneva: WHO; 2016. Available from: https://apps.who.int/iris/handle/10665/25014
4. South African Department of Environmental Affairs (DEA). National ambient air quality standards [document on the Internet]. c2009 [cited 2019 Feb 04]. Available from: https://www.environment.gov.za/sites/default/files/legislations/nemaqa_airquality_g32816gon1210.pdf
5. Western Cape Department of Environmental Affairs and Development Planning. State of Air Quality Management 2015 [document on the Internet]. c2015 [cited 2019 Feb 04]. Available from: https://www.westerncape.gov.za/eadp/files/atoms/files/State%20Of%20Air%20Quality%20Monitoring%20Report%202015.pdf
6. South African Air Quality Information System (SAAQIS). The Vaal Triangle Air-Shed Priority Area Network AQMP. Pretoria: South African Weather Service; 2009. Available from: http://www.saaqis.org.za/documents/Vaal%20Triangle%20Air-Shed%20Priority%20Area%20(VTAPA)%20AQMP%20Regulations_29-05-2009.pdf
7. South African Air Quality Information System (SAAQIS). Declaration of the Highveld Priority Area. Pretoria: South African Weather Service; 2007. Available from: http://www.saaqis.org.za/documents/HIGHVELD%20PRIORITY%20AREA%20AQMP.pdf
8. South African Department of Environmental Affairs (DEA). Declaration of the Waterberg Bojanala Priority Area. Pretoria: South African Weather Service; 2013. Available from: https://www.environment.gov.za/sites/default/files/gazetted_notices/nemaqa_waterberg_declaration_g35435gen495_0.pdf
9. World Bank Group. Ground-level ozone. Washington DC: World Bank; 1998. Available from: https://www.ifc.org/wps/wcm/connect/dd7c9800488553-e0b0b4f26a6515bb18/HandbookGroundLevelOzone.pdf?MOD=AJPERES

10. Maponya P, Rampedi IT. Impact of air pollution on maize production in the Sasolburg Area, South Africa. J Agric Sci. 2013;5(11):181–188. https://doi.org/10.5539/jas.v5n11p181

11. Keen S, Altieri K. The health benefits of attaining and strengthening air quality standards in Cape Town. Clean Air J. 2016;26(2):22–27. https://doi.org/10.17159/2410-972X/2016/v26n2a9

12. Romualt KS. Democratic institutions and environmental quality: Effects and transmission channels. Paper presented at: EAAE 2011 Congress on Change and Uncertainty Challenges for Agriculture, Food and Natural Resources; 2011 August 30 – September 02; Zurich, Switzerland. Available from: https://ageconsearch.umn.edu/bitstream/120396/2/Somlanare_Kinda_354.pdf

13. Bhatia SC. Environmental pollution and control in chemical process industries. Delhi: Khanna Publishers; 2001; p. 163.

14. Kicinski M, Nawrot TS. Neurobehavioral effects of air pollution in children. In: Costa L, Aschner M, editors. Environmental factors in neurodevelopmental and neurodegenerative disorders. London: Academic Press; 2015. p. 89–105. https://doi.org/10.1016/B978-0-12-800228-5.00005-4

15. Singh OP. Air pollution: Types, sources and abatement. Environment and natural resources: Ecological and economic perspective. New Delhi: Regency Publications; 2015. p. 101–124.

16. Ediagbona TF, Ukpebor EE, Okieimen FE. Correlation of meteorological parameters and dust particles using scatter plot in a rural community. Ife J Sci. 2013;15(3):445–453.

17. South African Air Quality Information System (SAAQIS). [National air quality officer's annual report on air quality management [document on the Internet]. c2015 [cited 2019 Feb 07]. Available from: https://saaqis.environment.gov.za/Pagesfiles/NAQO%27s_Annual%20Report_2015.pdf

18. South African Department of Environmental Affairs (DEA). Vaal Triangle Airshed Priority Area source apportionment study: Preliminary results [document on the Internet]. c2018 [cited 2019 Feb 13]. Available from: http://www.airqualitylekgotla.co.za/assets/2018_5.4-vtapa-source-apportionment-study.pdf

19. South African Government. [Local government]. c2019 [cited 2019 Feb 16]. Available from: https://www.gov.za/about-government/government-system/local-government

20. Eskom Holdings SOC Limited. The execution of a household emission offset pilot study in the Highveld Priority Area, Mpumalanga [document on the Internet]. c2015 [cited 2019 Feb 20]. Available from: http://www.eskom.co.za/AirQuality/Documents/PilotStudySemi-FinalReport.pdf

21. groundWork. Government: Wheels come off the Eskom offset [webpage on the Internet]. c2018 [cited 2019 Feb 22]. Available from: http://www.groundwork.org.za/archives/2018/news20180814-Wheels_come_off_the_Eskom_offset.php

22. South African Air Quality Information System (SAAQIS). AQ Planning [webpage on the Internet]. No date [2019 Jan 23]. Available from: https://saaqis.environment.gov.za//home/text/358).

SUPPLEMENTARY MATERIAL TO:

Tshehla and Wright. S Afr J Sci. 2019;115(9/10), Art. #6100, 4 pages.

HOW TO CITE:

Tshehla C, Wright CY. 15 Years after the *National Environmental Management Air Quality Act*: Is legislation failing to reduce air pollution in South Africa? [supplementary material]. S Afr J Sci. 2019;115(9/10), Art. #6100, 12 pages. https://doi.org/10.17159/sajs.2019/6100/suppl

Table 1: Mpumalanga Department of Agriculture, Rural Development, Land and Environmental Affairs 2018 status quo

Mpumalanga Department: Agriculture, Rural Development, Land and Environmental Affairs			
Requirement		**Status**	**Comment**
Appointment of Air Quality Officer (AQO)		**Yes**	One provincial AQO
Air Quality Management Plan (AQMP)		**Planned**	Currently underway
Capacity	Human Resources	**Yes**	Environmental Department
	Equipment	**No**	
	Skills	**No**	
Atmospheric Emissions Licence (AEL) capacity		**Yes**	Issue AELs
Cooperative governance		**Yes**	Involve other departments when conducting air quality functions
Ambient Air Quality Monitoring		**Yes**	Five stations within Mpumalanga Department managed by SAWS

Table 2: Gert Sibande District Municipality and local municipalities' 2018 status quo

Gert Sibande District Municipality			
Requirement		**Status**	**Comment**
Appointment of Air Quality Officer (AQO)		Yes	An AQO has been designated and the department has adequate capacity to perform the function
Air Quality Management Plan (AQMP)		Yes	AQMP draft in place
Capacity	Yes	Yes	One AQO designated, one Enforcement Officer, 2 Compliance Officers and four AQOs
	Yes	Yes	Able to perform with resources they have
	Yes	Yes	Staff have appropriate qualifications in air quality
Atmospheric Emissions Licence (AEL) capacity		Yes	All AELs are issued by the district for all local municipalities
Cooperative governance		Yes	Involvement of political officials, Councillors, Portfolio Committee, Mayoral Committee
AQM factored into IDP		Yes	Yes, R800 000
Ambient Air Quality Monitoring		Yes	Ermelo Station

Chief Albert Luthuli Local Municipality			
Requirement		**Status**	**Comment**
Appointment of Air Quality Officer (AQO)		No	No staff
Air Quality Management Plan (AQMP)		No	No plans in place
Capacity	Human Resources	No	District function
	Equipment	No	
	Skills	No	
Atmospheric Emissions Licence (AEL) capacity		No	This function is undertaken by the district
Cooperative governance		Yes	Meeting held with different stakeholders in air quality
AQM factored into IDP		No	Proposed to the local municipality
Ambient Air Quality Monitoring		No	No plans to have a station

Dipaleseng Local Municipality			
Requirement		**Status**	**Comment**
Appointment of Air Quality Officer (AQO)		No	No staff
Air Quality Management Plan (AQMP)		No	No plans in place
Capacity	Human Resources	No	District function
	Equipment	No	
	Skills	No	
Atmospheric Emissions Licence (AEL) capacity		Yes	This function is undertaken by the district
Cooperative governance		Yes	Meeting held with different stakeholders in air quality
AQM factored into IDP		Planned	Proposed to the local municipality
Ambient Air Quality Monitoring		Yes	Privately owned station

Dr Pixley ka Isaka Seme Local Municipality			
Requirement		**Status**	**Comment**
Appointment of Air Quality Officer (AQO)		No	No staff
Air Quality Management Plan (AQMP)		No	No plans in place
Capacity	Human Resources	No	District function
	Equipment	No	
	Skills	No	
Atmospheric Emissions Licence (AEL) capacity		No	This function is undertaken by the district
Cooperative governance		Yes	Meeting held with different stakeholders in air quality
AQM factored into IDP		No	Only priority services
Ambient Air Quality Monitoring		No	No plans to have a station

Govan Mbeki Local Municipality			
Requirement		**Status**	**Comment**
Appointment of Air Quality Officer (AQO)		No	No staff
Air Quality Management Plan (AQMP)		No	No plans in place
Capacity	Human Resources	No	District function
	Equipment	No	
	Skills	No	
Atmospheric Emissions Licence (AEL) capacity		No	District function
Cooperative governance		Yes	Meeting held with different stakeholders in air quality
AQM factored into IDP		No	
Ambient Air Quality Monitoring		Yes	Two ambient stations

Lekwa Local Municipality			
Requirement		**Status**	**Comment**
Appointment of Air Quality Officer (AQO)		No	There is no designated AQO for the function of air quality
Air Quality Management Plan (AQMP)		No	No plan in place
Capacity	Human Resources	No	This will be addressed once there is a budget for AQMP
	Equipment	No	This will be addressed once there is a budget for AQMP
	Skills	No	This will be addressed once there is a budget for AQMP
Atmospheric Emissions Licence (AEL) capacity		Yes	Function of the district
Cooperative governance		No	Meeting held with different stakeholders in air quality
AQM factored into IDP		No	
Ambient Air Quality Monitoring		Yes	One station

Mkhondo Local Municipality			
Requirement		**Status**	**Comment**
Appointment of Air Quality Officer (AQO)		No	The is no designated AQO for the function of air quality
Air Quality Management Plan (AQMP)		Yes	In the developmental stage
Capacity	Human Resources	Yes	
	Equipment	Yes	
	Skills	Yes	
Atmospheric Emissions Licence (AEL) capacity		No	Function of the district
Cooperative governance		Yes	
AQM factored into IDP		No	
Ambient Air Quality Monitoring		No	No monitoring station
Msukaligwa Local Municipality			
Requirement		**Status**	**Comment**
Appointment of Air Quality Officer (AQO)		No	
Air Quality Management Plan (AQMP)		No	
	Human Resources	No	
	Equipment	No	
	Skills	No	
Atmospheric Emissions Licence (AEL) capacity		No	Function of the district
Cooperative governance		Yes	Meeting held with different stakeholders in air quality
AQM factored into IDP		No	
Ambient Air Quality Monitoring		Yes	National monitoring stations

Table 3: Nkangala District Municipality and local municipalities' 2018 status quo

Nkangala District Municipality			
Requirement		**Status**	**Comment**
Appointment of Air Quality Officer (AQO)		Yes	Three AQOs
Air Quality Management Plan (AQMP)		Yes	AQMP completed in 2015
Capacity	Human Resources	Planned	
	Equipment	Planned	
	Skills	Planned	
Atmospheric Emissions Licence (AEL) capacity		Yes	Issues AELs for local industries
Cooperative governance		Yes	Liaison with the provincial department
AQM factored into IDP		No	
Ambient Air Quality Monitoring		No	

Dr JS Moroka Local Municipality			
Requirement		**Status**	**Comment**
Appointment of Air Quality Officer (AQO)		No	
Air Quality Management Plan (AQMP)		No	
Capacity	Human Resources	Yes	One Waste Manager
	Equipment	No	
	Skills	No	
Atmospheric Emissions Licence (AEL) capacity		No	
Cooperative governance		No	
AQM factored into IDP		No	
Ambient Air Quality Monitoring		No	

eMalahleni Local Municipality			
Requirement		**Status**	**Comment**
Appointment of Air Quality Officer (AQO)		Yes	One AQO
Air Quality Management Plan (AQMP)		Planned	Currently under development
Capacity	Human Resources	Planned	Various air quality management roles mandated in terms of *NEMAQA* are yet to be resourced
	Equipment	Planned	
	Skills	Planned	
Atmospheric Emissions Licence (AEL) capacity		No	
Cooperative governance		No	
AQM factored into IDP		No	
Ambient Air Quality Monitoring		Yes	One monitoring station (Witbank)

Emakhazeni Local Municipality			
Requirement		**Status**	**Comment**
Appointment of Air Quality Officer (AQO)		No	
Air Quality Management Plan (AQMP)		No	
Capacity	Human Resources	Yes	Three Environmental Health Officers from the district
	Equipment	No	
	Skills	No	
Atmospheric Emissions Licence (AEL) capacity		No	
Cooperative governance		No	
AQM factored into IDP		No	
Ambient Air Quality Monitoring		No	

Steve Tshwete Local Municipality			
Requirement		**Status**	**Comment**
Appointment of Air Quality Officer (AQO)		No	
Air Quality Management Plan (AQMP)		Planned	Currently under development
Capacity	Human Resources	Yes	One Environmental Officer, two Environmental Management Inspectors and three Environmental Health Officers (from the district)
	Equipment	No	
	Skills	No	
Atmospheric Emissions Licence (AEL) capacity		No	
Cooperative governance		No	
AQM factored into IDP		No	
Ambient Air Quality Monitoring		Yes	Five monitoring stations (Hendrina, Middelburg, Mhluzi, Golfsig, Columbus Steel)

Thembisile Hani Local Municipality			
Requirement		**Status**	**Comment**
Appointment of Air Quality Officer (AQO)		No	
Air Quality Management Plan (AQMP)		No	
Capacity	Human Resources	Yes	Nine Environmental Health Officers
	Equipment	No	
	Skills	No	
Atmospheric Emissions Licence (AEL) capacity		No	
Cooperative governance		No	
AQM factored into IDP		No	
Ambient Air Quality Monitoring		No	

Victor Khanye Local Municipality			
Requirement		**Status**	**Comment**
Appointment of Air Quality Officer (AQO)		No	Environmental Officer
Air Quality Management Plan (AQMP)		No	
Capacity	Human Resources	Yes	Three Environmental Health Officers (from the district)
	Equipment	No	
	Skills	No	
Atmospheric Emissions Licence (AEL) capacity		No	
Cooperative governance		No	
AQM factored into IDP		No	
Ambient Air Quality Monitoring		Yes	One monitoring station (Delmas)

Table 4: Ehlanzeni District Municipality and local municipalities' 2018 status quo

Ehlanzeni District Municipality			
Requirement		**Status**	**Comment**
Appointment of Air Quality Officer (AQO)		Yes	One designated AQO One appointed AQO
Air Quality Management Plan (AQMP)		Planned	AQMP underway development
Capacity	Human Resources	Yes	Two AQOs Five Environmental Management Inspectors
	Equipment	No	No air quality monitoring equipment and no plan in place for procurement
	Skills	Yes	Training on AEL and Emissions Management
Atmospheric Emissions Licence (AEL) capacity		Yes	AEL training completed
Cooperative governance		Yes	MDARDLEA, SAWS and local authorities
AQM factored into IDP		Planned	Environmental profile was developed by the province and will be included in the IDP
Ambient Air Quality Monitoring		No	No plan in place to implement air quality monitoring

Bushbuckridge Local Municipality			
Requirement		**Status**	**Comment**
Appointment of Air Quality Officer (AQO)		No	No designated AQO
Air Quality Management Plan (AQMP)		Yes	Draft AQMP 2017/2018
Capacity	Human Resources	No	One AQO advertised
	Equipment	No	No air quality monitoring equipment
	Skills	No	No air quality related skills. Training to be provided once the AQO is appointed
Atmospheric Emissions Licence (AEL) capacity		No	Done by EDM
Cooperative governance		Yes	DARDLEA, EDM, IUCMA and SANPARKS
AQM factored into IDP		No	Available 2017/2018 AQMP draft to be factored in the IDP once approved
Ambient Air Quality Monitoring		No	No plan in place to implement air quality monitoring

City of Mbombela Local Municipality			
Requirement		**Status**	**Comment**
Appointment of Air Quality Officer (AQO)		Yes	One AQO
Air Quality Management Plan (AQMP)		Planned	AQMP development planned for 2018/2019 financial year
Capacity	Human Resources	Yes	One AQO. Three Environmental Management Inspectors vacant but not funded
	Equipment	No	No air quality monitoring equipment
	Skills	Yes	Emissions Management Training provided
Atmospheric Emissions Licence (AEL) capacity		No	Done by EDM
Cooperative governance		Yes	National: DEA, DWS and DAFF Provincial: DARDLEA, CoGTA & DWS Specialists: ARC, UMP
AQM factored into IDP		Yes	AQMP development is factored into IDP
Ambient Air Quality Monitoring		No	No plan in place to implement air quality monitoring

Nkomazi Local Municipality			
Requirement		**Status**	**Comment**
Appointment of Air Quality Officer (AQO)		Yes	No designated AQO Waste Manager assists with air quality related matters
Air Quality Management Plan (AQMP)		No	
Capacity	Human Resources	Yes	Waste Manager. EO position is vacant as per organogram but stills need to be approved
	Equipment	No	No air quality monitoring equipment
	Skills	No	No air quality training provided to Waste Manager
Atmospheric Emissions Licence (AEL) capacity		No	Done by EDM
Cooperative governance		Yes	Internal departments
AQM factored into IDP		No	No Environmental Plan. AQM factored in from a plan developed by DEA for EDM
Ambient Air Quality Monitoring		No	No plan in place to implement air quality monitoring

Thaba Chweu Local Municipality			
Requirement		**Status**	**Comment**
Appointment of Air Quality Officer (AQO)		No	No designated AQO. One official to assist with air quality related matters
Air Quality Management Plan (AQMP)		No	Still rely on AEP that elapsed in 2012 and needs to be reviewed
Capacity	Human Resources	Yes	Support staff One Environmental Management Inspector
	Equipment	No	No air quality monitoring equipment
	Skills	No	No air quality personnel
Atmospheric Emissions Licence (AEL) capacity		No	Done by EDM
Cooperative governance		Yes	National, provincial and district
AQM factored into IDP		No	Rely on AEP that needs to be reviewed
Ambient Air Quality Monitoring		No	No plan in place to implement air quality monitoring

Table 5: Number of ambient air quality stations reporting to SAAQIS

Station type	Number of stations	Percentage of total stations in South Africa
Total number of private electronic stations	43	26
Total number of government electronic stations	121	74
Total number of electronic stations	164	

Table 6: Vaal Traingle Airshed Priority Area VTAPA) 2018 exceedances

Pollutant & Averaging Period	Standard	Annual Number of Permitted Exceedances	Station Name	Exceedances Per Month												Total Exceedances to Date
				January	February	March	April	May	June	July	August	September	October	November	December	
PM10 24h	75 µgm^{-3}	4	Zamdela	0	0	0	0	0	0	0	0	0	0	1	0	1
			Three Rivers	0	0	0	0	1	21	14	24	24	13	5	5	107
			Sharpeville	0	0	0	1	8	19	11	11	11	0	0	1	62
			Sebokeng	0	0	0	0	0	5	0	0	0	0	0	0	5
			Kliprivier	0	0	0	2	5	21	11	13	11	2	1	0	66
			Diepkloof	0	0	0	0	0	1	0	0	1	0	0	0	2
PM2.5 24h	40 µgm^{-3}	4	Zamdela	0	0	1	3	5	18	12	6	10	10	1	0	66
			Three Rivers	0	0	1	0	0	3	1	0	2	0	0	1	8
			Sharpeville	0	2	0	10	14	23	13	12	5	0	0	0	79
			Sebokeng	0	0	0	0	8	19	7	7	7	0	0	0	48
			Kliprivier	7	6	11	16	15	28	18	13	14	4	0	2	134
			Diepkloof	0	1	0	2	0	5	0	0	5	0	0	0	13
SO_2 10 min	191 ppb	526	Zamdela	0	0	1	3	0	0	0	0	1	0	0	0	5
			Three Rivers	0	0	1	0	2	0	0	0	0	1	0	0	4
			Sharpeville	0	0	0	0	0	0	1	1	5	0	0	0	7
			Sebokeng	0	0	0	0	1	0	0	0	0	0	0	0	1
			Kliprivier	0	0	0	0	0	0	0	0	0	0	0	0	0
			Diepkloof	0	0	2	0	0	0	0	0	0	0	0	0	2
SO_2 1h	134 ppb	88	Zamdela	0	0	0	0	0	0	0	0	0	0	0	0	0
			Three Rivers	0	0	0	0	1	0	0	1	0	0	0	0	2
			Sharpeville	0	0	0	0	1	0	0	1	2	0	0	0	4
			Sebokeng	0	0	0	0	0	0	0	0	0	0	0	0	0
			Kliprivier	0	0	0	0	0	0	0	0	0	0	0	0	0
			Diepkloof	0	0	0	0	0	0	0	0	0	0	0	0	0
SO_2 24h	48 ppb	4	Zamdela	0	0	0	0	0	0	0	0	0	0	0	0	0
			Three Rivers	0	0	0	0	0	0	0	0	0	0	0	0	0
			Sharpeville	0	0	0	0	0	0	0	0	0	0	0	0	0
			Sebokeng	0	0	0	0	0	0	0	0	0	0	0	0	0
			Kliprivier	0	0	0	0	0	0	0	0	0	0	0	0	0
			Diepkloof	0	0	0	0	0	0	0	0	0	0	0	0	0
NO_2 1h	106 ppb	88	Zamdela	0	0	0	0	0	0	0	0	0	0	0	0	0
			Three Rivers	0	0	0	0	0	0	0	0	0	0	0	0	0
			Sharpeville	0	0	0	0	0	0	0	0	0	0	0	0	0
			Sebokeng	0	0	0	0	0	0	0	0	0	0	0	0	0
			Kliprivier	0	0	0	0	0	0	0	0	0	0	0	0	0
			Diepkloof	0	0	0	0	0	0	0	0	0	0	0	0	0
O_3 8h (Running)	61 ppb	11	Zamdela	12	6	26	0	0	0	0	0	0	0	4	0	48
			Three Rivers	4	0	17	0	0	0	0	23	68	25	24	21	182
			Sharpville	15	33	25	5	5	0	0	0	0	5	10	0	98
			Sebokeng	132	133	106	15	9	12	10	139	161	157	13	5	892
			Kliprivier	14	2	9	0	0	0	0	0	21	5	23	9	83
			Diepkloof	0	0	5	5	0	0	0	0	0	0	0	0	10
CO 1h	26 ppm	88	Zamdela	0	0	0	0	0	0	0	0	0	0	0	0	0
			Three Rivers	0	0	0	0	0	0	0	0	0	0	0	0	0
			Sharpeville	0	0	0	0	0	0	0	0	0	0	0	0	0
			Sebokeng	0	0	0	0	0	0	0	0	0	0	0	0	0
			Kliprivier	0	0	0	0	0	0	0	0	0	0	0	0	0
			Diepkloof	0	0	0	0	0	0	0	0	0	0	0	0	0
CO 8h (calculated on 1 hourly averages)	8.7 ppm	11	Zamdela	0	0	0	0	0	0	0	0	0	0	0	0	0
			Three Rivers	0	0	0	0	0	0	0	0	0	0	0	0	0
			Sharpeville	0	0	0	0	0	0	0	0	0	0	0	0	0
			Sebokeng	0	0	0	0	0	0	0	0	0	0	0	0	0
			Kliprivier	0	0	0	0	0	0	0	0	0	0	0	0	0
			Diepkloof	0	0	0	0	0	0	0	0	0	0	0	0	0

Table 7: Highveld Priority Area (HPA) 2018 exceedances

Pollutant & Averaging Period	Standard	Annual Number of Permitted Exceedances	Station Name	Exceedances Per Month												Total Exceedances to Date
				January	February	March	April	May	June	July	August	September	October	November	December	
PM10 24h	75 µgm^{-3}	4	Ermelo	4	15	8	5	17	20	20	18	19	9	4	4	143
			Hendrina	-	-	-	-	-	4	5	7	-	-	0	0	16
			Middelburg	0	0	0	1	0	0	0	0	0	0	0	0	1
			Secunda	18	5	1	4	16	16	3	22	17	1	0	0	103
			Witbank	-	0	0	7	11	13	10	21	21	8	1	0	92
PM2.5 24h	40 µgm^{-3}	4	Ermelo	4	12	4	6	17	19	17	11	10	0	0	0	100
			Hendrina	-	-	-	-	-	3	1	3	-	-	0	0	7
			Middelburg	0	0	0	1	0	0	0	0	0	0	0	0	1
			Secunda	20	5	2	5	16	17	9	17	12	0	0	0	103
			Witbank	-	0	1	7	9	12	11	16	17	1	0	0	74
SO_2 10 min	191 ppb	526	Ermelo	0	6	0	0	0	0	0	0	0	0	0	0	6
			Hendrina	3	0	3	1	2	0	1	0	4	0	4	1	19
			Middelburg	0	0	0	0	2	0	0	0	0	0	0	0	2
			Secunda	0	0	0	0	0	0	0	0	0	0	0	0	0
			Witbank	0	0	0	1	2	0	4	0	0	6	1	0	14
SO_2 1h	134 ppb	88	Ermelo	0	3	0	0	1	0	0	0	0	0	0	0	4
			Hendrina	1	0	1	1	2	0	0	0	1	0	0	0	6
			Middelburg	0	0	0	0	0	0	0	0	0	0	0	0	0
			Secunda	0	0	0	0	0	0	0	0	0	0	0	0	0
			Witbank	0	0	0	0	0	0	2	0	0	1	0	0	3
SO_2 24h	48 ppb	4	Ermelo	0	0	0	0	0	0	0	0	0	0	0	0	0
			Hendrina	0	0	0	0	0	0	0	0	0	0	0	0	0
			Middelburg	0	0	0	0	0	0	0	0	0	0	0	0	0
			Secunda	0	0	0	0	0	0	0	0	0	0	0	0	0
			Witbank	0	0	0	0	0	0	1	0	0	0	0	0	1
NO_2 1h	106 ppb	88	Ermelo	0	0	0	0	0	0	0	0	0	0	0	0	0
			Hendrina	0	0	0	0	0	0	0	0	0	0	0	0	0
			Middelburg	0	0	0	0	0	0	0	0	0	0	0	0	0
			Secunda	0	0	0	0	0	0	0	0	0	0	0	0	0
			Witbank	0	0	0	0	0	0	0	0	0	0	0	0	0
O_3 8h (Running Averages)	61 ppb	11	Ermelo	4	0	2	0	0	0	0	7	36	3	0	10	62
			Hendrina	7	2	0	0	0	0	0	9	69	15	14	0	116
			Middelburg	0	2	0	0	0	0	0	0	0	0	3	0	5
			Secunda	-	0	0	0	0	0	0	6	11	5	0	0	22
			Witbank	187	90	7	0	0	0	0	0	0	0	0	0	284
CO 1h	26 ppm	88	Ermelo	0	0	0	0	0	0	0	0	0	0	0	0	0
			Hendrina	0	0	0	0	0	0	0	0	0	0	0	0	0
			Middelburg	0	0	0	0	0	0	0	0	0	0	0	0	0
			Secunda	0	0	0	0	0	0	0	0	0	0	0	0	0
			Witbank	0	0	0	0	0	0	0	0	0	0	0	0	0
CO 8h (Running Averages)	8.7 ppm	11	Ermelo	0	0	0	0	0	0	0	0	0	0	0	0	0
			Hendrina	0	0	0	0	0	0	0	0	0	0	0	0	0
			Middelburg	0	0	0	0	0	0	0	0	0	0	0	0	0
			Secunda	0	0	0	0	0	0	0	0	0	0	0	0	0
			Witbank	0	0	0	0	0	0	0	0	0	0	0	0	0

Table 8: Waterberg Bojanala Priority Area (WBPA) 2018 exceedances

Pollutant & Averaging Period	Standard	Annual Number of Permitted Exceedances	Station Name	January	February	March	April	May	June	July	August	September	October	November	December	Total Exceedances to date
PM10 24h	75 μgm^{-3}	4	Lephalale	0	0	0	0	0	0	0	0	0	0	0	0	0
			Mokopane	0	0	2	1	12	23	12	26	23	9	0	1	109
			Thabazimbi	0	0	0	0	2	8	5	3	9	0	0	0	27
			Xanadu	0	0	0	2	3	3	1	20	7	0	0	0	36
PM2.5 24h	40 μgm^{-3}	4	Lephalale	0	0	0	0	0	0	0	0	0	0	0	0	0
			Mokopane	0	0	0	0	0	0	0	2	2	0	0	0	4
			Thabazimbi	0	0	1	0	0	7	1	0	1	0	0	0	10
			Xanadu	0	0	10	9	1	26	9	27	26	8	12	2	130
SO_2 10 min	191 ppb	526	Lephalale	0	0	1	0	0	0	0	0	0	0	0	0	1
			Mokopane	0	0	0	0	0	0	0	0	0	0	0	0	0
			Thabazimbi	0	0	0	0	0	0	0	0	0	0	0	0	0
			Xanadu	0	0	0	0	0	0	0	0	0	0	0	0	0
SO_2 1h	134 ppb	88	Lephalale	0	0	1	0	1	0	0	0	0	0	0	0	2
			Mokopane	0	0	0	0	0	0	0	0	0	0	0	0	0
			Thabazimbi	0	0	0	0	0	0	0	0	0	0	0	0	0
			Xanadu	0	0	0	0	0	0	0	0	0	0	0	0	0
SO_2 24h	48 ppb	4	Lephalale	0	0	0	0	0	0	0	0	0	0	0	0	0
			Mokopane	0	0	0	0	0	0	0	0	0	0	0	0	0
			Thabazimbi	0	0	0	0	0	0	0	0	0	0	0	0	0
			Xanadu	0	0	0	0	0	0	0	0	0	0	0	0	0
NO_2 1h	106 ppb	88	Lephalale	0	0	0	0	0	0	0	0	0	0	0	0	0
			Mokopane	0	0	0	0	0	0	0	0	0	0	0	0	0
			Thabazimbi	0	0	0	0	0	0	0	0	0	0	0	0	0
			Xanadu	0	0	0	0	0	0	0	0	0	0	0	0	0
O_3 8h (Running)	61 ppb	11	Lephalale	0	0	0	0	0	0	0	8	54	0	0	0	62
			Mokopane	0	0	0	0	0	0	0	0	0	0	0	0	0
			Thabazimbi	0	0	0	0	0	0	0	0	0	0	0	0	0
			Xanadu	12	9	4	0	0	0	0	24	75	48	42	51	265
CO 1h	26 ppm	88	Lephalale	0	0	0	0	0	0	0	0	0	0	0	0	0
			Mokopane	0	0	0	0	0	0	0	0	0	0	0	0	0
			Thabazimbi	0	0	0	0	0	0	0	0	0	0	0	0	0
			Xanadu	0	0	0	0	0	0	0	0	0	0	0	0	0
CO 8h (calculated on 1 hourly averages.	8.7 ppm	11	Lephalale	0	0	0	0	0	0	0	0	0	0	0	0	0
			Mokopane	0	0	0	0	0	0	0	0	0	0	0	0	0
			Thabazimbi	0	0	0	0	0	0	0	0	0	0	0	0	0
			Xanadu	0	0	0	0	0	0	0	0	0	0	0	0	0

CHAPTER 7
Conclusions

7.1 Introduction

This Chapter gives a summary of the major findings of the study, makes conclusions based on the findings, and describes limitations and challenges encountered during the study. It further provides implications of the research and future directions and research needs. It does this by aligning the results to the objectives listed in the beginning of the thesis.

7.2 Major findings of the study by research objective

(1) *To collect particulate matter samples using University of North Carolina (UNC) gravimetric passive samplers.*

The study was conducted in the Greater Tubatse Municipality (GTM) home to a number of air pollution sources in a rural area within a complex terrain in Limpopo, South Africa. The main towns in the area are Steelpoort and Burgersfort which are sustained through economic activities such as mining and smelting of chromium ores. PM samples were collected using inexpensive UNC gravimetric samplers. The samplers were deployed for a period of ±30 days from July 2015 to June 2016, except for the months of August–September and September–November for which they were deployed for a period of >35 days. In the passive sampler, particles travel through a protective stainless steel mash and deposit on a collection surface by gravity and diffusion. The samplers collect total suspended PM which is then analysed for mass concentration of $PM_{2.5}$, PM_{10} and PM chemical components.

(2) *To characterize the mass concentrations of $PM_{2.5}$, PM_{10} and PM chemical components using Computer Controlled Scanning Electron Microscopy (CCSEM).*

The samples collected by UNC samplers were analysed using computer-controlled scanning electron microscopy with energy-dispersive X-ray spectroscopy (CCSEM-EDS) to determine the mass concentration of $PM_{2.5}$, PM_{10} and PM chemical components. The particle classes

obtained from the analysis included carbon-rich (C-rich), chromium-rich (Cr-rich), iron-rich (Fe-rich), iron/chromium-rich (FeCr-rich), silicon-rich (Si-rich), calcium-rich (Ca-rich), silicon/aluminium/iron-rich (SiAlFe-rich), silicon/magnesium-rich (SiMg-rich) and silicon/aluminium-rich (SiAl-rich).

The annual concentrations of PM_{10} at the different study sites varied from 20.98 $\mu g.cm^{-3}$ to 38.11 $\mu g.cm^{-3}$. Annual PM_{10} concentrations were below the South African National Ambient Air Quality Standard (DEA, 2009) of 40 $\mu g.cm^{-3}$. The $PM_{2.5}$ annual concentrations from CCSEM analysis ranged between 2.5 $\mu g.cm^{-3}$ and 11.8 $\mu g.cm^{-3}$. SiAl-rich and SiAlFe-rich particles were the most abundant particles with Fe-rich particles being less abundant.

The $PM_{2.5}$ concentrations are on average lower than the concentrations of SiAl-rich particles. The UNC passive samplers were likely underestimating the $PM_{2.5}$ mass concentration when deployed for a longer period due to possible evaporation of sulphates and nitrates. This was the first study in which the samplers together with CCSEM were used to analyse $PM_{2.5}$ concentrations. Therefore, without other PM measurements in the study area, it was not possible to carry out a correlation study to measure the accuracy of $PM_{2.5}$ measurement. However, the accuracy of UNC passive samplers on PM measurements (>2.5 $\mu g.cm^{-3}$ in aerodynamic diameter) has been discussed in other studies such as Shirdel *et al*. (2018).

(3) *To characterise the spatial distribution of $PM_{2.5}$, PM_{10}, and PM chemical components.*

The spatial analysis of $PM_{2.5}$, PM_{10} and PM chemical components was undertaken using the geographic information system (GIS) software. The inverse distance weighted (IDW) interpolation tool within the mapping software (ArcMap version 10.0) was used in the analyses. The analysis revealed that there is a distinct spatial heterogeneity in the study area with variability in both low and elevated concentrations observed at different sites for $PM_{2.5}$, PM_{10} and PM chemical components. The highest concentrations for annual PM_{10} (38.11 $\mu g.cm^{-3}$), Cr-rich (1.4 $\mu g.cm^{-3}$), Si-rich (2.6 $\mu g.cm^{-3}$), SiAl-rich (11.8 $\mu g.cm^{-3}$), SiAlFe-rich (7.0 $\mu g.cm^{-3}$) and SiMg-rich (3.9 $\mu g.cm^{-3}$) particles were observed at Site 3, which is located about 1.7 km and 1.9 km west north-westerly of Samancor chrome smelter and a Silicone mine, respectively. The lowest concentrations were observed at Site 6 (PM_{10} = 20.98 $\mu g.cm^{-3}$, Cr-rich = 0.2 $\mu g.cm^{-3}$, SiAlFe-rich 3.2 $\mu g.cm^{-3}$, Si-rich 0.9 $\mu g.cm^{-3}$ and SiMg-rich 0.8 $\mu g.cm^{-3}$) with exception of

SiAl-rich (7.3 μg.cm^{-3}) at Site 5. The C-rich particles had the same signature as $PM_{2.5}$, with the lowest concentration being at Site 6 (C-rich = 1.9 μg.cm^{-3}, $PM_{2.5}$ = 2.5 μg.cm^{-3}) and highest concentration at Site 1 (C-rich = 5.4 μg.cm^{-3}, $PM_{2.5}$ = 11.8 μg.cm^{-3}).

The highest concentrations for Ca-rich particles were observed at Site 6 (3.4 μg.cm^{-3}) which was located about 1.6 km west-northwest of Marula Platinum Mine, with the lowest concentration at Site 4 (1.7 μg.cm^{-3}). The highest observed concentrations for FeCr-rich particles (2.8 μg.cm^{-3}) were at sampling Sites 3 and 5 (Site 5 is about 2 km from the ASA chrome smelter). The Cr-rich particles were highest at Site 3 (1.4 μg.cm^{-3}) followed by Site 1 (1.3 μg.cm^{-3}) which is about 2.5 km from the Glencore chrome smelter and Site 5 (1.3 μg.cm^{-3}). The annual concentrations of Cr-rich particles across all the sites were above the 0.11 μg.cm^{-3} annual limit set by the New Zealand Ministry of Environment (Fisher and Metcalfe, 2016). FeCr-rich particles showed highest concentrations closer to the smelters around Site 3 (2.8 μg.cm^{-3}) and Site 5 (2.8 μg.cm^{-3}). Since the sites were not equally spaced in the study area, other methods such as the coefficient of divergence (COD) were used to confirm and validate the results of the spatial analysis determined using the geographic information system. COD values higher than 0.2 indicated spatial heterogeneity, while COD values less than 0.1 indicated homogeneity of concentrations. All components in the study area had COD values greater than 0.2 which is an indication that there was a heterogeneous relation observed between the sites in the study area. The lowest heterogeneity values for COD ranged from 0.24 to 0.4 and were observed for PM_{10} (0.24), C-rich (0.25), SiAlFe-rich (0.28), PM2.5 (0.29), SiAl-rich (0.3), Si-rich (0.35) and Ca-rich (0.38) particles. The moderate to high COD values were observed for Fe-rich (0.41), SiMg-rich (0.42), FeCr-rich (0.59) and Cr-rich (0.6) particles. The highest COD values were observed for sites located in the vicinity of point source emitters, which suggests that the communities residing in the vicinity of these point sources are more vulnerable to exposure of these particles than those living further downwind.

(4) *To determine the relationship between calculated mixing height, Monin-Obukhov length, ventilation coefficient and air pollution potential with PM_{10} concentration.*

The Air Pollution Model (TAPM) was used to calculate mixing height, Monin-Obukhov length, ventilation coefficient (VC) and air pollution potential. The spatial distribution of these parameters were plotted against the PM_{10} distribution to determine their relationship. Only the

VC was able to predict areas of high PM_{10} concentrations near the valley openings. The VC is possibly influenced by the impact of pressure gradient on the wind strength. The inverse correlation between PM_{10} concentration and the meteorological parameters of interest could be attributed to the use of monthly average data. These finding suggest that investment in ground based meteorological monitoring equipment is of high importance for observed data.

(5) *To determine source profiles of PM, the number of sources, and the contribution of identified sources in the GTM.*

The $PM_{2.5}$, PM_{10} concentrations and the elemental composition of individual particles deposited on the UNC passive sampler were determined using CCSEM-EDS (Tescan Vega 3 model). These data was then used as input to the PMF model. The most subjective and least quantifiable step in applying PMF for PM source apportionment is assignment of identities to the p factors. A common strategy for identifying source profiles which was applied in this study was to use statistical analysis in PMF coupled with knowledge of sources in the study area and atmospheric science experience supported by literature for measured PM source profiles with characteristics similar to factor profiles in the F matrix. After applying this method, three to five factors were deemed to be appropriate for a five source solution. The factors were identified according to the type of elements dominating in percentage in that factor. Agricultural and wood combustion was associated with the dominance of C as primary species and Fe elements. Ferrochrome smelter was identified by the domination of Cr and Fe elements. Crustal / road dust factor was associated with Si, Al, Ca and Mg as the primary elemental species. Industrial coal combustion factor was identified by Ca, C, Al and Si as the dominating elements. Vehicular emission factor was associated with Fe as the primary species, in addition to C, Al, Si, and Ca elements. The most interesting outcome was that Cr was also associated with crustal / road dust and agricultural / wood burning which is an indication that once this element is emitted from the source it is then deposited onto the soil and water bodies before it is absorbed by plant material and released into the atmosphere during burning.

The PM_{10} sources contribution to the GTM were identified as follows: Site 1 included chrome smelters (32.9%), coal combustion (21.3%), wood / agricultural combustion (37.3%), and crustal/road dust (8.6%)). At Site 2, sources were vehicle (14.7%), chrome smelters (15%), coal combustion (22.4%), wood / agricultural combustion (28.3%) and crustal / road dust

(19.6%). Sources in site 3 were similar with vehicle (20.17%), chrome smelters (13.6%), coal combustion (26.1%), wood / agricultural combustion (10.1%), and crustal/road dust (30.1%) sources. Site 4 sources were vehicle (8.4%), chrome smelters (14.8%), coal combustion (17.9%), wood / agricultural combustion (33.1%) and crustal/road dust (25.8%). Site 5 had vehicle (14.1%), chrome smelters (23.3%), coal combustion (21.3%), wood / agricultural combustion (20.9%), and crustal / road dust (20.4%) sources. Site 6 sources included vehicle (18.2%), chrome smelters (10.5%), coal combustion (9.7%), wood / agricultural combustion (25.9%), and crustal / road dust (35.7%).

(3) *To determine the regional and trans-boundary air transport to the receptor locations using the HYSPLIT model.*

In this study, the HYSPLIT air mass back trajectories were run for 24-hours (from mid-night to mid-morning) from 1 July 2015 to 30 June 2016 at all sites. The back trajectories were defined by their spatial position (longitude, latitude) at 30-minute intervals for 24 hours back from the receptor sites. Trajectory cluster analysis was performed to identify major transport pathways.

For Site 1, cluster 1 with 36% of trajectories originated from Mozambique and arrived at the receptor site by passing through mining areas and a smelter northeast of the sampling site. Cluster 2 with 12% of the trajectories originated from Zimbabwe and arrived at the receptor site from the northwest and away from the mines and smelters in the area. Cluster 3 with 20% of trajectories originated from the west while clusters 4 and 5 originated from the Indian Ocean. Only clusters 1, 4 and 5 passed through areas with mines and smelters within the study area. This makes them potential transporters of heavy metals to the receptor site. For Site 2, all clusters except for cluster 4 passed over the mines and smelters and as such had the potential of carrying elemental particles to the site. For Site 3, all the clusters passed over the mining areas and only clusters 3 and 5 passed over the smelters. Hence, all these clusters can transport elemental particles to the receptor sites. For Site 4, all the clusters pass over mining areas and only cluster 2 and 3 pass over the smelters before arriving at the receptor site. For Site 5, only cluster 1 did not pass over any industrial facility in the area. For Site 6, only clusters 2, 3 and 5 passed over industrial facilities. Cluster 2 with 30% of trajectories was recirculating within the vicinity of the receptor site and this made it the most likely contributor of local pollutants.

Therefore, both regional and trans-boundary transport of air masses were possibly adding to the pollution sources in the GTM.

(6) *To determine the distribution of PM_{10} from industrial point sources and evaluate their possible impact on human health using modelled hourly data from the TAPM model and GIS software.*

The Air Pollution Model (TAPM) version 4 was run for the period of July 2015 to June 2016. Four grids with nested domains of 25 x 25 horizontal grid points at 30 km, 20 km, 10 km spacing for the meteorology and 4 km for pollution simulation were used. A total of 49 receptor points were used for calculating pollution concentration fields. The GIS software was then used to display the seasonal, annual, daytime and night-time spatial variation of PM_{10} concentrations from industrial point sources.

The highest PM_{10} concentration ranged from 16.6 - 27.3 $\mu g.m^{-3}$ and were observed between X-Strata chrome smelter and Samancor chrome smelter, spreading to the west of Strata chrome smelter and south-west of Samancor chrome smelter (see Figure 3.1b in Chapter 3, page 87). Concentrations ranging from 10.7 – 16.6 $\mu g.m^{-3}$ were observed to the west of Smelter 1. Though the highest value is lower than the 40 $\mu g.m^{-3}$ of the South African annual PM_{10} National Ambient Air Quality Standards, it is higher than the WHO annual mean guideline of 20 $\mu g.m^{-3}$. The wind profile for the area (Figure 3.2) showed that the dominant winds were easterly to north-easterly. These winds were responsible for dispersing pollutants to the west and south-west of the smelters.

The seasonal PM_{10} concentration showed that the highest concentration occurred in winter (27.3 $\mu g.m^{-3}$), followed by summer (25.4 $\mu g.m^{-3}$), spring (24 $\mu g.m^{-3}$), and autumn (15.2 $\mu g.m^{-3}$). The seasonal distribution was similar to the annual distribution but varied in intensity of the PM_{10} distribution. The seasonal wind patterns did not provide a clear picture of the wind profiles in the GTM which can be attributed the complex nature of the topography in the area. The night-time PM_{10} concentration (16.5 $\mu g.cm^{-3}$) was higher than the day-time concentration of 15.9 $\mu g.cm^{-3}$. The high concentrations at night were spreading over a larger area compared to high day-time concentrations which were localised closer to the ASA chrome smelter and X-strata chrome smelter. The observed high concentration at night could be attributed to stable

atmospheric conditions which suppressed vertical distribution and lead to accumulation and distribution of pollution over a shallow and larger area. During the day the atmosphere is mostly unstable and disperses pollution resulting in lower concentrations.

(4) *To reflect on the findings of objectives (1) – (6) and consider gaps in the current implementation of air quality legislation in South Africa.*

The information used to conceptualise the commentary was gathered through desktop analysis of air quality monitoring reports, AQMP documents, AEL compliance reports, Air Quality legislations, and through active involvement in the DEFF's AQMP implementation task team meetings. There is evidence from air quality monitoring reports showing that $PM_{2.5}$, PM_{10} and ozone are in non-compliance with the South African NAAQSs. The gaps identified by the analysis of all the documents indicated that there were no formal scientific source apportionment studies done in the development of AQMPs. There are also not enough air quality monitoring sites to evaluate the behaviour of air pollution on a spatial scale in most local municipalities. Passive sampling had not been considered to monitor and diagnose air pollution problems in South Africa. Lastly, industrial facilities were not required to model the cumulative impacts of neighbouring facilities when applying for atmospheric emission licenses. Therefore, the findings of objectives 1 to 6 help inform appropriate scientific and decision-making for effective air quality management in South Africa. Findings from objective 1 to 3 provide an opportunity for environmental authorities to invest in inexpensive methods of collecting much needed data to assess the impacts of air pollution in South Africa, and allocate resources in areas that are heavily impacted by pollution. Objective 4 highlighted the need to consider meteorological parameters in all analyses of the data to inform spatial planning policies and demarcation of residential and industrial zones. Objectives 5 and 6 provided qualitative and quantitative evidence of various sources and thus inform pollution abatement policies.

7.3. Study limitations

There is lack of credible continuous ambient air quality data in South Africa which makes analysis of long-term trends very difficult. There is also no PM chemical characterization database (which exists in other developed countries) in South Africa. These data are needed as

input to the PMF model for source apportionment. Additionally, there is little or no source fingerprint information in South Africa to assist in eliminating the ambiguity when identifying the sources with a similar signature. However, other statistical tools such as potential source contribution function (PSCF), concentration weighted trajectories (CWT), and conditional probability function (CPF) can be used as an alternative to identify possible sources. The lack of credible ambient air quality data (or no data at all) makes it impossible to evaluate the accuracy of dispersion model results. Passive samplers used in the study were in part not appropriate for $PM_{2.5}$ measurements over long periods to due to the present of reactive species in $PM_{2.5}$. Lastly, the lack of emissions databases in South Africa hampers the comparison of studies of receptor models and dispersion models in source apportionment studies.

7.4 Future directions and research needs

The air quality management systems designed to improve the quality of air require constant review and improvement to ensure their effectiveness in addressing the poor state of air quality and the well-being of humans. Their effectiveness is largely dependent on the identification and quantification of pollution sources. The levels of pollution in the atmosphere are determined by physical and chemical processes, hence, a chemical composition and spatiotemporal analysis was undertaken to assess the distribution of pollutants in the study area. The fundamental principle of air pollution management is to reduce emissions from the sources. Therefore, to quantify the impact of such sources on air quality and to develop emission reduction strategies requires source profiling and apportionment.

The observed high level of chromium concentrations exceeded the WHO guidelines and requires urgent interventions by all spheres of government responsible for air quality management in South Africa (Research Objective 7). Source profiling and apportionment are scientific tools that assist policymakers to identify and quantify the different sources of air pollution, and thereby to increase the capacity to put in place effective policy measures to reduce air pollution to acceptable levels.

There is a need for future collaborations between government entities to ensure that Section 24 of the 1996 Constitution of South Africa (which stipulates that everyone has the right to live in an environment that is not harmful to their health or well-being) is adhered to. Collaborations

between government departments such as the Department of Environment, Forestry and Fishers, Spatial Planning and Land Use Management, and Health, are currently lacking in South Africa. Such collaborations should be in the monitoring, data collection and research activities that are aimed at improving air quality. The lack of credible continuous ambient air quality data (or no data at all in some areas) makes it impossible to evaluate the accuracy of dispersion model results. A database of PM chemical speciation data is needed not only as input to the PMF model, but also to assess the impact of PM on human health. Manuscript 1 showed that the use of monthly average data resulted in the inability to determine the relation between meteorological parameters (mixing height, Monin-Obukhov length) and PM_{10} distribution. Therefore, for future analysis of the behaviour of pollutants in a complex terrain, a network of meteorological station balloon soundings within the valley floor and adjacent slopes needs to be set up in order to capture the actual meteorological parameters that influence the behaviour of air pollution. The ambient air quality and meteorological parameters should be monitored continuously to verify the findings of this study.

Source apportionment studies need chemical species, emissions data, and continuous ambient air quality data. The availability of sufficient data will ensure that there is adequate information to perform comparison studies for top-down and bottom-up approaches to receptor modelling. The combination of continuous ambient air quality data with trajectory models allows for statistical analysis, such as potential source contribution function (PSCF) to identify the geographical origin of sources that are likely to contribute to concentrations above the emission limit values. This analysis should be incorporated in future source apportionment studies to identify which sources (identified by models such as PMF) are likely to contribute to values above the prescribed limits.

7.5 References

Environment Agency, 2014: Technical Guidance Document for Air Quality Modelling. Doc. ID:EAD-EQ-PCE-TG-12. [Online] Available from: https://www.ead.ae/Documents/Business%20and%20Industry/Technical%20Guidance%20Document%20for%20Air%20Quality%20Modelling.pdf [Accessed 19 August 2019].

Fisher, G., Metcalfe, J., 2016: Good practice guide for assessing discharges to air from industry. Wellington: NZ Ministry for the Environment. https://doi. org/10.13140/RG.2.1.3803.4162

Shirdel, M., Andersson, B.M., Bergdahl, I.A., Sommar, J.N., Wingfors, H. and Liljelind, I.E., 2018: Improving the UNC Passive Aerosol Sampler Model Based on Comparison with Commonly Used Aerosol Sampling Methods. *Annals of Work Exposures and Health*, 62 (3): 328 – 338. https://doi.org/10.1093/annweh/wxx110

South African Department of Environmental Affairs (DEA).: National Environmental Management: Air Quality Act (No. 39) of 2004 [Online] Available from https://www.environment.gov.za/sites/default/files/.../nema_amendment_act39.pdf [Accessed 19 August 2018]

South African Department of Justice and Constitutional Development (DOJ & CD), 1997: Constitution of the republic of South Africa No. 108 of 1996. [Online] Available from: http://www.justice.gov.za/legislation/constitution/SAConstitution-web-eng.pdf .

South African Department of Environmental Affairs (DEA). National ambient air quality standards [document on the Internet]. c2009 [cited 2019 Feb04]. Available from: https://www.environment.gov.za/sites/default/files/legislations/nemaqa_airquality_g32816gon1210.pdf

World Health Organization (WHO), 2017. Evolution of WHO air quality guidelines: Past, present and future. Available from: http://www.euro.who.int/__data/assets/pdf_file/0019/331660/Evolution-air-quality.pdf

CHAPTER 8

Appendices

Appendix 1: Poster presentation.

POSTERS INDEX (continued)

Characterization of airborne particles in Greater-Tubatse, South Africa

Cheledi Tshehla
SA Weather Service, 442 Rigel Avenue, Erasmusrand, Pretoria 0181.
cheledi.tshehla@weathersa.co.za

South African Weather Service
ISO 9001 Certified Organisation

Abstract

The Greater-Tubatse area is a rural industrialized area in the Limpopo Province, South Africa. To characterize the ambient particulate pollution, samples were collected using University of North Carolina passive samplers from 6 sites during a five month campaign. Computer Controlled Scanning Electron Microscopy was used to analyze individual particles to determine the PM10 concentrations and the chemical composition of the particles. The PM10 concentrations were found to vary across all sites. The chemical composition determined by CCSEM identified high temperature industrial processes as the major source of particles in the area.

Objectives

- Determine PM10 levels using University of North Carolina (UNC) passive samplers.
- Determine sources of heavy metals in a rural mining area.

Introduction

The Greater-Tubatse Municipality (GTM) is located under Sekhukhune District Municipality in the Limpopo Province, South Africa. The area falls within the eastern limb of the Bushveld Complex. The main towns in the area are Steelpoort and Burgersfort which are sustained through economic activities such as mining and smelting. There are 15 operational mines and 7 prospecting mines, and 3 operational smelters in the area.
Furthermore there are agricultural and forestry activities, brick manufacturing factories and transportation that also add to the economic activities in the area. These activities result in the release of particulate matter (PM) into the atmosphere.

PM is composed of various chemical components (Seinfeld, 1989). This complex mixtures includes both organic and inorganic particles with varying size, composition and origin. Information about the size, morphology and composition of PM10 in the atmosphere can provide clues about its sources (Xie *et al*., 2009).

The topography of the GTM (Figure 1.1) is mountainous with ridges and broad, flat-bottomed valleys. The ridges and the mountains form linear dividers between the settlements. The flat-bottomed valleys are mainly used for settlements and agricultural farming. The topography and land use play a critical role in influencing the development of mesoscale systems such as heat islands, mountain winds and anabatic/katabatic winds (Stull, 1991), which in turn influence the dispersion of air pollutants.

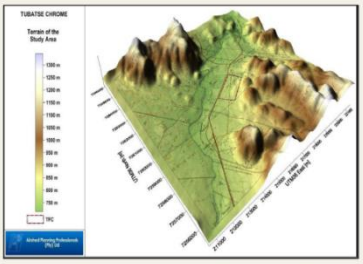

Figure 1.1: The topography of GTM (Airshed, 2012)

Computer Controlled Scanning Electron Microscopy (CCSEM) system comprising the SEM, and X-ray analyzer can determine particle size, shape, and elemental composition of particles from a few hundred particles per hour (Mamane *et al*., 2010). Statistical methods can be used to sort particles into distinct particle classes based on chemical characteristics to aid in source apportionment (Xie *et al*., 2009).

Methods

The UNC passive samplers (Fig 1.2) were deployed at 6 sites selected using the sequential sampling techniques (Goovaerts, 1997).
The samplers were deployed for a period of ±30 days from July 2015 to September 2015.
Computer Controlled Scanning Electron Microscopy (CCSEM) was used to determine PM10 and elemental composition. The instrument was set up such that within each field only particles less than 10 µm were analyzed.

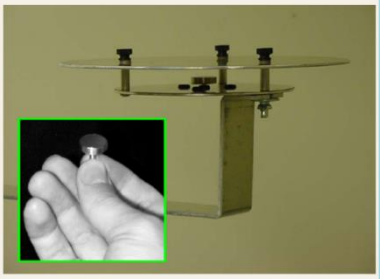

Figure 1.2: UNC passive sampler

Results

Figure 1.3 below show results for PM10 that were determined using CCSEM based on projected area diameter. While Figure 1.4 shows particle classes for elemental particles

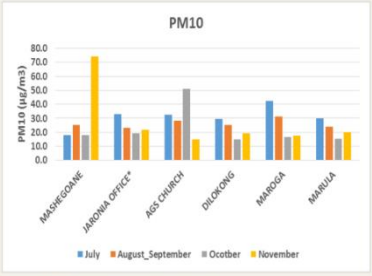

Figure 1.3: PM10 concentrations.

Particles within nested subsets were independently sorted into chemically distinct particle classes using a sorting algorithm provided with ZepSum. Abundance of each particle class were then compared across the subsets to determine the convergence of particle classification results as a function of number of particles (Fig. 1.4). Seven particle groups were created in this way for the samples from low energy analysis.

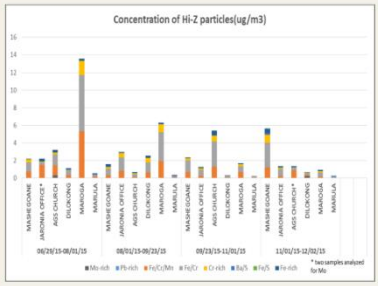

Figure 1.4: Particle classes. The height of digital color histogram represents the number fraction of particles containing an element. Color represents relative area.

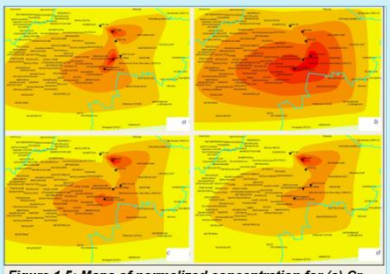

Figure 1.5: Maps of normalized concentration for (a) Cr-rich; (b) Fe-rich; © Fe/Cr-rich and (d) Fe/Mn/Cr-rich particles.

Discussion

CCSEM was applied to the analysis of 24 particulate matter samples from the GTM. The analysis indicated that were monthly variation of PM10 levels at each site and across all sites.
Four distinct particle classes of particles were identified by applying the sorting algorithm built in ZepSum: Fe/Cr/Mn particles; Fe/Cr particles; Cr-rich particles.
The normalized concentration maps (Fig 1.5) allows visualization of spatial heterogeneity with dark (red) regions indicating concentrations greater than the mean and lighter regions indicating those less than the mean. Figure 1.5a (Cr-rich) indicates higher concentrations on sites closer to ASA and Samancor smelters, Figure 1.5b (Fe-rich) indicates higher concentrations closer to Samancor and Glencore smelters, Figure 1.5c (Fe/Cr-rich) indicates higher concentrations closer to ASA smelter and Figure 1.5d (Fe/Mn/Cr-rich) indicating highest concentrations closer to ASA smelter.

Conclusion

CCSEM analysis is an excellent method for characterizing airborne particulate matter. The information derived form CCSEM is semi-quantitative but can serve as the basis for classification of particles into homogenous particle classes to assist in identifying the major particle sources. The variety of particle types reveals the complexity of particulate pollution and reflects the multiple contributions of different sources in the area. Industrial sources are the main sources of particles in the GTM area. This conclusion is consistent with the fact that the area is highly industrialized and is situated in a valley which makes it difficult for pollutants to disperse easily.

Implications

- Passive sampling can help identify local heavy metal sources.
- An inexpensive network of passive samplers provides information typically unavailable with conventional PM10 instruments.

Limitations

- Concentrations are not available in real-time.
- Currently only 1 commercial lab (RJ Lee Group) provides CCSEM analysis of passive samplers

Recommendations

- Perform Adaptive Resonance Theory (ART 2A) on CCSEM semi-quantitative data to obtain quantitative variables.
- Apply various approaches such Positive Matrix Factorization (PMF), trajectory cluster analysis and Potential Source Contribution Function (PSCF) to identify possible source contributions in addition to CCSEM
- Compare PM10 levels measured using UNC passive samplers to PM10 from continuous monitors in the area.

References

- Goovaerts, P., 1997. Kriging vs stochastic simulation for risk analysis in soilcontamination. In: Soares, A., Gomez-Hernandez, J., Froidevaux, R. (Eds.), geo-ENV I- Geostatistics for Environmental Applications. Kluwer Academic Publishers, Dordrecht, pp. 247e258.
- Mamane Y, Willis R, & Conner T. 2001, Evaluation of CCSEM applied to an Ambient Urban Aerosol Sample, *Aerosol Sci. Technol.* 34:97-107.
- Seinfeld, John H., and Spyros N. Pandis. 1989. Atmospheric Chemistry and Physics: From Air Pollution to Climate Change. John Wiley & Sons.
- Xie R.K, Seip H.M, Liu L, & Zhang D.S. 2009, Characterization of individual airborne particles in Taiyua City, China. *Air Qual Atmos. Heal.* 2: 123 131.

Appendix 2: Ethics Approval.

UNIVERSITEIT VAN PRETORIA
UNIVERSITY OF PRETORIA
YUNIBESITHI YA PRETORIA

Faculty of Natural and Agricultural Sciences
Ethics Committee

E-mail: ethics.nas@up.ac.za

05 March 2019

ETHICS SUBMISSION: LETTER OF APPROVAL

Mr CE Tshehla
Department of Geography Geoinformatics and Meteorology
Faculty of Natural and Agricultural Science
University of Pretoria

Reference number: 180000149
Project title: DETERMINATION OF HEAVY METAL COMPOSITION OF PARTICULATE MATTER IN A TYPICAL CHROME AND PLATINUM MINE AREA IN THE LIMPOPO PROVINCE, SOUTH AFRICA

Dear Mr CE Tshehla,

We are pleased to inform you that your submission conforms to the requirements of the Faculty of Natural and Agricultural Sciences Ethics committee.

Note that you are required to submit annual progress reports (no later than two months after the anniversary of this approval) until the project is completed. Completion will be when the data has been analysed and documented in a postgraduate student's thesis or dissertation, or in a paper or a report for publication. The progress report document is accessible on the NAS faculty's website: Research/Ethics Committee.

If you wish to submit an amendment to the application, you can also obtain the amendment form on the NAS faculty's website: Research/Ethics Committee.

The digital archiving of data is a requirement of the University of Pretoria. The data should be accessible in the event of an enquiry or further analysis of the data.

Yours sincerely,

Chairperson: NAS Ethics Committee

Appendix 3: Department of Environmental Affair data Permission.

Department:
Environmental Affairs
REPUBLIC OF SOUTH AFRICA

Enquiries: Mr. T. Setshedi, _____@_____
Environment House· 473 Steve Biko Street· Arcadia · PRETORIA
Tel (+ 27 12) 399 9197 · Fax (+ 2712) 359 3619

To whom it may concern

It is herewith confirmed that Cheledi Tshehla, student number 21309592, registered for PhD Air Quality Management at the University of Pretoria, for the project: **Determination of heavy metal composition in particulate matter in a typical chrome and platinum mine area in the Limpopo Province, South Africa** under the supervision of Dr Caradee Wright, has requested emissions data from the Department of Environmental Affairs. The data requested will be used in a research article with preliminary title: "**Evaluation of the impacts of point source emissions using TAPM model in an industrialized rural area in Limpopo, South Africa**".

The data requested was 2016 annual emissions from point source in the Greater Tubatse Municipality, Limpopo, South Africa.

The agreement between the student and DEA stipulates amongst other as follows:

- DEA will be provided with a copy of the results in printed or electronic format.
- The data received shall not be provided to any the third party.

Yours Sincerely

Mr. Thabo Setshedi
Directorate: Atmospheric Quality Information
Branch: Climate Change and Air Quality
Department of Environmental Affairs
Tel: +27 (0) 12 399 9197
Email: TSetshedi@environment.gov.za

Appendix 4: Conference programme and paper

CONFERENCE PROGRAMME

27th International Conference on
Modelling, Monitoring and
Management of Air Pollution

Air Pollution 2019

NOTES TO CHAIRMEN AND PRESENTERS

Chairmen must be in their respective rooms 10 minutes before the start of their session to meet with the presenting authors.

Authors must meet with the Chairman of their session 10 minutes before the start of the session.

Authors must keep strictly to the time allocated for their presentation to ensure the smooth running of the programme.

This programme is subject to last-minute alterations, please refer to the conference noticeboard for the most up-to-date information.

26 – 28 June 2019

Aveiro, Portugal

Organised by:

Wessex Institute, UK
University of Aveiro, Portugal
University of The West of England, UK

Supported by:

WIT Transactions on Ecology and the Environment
International Journal of Environmental Impacts

CONFERENCE COMMITTEE

Air Pollution 2019
26 – 28 June 2019, Aveiro, Portugal

Conference Chairmen:

C. Borrego
University of Aveiro, Portugal

J. Longhurst
University of The West of England, UK

S. Syngellakis
Member of WIT Board of Directors

M. Lopes
University of Aveiro, Portugal

J. Barnes
University of The West of England, UK

International Scientific Advisory Committee:

D. Almorza
University of Cadiz, Spain

S. Nagendra
Indian Institute of Technology Madras, India

I. Felzenszwalb
State University of Rio de Janeiro, Brazil

N. Ngcukana
South African Weather Service, South Africa

J. Ferreira
University of Aveiro, Portugal

R. Parra
University San Francisco of Quito, Ecuador

J. Souto Gonzalez
University of Santiago of Compostela, Spain

E. C. Rada
Insubria University, Italy

R. Ippolito
University of Rome "La Sapienza", Italy

A. Riccio
University of Naples Parthenope, Italy

K. Lach
Institute of Public Health, Czech Republic

M. Schiavon
University of Trento, Italy

E. Magaril
Ural Federal University, Russia

C. Trozzi
Techne Consulting srl, Italy

A. I. Miranda
University of Aveiro, Portugal

Q. Wang
Saitama University, Japan

B. Williams
University of the West of England, UK

CONFERENCE PROGRAMME

Air Pollution 2019

26 – 28 June 2019, Aveiro, Portugal

Wednesday, 26th June 2019

08.30 Registration
09.00 Opening Addresses by Chairmen

Session 1 : Air quality **Session Chairman: S. Syngellakis**

09.30 **Keynote Address by J. Longhurst**
The UK clean air strategy 2019 – Is this a new start for the management of air quality?

10.00 **Invited:**
Using game technology to engage citizens and understand the public acceptability of air quality interventions in European cities
E. Hayes, A. King, A. Callum, K. Vaherle, J. Barnes, C. Boushel, L. Fogg-Rogers & J. Longhurst

10.30 Air quality index as a tool for environmental degradation campaign
M. S. Awopetu & J. O. Aribisala

10:50 Air quality community action network
M. R. Ogletree & G W. Thomas

REFRESHMENT BREAK

Session 2 **Session Chairman: J. Longhurst**

11:30 **Keynote Address by J. Barnes**
Evidence from ClairCity: citizen demand for a clean air, low carbon, healthy city

12:00 Air pollution, citizen data collectives and communication agenda setting in Colombia
J. Valencia & O. Fonseca

12.20 An IOT platform for indoor air quality monitoring using the "Web of Things"
D. Ibaseta, J. Molleda, F. Di´ez & J. C. Granda

12:50 Indoor air NO2 depollution by photocatalysis - comparing reactor and experimental chamber results
J. Topalov, J. Hot, E. Ringot & A. Bertron

13:00 Climatic classifications and their applicability to building
J. J. de la Torre Bayo, C. Díaz López, M. L. Rodríguez González, E. Martínez Ibarra & M. Zamorano Toro

LUNCH

Wednesday, 26th June 2019

JOINT SESSION WITH URBAN TRANSPORT 2019 - Transport and air quality in Portugal

Session Chairs: M. Coelho, J. Ferreira & A. Monteiro

14:00 **Invited:**
Assessing road transportation impacts of connected and automated vehicles for a clean and sustainable mobility
P. Fernandes, R. Tomas & M.C. Coelho

14.30 **Invited:**
Shipping emissions and its impact on air quality on urban coastal areas: present and future scenarios
A. Monteiro, M. Russo, C. Gama & C. Borrego

15:00 **Invited:**
Assessment of local air quality for different penetration levels of connected autonomous vehicles
L.P. Correia, S. Rafael, D. Lopes, J. Bandeira, M. Coelho, M. Andrade, C. Borrego & A.I. Miranda

15:30 **Invited:**
Using air quality modelling and emission projections as a support to the 1st air pollution control program under NEC directive targets for 2030
J. Ferreira, D. Lopes, S. Coelho, A. Monteiro, M. Lopes & A.I. Miranda

16:00 Urban mobility strategies to improve local air quality – Lisbon case study
D. Lopes, J. Ferreira, S. Rafael, P. Baptista, M. Faria, M. Almeida-Silva & S. M. Almeida

16:20 Characterization of traffic-related particulate matter at urban scale
D. Dias, N. Pina & O. Tchepel

REFRESHMENT BREAK

Session 4 continues in ROOM A **Session Chairman: R. Parra**

17:00 Applying hybrid feature selection methods for statistical modelling of roadside particle concentrations (PM2.5 and PNC)
A. Suleiman, M. R. Tight & A. D. Quinn

17.20 Assessment of primary air pollutants in a tropical metropolitan region by combining local and global emissions inventories
Y. K. L. Kitagawa, E. G. Sperandio Nascimento, L. L. N. Guarieiro, T. Toledo de Almeida Albuquerque & D. Martins Moreira

17.40 Comparison of two PM2.5 forecasting models in Osorno, Chile
P. Perez & B. Nuñez

18:00 Sensor based monitoring techniques - their potential for use in local air quality management
H. Jaakkola, M. Laakso, T. Pekkanen, J. Suikkola

18.20 Factors affecting mercury loading in urban atmosphere
D. Prete, M. David & J. Lu

END OF DAY 1
CONFERENCE DINNER*—Please check the notice board or ask Conference Coordinator for more information*

Thursday, 27th June 2019

Session 5: Air pollution modelling **Session Chairman: K. Lach**

09.00 **Invited:**
Influence of spatial resolution in modelling the dispersion of volcanic ash in Ecuador
R. Parra

09.30 **Invited:**
Real time atmospheric monitoring for urban air pollution by using unmanned aerial vehicles (UAVs)
Q. Wang

10:00 PM10 forecasting through applying convolution neural network techniques
P. A. Kowalski, K. Sapala & W. Warchalowski

10:20 Short and long-term forecasting of ambient air pollution levels using wavelet-based non-linear autoregressive artificial neural networks with exogenous inputs
S. M. Cabaneros, J. K. Calautit & B. Hughes

10:40 Macao air quality forecast using statistical methods
M. T. Lei, J. Monjardino, L. Mendes & F. Ferreira

11:00 Chemical characteristics of water soluble ions and metal elements in ambient particles of Saitama, Japan, during the Spring Asian dust event, 2017
W. Wang & Q. Wang

REFRESHMENT BREAK

Session 6: Special Session: E. C. Rada —Strategies for human exposure reduction

11:40 **Invited:**
CO2 measurements for an unconventional managemenet of indoor air quality
M. Ragazzi, R. Albatici, M. Schiavon, N. Ferronato & V. Torretta

12:10 An integrated methodology for the management of human exposure to air pollutants
M. Schiavon, E. C. Rada, L. Adami, F. Fox & M. Ragazzi

12:30 The influence of key parameters on the removal efficienty of air pollutants by a biotrickling filter
V. Torretta, M. Schiavon, P. Caruson & M. Ragazzi

12:50 Environmental tobacco smoke exposure and children's cardiorespiratory fitness: a pilot study
M. J. Parnell, I. Gee, L. Foweather, G. Whyte, Z. Knowles & J. Dickinson

13:10 **Invited:**
Perspectives of stack and environmental monitoring in the surrounding of a waste-to-energy plant
L. Adami, M. Schiavon, M. Ferrai, L. Dallago, E. C. Rada, M. Tubino & M. Ragazzi

LUNCH

Thursday, 27th June 2019

Session 7: Air Pollution Modelling **Session Chairman: E. Magaril**

14.00 **Invited:**
The emission of ultrafine particles in the manufacture of fireplace ceramic tiles
K. Lach & I. Smolova

14:30 Characterization of odorous emissions from a civil wastewater treatment plant in Italy
M. Ravina, D. Panepinto, J. M. Estrada, L. De Giorgio, P. Salizzoni, M. C. Zanetti & L. Meucci

14:50 Nanotechnology based control of hazardous air pollutants emission– pilot scale trials for simultaneous capture of H2S, NH3, and odours from livestock facilities
G. Valdes Labrada, S. Kumar, B. Predicala & M. Nemati

15:10 Estimating concentrations of suspended particulate matter over the metropolitan area of Mexico City using satellite and geospatial imagery: preliminary results
R. T. Sepulveda Hirose, A. B. Carrera A., M. G. Martinez R, P. de J. Ángeles S & C. Herrera V.

15:30 Estimation of fuel loss and spatial-temporal dispersion of vehicular pollutants at a signalised intersection in Delhi city
R. Dhyani, N. Sharma & M. Advani

15:50 Integrated environmental health risk assessment framework for firewood induced indoor air pollution at Senwabarwana Villages, RSA
K. Semenya & F. Machete

REFRESHMENT BREAK

Session 8 **Session Chairman: J. Barnes**

16:30 **Invited:**
The prospects for the use of alternative fuels and energy by motor transport in Russia
A. Gobuleva & E. Magaril

17:00 VOC and particle concentrations in new and old model automobiles
J. E. Dotherow, D. Martin & A. Adhikari

17:20 Investigating ozone ambient levels: the case study of Fahaheel urban area, state of Kuwait
M. Al-Qassimi & S. M. Al-Salem

17:40 Long–term trends of tropospheric ozone in the Czech Republic 1992-2018
M. Vana & J. Pekarek

18:00 Hourly tropospheric ozone concentration forecasting using deep learning
L. V. Boas Alves, E. G. Sperandio Nascimento & D. Martins Moreira

18:20 Health and economic impacts of ozone ship-related air pollution in Portugal
R. A. O. Nunes, M. C. M. Alvim-Ferraz, F. G. Martins, J. P. Jalkanen, H. Hannuniemi & S. I. V. Sousa

18:40 Assessment of source contributions to the urban air quality for Bristol ClairCIty pilot case
K. Oliveira, V. Rodrigues, S. Coelho, A. P. Fernandes, S. Rafael, C. Faria, J. Ferreira, C. Borrego et al

END OF DAY 2

Friday, 28th June 2019

Session 9: Special Session: R. Ippolito—Naturally occurring ionizing pollutants

09.00 **Invited**
Radon entry models into buildings vs environmental parameters, building shape and types of foundations
R. Ippolito & R. Remetti

09.30 Indoor radon survey in university buildings: a case study at Sapienza - University of Rome
C. Di Carlo, R. Remetti, F. Leonardi, R. Trevisi, L. Lepore & R Ippolito

09:50 An inexpensive and continuous radon progeny detector to indoor air-quality monitoring
C. Di Carlo, L. Lepore, L. Gugliermetti & R. Remetti

10:10 Children's exposure to indoor air in schools – impact on wheezing
J.P. Sa, P.T.B.S. Branco, M.C.M. Alvim-Ferraz, F.G. Martins & S.I.V. Sousa

10:30 Unpaved road influence areas in hydrocarbons exploration projects
M. A. De Luque Villa & A. Valencia Cruz

REFRESHMENT BREAK

Session 10 **Session Chairman: S. Syngellakis**

11:10 Real life emission factor assessment for bimass heating appliances at a field measurement campaign in Styria, Austria - results of the Clean Air biomass project
R. Sturmlechner, C. Schmidl, E. Carlon, G. Reichert, H. Stressler, F. Klauser, J. Kelz, M. Schwabl, B. Kirchsteiger, A. Kasper-Giebl, E. Hoftberger & W. Haslinger

11:30 Atmospheric dispersion patterns of radionuclides originating from nuclear power plant accidents under various release types
E. Bilgic & O. Gunduz

11:50 Source profiling and source apportionment of PM using PMF model and evaluation of the impacts of point source emissions using TAPM model in an industrialized rural area in Limpopo, South Africa
C. Tshehla, G. Djolov & C. Y. Wright

12:10 SO_2 and NO_2 simulation and validation in metropolitan Lima using WRF-Chem model
A. Luna Adan, H. Navarro Barboza & A. Moya Alvarez

12:30 Bioaerosol property and viability affected by various environmental factors
Y. L. Pan, A. Kalume, S. Kinahan, M. Tezak & J. Santarpia

CLOSURE OF AIR POLLUTION 2019 BY CHAIRMEN

We hope you have enjoyed the conference and look forward to seeing you at the next meeting in the series, have a safe and pleasant journey home.

SOURCE PROFILING AND SOURCE APPORTIONMENT OF PM USING PMF IN AN INDUSTRIALIZED RURAL AREA IN LIMPOPO, SOUTH AFRICA

CHELEDI TSHEHLA[1,2], CARADEE WRIGHT[3]
[1]Department of Geography, Geoinformatics and Meteorology, University of Pretoria, Pretoria, South Africa
[2]Department Air Quality Services, South African Weather Service, Pretoria, South Africa
[3]Evironment and Health Research Unit, South African Medical Research Council, Pretoria, South Africa

ABSTRACT

The Greater Tubatse Municipality in Limpopo is home to three ferrochrome smelters and chromium, platinum and silica mining operations. Source apportionment in this study was performed by combining air mass back trajectories and receptor modelling. The PM samples were collected using Passive Samplers. The samples were collected for a period of 4-5 weeks, except for August-September and September-October 2015 were the samples were collected for up to 6 weeks. Elementary analysis was performed using Computer Controlled Scanning Electron Microscopy coupled with Energy-Dispersive X-ray Spectroscopy (CCSEM-EDS). This paper will focus on the results of Site 3. The chemical analysis resulted in elements such as carbon (C), calcium (Ca), chromium (Cr), iron (Fe), aluminium (Al), silicon (Si), magnesium (Mg) and lead (Pb). The PM_{10} concentrations exceeded the WHO annual guidelines of 20µg/m3. The annual chromium concentrations exceeded the 0.0001 µg/m3 and 0.11µg/m3 for Cr(IV) and Cr(III) respectively. Back trajectory clusters computed by HYSPLIT model identified 5 transport pathwayse. The main transport patterns were northerly to north-easterly, easterly to south-easterly, and south-westerly to north-westerly clusters. The US EPA PMF model version 5.0 used in source profiling and source apportionment identified agriculture/wood combustion, coal combustion, crustal/road dust, ferrochrome smelters, and vehicle emissions as the main sources. The transport pathways indicate that the pollution can either be from local or regional

Keywords: Particulate matter; source apportionment; back trajectories.

1 INTRODUCTION

South Africa is one of the developing countries in the world, and as such the country has considered economic growth, social and educational development and industrialization as key development priorities. In the Greater Tubatse Municipality (GTM) in Limpopo Province, South Africa, mining is viewed as one of the important economic activities which has the potential of contributing to the development of the area's economy [1]. Though the contribution of mining activities to economic development of GTM is well acknowledged, this might be achieved at a significant environmental, health and social costs to the region due to urbanization, high traffic volumes and higher industrial and domestic waste production. Environmental pollution due to heavy metals from mining activities, vehicular emissions, agricultural and biomass burning are a major concern in many parts of the world [2]. Extensive mining of chromite, platinum and silica in the GTM mining belt may pose a serious threat to the environment. Mining of these ores may release toxic metals such as hexavalent chromium and platinum group metals which are carcinogenic and mutagenic to human health [3]. Studies worldwide have found that ambient levels of PM_{10} are associated with adverse health effects including increase in premature deaths, hospital admissions and emergency attendances for respiratory and cardiovascular disease and exacerbation of asthma [4]. $PM_{2.5}$ which is smaller in aerodynamic diameter than PM_{10}, can penetrate deeper into the lungs and reach the blood system and it can also impact on visibility and climate change [5].

The potential of adverse health effects of particulate pollution has triggered extensive research on PM chemical composition and source apportionment in many countries over the past decade [6]. Understanding the chemical components of PM is crucial to adequately assess the impacts of these chemicals on the receiving environment. A number of ferrochrome smelters are found in the GTM. Ferrochrome is a major chromium source used as raw material for the production of stainless steel and ferro-metal alloys. The morphology of the chromite spinel ore can be described stoichiometrically as $(Fe, Mg)(Cr, Al, Fe)_2O_4$ and they often contain gangue compounds of SiO_2 and MgO. Submerged-arc furnaces are commonly used to smelt chromite ores by using carbonaceous reductants such as coke, bituminous coal and char. The ferrochrome slag created during the smelting process mainly consists of SiO_2, Al_2O_3 and MgO in different proportions but also smaller amounts of CaO, chromium and iron oxides [7]. These elements may find their way into the atmosphere during the smelting operations and they can cause serious harm to human health.

In South Africa, the National Environmental Management: Air Quality Act [8] was promulgated in 2005 as an approach to manage air quality in the country. The Act requires national, provincial and local authorities to identify substances or mixtures of substances in ambient air which may reasonably be anticipated to endanger public health, and to establish air quality standards to limit emission of such substances. However, to date no ambient metal standards (with the exception of Pb) have been promulgated to define the level of air quality that is necessary to protect the public welfare from known or anticipated adverse effects of these pollutants on the receiving environment in South Africa. There is also little information on PM source apportionment studies to assist in developing effective policies to mitigate the impacts of PM in South Africa.

Numerous methods have been developed over the years to collect and analyse air pollutant samples, using both active and passive techniques. Easy to use passive samplers are available in the market and are less expensive than conventional samplers. Therefore, a large number of passive samplers can be deployed at a given time to capture representative spatial measurements in an airshed [9].

There are two types of models (source-oriented models and receptor models) used to identify sources of pollution in the environment [10]. Source-oriented (dispersion) models require knowledge of all emissions from the contributing sources [11]. Receptor modes are statistical analysis tools used to identify contributions from different sources using multivariate measurements from different receptor locations. These models use ambient data and the chemical components in source emissions to quantify contributions, unlike the source models that use emissions and meteorological parameters to estimate concentrations at the receiving environment [12]. Positive Matrix Factorization (PMF) is one of the recent models developed by the United State (U.S) Environmental Protection Agency (EPA). PMF has been used widely in source apportionment of ambient PM because of its ability to account for the uncertainty variables that are often associated with sample measurements and also the output values in the solution profiles and contributions are nonnegative [13]. The key output of PMF is the percentage contributions of different sources to ambient pollutant concentration at specific receptors [11]. The PMF model has been used by many researchers across the world for source identification and profiling. A study by [14] characterized Ca, Al, Mg, Si, K, Fe, Mn and Zn as elements emitted from metal smelters. Soil was found to contain elements such as Fe, Al, K, Ca, Ti in a study by [15], while road dust contributed to Fe, Al, K, Ca, Si, Mg, P, S, Na and BC [16]. However, these profiles can vary from one area to the other due to varying soil types. A source profiling study by [17] and [18] identified motor vehicle

emissions as the source of Mg, Al, Fe, Si, S and BC (black carbon). Biomass burning emissions are a mixture of both organic carbon and elemental carbon and their ratio depends on the type of fuel used [19].

The quantitative assessment of sources contributing to the ambient PM on the receiving environment is required to develop sound and effective control strategies to address the scourge of PM pollution in South Africa. However, the bottom-up approach based on emission inventories is hindered by poor availability of the emissions data particularly from industries. The objective of this study is to identify sources of PM in a mountainous terrain in Limpopo, South Africa and estimate their contributions through receptor modelling (PMF) application. The sampling data obtained during the sampling campaign from July 2015 to June 2016 will be used.

2 METHODS

Ambient PM sampling was undertaken in a rural area of the Greater Tubatse Municipality (GTM) in Limpopo Province, South Africa (Fig. 1). The main towns in the area are Steelpoort and Burgersfort which are sustained through economic activities such as mining and smelting of chromium ores. Furthermore there are agricultural and forestry activities and transportation that also add to the economic activities in the area.

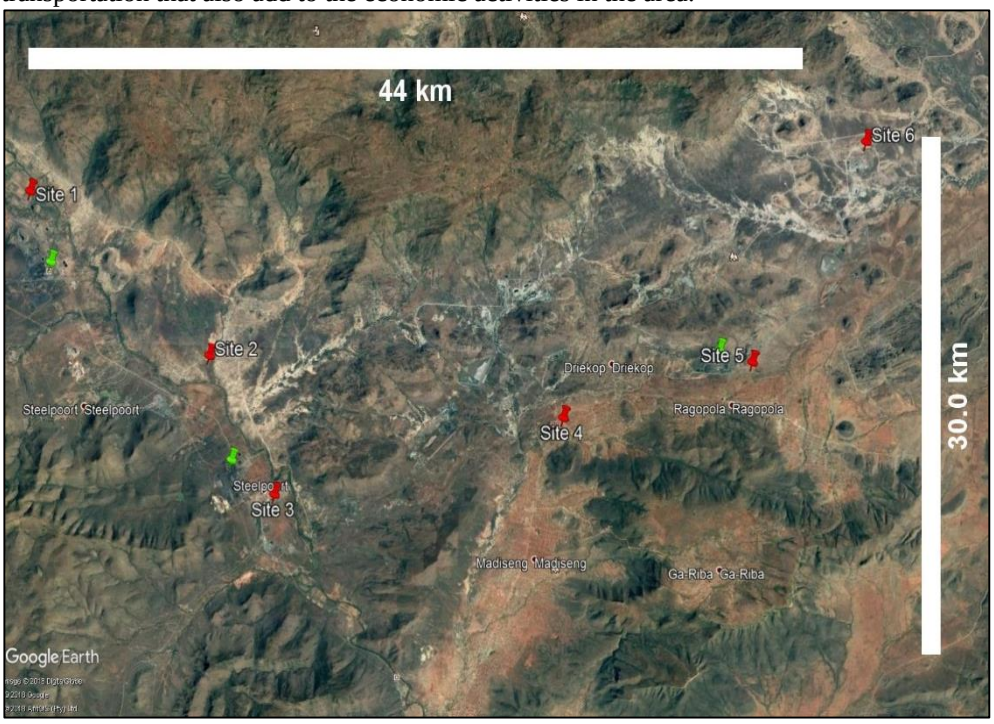

Figure 1: Map of the study area showing passive sampler locations (red place-marks on Google map), with smelters shown as green place-marks.

Most of the households in the area are dependent on wood burning for space heating and cooking [20]. The GTM has a complex terrain with high mountains and steep inclinations. The elevation of the surface area is approximately 740 m above sea level with the surrounding

mountains extending to a height of approximately 1200-1900 m above sea level. The area is located in the subtropical climate zone where the maximum average temperature reaches 35 °C with minimum average temperature of 18 °C in summer. In winter the maximum average temperature reaches 22 °C with average minimum of 4 °C (Schulze, 1986). The annual rainfall for the area ranges between 500 and 600mm [21].

2.1 Sampling and sample analysis

The University of North Carolina (UNC) passive samplers designed by [22] and housed in a protective shelter designed by [23] were deployed at six sites for PM sampling. [24], designed the shelter to shield the passive sampler from precipitation and to minimize the influence of wind speed on particle deposition [25]. The samplers consist of a scanning electron microscopy (SEM) stub, a collection substrate, and a protective mesh cap [11]. The samplers were deployed for sequential periods of approximately 30 days from July 2015 to June 2016, except for the month of August and September when they were deployed for a period of approximately 40 days. The longer sampling periods of 3-4 weeks were selected to ensure that there was sufficient particle loading on the samplers as suggested by [23].

The $PM_{2.5}$, PM_{10} concentrations and the elemental composition of individual particles deposited on the passive sampler were determined by CCSEM-EDS (Tescan Vega 3 model). Before sample analysis with Personal Scanning Electron Microscopy (PSEM) (method by [26]), the samples were coated with a thin layer of graphitic carbon under vacuum to bleed off the charges induced by the electron beam in the SEM. The PSEM was operated with a 20-kV beam [23]. [9], gave a brief description of the CCSEM analysis. The elements obtained from the analysis were Carbon (C), Chromium (Cr), Calcium (Ca), Iron (Fe), Silicon (Si), Aluminium (Al), Magnesium (Mg), Lead (Pb), and other miscellaneous elements. Pb and miscellaneous elements were not included in further analysis due to their insignificant weight. The concentrations of $PM_{2.5}$, PM_{10} and each particle was determined using the method outlined in Ott and Peters (2008). Data obtained from CCSEM is semi-quantitative, and therefore, in order to use the data in PMF for source contributions the particles needs to be classified into homogenous groups by applying cluster analysis [27].

2.1.1 Cluster analysis

[28], described cluster analysis in detail. In this study, hierarchical cluster analysis was performed on single particle data from CCSEM using the open source clustering software (Cluster 3) developed by the Institute of Medical Science (IDS) at the University of Tokyo. Once the analyses were completed, all the cluster groups with less than 4 (excluding Pb and miscellaneous elements) particles were chosen as potential homogenous classes. This is because as the number of classes created for each source sample increases, the number of particles assigned to each class decreases (Kim and Hopke, 1988). The particle classes obtained from cluster analysis include Carbon-rich (C-rich), Chromium-rich (Cr-rich), Iron-rich (Fe-rich), Iron/Chromium-rich (FeCr-rich), Silicon (Si-rich), Silicon/Aluminium/Iron-rich (SiAlFe-rich), Calcium-rich (Ca-rich), Silicon/Magnesium-rich (SiMg-rich) and Silicon/ Aluminium-rich (SiAl-rich).

2.1.2 Positive Matrix Factorization

PMF 5.0 was used to apportion the contribution from emission sources [29]. The guidelines specified in the user manual were closely followed in this study. Two input files are required by the model: the sample species concentration values and the sample species uncertainty values or parameters for calculating uncertainty. In this study, the sample species uncertainties were obtained during CCSEM analysis of samples.

The receptor modelling in principle relies on the observed concentrations of chemical species in the atmosphere and these species must be conserved during transport between the source and the receptor. The conserved mass is then used during the analysis in the identification and apportionment of these species [8]. The PMF model identifies the sources by applying the following mass balance equation:

$$X_{ij} = \sum_{k=1}^{p} g_{ik} f_{kj} + e_{ij} \quad (1)$$

where x_{ij} is the concentration of the j^{th} species in the i^{th} sample, g_{ik} the contribution of k^{th} source to the i^{th} sample, f_{kj} the concentration of the j^{th} species in the k^{th} source, and e_{ij} is the difference between the measured and fitted value. If the number and sources in the area being modelled are known, (f_{kj}), then the mass contribution of each source to each sample, g_{ik}, in equation (1) is known [30]. However, the objective is to calculate values of g_{ik}, f_{kj}, and p that can reproduce *x*. An adjustment is then made to g_{ik} and f_{kj} until the minimum value of *Q* for a given *p* is found. *Q* is defined as: Where σ_{ij} is the uncertainty of the j^{th} species concentration in sample I, *n* is the number of samples, and *m* is the number

$$Q = \sum_{i=1}^{n} \sum_{j=1}^{m} \left(\frac{e_{ij}}{\sigma_{ij}}\right)^2 \quad (2)$$

of species [15]. In most cases, a given chemical constituent will have multiple sources and the program performs correlation analysis to generate chemical profiles of 'factors' characteristic of the sources. Past knowledge of source chemical profiles is then used to assign factors to sources [11]. However, in South Africa there are few source chemical profiles available. Therefore, the international source chemical profiles [31] were used as a guide.

2.1.2 HYSPLIT model

Backward air trajectories arriving at the six sampling sites were calculated using the Windows PC version of the Hybrid Single Particle Integrated Trajectory (HYSPLIT-4) model. This model is a system for computing air mass trajectories and complex dispersion and deposition simulations [32]. Meteorological data fields to run the model are available from routine archives. In this study, 24-hour back trajectories were calculated at a height 500 meters above ground level (Table 2) using reanalysis data from National Centre for Environmental Prediction (NCEP) and National Centre for Atmospheric Research (NCAR) available from the National Oceanic and Atmospheric Administration's (NOAA) Air Resources Laboratory (ARL) archives. The reanalysis data covers the globe from 1948 to the present with a horizontal resolution of about 2.5 x 2.5 degrees latitude-longitude and with an output every 6- hours.

Table 1: Model parameters used for HYSPLIT runs.

Meteorological dataset	NCEP/NCAR Reanalysis, 2.5 degree latitude-longitude
Trajectory direction	Backward
Trajectory duration	24Hr
Site 3	(-24.726582, 30.205004)
Start time	00:00 UTC
Start height	500m AGL

2.1.3 HYSPLIT model

In this study trajectory cluster analysis was performed using the HYSPLIT_4 model. The model uses Ward's method described by [33]. The HYSPLIT clustering method is described in detail by [34]. Five clusters were chosen for each set of trajectory end point files because this number was sufficient to identify all major flow patterns, as well as several less common but nonetheless important patterns. Once the number of clusters has been decided, 'Special Runs' was chosen as the technique to produce standard clusters for all trajectory end points for the period starting from July 2015 to June 2016. A practical advantage of 'Special Runs' it's its ability to accommodate large volumes of data. The variables clustered were the latitude and longitude of trajectory segment endpoints at 1-hour intervals along each 24-hour back trajectory. Individual trajectories were further averaged to produce "cluster-mean" trajectories. Thus, our large data base (annual trajectories) was reduced to a number of cluster-mean plots that can be interpreted in terms of known mesoscale and synoptic features. For each cluster, ensemble plots of all individual trajectories belonging to that cluster were produced. These ensembles or "cluster membership" plots were used to validate the mean and to assess the variability within the cluster.

2.1.3 Cluster analysis

In this study trajectory cluster analysis was performed using the HYSPLIT_4 model. The model uses Ward's method described by [35]. The HYSPLIT clustering method is described in detail by [36]. Five clusters were chosen for each set of trajectory end point files because this number was sufficient to identify all major flow patterns, as well as several less common but nonetheless important patterns. Once the number of clusters has been decided, 'Special Runs' was chosen as the technique to produce standard clusters for all trajectory end points for the period starting from July 2015 to June 2016. A practical advantage of 'Special Runs' it's its ability to accommodate large volumes of data. The variables clustered were the latitude and longitude of trajectory segment endpoints at 1-hour intervals along each 24-hour back trajectory. Individual trajectories were further averaged to produce "cluster-mean" trajectories. Thus, our large data base (annual trajectories) was reduced to a number of cluster-mean plots that can be interpreted in terms of known mesoscale and synoptic features. For each cluster, ensemble plots of all individual trajectories belonging to that cluster were produced. These ensembles or "cluster membership" plots were used to validate the mean and to assess the variability within the cluster).

3 RESULTS AND DISCUSSION

The mean annual concentrations for $PM_{2.5}$, PM_{10}, and particle classes obtained through cluster analysis are shown in Table 3. The $PM_{2.5}$ and PM_{10} annual mean concentrations were below the South Africa National Ambient Air Quality Standard (NAAQS) of 20 µg/m3 and 40 µg/m3, respectively. However, the PM_{10} concentrations at the site exceeded the WHO 20 µg/m3 annual guidelines [37]. The chromium concentrations exceeded the New Zealand annual chromium limits [38] of 0.0011µg/m3 and 0.11 µg/m3 for Cr(VI) and Cr(III), respectively. This is an indication that the area may experience negative impacts on human health due to the toxicity of Cr(VI).. The existence of SiAl-rich particles with concentrations of 11.8 µg/m3, may result in cardio metabolic effects on animals and humans [39].

Table 3: Species mean concentrations and range.

Mean concentrations											
Species	PM_{10}	$PM_{2.5}$	Ca-rich	C-rich	Cr-rich	Fe-rich	FeCr-rich	Si-rich	SiAl-rich	SiAlFe-rich	SiMg-rich
Site 3	38.11	4.8	2.7	2.6	1.4	0.6	2.8	2.6	11.8	7.0	3.9

3.1 HYSPLIT transport pathways

Fig. 3 shows transport pathways arriving at the receptor site. All the trajectory clusters pass over the mining areas and only cluster 3 and 5 passes over the smelters. Hence all these clusters can transport elemental particles to the receptor. However, it should be noted that even though some trajectories are not passing through the industrial facilities, they can also transport pollutants from a variety of sources such as transport, agriculture, domestic, crustal and oceans, and that these pollutants also contribute to the observed concentrations as shown in Table 3.

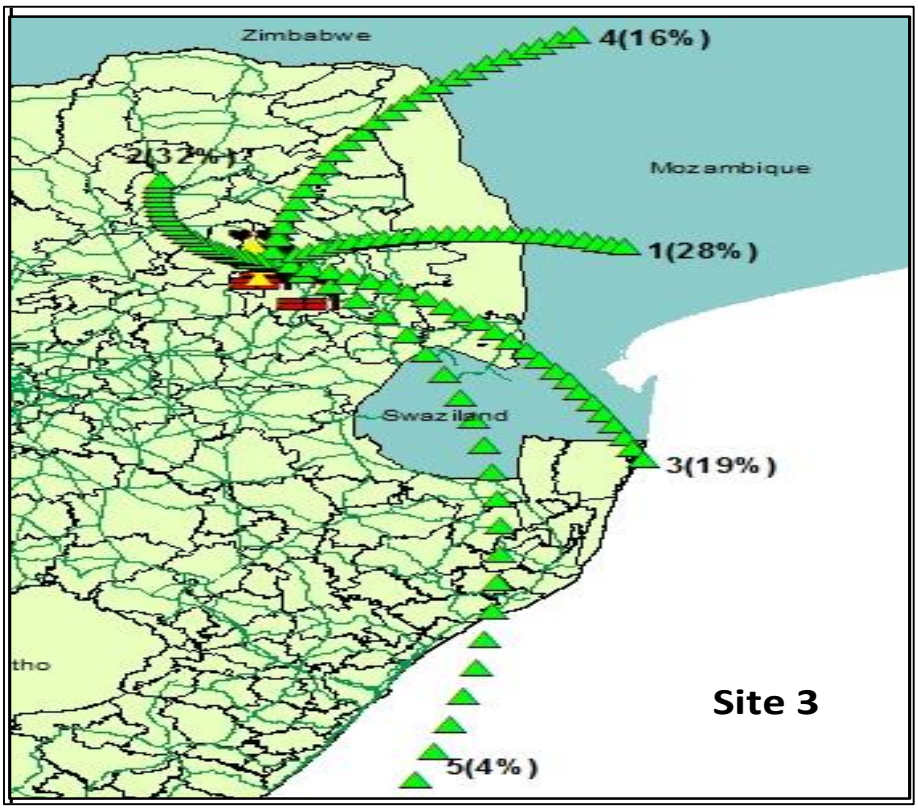

Figure 3: Five transport pathways (clusters) arriving at the six sampling sites.

3.2 PMF source profiling.

The most important step in PMF is to determine the number of factors which correspond to potential particle sources. After applying bootstrap and displacement tests on the data sets, three to five factors were deemed to be appropriate for a five source solution. The profile graph (Fig. 4) displays the mass of each species apportioned to the factor (blue bar) and the percentage of each species apportioned to the factor (red bar). The factors were identified according to the type of elements dominating in percentage in that factor. Agricultural/ wood combustion was associated with the dominance of C as a primary species and Fe elements. Ferrochrome smelter was identified by the domination of Cr and Fe elements. Crustal/ road dust factor was associated with Si, Al, Ca and Mg as the primary elemental species. Industrial coal combustion factor was identified by Ca, C, Al and Si as the dominating elements. Vehicular emission factor was associated with Fe as the primary species, C, Al, Si, and Ca. The most interesting outcome is that Cr was also associated with crustal/road dust and agricultural/ wood burning which is an indication that once this element is emitted from the source it is then deposited on to the soil and water bodies before it is absorbed by plant material and released into the atmosphere during burning.

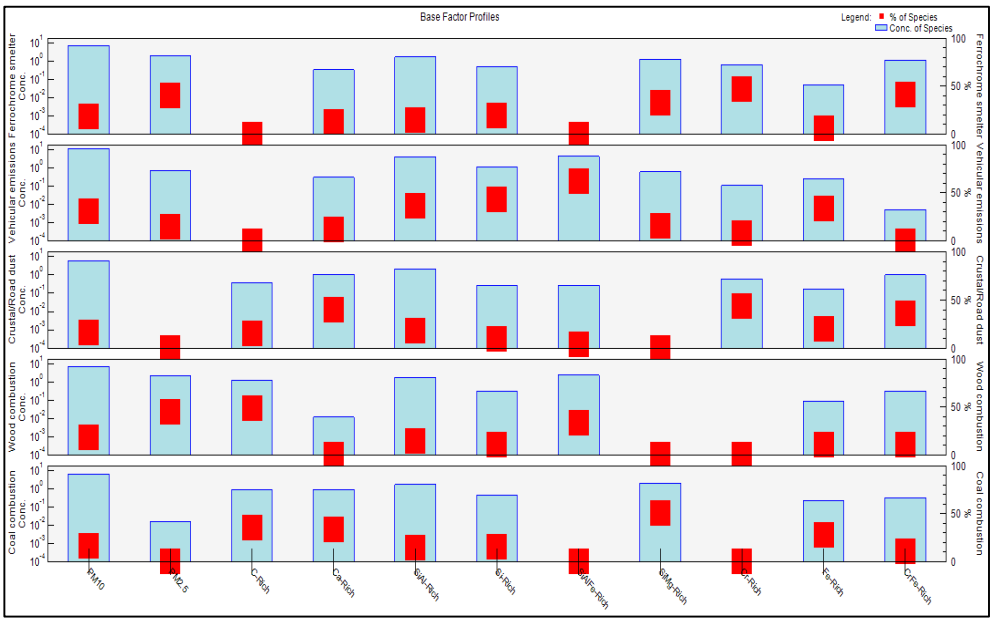

Figure 4: Factor fingerprints for species.

3.3 PM source contributions

PMF analysis determines the number of factors which correspond to potential particle sources. Source categories that potentially have contributed to ambient PM in the GTM rural area were identified as crustal/road dust, coal combustion fly ash, vehicle exhaust dust, agricultural/wood burning and industrial sources (Table 4). The average PM source contributions indicate that industrial coal combustion is the dominant polluter in the area followed by geological material (crustal/road dust). Most coal ash contain aluminium oxide (Al2O3), calcium oxide (CaO) and silicon dioxide (SiO2) (Coal Ash, 2016). And regardless of the by-product produced, there are many toxic substances that are present in coal ash (such as arsenic, chromium, lead, mercury and uranium) that can cause major health problems in humans (Lockwood and Evans, 2016). The crustal material could be mainly from re-suspended dust from mine tailing in the area or transported from regional sources as indicated by the HYSPLIT transport pathways. Motor vehicles emissions are the third largest source of pollution in the GTM and maybe associated with tail pipe, emissions, tire and brake wear, road surface abrasion, wear and tear of other vehicle components such as the clutch, and re-suspension of road surface. The Ferro-chrome smelters are the fourth largest source of pollution in the GTM with agricultural and wood burning coming last. The distribution of Cr elements across all source types indicate that ferrochrome smelters have a potential to pollute the water bodies, which can impact on the human health since some of the communities in the area depend on water from the river streams for cooking and bathing.

Both PMF results and HYSPLIT clusters can be combined to make informed decisions on the sources and origin of PM sources. Crustal/road and soil dust can be transported by trajectories from both local and regional anthropogenic sources as shown in Fig. 2. However, it should be noted with caution that the trajectories are not accurately terrain following.

Therefore, high-ending trajectories were chosen to represent more accurate boundary layer flow above the local terrain.

Table 4: PM source contributions.

		Vehicular emissions	Ferrochrome smeltering	Coal combustion	Agricultural/Wood combustion	Crustal/Road dust
Site 3	C-rich	52%		45%	3%	
	Ca-rich	6%	21%	60%		14%
	SiAl-rich	18%	14%	26%	7%	36%
	Si-rich	13%	10%	20%	15%	42%
	SiAlFe-rich	36%		2%		62%
	SiMg-rich		1%	44%	41%	14%
	Cr-rich	1%	52%	31%	7%	9%
	Fe-rich	15%	6%	39%	6%	34%
	CrFe-rich	12%	40%	36%	12%	

4 CONCLUSION

The results showed that the composition and levels of PM in GTM varied significantly among the six sites, however, systematic sampling and characterization of PM is needed in order to increase the sampling numbers and improve PMF results.

The PMF analysis identified a mixture of tracer elements as markers for source identification. However, differentiating these markers for different sources in the area has proved to be very difficult. This is because some of the chemical components that are solely industrial can find their way into other source categories such soil and road dust through deposition, and wood and agricultural plantation through absorption from the soil. The average source contributions were dominated by crustal/road dust, industrial activities such as ferrochrome smelters, and wood burning for space heating, with industrial coal burning, agricultural activities and vehicle emissions being other sources identified in the area. The contribution of this sources varied across the study area with chromium pollution being concentrated closer to the sources. These results show that the composition and levels of PM in GTM varied significantly among the six sites indicating the existence of varying microenvironments within the GTM airshed, however, systematic sampling and characterization of PM is needed in order to increase the sampling numbers and improve PMF results.

This study can serve as a base for siting of AQ monitoring stations to ensure harmonized AQ assessments throughout the GTM. It can also be used as a guiding document for strengthening intervention strategies in the industrialized areas across South Africa.

ACKNOWLEDGEMENTS

The author acknowledges the South African Weather Service for financial assistance during the sampling period. RJ Lee for chemical analysis, NOAA Air Resources Laboratory for providing the HYSPLIT model and NOAA/OAR/ESRL PSD, Boulder, Colorado, USA for the NCEP Reanalysis data. The author also acknowledges Prof. Phillip Hopke from Clarkson

University for his advice on the treatment of CCSEM results before application of PMF, and Dr. Thomas M Peters from University of Iowa for providing the formula for calculating single particle concentrations.

REFERENCES

[1] Community Empowerment Impact Assessment Report: Phase 1. 2007. https://www.nra.co.za/content/Tubatse1.pdf

[2] UNEP, 2006. African Regional Implementation Review for the 14th Session of the Commission on Sustainable Development.

[3] Zayed A.M and Terry M., 2003. Chromium in the environment: factors affecting biological remediation. Plant and Soil 249: 139–156.

[4] Pope CA III. 2000. What do epidemiologic findings tell us about health effects of environmental aerosols? Aerosol Med. 13(4):335–354.

[5] Chen, W.N., Chen, Y.C., Kuo, C.Y., Chou, C.H., Cheng, C.H., Huang, C.C., Chang, S.Y., Ramana, M.R., Shang, W.L., Chuang, T.Y. and Liue, S.C. 2014. The real-time method of assessing the contribution of individual sources on visibility degradation in Taichung. Sci. Total Environ. 497–498: 219–228.

[6] Liu, Y., Zhang W., Yang W., Bai Z., and Zhao X., 2018. Chemical Compositions of PM2.5 Emitted from Diesel Trucks and Construction Equipment. Aer. Sci. & Eng 2:51–60.

[7] Nkohla, M.A., 2006. Characterization of Ferrochrome Smelter Slag and its Implications in Metal Accounting, Cape Peninsula University of Technology, Cape Town, South Africa. 1-10.

[8] https://www.environment.gov.za/sites/default/files/legislations/nema_amendment_act39.pdf.

[9] Lagudu U.R.K, Raja S, Hopke P.K, Chalupa D.C, Utell M.J, Casuccio G, Lersch T.L, and West R.R., 2011. Heterogeneity of Coarse Particles in an Urban Area. Environ. Sci. Technol. 45: 3288–3296.

[10] Schauer, J.J., W.F. Rogge, L.M. Hildemann, M.A. Mazurek, G. R. Cass, and B.R.T. Simoneit. 1996. Source apportionment of airborne particulate matter using organic compounds as tracers. Atmos. Environ. 30:3837–55.

[11] Pant P. and Harrison R. M. 2012. Critical review of receptor modelling for particulate matter: A case study of India. Atmos. Environ. 49: 1-12.

[12] Watson, J.G. 2002. Visibility: science and regulation. J. of Air and Waste Manag. Ass. 52: 628–713.

[13] Reff, A., Eberly, S. I., and Bhave, P. V. 2007. Receptor modeling of ambient particulate matter data using positive matrix factorization: review of existing methods. JAPCA J. Air Waste Manag. 57: 146–154.

[14] Harris, A.R. and Davidson, C.I. 2005. The Role of Resuspended Soil in Lead Flows in the California South Coast Air Basin. Environ. Sci. Technol. 39: 7410-7415.

[15] Watson, J.G. and Chow, J.C. 2001a. PM2.5 Chemical Source Profiles for Vehicular Exhaust, Vegetation Burning, Geological Materials and Coal Burning in Northwestern Colorado during 1995. Chemosphere. 43: 1141-1151.

[16] Bhave, P.V., Fergenson, D.P., Prather, K.A. and Cass, G.R. 2001. Source Apportionment of Fine Particle Matter by Clustering Single-Particle Data: Tests of Receptor Model Accuracy. Environ. Sci. Technol. 35: 2060-2072.

[17] Kim, E., T.V. Larson, P.K. Hopke, C. Slaughter, L.E. Sheppardand Claiborne, C. 2003b. Source Identification of PM2.5 in an Arid Northwest U.S. City by Positive Matrix Factorization. Atmos. Res. 66: 291-305.

[18] Begum, B.A., Kim, E., Biswas, S.K. and Hopke, P.K. 2004. Investigation of Sources of Atmospheric Aerosol at Urban and Semi-Urban Areas in Bangladesh. Atmos. Environ. 38: 3025-3038.
[19] Karanasiou A., Minguillón M. C., Viana M., Alastuey A., Putaud J. P., Maenhaut W., Panteliads P., Močnik G., Favez O., and Kuhlbusch T. A.J. 2015. Thermal-optical analysis for the measurement of elemental carbon (EC) and organic carbon (OC) in ambient air: a literature review. Amos. Meas. Tech. Discuss., 8: 9649-9712.
[20] Schulze B. R. 1986. Climate of South Africa. Part 8. General Survey, WB 28, Weather Bureau, Department of Transport, Pretoria, 330 pp.
[21] DWAF, 2005. Water Services Planning Reference Framework, Sekhukhune District Municipality. DWAF, inviromap and GPM Consultants, Pretoria, 124pp.
[22] Wagner, Jeff, and David Leith. 2001b. "Passive Aerosol Sampler. Part II: Wind Tunnel Experiments." Aeros. Sc. & Tech. 34 (2): 193– 201.
[23] Ott, D. K., Cyrs, W, and Peters T.M. 2008. "Passive Measurement of Coarse Particulate Matter, PM10-2.5." J. of Aeros. Sc. 39 (2): 156– 167.
[24] Sawvel, E.J., Willis, R., West, R.R., Casuccio, G.S., Norris, G., Kumar, N., Hammond, D., and Peters T.M. 2015. Passive sampling to capture the spatial variability of coarse particles by composition in Cleveland, OH. Atmos. Environ., 105: 61-69.
[25] Hopke, P.K., and Casuccio, G. 1991. Scanning Electron Microscopy. In: Receptor Modeling for Air Quality Management. Elsevier, p. 7.
[26] Song, X.H., Hopke, P.K., 1996b. Solving the chemical mass balance problem using an artificial neural network. Environ. Sci. Technol. 30 (2): 531–535.
[27] Kim, E. and Hopke, P. K. 2008: Source characterization of ambient fine particles at multiple sites in the Seattle area, Atmos. Environ., 42: 6047–6056.
[28] Buhot, A and W. Krauth. 1999. Phase separation in two dimensional additive mixtures. Phys. Rev. E 59: 2939-2941.
[29] Kim, D.S., Hopke, P.K., 1988. The classification of individual particles based on computer-controlled scanning electron microscopy data. Aerosol Sci. Technol. 9: 133–151.
[30] Lee, E., Chan, C.K., Paatero, P., 1999. Application of positive matrix factorization in source apportionment of particulate pollutants in Hong Kong. Atmos. Environ. 33 (19): 3201– 3212.
[31] European Commission. 2014. European Guide on with Receptor Models Air Pollution Source Apportionment. doi: 10.2788/9307.
[32] Central Pollution Control Board. Delhi, India (2010). Air quality monitoring, Emission Inventory and source apportionment study for Indian Cities – National Summary Report. http://moef.nic.in/ downloads/public-information/Rpt-air-monitoring-17-01-2011.pdf.
[33] Barrera, V. A., Miranda, J., Espionosa, A. A., Meinguer, J. N., Ceron, E., Morales, J. R., Miranda, P. A., and Dias., J. F. 2012. Contribution of Soil, Sulfate, Biomass Burning Sources to the Elemental Composition of PM10 from Mexico City. Int. J. Environ. Res., 6(3): 597-612.
[34] Draxler, R. R. and G. D. Hess, 1997: Description of HYSPLIT_4 modelling system. NOAA technical memorandum ERL ARL-224: 24pp.
[35] Romesburg, H. C. 1984: Cluster analysis for researchers. Lifetime Learning, Belmont, Calif., 334pp.
[36] Draxler, R., Stunder, B., Rolph, G., and Stein, A. 2018. HYSPLIT4 USER's GUIDE. Version 4. NOAA Air Resources Laboratory.
[37] WHO 2017. Evolution of WHO air quality guidelines: past, present and future.

[38] Ministry for the Environment, 2009. Good Practice Guide for Air Quality Monitoring and Data Management 2009.
[39] Sun H, Shamy M, Kluz T. 2012. Gene expression profiling and pathway analysis of human bronchial epithelial cells exposed to airborne particulate matter collected from Saudi Arabia. Toxicol. Appl. Pharmacol. 265:147–57.